The role of adenylyl cyclase 6 in platelet function and thrombosis

Bethany Ann Webb

Submitted in accordance with the requirements for the degree of
Doctor of Philosophy

The University of Leeds
Faculty of Medicine and Health
Leeds Institute of Cardiovascular and Metabolic Medicine

July 2022

The candidate confirms that the work submitted is her own and that appropriate credit has been given where reference has been made to the work of others. This copy has been supplied on the understanding that it is copyright material and that no quotation from the thesis may be published without proper acknowledgement.

Acknowledgements

First and foremost, I would like to thank my supervisor Prof. Khalid Naseem for the opportunity to work on this project, supporting me throughout and for taking a leap of faith in that shy girl that walked into his office 4 years ago. Khalid has been a great mentor and has allowed me to develop not only my skills as a researcher but my confidence too, to which I am very grateful.

Thank you to Dr Kerrie Smith, who provided me with great support in the early stages of my PhD and encouraging me to have faith in myself. I would also like to thank Dr Neil Turner for all his support and encouragement as well as taking on the role as my secondary supervisor.

I would like to acknowledge the support of Dr Nadira Yuldasheva who helped me establish the early stages of breeding (Figure 16) and Dr Lih Cheah for training me and providing a huge amount of support for all the murine techniques described in this study. As well as Dr Cedric Duval for his support and advice upon analysing *in vivo* embolic events (Figure 62).

A huge thank you, to everyone in the Naseem lab group both past and present, for making coming into the labs an absolute pleasure. I feel incredibly lucky to have worked with some great people over the past 3.5 years. My sincere thanks to Dr Matt Hindle and Dr Lih Cheah for welcoming me to the group and teaching me all what I know today as well as alleviating the pressure during busy lab days. I would also like to thank Dr Clare Wilson for being a great friend and supporting me throughout the years. I must also acknowledge the work carried out by others in this study, to which I am grateful. Matt carried out murine phospho-flow experiments and analysis (Figure 40 and 68) as well as spreading analysis presented in section 4.5. In addition, Lih and I worked together to assess thrombosis injury *in vivo* (Figure 61).

I would whole heartedly like to thank my incredible friends and my parents, for always supporting me and encouraging me throughout my studies. Lastly, a special heartfelt thank you to my fantastic partner Zach, who is my absolute rock and has been there through all the highs and lows of the PhD process.

Thank you for everything you do for me and for always making me smile, even when the going gets tough. I don’t think I would have made it this far without you.

List of Abbreviations

AA	Arachidonic Acid
AC	Adenylyl Cyclase
ACD	Acid-citrate dextrose
ACS	Acute coronary syndrome
ADP	Adenosine Diphosphate
aIIbB3	Integrin alpha 2b beta 3
AKAPs	A-kinase anchoring proteins
AMP	Adenosine Monophosphate
AMR	Ashwell-Morrell Receptor
APC	Allophycocyanin
ApoE	Apolipoprotein-E
ATP	Adenosine Triphosphate
BB	Brilliant blue
BCL-XL	B-cell lymphoma-extra large
BSA	Bovine serum albumin
Ca2+	Calcium ion
CaM	Calmodulin
cAMP	cyclic-adenosine 3',5'-monophosphate
cGMP	cyclic-guanosine 3',5'-monophosphate
COX	Cyclooxygenase
DNA	Deoxyribonucleic Acid
DTS	Dense tubular system
ECL	Enhanced chemi-luminescence
ECM	Extracellular matrix
FFC	Fluorescent flow cytometry
FITC	Fluorescein
FSC	Forward scatter
GPIb-IX-V	Glycoprotein Ib-IX-V
GPVI	Glycoprotein VI
GS	Glycogen synthase
GSK3	Glycogen synthase kinase 3
GTP	Guanosine triphosphate
HRP	Horseradish peroxidase
HSCs	Haematopoietic Stem Cells
ITAMs	Immunoreceptor Tyrosine-based Activation Motifs
IVC	Inferior vena cava
MI	Myocardial infarction
MKs	Megakaryocyte
mRNA	Messenger ribonucleic acid
NO	Nitric Oxide

OCS	Open canalicular system
PAGE	Polyacrylamide gel electrophoresis
PAR	Protease-activated receptor
PBS	Phosphate-buffered saline
PCR	Polymerase chain reaction
PDE	Phosphodiesterase
PE	phycoerythrin
PE	Pulmonary embolism
PGE1	Prostaglandin E1
PGG2	prostaglandin G2
PGH2	prostaglandin H_2
PGI2	Prostacyclin
PKA	Protein Kinase A
PKC	Protein Kinase C
PKG	Protein kinase G
PLA	Proximity ligation assay
PLA2	phospholipase A_2
PPP	Platelet poor plasma
PROTACs	proteolysis-targeting chimeras
PRP	Platelet rich plasma
PS	Phosphatidylserine
qPCR	Quantitative polymerase chain reaction
RNA	Ribonucleic Acid
SD	Standard deviation
SDS	Sodium dodecyl sulphate
Ser	Serine
sGC	Soluble guanylyl Cyclase
siRNA	Small interfering RNA
SMC	smooth muscle cells
SSC	Side scatter
TBS	Tris-buffered saline
TBT	Tail bleeding time
Thr	Threonine
TPO	Thrombopoietin
TxA_2	Thromboxane A_2
VASP	Vasodilator-stimulated phosphoprotein
VSMC	Vascular smooth muscle cells
vWF	von Willebrand factor
WCL	Whole cell lysate
WP	Washed platelets

Abstract

Platelet activation is constrained by endothelial-derived prostacyclin (PGI_2) acting through a cyclic adenosine-5'-monophosphate (cAMP) signalling pathway. Cyclic-AMP signalling in platelets involves a complex network of multiple isoforms of adenylyl cyclase (AC), protein kinase A (PKA) and phosphodiesterase's (PDEs). AC6 is the predominant isoform in both human and murine platelets, although its importance to platelet function is unclear. To address this, we generated a novel platelet-specific AC6 deficient mouse (AC6-KO). This new murine strain was fertile and showed no differences in platelet counts or morphology. *In vitro* studies showed that the absence of AC6 compromised the ability of PGI_2 to control thrombin-mediated aggregation, fibrinogen binding, P-selectin expression, and PS exposure. In contrast, there were no effects on inhibition of platelet activation stimulated by collagen. *In vivo* studies indicated an accelerated rate of thrombosis in response to ferric chloride injury, as well as impaired thrombus stability in the AC6-KO compared to controls. Having found that inhibition of thrombin-mediated platelet activation was compromised in the absence of AC6, we examined the role of AC6 in cAMP signalling. Interestingly, no differences in basal cAMP concentrations were observed between AC6-KO and littermate controls, suggesting that AC6 does not control basal cAMP production. In contrast, AC6-KO showed significantly reduced responses to PGI_2-induced cAMP generation, although this was not completely ablated. We found that phosphoVASP^{Ser239}, phosphoVASP^{Ser157} and phosphoGSK3β^{Ser9} were all significantly impaired in AC6-KO platelets in response to both PGI_2 and forskolin, indicating that reduced cAMP led to diminished signalling responses. Overall, these data confirm a key role of AC6 in controlling cAMP-mediated platelet regulation *in vitro* and *in vivo*. However, given that the effects of PGI_2 and cAMP signalling are not ablated, suggests that the regulation of platelet function and thrombosis is linked to multiple AC isoforms.

Table of Contents

List of Tables

List of Figures

Publications

Oral presentations

Platelet Society Meeting, April 2022. The University of Hull. 4-minute flash oral presentation: The role of Adenylyl cyclase 6 in platelet function and thrombosis. (Awarded joint-first place)

LICAMM early career conference, December 2021. Online. Oral presentation: The role of Adenylyl cyclase 6 in platelet function and thrombosis. (Awarded runner-up prize).

British Society of Haemostasis and Thrombosis (BSHT), April 2020. Online. 3-minute flash oral presentation: Acute coronary heart disease is characterised by circulating procoagulant platelets and hyposensitivity to prostacyclin.

Poster presentations

Platelet Society Meeting, April 2021. The University of Hull. Poster presentation: The role of Adenylyl cyclase 6 in platelet function and thrombosis.

Platelet Society Meeting, April 2020. Online. Poster presentation: Acute coronary heart disease is characterised by circulating procoagulant platelets and hyposensitivity to prostacyclin. (Awarded joint-first place)

Journal articles

Webb BA, Cheah LT, Hindle MS, Khalil JS, Duval C, Turner NA, Ariëns RAS, and Naseem KM (2022). Adenylyl cyclase 6 mediates platelet function and thrombosis, in preparation

Hindle MS, Spurgeon BEJ, Cheah LT, **Webb BA**, Naseem KM. Multidimensional flow cytometry reveals novel platelet subpopulations in response to prostacyclin. J Thromb Haemost. 2021 Jul;19(7):1800-1812. doi: 10.1111/jth.15330. Epub 2021 Apr 26. PMID: 33834609.

Aburima A, Berger M, Spurgeon BEJ, **Webb BA**, Wraith KS, Febbraio M, Poole AW, Naseem KM. Thrombospondin-1 promotes hemostasis through modulation of cAMP signaling in blood platelets. Blood. 2021 Feb 4;137(5):678-689. doi: 10.1182/blood.2020005382. PMID: 33538796.

Chapter 1
Introduction

1.1. Platelets

Haemostasis is a major physiological process that prevents blood loss, maintains fluidity, and removes haemostatic plugs upon vascular repair. It is a complex and dynamic system involving proteins and cells of the blood vessel wall, plasma enzymes and circulating platelets to repair damage and prevent bleeding (Versteeg et al., 2013; Brass et al., 2016).

Under normal and healthy conditions, endothelial cells that line blood vessel walls serve as an anti-thrombogenic surface and a physical barrier to separate blood from these anti-thrombogenic agents that reside within the endothelium (Azuma et al., 1986; Radomski et al., 1987a; Radomski et al., 1987b). Platelets circulate within the blood in proximity to the endothelium and are maintained in a quiescent state via endothelial-derived platelet inhibitors, prostacyclin (PGI_2) and nitric oxide (NO) (Radomski et al., 1987b). Upon vascular injury whereby subendothelial collagen is exposed, platelets adhere, activate and aggregate over the injury site to form a haemostatic plug alongside the coagulation cascade (Hoffman and Monroe, 2001). The extent of platelet activation and thrombus size is regulated by the constant exposure to PGI_2 and NO secreted by intact neighbouring endothelial cells (Clemetson, 2012).

Yet, pathological conditions that compromise endothelial function and sensitivity to endothelial-derived inhibitors can lead to uncontrolled and occlusive thrombus formation, resulting in cardiovascular events such as stroke or myocardial infarction (MI) (Lindemann et al., 2007). Therefore, improving our understanding of the mechanisms that control platelet function may allow us to establish novel therapeutic or diagnostic targets for pathological thrombosis.

1.2. Platelet formation and clearance

Platelets are small anucleate cells of the blood, first discovered by Giulio Bizzozero in 1882 (Ribatti and Crivellato, 2007), that play a key role in

haemostasis, thrombosis, innate immunity, wound healing, and angiogenesis (Gibbins, 2004; Blair and Flaumenhaft, 2009; Golebiewska and Poole, 2015; Koupenova, M. et al., 2018). In circulation, the average human platelet lifespan is 8-10 days. The typical blood concentration of platelets is 150-450 $x10^9$ platelets per litre (Bonaccio et al., 2016) and is maintained via a daily turnover of ~10^{11} cells (Pluthero and Kahr, 2018; Grozovsky, R. et al., 2015). Platelets are primarily formed in the bone marrow by the shedding of mature megakaryocytes (MKs), a process known as thrombopoiesis (Deutsch and Tomer, 2006), although, there is some evidence that platelets are formed from megakaryocytes that reside in the pulmonary system (Lefrançais et al., 2017).

MKs are large diffuse cells that are derived from haematopoietic stem cells (HSCs) (Deutsch and Tomer, 2006). Upon maturation, MKs exhibit polyploidy and expansion of the cytoplasmic mass (Patel, 2005). Enlargement is mediated by several rounds of endomitosis which amplifies the DNA by as much as 64-fold (Ebbe et al., 1965; Odell et al., 1968; Ravid et al., 2002). Maturation of MKs leads to the formation of pro-platelet projections which are released into circulation, where they fragment into circulating platelets (Deutsch and Tomer, 2006). This release of platelets is thought to be a consequence of apoptosis of mature polyploid MKs. It is thought that a specialised apoptotic process may lead to pro-platelet projections and platelet assembly (Patel, 2005; Gordge, 2005). Apoptotic inhibitory factors (pro-survival), BCL-2 and BCL-XL are expressed in early MKs but when overexpressed they inhibit pro-platelet formation (Ogilvy et al., 1999; Kaluzhny et al., 2002; Kaluzhny and Ravid, 2004) suggesting that apoptosis of MKs may play a role in platelet formation. It has also been found that caspase-3 and caspase-9 are active in mature MKs and has been established as a requirement for pro-platelet formation (De Botton, 2002). Inhibition of caspases was also found to block the biogenesis of pro-platelets (De Botton, 2002; Clarke et al., 2003). Different mechanisms of apoptosis in MKs and platelets suggest that specific apoptotic factors are required for MKs compared to platelets (Josefsson et al., 2011; Josefsson et al., 2014). Alternatively, it has been proposed that platelets are formed from explosive fragmentation of MKs in the bone marrow and pulmonary system (Kosaki, 2005), though the pro-platelet theory is more widely accepted.

Each MK can produce thousands of platelets (Ghoshal and Bhattacharyya, 2014) and this is primarily controlled by thrombopoietin (TPO), a growth factor of the MK lineage (Hitchcock and Kaushansky, 2014; Cho et al., 2018; Kelemen et al., 1958). The main source of TPO are hepatocytes, inducing both proliferation and maturation of MKs to ensure a steady platelet count is maintained within the body (Hoffmeister, 2012; Grozovsky et al., 2015a; Grozovsky et al., 2015b). After 8-10 days, platelets are removed by hepatic Ashwell-Morrell receptors (AMR) which recognise desialylated surface proteins on aged platelets (Harker and Finch, 1969; Grozovsky et al., 2015a; Hoffmeister and Falet, 2016; Cho et al., 2018). The removal of desialylated platelets by AMR regulates TPO synthesis in the liver, increasing thrombopoiesis to maintain a steady state of platelet production (Grozovsky et al., 2015a). Additionally, studies have shown that glycan modifications on platelet surface proteins can also mediate platelet clearance (Rumjantseva and Hoffmeister, 2010; Hoffmeister, 2011).

Although platelets are anucleate, studies have shown that platelets contain the necessary components and programming for apoptosis, controlling their survival and lifespan (Mason et al., 2007; Leytin, 2012; Deng et al., 2017). Platelet apoptosis displays several distinct events including mitochondrial depolarisation, cytochrome C release, activation of apoptotic caspases, exposure of phosphatidylserine and cellular blebbing, along with fragmentation (Gyulkhandanyan et al., 2012; Mcarthur et al., 2018). The ageing of platelets is controlled by the anti-apoptotic protein, BCL-XL which has been suggested to be regulated by the cAMP/PKA signalling pathway (Vogler et al., 2011; Zhao et al., 2017).

Complications in the processes controlling platelet production and clearance can lead to disorders such as thrombocytopenia (platelet counts less than 150,000/μL) resulting in insufficient clot formation and increased bleeding risk. While thrombocythemia (platelet counts greater than 600,000/μL) can induce a greater risk of thrombotic events such as stroke, deep vein thrombosis and myocardial infarction (Patel, 2005; Griesshammer et al., 1998; Kuter and Gernsheimer, 2009; Martin et al., 2012).

1.2.1. Platelet structure

Platelets are discoid in shape with a diameter of 2-4 μm and are the smallest cells in the blood. Though despite their size they contain over 4000 unique proteins, owing to their complexity as cells (Burkhart et al., 2012). Platelets have evolved to allow for rapid haemostatic function and activation upon injury to cessate bleeding at vascular sites, including; tethering, degranulation, spreading over injury sites, binding to, as well as recruiting other platelets, and facilitating the coagulation cascade (Gibbins, 2004).

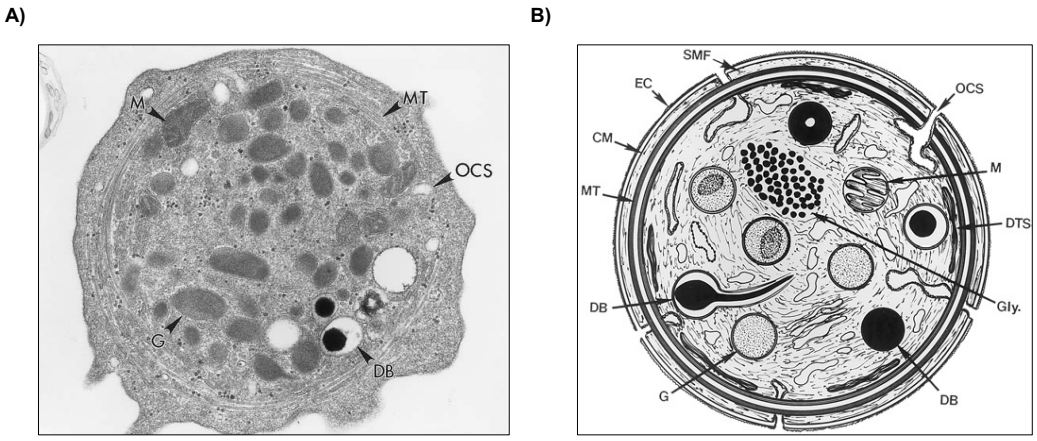

Figure 1. Platelet structure and contents

Cross-section of a resting human platelet take by transmission electron microscopy (x36,000) (A). The ultrastructural components of resting human platelets (B). Abbreviations include Exterior coat (EC), trilaminar unit membrane (CM), submembrane (SMF), and open canalicular system (OCS), mitochondria (M), alpha granules (G), dense bodies (D) and dense tubular system (DTS). Figures and legend adapted from (White, 2004).

1.2.2. Membrane

The platelet membrane is a typical phospholipid bilayer composed of proteins and lipids. Phospholipids form the basic structure, while cholesterol is distributed asymmetrically throughout the phospholipids. Cholesterol acts to stabilise the membrane, maintain fluidity, and control the transmembrane passage of materials. The platelet membrane bilayer consists of phosphatidylcholine on the exterior and phosphatidylserine on the interior (Lhermusier et al., 2011). Phosphatidylserine (PS) is regulated by flippase and scramblase enzymes and upon platelet activation some platelets present PS on their surface (Agbani and Poole, 2017), thus creating a negatively charged surface to facilitate coagulation (Hoffman and Monroe, 2001; Monroe et al., 2002). The platelet membrane surface known as the glycocalyx, as it is heavily glycosylated, absorbs albumin, fibrinogen, and other plasma proteins, transporting them to storage organelles. It is here where platelet glycoprotein surface receptors sit, anchored within the membrane (Bennett, 1963). The plasma membrane is selectively permeable, and the membrane bilayer acts to support platelet activation internally and plasma coagulation externally. Platelets also exhibit membrane folding called the open canalicular system (OCS) which is important for rapidly increasing surface area upon activation and spreading (Escolar and White, 1991). Changes to the OCS have been implicated in disease, which has been suggested to play a role in platelet activation, though further understanding is required (Selvadurai and Hamilton, 2018) (Figure 1).

The platelet plasma membrane is a dynamic environment which can undergo broad reorganisation (Lopez et al., 2005). Plasma membrane lipids are not homogenously distributed, and these membranes may contain microdomains or compartments. Glycosphingolipid- and cholesterol-rich microdomains are known as lipid rafts (Simons and Gerl, 2010). Lipid rafts are specialised membrane microdomains that are involved in various stages of haemostasis and thrombosis (Lopez et al., 2005; Jin et al., 2007). They are said to form distinct islands within the phospholipid bilayer in a fluid mosaic-like structure, which can readily move and rearrange to facilitate membrane-bound protein reorganisation. Rafts containing receptors are suggested to play a key role in receptor clustering, a central prerequisite for Immunoreceptor Tyrosine-based

Activation Motifs (ITAMs) signalling, including GPVI clustering and signalling (Locke et al., 2002). Lipid rafts have also been linked to cyclic-nucleotide signalling, which has been postulated to control spatiotemporal regulation of platelet inhibitory pathways (Raslan, Z. and Naseem, K.M., 2015).

1.2.3. Cytoskeleton

A vital aspect of the structure of platelets is the cytoskeleton. At rest, the cytoskeleton is distinct, as it displays a cell-spanning coil of microtubules that support the discoid shape of resting platelets (Behnke, 1965). However, it allows for platelets to rapidly change morphology upon activation and contributes to their role in clot retraction. Upon platelet activation, the coil of microtubules contracts, losing its discoid shape and undergoing significant remodelling. The cytoskeletal rearrangement leads to the formation of actin structures such as filopodia, lamellipodia, actin nodules and stress fibres (Yusuf et al., 2017; Atkinson et al., 2018). Together, these processes lead to the collapse of discoid shape and ensure the ability of platelets to spread over a large surface area during injury.

1.2.4. Cytosol and granules

The platelet cytosol, like other cells, contains many organelles typical to eukaryotic cells, though platelets have distinct granules. The platelet cytosol contains mitochondria to ensure efficient production of ATP. It also contains a platelet-specific organelle known as the dense tubular system (DTS) which stores intracellular Ca^{2+} (Ebbeling et al., 1992) (Figure 1). In addition, platelets also include three types of granules: α-granules, δ-granules, and lysosomal granules. The α-granules are the most abundant, with numbers of ~65 α-granules per platelet and roughly 0.2-0.5 μm in diameter (Blair and Flaumenhaft, 2009). Though extremely small, α-granules contain adhesion proteins, chemokines, coagulation factors, fibrinolytic enzymes, and growth factors. Giving α-granules an expansive role across haemostasis, thrombosis, repair and growth, as well as immunity (Golebiewska and Poole, 2015). In contrast, δ-granules contain small molecules such as polyphosphates, ADP, ATP, Ca^{2+} and serotonin, supporting coagulation or further enhancing platelet activation (Stalker et al., 2013; Brass et al., 2016).

1.3. Platelet activation

Platelet activation is a dynamic process with multiple signalling pathways working in harmony to promote the formation of a haemostatic platelet plug in response to injury (Figure 2). Vascular injury leads to exposure of prothrombotic extracellular matrix (ECM) proteins such as von Willebrand factor (vWF) and collagen, which facilitate platelet adhesion (Varga-Szabo et al., 2008; Clemetson, 2012) (Figure 2 A). The initial adhesion to vWF via the GPIb-V-IX (GPIbα) receptor complex leads to transient platelet tethering and rolling (Jennings, 2009; Broos et al., 2011; Clemetson, 2012; Thomas and Storey, 2015). The subsequent binding of collagen to GPVI then activates the platelets leading to a series of functional changes that drive the formation of a haemostatic platelet plug (Jackson et al., 2003; Stepanyan et al., 2021) (Figure 2 B). Notably, the absence of vWF and GPIbα are linked to bleeding disorders such as von Willebrand disease and Bernard-Soulier syndrome, respectively, highlighting their important role in haemostasis (Salles et al., 2008; De Meyer et al., 2009).

Next, inside-out signalling drives conformational changes in integrins $\alpha_2\beta_1$ and $\alpha_{IIb}\beta_3$, to facilitate stable platelet adhesion and platelet-platelet aggregation, respectively (Kulkarni et al., 2000; Jackson et al., 2003). The subsequent release of the soluble platelet agonist, adenosine diphosphate (ADP), adhesive proteins such as vWF, and fibrinogen, and the synthesis of thromboxane A_2 (TxA_2), act to promote both activation and recruit additional platelets into the growing thrombi (Offermanns, 2006; Jennings, 2009) (Figure 2 C). In addition to morphological changes, the exposure of phosphatidylserine on the surface of platelets facilitates the generation of thrombin, a potent platelet agonist (Monroe et al., 2002). Thrombin also plays an important role in the coagulation cascade and thrombus formation via the cleavage of fibrinogen to fibrin (Hoffman and Monroe, 2001).

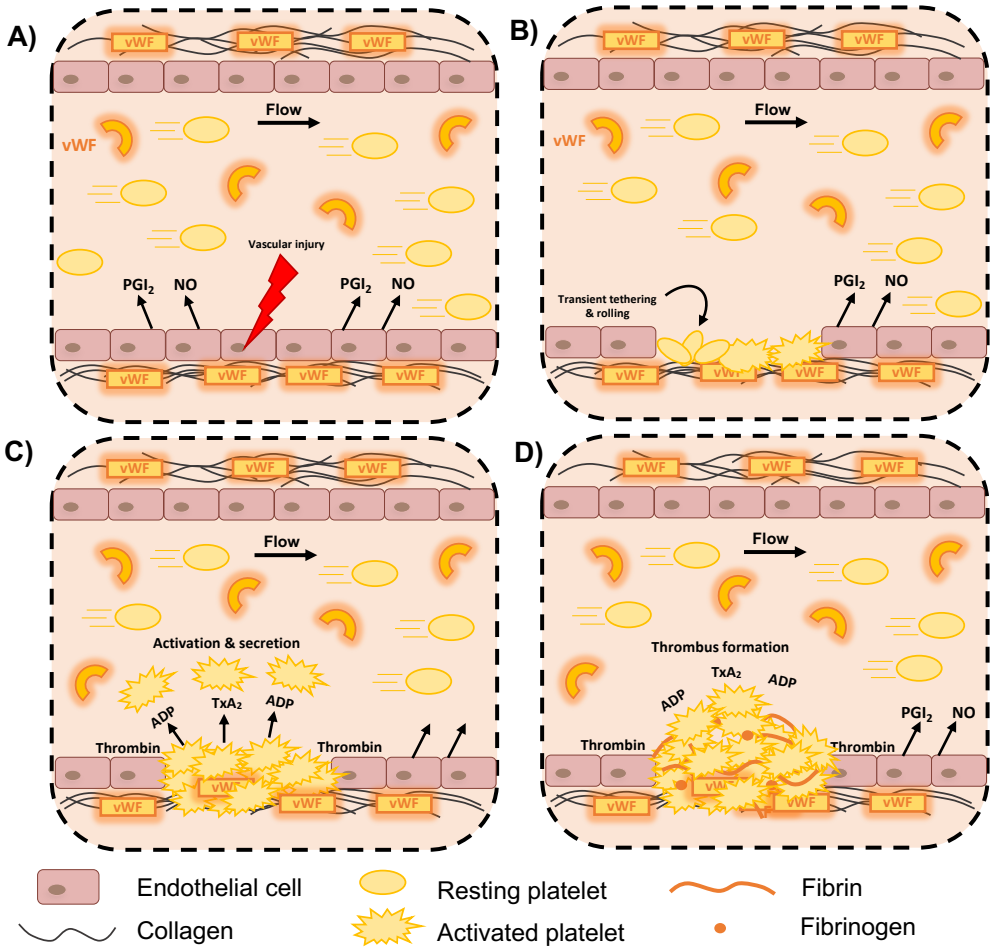

Figure 2. Platelet activation in response to vascular injury

Simplified schematic of the stages of platelet activation in response to injury. (A) vascular injury causing damage to the endothelium, (B) transient tethering and rolling over the injury site, (C) platelet activation and secretion, leading to amplification of platelet activity, and (D) formation of fibrin-rich thrombus, leading to the cessation of bleeding. Schematic and caption adapted from (Gibbins, 2004).

The downstream signalling pathways associated with agonist-dependent platelet activation begins with the activation of one of the phospholipase C (PLC) isoforms (Stalker et al., 2012). PLC hydrolyses phosphatidylinositol 4,5 bisphosphate (PIP_2) to produce membrane bound inositol-1,4,5-trisphosphate (IP_3), the second messenger required to raise intracellular Ca^{2+} levels and membrane bound diacylglycerol (DAG) (Broos et al., 2011; Stalker et al., 2012). The increase in Ca^{2+} is what leads to integrin activation via a pathway that includes CalDAG-GEF, Rap1, RIAM, talin and kindlin (Crittenden et al., 2004). The binding of collagen to GPVI activates PLCγ2 via a mechanism that is dependent on scaffold molecules and protein tyrosine kinases (Watson et al., 2005; Shattil et al., 2010; Stalker et al., 2012) (Figure 3). Thrombin binds to and cleaves G-protein coupled Protease Activated Receptors (PAR) on the surface of platelets activating PLCβ, with ADP and TxA_2 activating PLCβ in a similar fashion (Brass et al., 2011) (Figure 3).

The functional significance of soluble platelet agonists such as ADP, TxA_2 and thrombin are underscored by their pharmacological targeting as anti-platelet therapies (Tello-Montoliu et al., 2011; Wijeyeratne and Heptinstall, 2011; Fontana et al., 2014; Metharom et al., 2015). In the clinic, $P2Y_{12}$ receptor antagonists such as ticagrelor or clopidogrel, prevent ADP binding to $P2Y_{12}$ and are typically given to patients post-MI (Zhang et al., 2017). While other anti-platelet therapies such as aspirin target endothelial COX to inhibit the production of TxA_2 (Abramson et al., 1985; Schror, 1997; Warner et al., 2011). Aspirin and $P2Y_{12}$ receptor antagonists are often used together, known as dual anti-platelet therapy (DAPT) (Warlo et al., 2019). Both aspirin and $P2Y_{12}$ receptor antagonists act by reducing platelet amplification responses to control platelet activation, however they can be associated with bleeding complications (Becker et al., 2011; Garcia Rodriguez et al., 2016). Yet, despite DAPT, some patients still experience recurrent cardiovascular events, likely due to insufficient platelet inhibition or differences in treatment response, highlighting the need for more personalised and targeted anti-platelet agents (Zhang et al., 2017).

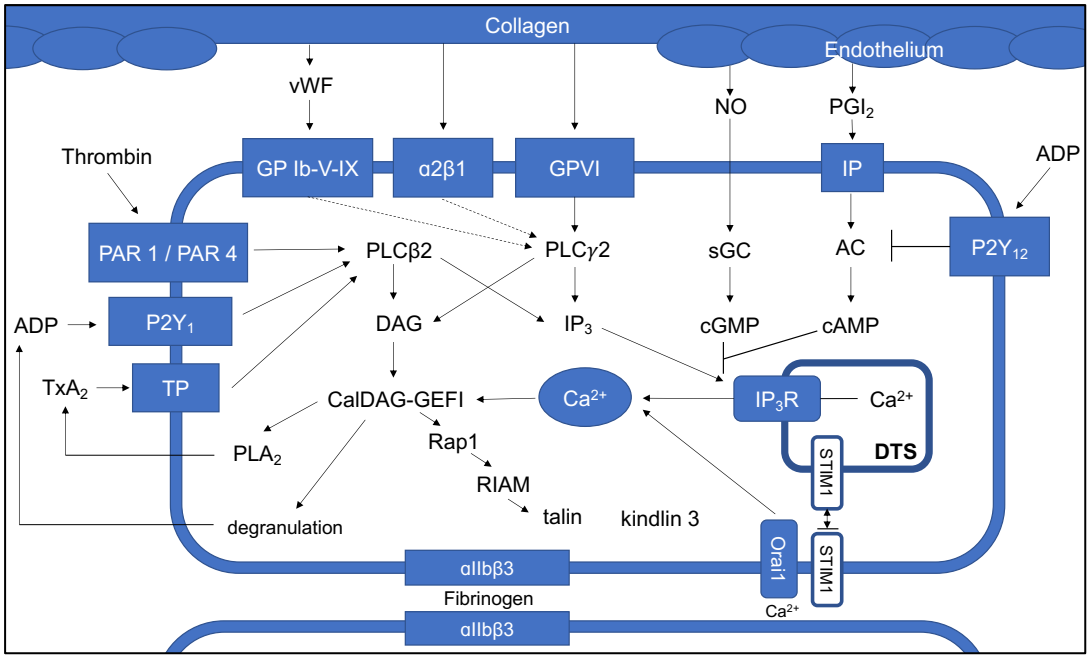

Figure 3. Platelet effectors and receptors controlling platelet activation.

Schematic representation of platelet agonists, receptors and intracellular signalling pathways that control platelet activation adapted from Broos et al., (2011).

Interestingly, recent studies examining the response to vascular injury *in vivo* highlight the complexity of platelet activation. Rather than a mass of uniformly activated platelets contained in a fibrin-mesh as previously described (Brass, 2003; Gibbins, 2004). Instead, thrombi plugs develop an ordered structure with gradation of platelet activation and fibrin distinctly localised in the core of the haemostatic plug (Tomaiuolo et al., 2017). The core region consists of highly irreversibly activated and densely packed platelets surrounded by a shell of less activated and weakly bound platelets (Diamond, 2016). This has been termed the 'shell and core' model of thrombus architecture and suggests a level of hierarchal platelet activation, whereby individual platelets are exposed to different combinations and concentrations of agonists that vary over time and space (Tomaiuolo et al., 2017; Stalker et al., 2013). The core is characterised by the presence of P-selectin positive cells, a key marker for platelet activation, while the shell has been reported to have little to no P-selectin positive cells (Stalker et al., 2013). It was also shown that thrombin was the main driver for full platelet activation in the core, whereas TxA_2 and ADP were primarily involved in platelet activation in the shell of the growing thrombus (Stalker et al., 2013; Brass et al., 2016). This is consistent with models of platelet inhibition whereby platelets only become activated when required as reviewed by Stalker et al., (2013) and Brass et al., (2016).

The marginalisation of platelets during blood flow, enables their continuous exposure to PGI_2 throughout circulation, ensuring that the platelets remain in a quiescent state, while still able to activate when required (Gibbins, 2004). Upon vascular injury, platelets overcome the inhibitory effect of PGI_2 to become rapidly active. This is achieved through two distinct mechanisms. Firstly, inhibition of cyclic adenosine 3',5'-monophosphate (cAMP) production by platelet-derived adenosine diphosphate (ADP), which binds to the $P2Y_{12}$ /$G\alpha_i$, coupled receptor, leading to the inhibition of AC activity (Nagy and Smolenski, 2018). Secondly, thrombin- and collagen-mediated increases in cAMP hydrolysis through the activation of phosphodiesterases (PDEs) (Zhang and Colman, 2007). The reduction of platelet cAMP concentrations is thought to lower the threshold for platelet activation. While pathological conditions of the vasculature such as atherosclerosis are thought to reduce the anti-thrombotic effect from endothelial-derived PGI_2 and NO (Ruggeri, 2002).

Additionally, defects in cyclic nucleotide signalling in platelets as a result of either a pathological condition or an inherited mutation have been linked to cardiovascular disease (Manrique and Manrique, 1987; Van Geet et al., 2009) resulting in disruption of this dynamic process. Consequently, the risk of vessel occlusion increases which can lead to an increased risk of stroke or MI (Nieswandt et al., 2011).

1.4. Regulation of platelet function

To moderate excessive activation and return platelets to their quiescent state after transient activation, the endothelium releases inhibitory agents such as prostaglandins (PGI_2 and PGE_1), adenosine and nitric oxide (NO), which inhibit platelets through cyclic nucleotide signalling pathways. Prostacyclin (PGI_2), Prostaglandin E_1 (PGE_1) and adenosine lead to the production of cAMP and downstream activation of protein kinase A (PKA). While, NO leads to the production of cyclic guanosine 3',5'-monophosphate (cGMP) and downstream activation of protein kinase G (PKG), with both signalling cascades resulting in platelet inhibition (Fukumoto et al., 1999) (Figure 4).

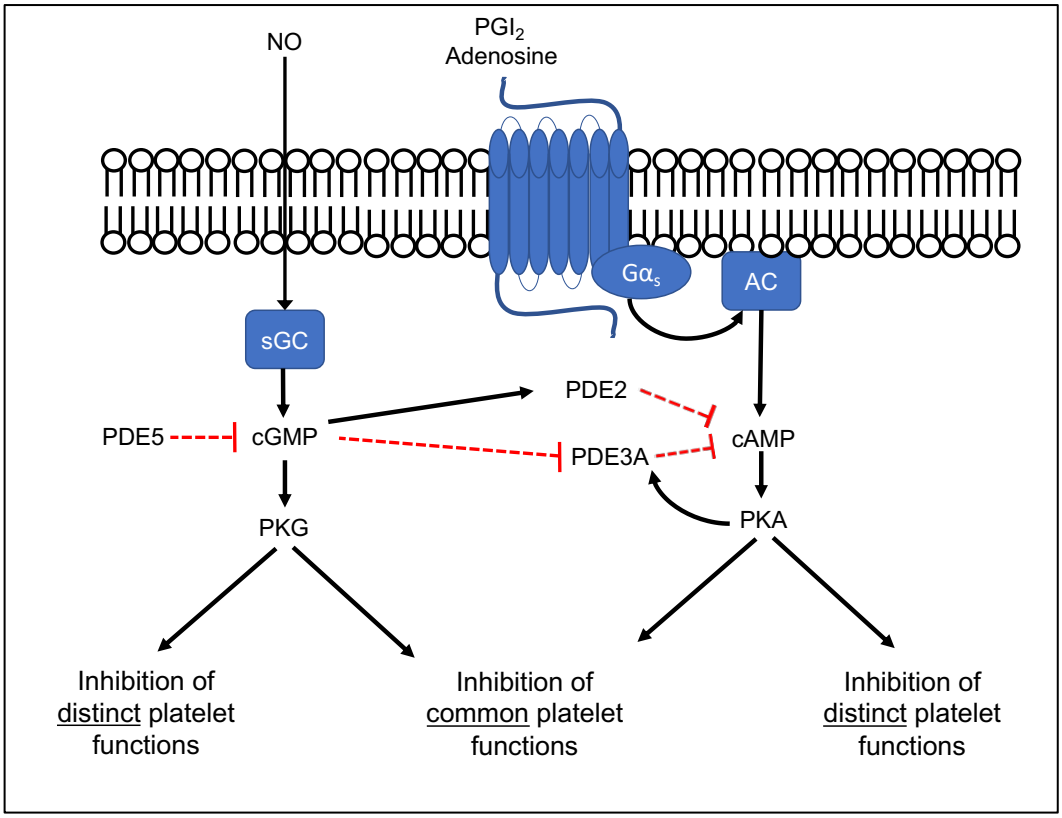

Figure 4. Platelet cyclic nucleotide signalling

A simplified schematic of platelet cyclic nucleotide signalling. Platelets are maintained at rest by cGMP and cAMP signalling pathways. Nitric Oxide (NO) binds to soluble guanylyl cyclase (sGC) which produces cGMP, leading to the activation of protein kinase G (PKG). PGI_2 or adenosine, bind to their receptors, leading to $G\alpha_s$ activation, which in turn activates adenylyl cyclase (AC). AC produces cAMP, which leads to the activation of protein kinase A (PKA). PKA and PKG then phosphorylate substrates lead to the inhibition of platelet function(s). The levels of cGMP are maintained by phosphodiesterase 5 (PDE5), while cAMP is controlled by PDE3A and PDE2.

1.4.1. Endothelial-derived cAMP elevating agents

PGI_2, the most potent endothelial-derived platelet inhibitor, is a prostanoid that belongs to the eicosanoid family of lipid mediators (Moncada et al., 1976). Eicosanoids are derived from the hydrolysis of arachidonic acid (AA) from membrane phospholipids by phospholipase A_2 (PLA_2) (Samuelss, 1965; Hamberg and Samuelss, 1974) (Figure 5). PGI_2 is produced by the endothelium upon stimulation, either by an agonist such as thrombin or via shear stress (Majed and Khalil, 2012). After PLA_2-mediated release of AA from the cell membrane (Corey et al., 1980), it is metabolised by cyclooxygenase (COX)-1 and -2, which in turn yields prostaglandin G_2 (PGG_2), then prostaglandin H_2 (PGH_2) in a sequential fashion. PGH_2 acts as a precursor for the prostaglandins PGD_2, PGE_2, PGF, PGI_2 and TxA_2 (Majed and Khalil, 2012) (Figure 5). PGI_2 is released both luminally and abluminally by the endothelium leading to platelet inhibition and muscle relaxation, respectively (Sandoo et al., 2010; Beaulieu and Freedman, 2013). The net effect of PGI_2 is to globally reduce the intracellular signalling events required to support platelet activation through elevating the intracellular levels of cAMP. The inhibitory effect of PGI_2 has been reported to be reversible, which is physiologically important, as platelets need to retain their ability to activate upon vascular injury, while being under constant exposure to PGI_2 to avoid spontaneous and unwanted platelet activation (Beaulieu and Freedman, 2013).

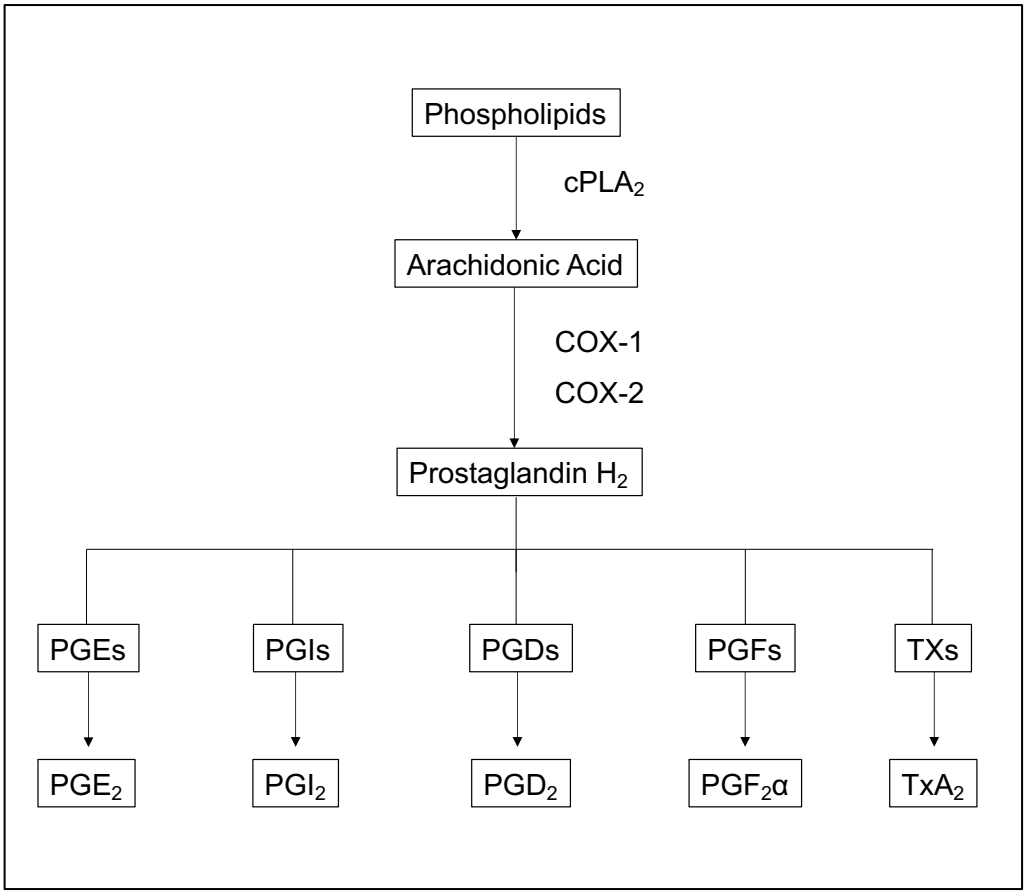

Figure 5. Synthesis of endothelial-derived prostacyclin

Schematic of the synthesis of prostacyclin from phospholipids within the endothelium adapted from Majed and Khalil (2012).

1.4.2. Adenylyl cyclase

A key player in mediating cAMP in platelets are the adenylyl cyclases (ACs). The adenylyl cyclases are a ubiquitously expressed family of transmembrane enzymes that catalyse the conversion of ATP into cAMP. They are key regulators in a broad range of cellular functions and are critical effectors for G-protein couple receptors (GPCRs) (Cooper, 2003). It's been suggested that ACs are the rate-limiting step in GPCR signalling cascades (Lohse et al., 2008). The α-subunit of the G_s protein is released from heterotrimeric α-β-γ-G-protein complexes following the binding of agonist ligands to GPCRs. The α-subunit binds to and activates AC with consequential cAMP generation within the cell (Pierce et al., 2002; Sassone-Corsi, 2012).

There are four distinct classes of ACs and nine known isoforms of AC shown in Table 1, each of which are differentially distributed in a cell type-dependent manner (Hanoune and Defer, 2001). Variability in cAMP synthesis is thought to be determined predominantly either by the extent of AC expression, the specific characteristics of GPCRs linked to enzyme activation or variation in concentration of regulatory factors such as G-proteins, protein kinases, ions and PDE activity (Sadana and Dessauer, 2009; Berger et al., 2018a). It has been shown that all isoforms exhibit basal activity, which is increased by $G\alpha_s$ activity. However, group I (AC1, AC3 and AC8) are also stimulated by calcium, group II (AC2, AC4 and AC7) are activated by $G_s\beta\gamma$, group III (AC5 and AC6) are inhibited by $G\alpha_i$, and group IV (AC9) are insensitive to forskolin.

Class I	AC1, AC3 and AC8	Also stimulated by calcium
Class II	AC2, AC4 and AC7	Activated by Gsβγ
Class III	AC5 and AC6	Inhibited by $G\alpha_i$
Class IV	AC9	Insensitive to AC activator; forskolin

Table 1. The four classes of adenylyl cyclase based on their biochemical properties

1.4.2.1. The structure of adenylyl cyclase

In the 1970s, AC from the rat renal medulla was successfully solubilised and partially purified (Neer, 1975). However, it wasn't until the late 1980s when Krupinski and colleagues (1989) purified, sequenced and cloned AC1 from bovine brain to reveal a protein with 12 transmembrane-spanning (TM) domains, two homologous ATP-binding regions and extensive NH_2 and COOH termini (Figure 6) (Willoughby and Cooper, 2007; Krupinski et al., 1989). To date at least nine isoforms of AC have been identified, cloned, and characterised (Iyengar, 1993; Sunahara et al., 1996; Hanoune et al., 1997; Simonds, 1999). ACs have two transmembrane domains termed TM1 and TM2 and two cytoplasmic domains; C1 and C2, which have important regulatory roles in all cells (Krupinski et al., 1989; Hurley, 1999; Zhang et al., 1997). The transmembrane domains are in tandem and are separated by the C1 domain. The interaction between C1 and C2 creates the catalytic core of AC (Hurley, 1999). AC has three nucleotide-binding sites and one Mg^{2+} binding site that are required for the conversion of ATP to cAMP upon activation. For the ATP molecule to bind to AC, Lys-923 and Asp-1000 on the C2 domain interact with N-1 and N-6 from the purine ring of the ATP molecule (Liu et al., 1997). These residues allow the AC to specifically interact with ATP as opposed to GTP (Tesmer et al., 1997). The two Mg^{2+} ions are most likely required to produce one cAMP molecule. The first allows for nucleophilic attack on the 3'-hydroxyl group of the ATP after mediating its deprotonation. The second helps to stabilise a transient ATP conformation that is produced from the nucleophilic attack. Following this, three residues Asn-1007, Arg-1011 and Lys-1047 mediate the release of the pyrophosphate group of the ATP molecule resulting in the production of cAMP (Zimmermann et al., 1998; Hurley, 1999). Additionally, Ludwig and Seuwen (2002) determined the gene structure of AC to be comprised of 11 – 26 exons, which were distributed over 16 – 430 kilobases (kb).

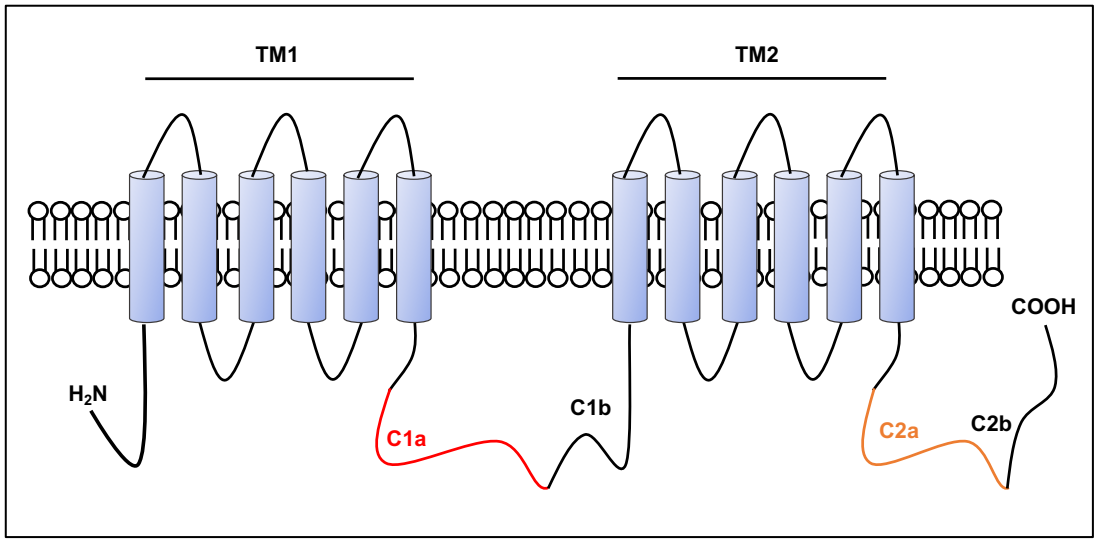

Figure 6. The structure of adenylyl cyclase

ACs have 5 major domains; the NH_2 terminus, the first transmembrane cluster (TM1, blue cylinders), the first catalytic loop comprised of C1a (red) and C1b (black), the second transmembrane domain (TM2, blue cylinders), the second catalytic loop containing C2a (orange) and C2b (black). The catalytic core is formed due to the dimerization of C1a and C2b upon Gαs activation. Figure and legend are modified from (Willoughby and Cooper, 2007).

The complex structure of AC is not characteristic of membrane-bound enzymes, it possesses a similar structure to that of transporters or ion channels. Although ACs appear to be related to a larger family of membrane transporters known as the ATP-binding cassette family of proteins based on their structure, they do not, however, possess an ATP-binding motif (Greenberger and Ishikawa, 1994). In addition to the unique structure, ACs showed significant homology to the sequences within both bacterial and yeast ACs, suggesting that eukaryotic and prokaryotic ACs share the same ancestral origin (Ishikawa and Homcy, 1997; Ludwig and Seuwen, 2002). To further add to the complexity of ACs, all AC isoforms are found on different chromosomes, these differences in chromosomal location even occur within the same class of AC, suggesting that each isoform must possess a different role (Ishikawa and Homey, 1997; Ishikawa and Homcy, 1997).

1.4.2.2. Regulation of Adenylyl Cyclase

The regulation of ACs is dependent on a variety of stimuli including intracellular calcium, protein kinases and G-proteins. In platelets, G-proteins can be either stimulatory ($G\alpha_s$) or inhibitory ($G\alpha_i$) and are responsible for mediating signalling pathways. The ligation of GPCR causes a conformational change whereby the α-subunit dissociates from the complex and a GTP molecule becomes bound, leading to the activation of $G\alpha_s$ (Smrcka, 2008). The $G\alpha_s$-GTP is proposed to move laterally within the confines of the membrane, where it binds to AC leading to its activation and cAMP synthesis (Godinho et al., 2015). All isoforms of AC are activated in response to $G\alpha_s$, including AC3 (human), AC5 (murine) and AC6 (human and murine) which are expressed in platelets. Additionally, IP (PGI_2 receptor), EP (PGE_2 receptor), A_{2A} and A_{2B} (adenosine receptors) are all coupled to $G\alpha_s$ and activate AC in platelets (Johnston-Cox and Ravid, 2011; Armstrong, 1996).

Inactivation of AC requires the deactivation of the $G\alpha_s$-GTP complex which is accomplished via GTP hydrolysis (Godinho et al., 2015). The α-subunits of G_i, G_z and G_o can inhibit specific isoforms of AC and the $\beta\gamma$ subunit of G-proteins can either be stimulatory or inhibitory depending on AC isoform (Table 2) (Sadana and Dessauer, 2009). The activation of the $G\alpha_i$ in platelets, triggered via ADP binding to its GPCR the $P2Y_{12}$ receptor, leads to the

selective inhibition of AC5 and AC6 (Godinho et al., 2015). The activation of ACs can also be controlled by calcium and calcium-bound calmodulin (CaM) (Willoughby and Cooper, 2007), although it is unclear if this is relevant to platelets. All isoforms of AC are inhibited by high non-physiological Ca^{2+} via competition for Mg^{2+} at the active site, but only AC5 and AC6 are inhibited by sub-micromolar concentrations of free Ca^{2+} (Cooper and Brooker, 1993; Guillou et al., 1999).

Class	AC isoform	Present in Platelets	G – protein		Protein kinases		Calcium
			Stimulatory	Inhibitory	Stimulatory	Inhibitory	
Class I	AC3	Human	$G\alpha_s$	$G\beta\gamma$	PKCα (weak)	CaMK II	↑ CaM
Class II	AC7	Human	$G\alpha_s$, $G\beta\gamma$	-	PKCα	-	-
Class III	AC5	Murine	$G\alpha_s$, $G\beta\gamma$	$G\alpha_{i, z}$	PKC (α, ζ)	PKA	↓ Free Ca^{2+}
	AC6	Human/ Murine	$G\alpha_s$, $G\beta\gamma$	$G\alpha_{i, z}$	-	PKA, PKC (α, e)	↓ Free Ca^{2+}
Class IV	AC9	Murine	$G\alpha_s$	-	-	PKC	↓ via calcineurin

Table 2. Regulation of adenylyl cyclases in platelets

Adapted from (Sadana and Dessauer, 2009). *CaMK = Calmodulin Kinase.

Protein kinases (A and C) have also been shown to regulate most ACs using insect cell lines (Iwami et al., 1995). Additionally, in smooth muscle (Murthy et al., 2002) and insect cell lines (Kawabe et al., 1994; Iwami et al., 1995; Chen et al., 1997), PKA serves as a feedback inhibitor and can regulate AC5 and AC6 through phosphorylation (Bauman et al., 2006). While PKC regulation can be stimulatory or inhibitory and the phosphorylation sites differ between AC isoforms, for example, certain isoforms of PKC (δ and ∈) have been shown to specifically inhibit AC6 (Kawabe et al., 1994). In addition, PKC has been shown to be stimulatory and PKA inhibitory for AC5, while PKA and PKC are both inhibitory for AC6 (Kawabe et al., 1994; Iwami et al., 1995), highlighting further differences between AC isoforms and their means of regulation. These protein kinase feedback mechanisms could maintain basal cAMP production by regulating AC activity, while differences in protein kinase phosphorylation of ACs remains unclear in platelets.

1.4.2.3. Adenylyl cyclase in other cell types

ACs are ubiquitously expressed across multiple cell types. AC6, in particular, has shown to be expressed in the brain, heart, kidney, liver and lung, among other potential tissues (Defer et al., 2000). Different isoforms of AC have distinct regulatory properties and may be differentially localised in each cell type (Hanoune and Defer, 2001; Cooper and Crossthwaite, 2006). The reason for multiple AC isoforms within the same cell is unclear, until recently, it was believed that the downstream consequences of cAMP synthesis were common to all isoforms of AC. However, studies now suggest that individual AC isoforms mediate distinct biological effects, often within the same cell, although this has yet to be established in platelets. In human embryonic kidney cells, AC6 specifically couples to IP_3R2 and regulates IP_3 sensitivity and actin polymerisation despite the presence of both AC2 and AC3 in the same cells (Zeiler et al., 2014). The most relevant cell model to platelets are vascular smooth muscle cells (VSMCs) which share many features of cAMP signalling with platelets, including PKA isoforms and their known protein targets (VASP, IP_3R1 and MYPT1). Overexpression of AC6, but not AC5, in rat VSMCs lead to VASP phosphorylation and inhibition of actin polymerisation (Nelson et al., 2011). In a separate study AC1, AC2, AC5 and AC6 were overexpressed to understand their relative roles in VSMC

proliferation (Gros et al., 2006b). Data demonstrated that AC6 was the predominant isoform driving cAMP synthesis, PKA-mediated signalling, and regulation of membrane potential in response to α-adrenoreceptor stimulation. Furthermore, only the siRNA knockdown of AC6 affected cAMP synthesis. Thus providing strong evidence for differential roles for specific AC isoforms, in directing the effect of intracellular cAMP in the regulation of vascular contractility in VSMCs (Gros et al., 2006a). In a study by Wong (2001), a global AC3 deficient mice displayed resistance to PGE_2-induced cAMP signalling that mediated growth inhibition of arterial smooth muscle cells (SMCs) suggesting that PGE_2 receptors could only couple specifically to AC3. Other studies now suggest that PGE_2 receptors can also couple to AC6 when overexpressed in rat arterial SMCs (Wong et al., 2001; Ostrom et al., 2002). The use of global deficient animal models can provide useful information for studying cAMP signalling in smooth muscle cells, but cell-specific models are required for further clarification of the specific roles of AC in cAMP signalling within different cell types, such as platelets.

1.4.2.4. Adenylyl cyclase in blood platelets

The expression of different AC isoforms in platelets was suggested by Hanoune and Defer (2001). In their 2001 review, it was proposed that the presence of AC2, along with ubiquitously expressed AC6 and AC7 were expressed in platelets through mRNA expression studies (Hanoune and Defer, 2001). More recent transcriptomic studies have suggested presence of AC3, AC6 and AC7 mRNA in human platelets, whereby AC3 was shown to be the most abundant. They also found differences in the murine transcriptome with AC9, AC6 and AC5 shown to be the most expressed AC isoforms in murine platelets (Rowley et al., 2011). In a more recent proteomic study, it was reported that AC3, AC5 and AC6 are expressed in human platelets with AC6 shown as the most predominant AC isoform, with a copy number of ~2500 per platelet (Burkhart et al., 2012) (Figure 7). The direct confirmation of which isoforms are present and their potential roles in platelet function is still lacking, but evidence suggests that AC6 is the predominantly expressed isoform in both human and murine platelets across three significant studies, suggesting that this is a key AC isoform in platelet biology (Hanoune and Defer, 2001; Rowley et al., 2011; Burkhart et al., 2012). Clinically,

dysfunction of AC is a major contributor to platelet resistance against $P2Y_{12}$ receptor antagonists in ACS patients (Imam et al., 2019), thereby highlighting an important role for AC in disease and respective treatments.

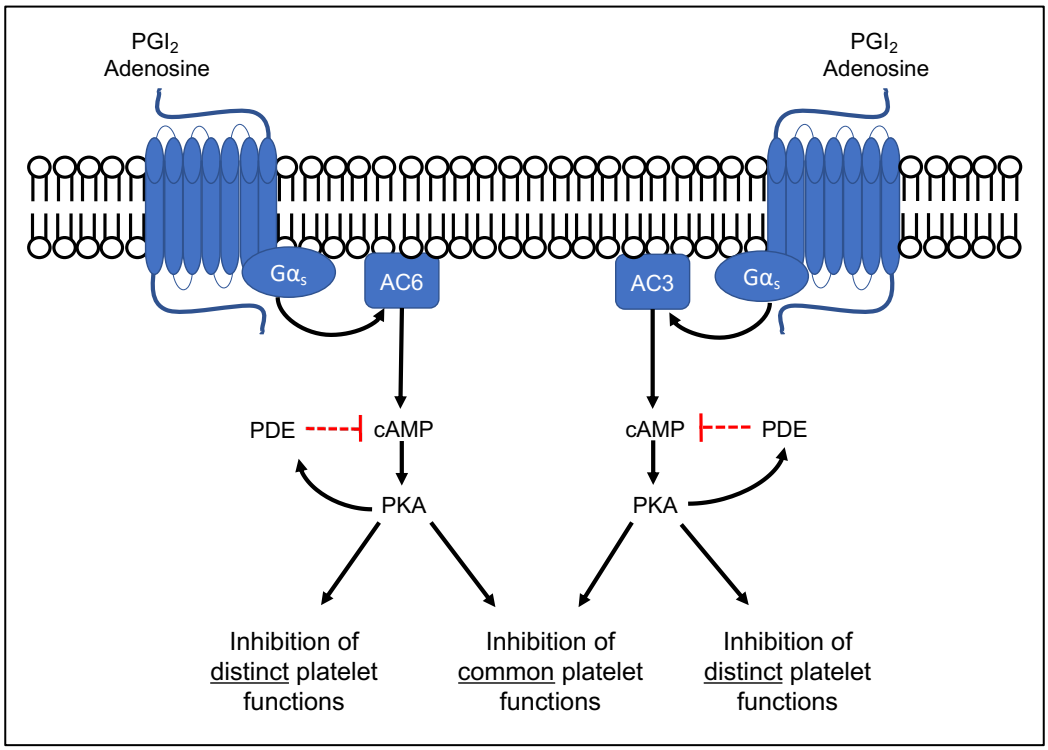

Figure 7. Schematic of cAMP signalling with AC isoforms in platelets

A simplified schematic of platelet cAMP signalling. Platelets are maintained at rest by cGMP and cAMP signalling pathways. PGI_2 or adenosine, bind to their receptors, leading to $G\alpha_s$ activation, which in turn activates adenylyl cyclase (AC6 or AC3). AC isoforms produce cAMP, leading to the activation of protein kinase A (PKA). PKA then phosphorylates specific substrates leading to the inhibition of platelet function(s). The levels of cAMP are maintained by PDEs.

1.4.3. Cyclic-AMP signalling

Cyclic-AMP activates a complex and dynamic signalling pathway that targets multiple aspects of platelet function (Figure 4). Critical to its effectiveness as a regulator of platelet function and haemostasis is the dynamic nature of the signalling events it controls. The cyclic nucleotide is generated through the activation of G-protein-coupled ACs in response to primarily PGI_2, but also to PGE_1 and adenosine. Increased cAMP leads to the activation of protein kinase A (PKA) isoforms, the primary effector of cAMP signalling in platelets (Figure 1). The holoenzyme of PKA is an inactive heterotetramer composed of two regulatory (R) and two catalytic (C) subunits. The binding of four cAMP molecules to their binding sites on R-subunits results in a conformational change unleashing the catalytic subunit and consequently the phosphorylation of adjacent protein substrates. Platelets express all the known isoforms of the regulatory and catalytic subunits (RIα, RIβ, RIIα, RIIβ, Cα, Cβ and Cγ) (Pidoux and Tasken, 2010; Burkhart et al., 2012), indicating that platelets likely possess multiple variations of the two PKA subtypes. Differentially localised in platelets PKA-I and PKA-II (Raslan et al., 2015b) have distinct biochemical properties which likely account for their broad targets. The phosphorylation of multiple substrates in response to cAMP elevating agents likely accounts for their ability to modulate platelet activity. To date sixteen substrates have been characterised in platelets by biochemical methods (Beck et al., 2014) and it is likely that there are many others, (Rivera et al., 2009) as proteomic studies suggests that over one hundred substrates may be present (Beck et al., 2014) (Table 3).

Increases in platelet cAMP is associated with reduced Ca^{2+} mobilisation, dense granule secretion, integrin ($\alpha_{IIb}\beta_3$) activation and aggregation *in vitro* (Graber and Hawiger, 1982) as well as, reduced platelet accrual at sites of vascular injury *in vivo* (Sim et al., 2004). Increased intracellular cAMP creates an activation threshold that ensures platelets remain in a quiescent state while still able to respond quickly to vascular injury. The constant opposition between activation and inhibition suggests that platelets should only become active when required, and the extent of activation is directly proportional to the relative amount of activatory stimuli. Unfortunately, this protective mechanism is abolished during diseases such as atherothrombosis (Yusuf et al., 2017),

yet the direct mechanisms behind this, remain unclear (Brass, 2003; Offermanns, 2006).

PKA substrate	Molecular Weight (kDa)	Role of phosphorylation in platelets	Reference
$G\alpha_{13}$	44	Inhibition of TxA_2-induced aggregation	(Manganello et al., 1999)
Inositol trisphosphate receptor (IP_3R)	260	Inhibition of Ca^{2+} release from intracellular stores	(Cavallini et al., 1996; El-Daher et al., 2000)
$VASP^{Ser157/Ser239}$	46-50	Inhibition of integrin $\alpha_{IIb}\beta_3$ activation	(Halbrugge and Walter, 1989)
Caldesmon	82	Inhibition of myosin and actin interaction	(Hettasch and Sellers, 1991)
$PDE3A^{Ser312}$	110	Activation of PDE3A to control cAMP levels	(Macphee et al., 1988; Hunter et al., 2009)
$RhoA^{Ser188}$	22	Inhibits RhoA membrane relocation and GTP loading	(Aburima et al., 2013)
$GPIb\beta^{Ser166}$	24	Inhibition of actin polymerisation and platelet vWF binding	(Wardell et al., 1989; Bodnar et al., 2002; Fox, 1985)
$GSK3\alpha^{Ser21}$/ $GSK3\beta^{Ser9}$	51 46	Inhibits glycogen synthase (GS) activity	(Beck et al., 2014; Fang et al., 2000)
$LASP^{Ser146}$	36	Reduces its ability to bind to F-actin	(Butt et al., 2003; Beck et al., 2014; Orth et al., 2015)
CalDAG-GEFI	72	Prevents CalDAG-GEFI-mediated Rap1b activation.	(Beck et al., 2014; Subramanian et al., 2013)

Table 3. PKA substrates and their phosphorylation role in platelets

1.4.3.1. Phosphodiesterases

To ensure optimal platelet function, the levels of intracellular cyclic nucleotides are controlled by a family of tightly regulated hydrolysing enzymes called phosphodiesterases (PDEs). Platelets contain three isoforms of PDE including PDE2, PDE3A and PDE5. PDEs act by hydrolysing cAMP and cGMP to 5-AMP and 5-GMP, respectively, thereby mediating signal termination (Moorthy et al., 2011). In platelets, PDE2 and PDE3A control the levels of cAMP while PDE5 controls the levels of cGMP (Haslam et al., 1999). PDE3A regulates cAMP via a cGMP-inhibited mechanism, whereas PDE2 works through a cGMP-stimulated mechanism (Figure 4). While PDE3A may be more abundant than PDE2 in platelets, inhibition of PDE2 resulted in a much higher increase of intracellular cAMP when compared with PDE3A inhibition (Manns et al., 2002). However, inhibition of PDE2 does not affect platelet function while inhibition of PDE3A leads to reduced platelet activation. Authors suggested that pools of cAMP may be localised and that different PDEs have the potential to regulate specific pools of cAMP. Inhibition of both PDE2 and PDE3A, however, resulted in synergism which demonstrated the importance of cGMP signalling regulating cAMP. Importantly, PDE2 has demonstrated dual specificity for both cAMP and cGMP, (Manns et al., 2002) recognising potential cross-talk between cAMP and cGMP signalling pathways (Weber et al., 2017).

PDE3 comprises two subfamilies, PDE3A and PDE3B, showing distinct and overlapping tissue and subcellular distributions (Conti and Jin, 2000; Shakur et al., 2001; Sun et al., 2007). PDE3A is more abundantly expressed in cells of the cardiovascular system whereas PDE3B is highly expressed in adipocytes, hepatocytes, and spermatocytes. Subcellular levels of PDE3 subtypes show distinct distributions and these differences may allow for differential regulation of PDE3 subtypes and could be important for cAMP compartmentalisation (Sun et al., 2007). Using genetically modified mice Sun et al (2007) showed that PDE3A plays a predominant role in regulating cardiovascular and platelet function.

The potent platelet activator, thrombin, and platelet secreted thrombospondin-1 (TSP-1) have also been shown to activate PDE3A to reduce intracellular cAMP (Gachet et al., 2006; Zhang and Colman, 2007; Roberts et al., 2010;

Aburima et al., 2021). Additionally, the elevation of cAMP levels is regulated by the opposing activity of both ACs and PDEs (Hunter et al., 2009), therefore an imbalance in this dynamic system can have profound effects on platelet function, which has been shown in congenital disorders whereby cAMP production is implicated (Van Geet et al., 2009). Additionally, the ability of cAMP to inhibit platelet activation has been exploited in the development of anti-platelet drugs such as dipyridamole, which works by inhibiting these PDEs that would typically degrade cAMP (Brass, 2003).

1.5. Remaining questions

PGI_2 remains the most potent endogenous inhibitor of platelets that has been identified and therefore plays a key role in regulating haemostasis and thrombosis. Given that ACs are critical to this regulatory haemostatic mechanism, the specific role of individual AC isoforms in platelets needs further exploration as the specific role of different AC isoforms and their downstream effects remains unclear. AC3 and AC6 are both expressed in human platelets but are differentially regulated, with the regulation of ACs differing between classes and even between isoforms within the same class. Further suggesting that AC isoforms have differential roles in response to different regulatory stimuli, which could potentially have differing downstream signalling effects on certain aspects of platelet function.

The compartmentalisation of cAMP in platelets is another aspect of cAMP signalling that requires further understanding. In different cell types, the enzymes involved in generating, propagating and terminating the cAMP signal are typically organised into restricted microdomains that focus the activity of cAMP signalling to specific downstream substrates (Tasken and Aandahl, 2004; Scott and Pawson, 2009; Zaccolo, 2011). The compartmentalisation of cAMP signalling events allows for specific control of distinct cell functions in response to different stimuli (Zaccolo, 2009; Zaccolo, 2011; Lefkimmiatis and Zaccolo, 2014). Importantly, in platelets, cAMP signalling is spatiotemporally controlled by the opposing effects of AC and PDE isoforms, and scaffolding proteins called A-kinase anchoring proteins (AKAPs) (Raslan et al., 2015a; Raslan, Z. and Naseem, K.M., 2015; Zaccolo et al., 2021). The cAMP signal

is constrained to specific regions of the cell where individual isoforms PKA interact with AKAPs to direct PKA activity to specific substrates.

In a study by Raslan et al (2015), it was shown through subcellular fractionation and immunostaining that PKA-I and PKA-II are differentially localised in platelets. It was reported that PKA-I was primarily found in the cell membrane while PKA-II resides in the cytosol. AC5, AC6 and PKA-I, but not PKA-II were shown to be localised to membrane microdomains in platelets where lipid rafts act to constrain PKA activity, thus further confirming compartmentalisation of cAMP signalling in platelets (Raslan et al., 2015a). PDEs are critical regulators of cAMP levels within platelets, they are considerably diverse and like cAMP, could also undergo compartmentalisation within the cell (Manns et al., 2002). It is therefore possible that different PDEs could co-locate with specific AC isoforms to play a role in regulating local or global cAMP levels in platelets. To add to the complexity of an already complex signalling pathway, different isoforms of AC could generate specific pools of cAMP, that activate distinct PKA isoforms, resulting in specific downstream phosphorylation events that alter platelet function. The different roles and relative contributions of these cAMP pools, PKAs, PDEs and AC isoforms to the inhibition of specific platelet functions are still lacking and require further investigation. However, due to the lack of reliable antibodies and the ability to perform siRNA knockdown in platelets, studying such a complex system requires the use of platelet-specific knockout animal models to identify the specific roles of AC and their isoforms, in platelet cAMP signalling.

1.6. Scope of study

The cAMP signalling cascade represents a major inhibitory pathway that controls platelet function, haemostasis and thrombosis and our understanding of its specific regulation is limited. The role of AC needs further exploration, as little is known about the specific downstream effects of AC production of cAMP and the phosphorylation events leading to platelet inhibition. Platelet hyperactivity is a typical phenotype associated with atherothrombotic disease (Berger et al., 2020). The protective mechanisms that typically control platelet activity are overcome in cases of atherothrombotic disease, but the reasons

remain unclear. Platelet hyperactivity is likely due to a reduction in intracellular cAMP levels which has been linked to activation of PDE3A, reduced platelet sensitivity to PGI_2 and IP receptor desensitisation (Fisch et al., 1997; Bunting et al., 1983; Berger et al., 2020). Though, IP receptor desensitisation has been shown to be reversible (Fisch et al., 1997) therefore, an alternative hypothesis for reduced sensitivity to PGI_2 and platelet hyperactivity, could be due to a loss of function or downregulation of AC activity, in particular, AC6, allowing platelet activation to outweigh platelet inhibition. AC6 expression could be a possible marker for platelet hyperactivity and potential cardiovascular events. The success of AC6 gene transfer clinical trial in heart failure patients led by the Hammond laboratory (Hammond et al., 2016) highlights the importance of AC6 and how potential upregulation of AC6 can have a positive effect in heart failure patients, bringing into question whether this could be the case in platelets. In addition, a recent study by Imam and colleagues (2019), highlights the importance of functional AC with the responsiveness to $P2Y_{12}$ receptor antagonists in ACS patients, indicating that AC activity could be implicated in disease and it's treatment.

Understanding the role of AC6 in platelet function, thrombosis and haemostasis could provide insight into how platelets become hyperactive in atherothrombotic disease and whether AC6 could be a potential therapeutic target.

1.6.1. Aims of study

The overall objective of this study was to establish the role of AC6 in murine platelet function, haemostasis, and thrombosis. The strategy for this study is shown in Figure 8.

1. Develop a novel platelet-specific AC6 knockout mouse model
2. Functionally characterise the AC6-KO mouse
3. Understand the relative contribution of AC6 to platelet cAMP signalling

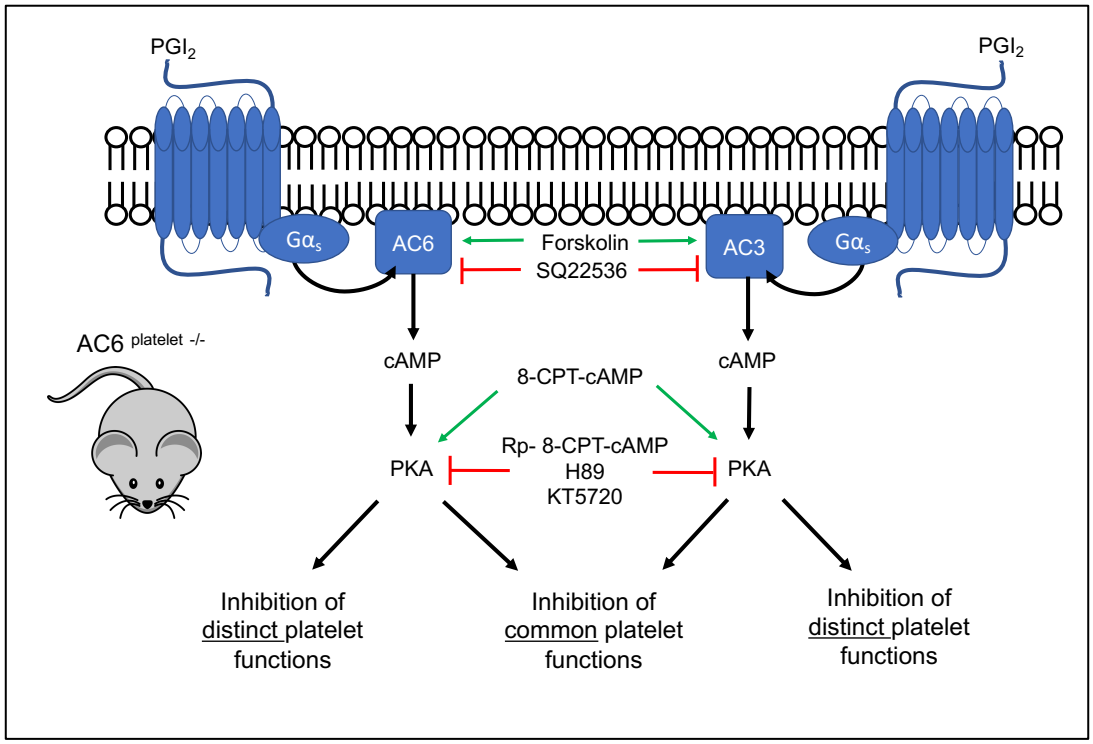

Figure 8. Strategy to assess the role of AC6 in platelet function

To assess the role of AC6 in platelet function we have a variety of tools available. A platelet specific AC6-KO mouse, SQ22536 an AC inhibitor, RP-8-CPT-cAMP, H89 and KT5720 which are direct PKA inhibitors, forskolin which is an AC activator and 8-CPT-cAMP which is a direct PKA activator. Together, these agents should allow us to identify the role of AC6 in platelet function.

Chapter 2
Methods & Materials

2.1. Reagents

2.1.1. Chemicals and reagents

Sodium Citrate (367691), ACD-A (8304451), Sodium Heparin BD Vacutainer Tubes (8516324) and BD Phosflow Lyse/Fix Buffer 5X (558049) were from BD Biosciences. The DC Protein Assay Kit (5000112) was from Bio-Rad. PAR1 (60679) and PAR4 (60218-1) (Protease-activated receptor) agonists were from Anaspec. Collagen-related peptide (CRP-XL) was from CambCol Laboratories. Collagen Reagens HORM® suspension (1130630) was from Takeda. Prostaglandin I2 (sodium salt) (61849-14-7), Prostaglandin E1 (745-65-3) and Forskolin (66575-29-9) were from Cayman Chemical. The Amersham cAMP Biotrak Enzyme immunoassay (EIA) system (RPN2551) was from Cytiva. VersaComp Antibody Capture Bead Kit (B22804) was from Beckman Coulter Life Sciences. 4% Paraformaldehyde Aqueous Solution (157-4) was from Electron Microscopy Sciences. S-Nitrosoglutathione (GSNO) (57564-91-7) and 8-CPT-cAMP (93882-12-3) were from Santa Cruz Biotechnology. SQ22536 (17318-31-9) and H89 Dihydrochloride (127243-85-0) were from Calbiochem. 8-CPT-cAMP (93882-12-3) and RP-8-CPT-cAMP (129735-01-9) were from Biolog Life Sciences. KT 5720 (108068-98-0) was from Merck. Restore Western Blot Stripping buffer (46430), SuperSignal West Pico Plus Pierce ECL (32106), TaqMan™ primers and TaqMan™ Fast Advanced Master Mix (4444556) were from Thermo Fisher Scientific. The Reverse Transcription System (A3500) was from Promega. All other reagents were from Sigma-Aldrich.

2.1.2. Antibodies

Annexin V APC Ready Flow conjugate (R37176) and Rabbit Anti-sheep IgG (H+L) Secondary Antibody HRP (31480) were from Invitrogen. BB700 Mouse Anti-Human CD42b (742219), APC Mouse Anti-Human CD42b (551061), FITC Mouse Anti-Human PAC-1 (340507), PE Mouse Anti-Human CD62P

(555524), PE Mouse IgG1 κ Isotype Control (556650), FITC Rat IgG isotype control (553995), FITC Rat Anti-mouse CD62P (553744), BB700 Rat Anti-mouse CD41 (742148), FITC Hamster Anti-rat CD49b (554999), Hamster IgG2 λ1 Isotype control (553964), FITC Rat Anti-mouse CD41 (553848), FITC Rat IgG1 κ (553924), FITC Hamster Anti-mouse CD61 (553346), and FITC Hamster IgG1 κ (553971) were all from BD Biosciences. PE Hamster Anti-mouse CD36 (102606) and PE Hamster IgG Isotype control (400908) were from Biolegend. PE Rat Anti-mouse JON/A (M023-2), FITC Rat Anti-mouse CD42b (M040-1), FITC Rat Anti-mouse CD49b (M071-1), FITC Rat Anti-mouse GPVI (M011-1) and FITC Rat IgG (P190-1) were from Emfret. Sheep Anti-PDE3A phospho Ser 312, Sheep Anti-PDE3A phospho Ser 465 and Sheep Anti-PDE3A were from the MRC Protein Phosphorylation and Ubiquitylation Unit, University of Dundee. Rabbit Anti-Phospho-VASP Ser157 (3111S), Rabbit Anti-Phospho-VASP Ser239 (3114S), Rabbit Anti-Phospho-PKA substrates (RRXS/T) (9624S), Rabbit Anti-Phospho-GSK3β Ser9 (9336S), Rabbit Anti-GAPDH (2118S), Rabbit VASP (3132S) and Rabbit Anti-β-tubulin (15115S) were from Cell Signalling Technology. Mouse Anti-Adenylate cyclase (sc-377243), Mouse Anti-Adenylyl cyclase 5/6 (sc-514785) and Mouse IgG_{2b} binding protein-HRP (sc-542741) antibodies were from Santa Cruz Biotechnology. Sheep Anti-mouse IgG HRP-linked (NA931) and Donkey Anti-rabbit IgG HRP-linked (NA934) were from Cytiva.

2.2. Methodologies used in the preparation of platelets from human whole blood

2.2.1. Procurement of human whole blood

Blood was obtained by trained phlebotomists from healthy volunteers in accordance with the declaration of Helsinki (Ethics Code: MREC19-006). All donors were consenting, presenting healthy and confirmed they had not taken any medication that could interfere with or affect platelet function.

Venepuncture was performed using a 21G-butterfly needle and the first 2 mL collected was discarded to avoid any artificial activation of platelets. Blood was collected into 8.5 mL acid citrate dextrose (ACD) vacutainers for washed

platelet studies or 4.5 mL sodium citrate vacutainers for the use of whole blood or PRP.

2.2.2. Procurement of whole blood from clinical samples

Blood was obtained from two patient cohorts: age-matched controls and patients with acute coronary syndrome (ACS) post-myocardial infarction (MI) in line with the declaration of Helsinki (IRAS code: 219491). Venepuncture was carried out as described in 2.2.1. Patient info displayed below (Table 4).

Parameter	Control	ACS
Age	56.1 ± 9.0	60.6 ± 9.0
Females	10	1
Males	5	6

Table 4. Patient parameters.

Clinical samples from the ACS patient study included n=7 (ACS) and n=15 (age-matched controls).

2.2.3. Isolation of platelets from human whole blood by lowering blood pH

Platelets were isolated using a reduced pH method, whereby the pH of the plasma is reduced to 6.4 by using a citric-acid based wash buffer, thus preventing any platelet activation during centrifugation (Mustard et al., 1989). Unlike prostaglandin-based methods of platelet isolation, pH-lowering methods avoid activation of cyclic-nucleotide signalling cascades and therefore maintain platelet sensitivity to cyclic nucleotide-elevating agents, which were used throughout this study.

Whole blood was centrifuged at 100 x *g* for 20 minutes at room temperature (RT) to obtain platelet rich plasma (PRP). The PRP was then transferred into a sterile 15 mL falcon tube and the plasma pH was reduced to 6.4 via addition of citric acid (0.3 M) at a ratio of 1:50. The PRP was then centrifuged at 1000 x *g* with 1 brake for 10 mins at RT to obtain a platelet pellet and platelet poor plasma (PPP). The PPP was discarded, and the pellet was resuspended in 5 mL of wash buffer (5 mM glucose, 5 mM KCl, 9 mM NaCl, 10mM EDTA, 36 mM citric acid, pH 6.4). The platelet suspension was then centrifuged again

at 1000 x *g* with 1 brake for 10 mins at RT to remove any residual plasma. The final pellet was re-suspended in 1 mL of Modified Tyrode's buffer (0.5 mM $MgCl_2$, 0.55 mM NaH_2PO_4, 2.7 mM KCl, 5 mM HEPES, 5.6 mM glucose, 7 mM $NaHCO_3$, 150 mM NaCl, pH 7.4) and counted using a Beckman Coulter Z1 particle counter.

2.2.4. Isolation of human washed platelets by PGI_2

In some cases, to compare isolation methods, platelets were isolated using the prostacyclin (PGI_2) method of isolation (Vargas et al., 1982) whereby the addition of prostacyclin prevents any platelet activation during centrifugation.

Platelet isolation method is as described in 2.2.3 except PGI_2 (200 µM) was added to the PRP give a final concentration of 200 nM (1:1000) and the platelet pellet after PPP discard was resuspended in Modified Tyrode's buffer (4 mL) and ACD (0.5 mL), along with the addition of PGI_2 (200 µM; 1:1000). Platelets were then rested for at least 30 minutes prior to usage to ensure recovery from cAMP stimulation.

2.3. Methodologies used in the preparation of platelets from murine whole blood

2.3.1. Procurement of murine whole blood

Under the authority of a United Kingdom Home Office approved project licence (Professor Khalid Naseem – PP0499799 and Professor Robert Ariens – PP9539458) and my personal licence (Miss Bethany Webb - I774212DC) mice were anesthetised under 2% constant inhalation of isoflurane (with oxygen). Blood was collected via the inferior vena cava using a 25G needle containing 200 µL of ACD (113.8 mM D-glucose anhydride, 29.9 mM Trisodium Citrate, 72.6 mM NaCl, 2.9 mM Citric acid). A volume of up to 1 mL of blood including ACD was collected into a 2 mL Eppendorf tube containing 200 µL of Modified Tyrode's buffer before isolating platelets.

2.3.2. Isolation of platelets from murine whole blood

Whole blood was transferred to a clean falcon tube diluted with addition of up to 500 µL of Modified Tyrode's Buffer to reduce risk of artificial platelet

activation. The blood was centrifuged at 100 *x g* for 5 min at RT to obtain PRP. The PRP was removed and transferred to a clean 15 mL falcon tube. The remaining red blood cells were then diluted via the addition of 500 µL of Modified Tyrode's buffer and centrifuged at 100 *x g* for a further 5 min. The PRP was then removed and added to the PRP that was collected originally. The total PRP was centrifuged at 1000 *x g* for 6 min at RT to obtain platelet pellet and PPP. The PPP was removed, and the platelet pellet was resuspended in 250 µL Modified Tyrode's buffer and counted using the Beckman Coulter Z1 particle counter.

2.3.3. Quantification of human and murine platelet counts

Platelet quantification was performed using a Beckman Coulter Z1 particle counter. Isolated washed platelets (WP) were diluted 1/2000 (5 µL in 10 mL) of isotonic buffer (Beckmann Coulter) and counted. The Coulter counter analyses particles between 2-7 µm in diameter using a 50 µm aperture. The count is automatically multiplied by 2000 to account for the dilution factor, the count of platelets was expressed as platelets/mL. Platelets were then diluted using Modified Tyrodes buffer to the desired count depending on requirement of the experiment (Equation 1).

$$\left(\frac{actual\ count}{count\ required}\right) * \ actual\ volume \ = \ volume\ to\ adjust$$

Equation 1. Calculation for platelet count dilutions

Equation used to calculate the volume of buffer required to adjust platelet count per experiment.

2.4. Assessment of platelet function

2.4.1. Light transmission platelet aggregometry

Platelet aggregation plays a vital role in thrombosis and is the final stage in a series of chemical and biophysical events that take place in platelets after activation (Ruggeri, 2002; Ruggeri and Mendolicchio, 2007; Jackson, 2007).

Light transmission aggregometry (LTA) was developed by Gustav Born in 1962, which allows for functional responses of washed platelets and PRP to be assayed (Born, 1962). The turbidimetric assay is based on changes in light scattering through a platelet suspension which is detected by a photocell. It assumes that when small volumes of resting platelets are stirred, they are homogenously distributed in the suspension allowing for an optically dense medium that is refractory to the passage of light. Upon platelet activation by agonist stimulation, the formation of aggregates disrupts the homogeneity of the suspension. This allows a greater amount of light to pass through the suspension depending on the size of the aggregates, therefore more light transmission. The extent of light transmission is proportional to the level of platelet aggregation, which in turn is dependent and an indicator of the level of platelet activation (Figure 9 A). Before aggregation, platelets also undergo shape change observed on the trace as a momentary decrease in light transmission (Figure 9 B).

Washed platelets (human; $2.5x10^8$ platelets/mL, murine; $2x10^8$ platelets/mL) were pre-incubated under constant stirring (800-1000 rpm) for 1 min at 37˚C to allow for temperature equilibrium. After the addition of a stimulus such as collagen (1 – 10 µg/mL) or thrombin (0.01 – 1U/mL), aggregation was monitored for up to 10 minutes using a multi-channel aggregometer (AggRAM or Chronolog). In some cases, platelets were treated with inhibitors such as PGI_2, GSNO, forskolin or 8-CPT-cAMP before addition of an agonist. The aggregometer was calibrated for every sample using untreated WP as 0% aggregation and Modified Tyrode's buffer as 100% aggregation.

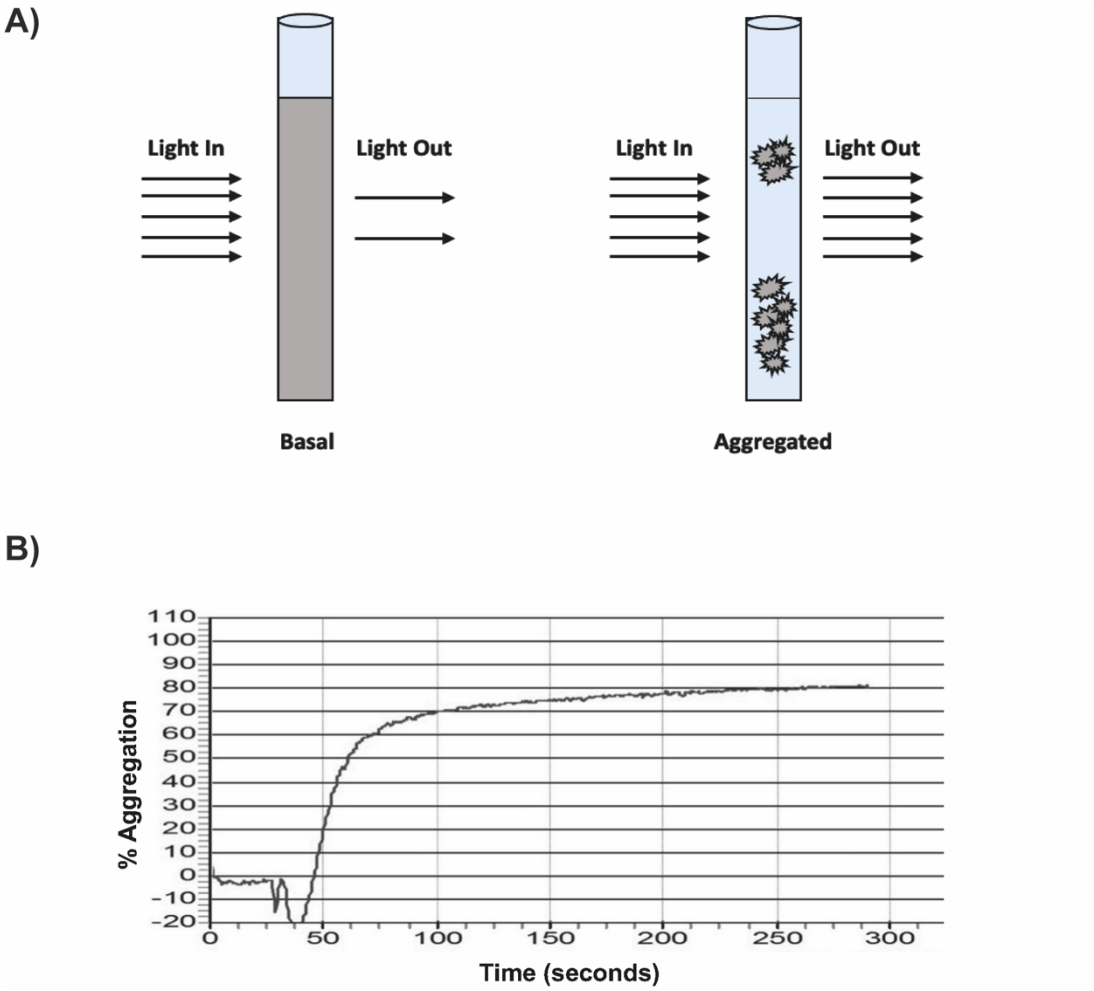

Figure 9. The general principle of platelet light transmission aggregometry

Resting platelets in suspension display a turbid solution where light cannot pass through. However, aggregation occurs upon stimulation with agonists, allowing light transmission through the cuvette (A). The extent of light transmission is proportional to the level of aggregation and, therefore, activation. Example trace generated by aggregometer during platelet aggregation upon agonist stimulation (B).

2.4.2. Flow cytometric analysis

Fluorescent flow cytometry (FFC) is a technique used for analysing individual cells within a population and is commonly used to assess platelet activation. FFC uses instrumentation that directs a single stream of cells past a light source and measures the resulting scatter and emission of light energy in various wavelengths. A flow cytometer uses excitation lasers paired with emission detectors to assess cells based on size and granularity, but also fluorophores that can be introduced against specific target proteins. This allows cellular populations, protein content, or the phosphorylation/cleavage stage of proteins to be analysed quantitatively (Cossarizza et al., 2017). The general principle of a flow cytometer is the capability of sheath fluid under pressure to force a suspension of cells or particles into a linear core and was first described by Crosland-Taylor (1953) as a method of counting particles within the suspension.

In modern flow cytometry analysis, fluorescent antibodies or dyes can be used with different excitation and emission characteristics to enable multiple readouts from a single cell. Forward scatter gating refers to the size of the cell, and side scatter gating relates to the complexity or granularity of the cell. A combination of forward and side scatter gating is used primarily to identify cells in a cell population and is confirmed using fluorescent antibodies (Figure 10).

To determine the expression of platelet activation markers, platelets were initially gated based on their physical properties, and 10,000 events were analysed for mean/median fluorescence intensity. To further establish that data was representative of the platelet population, we then gated on a platelet specific marker (e.g., CD41 or CD42b), ensuring that gates were adjusted until >95% of the gated population were stained positive for the desired platelet marker (Figure 10).

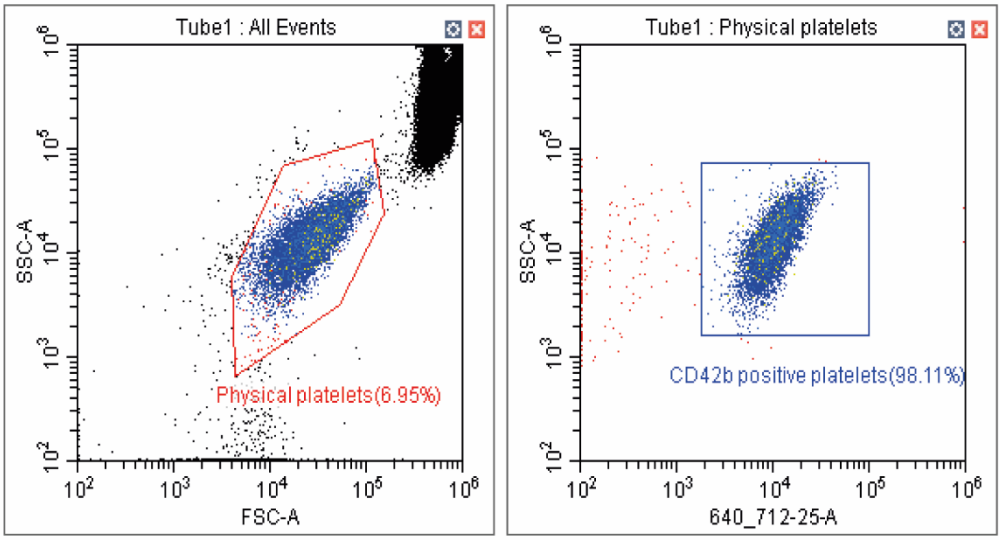

Figure 10. Example of platelet gating on a flow cytometer

Platelets can be gated for either physical characteristics based on FSC and SSC (left) or by CD42b positive cells (right). CD42b-BB700 was used to generate the positive platelet gate.

2.4.2.1. Platelet activation by flow cytometry

Platelet activation is shown by a right shift on histograms generated in CytExpert (Figure 11). This indicates greater fluorescence, which is directly proportional to antibody/dye binding and, therefore, protein expression. Data is typically presented as percent positive, mean/median fluorescence intensity (MFI) or fold over basal. Percent positive represents the percentage of cells in the platelet positive population stained or positive for the desired antibody or dye. This is generated by setting a background fluorescence of 2% on an IgG isotype control or fluorescence minus one (FMO) control. Based on this, any fluorescence that exceeds 2% is considered a positive signal, thus positive for the marker (Metcalfe et al., 1997). In contrast, MFI is the total reading of signal and represents the shift in fluorescence within the positive population of cells. Fold over basal also uses MFI; however, all data is normalised to basal preventing any comments on changes in basal activity. A combination of both percent positive and MFI present a more in-depth analysis of the data and is the preferred method of data presentation.

In this study, the expression of antigens on the surface of platelets was determined using both three-parameter and four-parameter assays to allow for simultaneous measurements of different surface antigens upon platelet activation. Flow cytometry can provide simple, single-targeted readouts or complex subpopulation phenotyping and cell signalling analysing, adding to its highly versatile and quantitative application (Cossarizza et al., 2017). Whole blood flow cytometry (Abrams and Shattil, 1991; Metcalfe et al., 1997) was primarily used throughout this study, but PRP or washed platelets were also explored, depending on assay requirements.

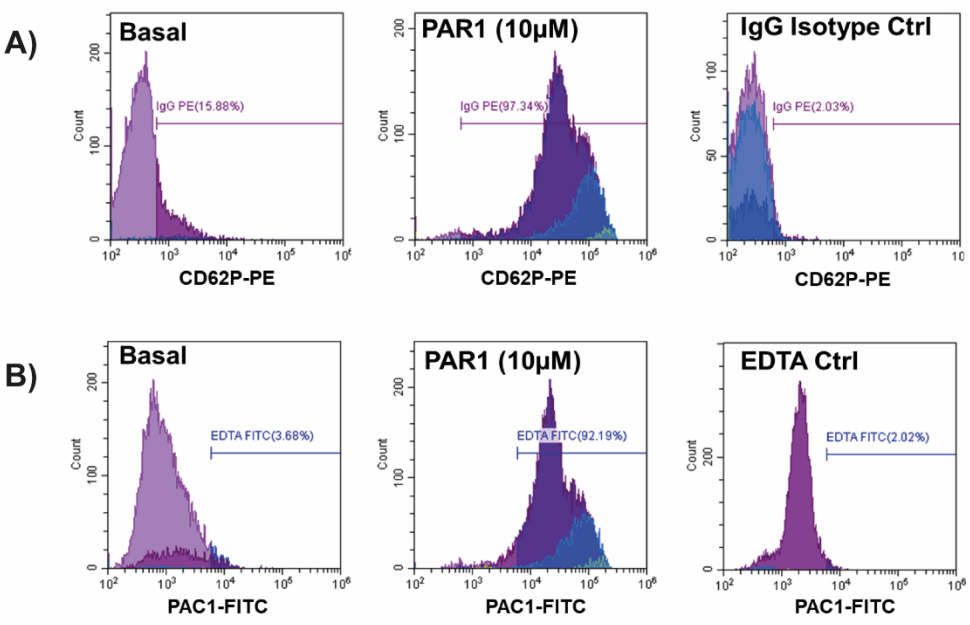

Figure 11. Representative histograms of platelet activation by flow cytometry

Histogram plots demonstrate the total fluorescence of the positive population; a shift towards the right shows an increase in fluorescence based on platelet activation. The percentage shift over control (2% of control fluorescence; horizontal line) can be plotted for comparison of PAR1 peptide treatments.

Whole blood, PRP or washed platelets were incubated with platelet agonists (CRP-XL, Convulxin, PAR1 or PAR4 peptide) and fluorescently labelled conjugates for specific surface antigens. A constitutive platelet marker (e.g., CD42b or CD41) stained the positive platelet population and inducible markers that bind to CD62P, fibrinogen, PAC1 or Annexin V were also used. CD62P is a marker that binds to P-selectin on the surface of activated platelets and is a marker for α-granule secretion (Holmsen, 1989; Kappelmayer et al., 2004). The anti-fibrinogen antibody binds to fibrinogen to analyse integrin activation (Kasahara et al., 1987), while PAC1 binds to the active conformation of $\alpha_{IIb}\beta_{3,}$ providing an alternative measurement for integrin activation (Shattil et al., 1985). The Annexin V (AnnV) conjugate binds to phosphatidylserine (PS) on the surface of activated platelets in a calcium-dependent manner. PS exposure can indicate a pro-coagulant or an apoptotic subpopulation of platelets (Gilbert et al., 1991; Fadok et al., 1992; Tait et al.,

1999). Activated platelets bind to these surface markers and thus, can be distinguished from resting platelets according to their fluorescent intensity.

2.4.2.2. Sample preparation for flow cytometric analysis

Freshly obtained citrated blood, PRP, or washed platelets ($5x10^8$ platelets/mL) were diluted in Modified Tyrode's buffer containing an antibody cocktail. Agonists were added, mixed, and left for 20 mins at RT in the dark. Samples were then fixed with 1% (v/v) paraformaldehyde and left for 10 mins to ensure fixation of cells. Cells were then analysed by flow cytometry using a CytoFLEX cytometer (Beckmann Coulter). In some cases, samples were fixed using 1.25x PhosFlow Fix/Lyse buffer (BD Biosciences) to lyse red blood cells.

Negative controls containing citrated blood, PRP or washed platelets, Modified Tyrode's buffer, and an IgG isotype control or EDTA (3 mM) were also prepared. EDTA was used to chelate calcium ions, preventing fibrinogen binding to $\alpha_{IIb}\beta_3$ and AnnV binding to PS.

In some cases, samples were incubated with PGI_2 prior to the addition of agonists and/or Gly-Pro-Arg-Pro (GPRP; 50 mM) was added to each sample to prevent clot formation by inhibiting fibrinogen polymerisation (Adelman et al., 1990; Michelson, 1994). Where AnnV was used, samples were re-calcified to ensure PS exposure could occur. In cases where whole blood was pre-treated, 10 µL of blood containing an inhibitor was added to the antibody cocktail, agonist, and Modified Tyrode's mix. An example experimental design is demonstrated in Table 5.

Condition	Modified Tyrodes (µL)	Platelet prep (µL)	Antibody mix (µL)	Agonists (µL)	Control Antibodies (µL)
Basal	40	5	5	0	0
Stimulated	35	5	5	5	0
Control	35	5	0	5	5

Table 5. Example experimental design for flow cytometry assays

Using a total volume of 50 µL, platelet preparation, antibodies and 10x agonists were added to the appropriate amount of Modified Tyrode's buffer. Modified Tyrode's buffer volume can be adjusted based on experimental design to account for additional inhibitors or larger volumes of antibodies.

2.4.2.3. Compensation

Upon using multi-parameter flow cytometry, it was essential to compensate for spectral overlap between fluorophores to avoid misinterpretation of the data. Compensation ultimately is a calculation to subtract fluorescence detected outside the target fluorophore emission.

Compensation experiments can be performed using antibody binding beads or cells. Individual tubes containing beads or cells and a single fluorophore are compared to an unstained control. Each tube is analysed separately to calculate the extent of bleeding of each fluorophore into the adjacent channels. Using CytExpert, a compensation matrix can be generated and applied to appropriate flow cytometry assays. The compensation matrix is specific to the fluorophores, gains, and spectral characteristics for the particular cytometer on which it was performed. If any of these aspects change, a new compensation matrix is required.

Beckmann Coulter VersaComp beads were stained with FITC, PE, APC, and BB700 or AF700 depending on the panel design. Each fluorophore was run separately to produce a compensation matrix which was calculated automatically by the compensation calculator within CytExpert. The compensation matrix generated can then be applied to experiments under the same conditions.

2.4.2.4. Platelet counting in whole blood by flow cytometry

Platelet counts in whole blood can be assessed via flow cytometry by diluting 5 µL of blood with 45 µL of stain mix. This mix contains an antibody which targets a platelet marker (e.g., CD41, CD42b or CD61). By adding 450 µL of PBS, the 1/100 dilution factor was maintained. Samples were then run at a low acquisition rate (10 µL / minute) for 2.5 minutes, allowing for platelet positive events/ µL to be calculated as shown in Equation 2.

$$Platelet\ positive\ events/\mu L\ of\ whole\ blood\ = \left(\frac{platelet\ positive\ events}{25}\right) * 100$$

Equation 2. Used to calculate platelet positive events / µL whole blood.

Samples were un at a low acquisition rate of 10 µL / minute for 2.5 minutes, giving a total volume of 25 µL read by the cytometer. The amount of platelet positive events, e.g., CD42b+, is then divided by 25 and multiplied by 100 to account for volume and dilution factor.

2.4.2.5. Assessment of reticulated platelets by flow cytometry

Immature platelets, known as reticulated platelets, can be analysed by flow cytometry using Rectic-COUNT™ reagent, using the Thiazole orange (TO) approach. TO is a nucleic-acid-specific dye that enters cells directly; when it binds to RNA or DNA, causing an increase in fluorescence. Immature platelets contain residual amounts of RNA and therefore differ from mature platelets, allowing for the identification of reticulated platelets.

Whole blood (10 µL) was added to Rectic-COUNT™ reagent (1 mL), mixed and left for 30 minutes in the dark at RT before flow cytometry analysis. An unstained sample, whereby whole blood was added to Phospho-Buffered Saline (PBS), was also run to account for background fluorescence. Platelets were gated based on physical properties for 10,000 events.

2.4.2.6. Phosphoflow cytometry

In addition to traditional flow cytometry techniques, we also used phosphoflow cytometry, a novel method that analyses the phospho-proteome by flow cytometry (Oberprieler and Tasken, 2011). It is a high throughput technique that can be used to assess intracellular signalling and can be applied to platelets (Spurgeon et al., 2014). Traditionally, phosphorylation events are evaluated via immunoblot and immunoprecipitation techniques, providing a total measurement of phosphorylation in the entire cell population. Phosphoflow cytometry allows us to analyse each cell as an individual event. Flow cytometry methods are high throughput and only require a small amount of starting sample, whereas immunoblotting techniques require larger volumes and can take over a day to process. Phosphoflow allows us to use freshly drawn whole blood, negating the need for isolating platelets, which traditional immunoblotting requires. This method uses permeabilisation of the cells to allow the entry of phospho-specific antibodies into the high throughput system (Spurgeon, B.E.J. and Naseem, 2018).

Whole blood (20 µL) was treated with increasing concentrations of PGI_2 (1 – 1000 nM) for 2 min and then fixed using PhosFlow Fix/Lyse buffer (BD Biosciences) according to manufactures instructions. Platelets were then pelleted by centrifugation at 1000 *x g* at 4°C for 10 mins. Supernatants were removed, and the remaining cells were permeabilised using ice-cold Triton X-100 (0.1%) in PBS for 10 mins at RT. Before incubation, cells were mixed by pipetting 20x, avoiding aeration. Permeabilised cells were pelleted (1000 x g; 4°C; 10 mins), washed with PBS and incubated with phospho-specific primary antibodies (p-PKA substrates, p-VASP^{Ser157} and p-VASP^{Ser239}; 1 µg/mL) for 30 mins at 4°C. After antibody incubation, cells were washed with PBS and incubated further with a fluorescently conjugated secondary antibody (Anti-Rabbit-PE; 1 µg/mL) in the dark for 30 mins at 4°C. After a final wash with PBS, cells were analysed by flow cytometry. Platelets were gated by physical characteristics at 10,000 events. In some cases, a platelet marker (CD41) was used to identify the platelet population.

2.4.3. Assessment of platelet spreading *in vitro*

In response to activation, quiescent, discoid platelets undergo a series of morphological changes that include rounding, generation of filopodia, actin nodules, lamellipodia and formation of stress fibres (Siess, 1989; Wurzinger, 1990; Morgenstern, 1997). These morphological changes can be visualised using static platelet spreading protocols and fluorescent microscopy.

2.4.3.1. Platelet spreading methodologies

Coverslips were incubated with either fibrinogen (100 µg/mL) or Collagen (50 µg/mL) overnight at 4°C, washed with PBS and blocked with BSA (5 mg/mL) for 1 hr a RT. Washed platelets (1-2 x 10^7 platelets/mL) were adhered to immobilised proteins for up to 60 minutes at 37°C in the presence or absence of PGI_2 (10-100 nM). At the required time point, the platelets were fixed with paraformaldehyde (4%) for 10 minutes, lysed with Triton X-100 (0.1%) and stained with FITC- or TRITC-phalloidin. Coverslips were mounted to slides using ProLong™ Diamond Antifade Mountant (Invitrogen) and visualised using Zeiss Axio Observer (Zeiss, Cambridge, UK) with a x63 oil immersion objective (1.4 NA) and Zen Pro software. Images of spread platelets were then analysed using ImageJ software (NIH, Bethesda, USA) to identify the surface area and the number of platelets adhered.

2.5. Methodologies used to analyse platelet signalling

2.5.1. Sodium dodecyl sulphate-polyacrylamide gel electrophoresis (SDS-PAGE)

This study analysed proteins involved in platelet signalling by solubilising cellular membranes and using one-dimensional sodium dodecyl sulphate-polyacrylamide gel electrophoresis (SDS-PAGE) to separate charged macromolecules based on mass via an electric current. The main principle of this technique is to combine the properties of negatively charged SDS, a polyacrylamide gel and electrophoresis. When an electrical current is applied to a porous matrix such as a gel, it can separate molecules based on their size and charge.

SDS-PAGE uses a combination of SDS and polyacrylamide gels to separate proteins according to their molecular masses by electrophoretic migration. Acrylamide molecules polymerise into long linear chains which are cross-linked by bisacrylamide. The presence of free radicals enhances this polymerisation. Ammonium persulphate (APS) is used during the gel casting process as it decomposes to release SO_4^- anions. Tetramethylethylenediamine (TEMED) is also included to catalyse APS decay. The percentage of the acrylamide used in these solutions determines the pore size and, therefore, the relative separation of the proteins within the mixture.

2.5.1.1. Sample preparation for SDS-PAGE

Sample preparation was performed based on methods described by Laemmli (1970), which uses SDS as a denaturing agent and 2-mercaptoethanol as a reducing agent to lyse cells and reduce all proteins to their primary structure.

Washed platelets ($5x10^8$ platelets/mL) were pre-treated with agonists and/or inhibitors and the reaction was terminated by the addition of Laemmli buffer (4% SDS (w/v), 10% 2-mercaptoethanol (v/v), 20% glycerol (v/v) 50 mM Tris base, trace bromophenol blue, pH 6.8) at a ratio of 1:1 to give a final platelet concentration of $2.5x10^8$ platelets/mL.

SDS is an anionic detergent that binds to and denatures proteins leaving them with similar, rod-shaped tertiary structures. This gives rise to an equal negative charge per unit of protein mass (1.4 g SDS per 1 g protein). Reducing agents such as 2-mercaptoethanol break disulphide bonds and allow proteins to become fully denatured.

Samples were then stored at -20˚C until use. Prior to SDS-PAGE and immunoblotting, samples were boiled for 10 mins to ensure the denaturation of all proteins further.

2.5.1.2. Quantification of platelet protein concentrations

Protein concentration was determined using the DC protein assay kit according to the manufacturer's protocol (Bio-Rad). It is based on the well-established Lowry assay (Lowry et al., 1951) applied to cell lysates that have been solubilised in a detergent. This colorimetric assay measures the intensity

of a characteristic blue colour at 750 nm, which develops as a result of a reaction between proteins in the sample with copper in an alkaline medium and the subsequent reduction of a folin reagent. The primary residues involved in this reaction are tyrosine and tryptophan residues. The extent of the blue colour produced is directly proportional to the amount of protein in the sample. Bovine serum albumin (BSA) solutions of defined concentrations were used to calculate sample protein concentration. Each sample (washed platelets; $5x10^8$ platelets/mL) and standards were diluted 1:2 in protein assay lysis buffer (150 mM NaCl, 10 mM Tris base, 1 mM EGTA, 1 mM EDTA, 1% Igepal (v/v)) and assayed in triplicate. Light absorption at 750 nm was obtained using a multiplate reader (ThermoFisher).

The average protein content calculated was ~0.55 mg/mL (human platelets) and ~1.4 mg/mL (murine platelets) based on three independent repeats. The volume of platelet lysate to add per well can be calculated using Equation 3; 36 µL of human platelet lysate and 14.3 µL of murine cell lysate were loaded to achieve 20 µg of protein across all experiments.

$$\left(\frac{Desired\ protein\ mass}{Protein\ content}\right) = volume\ of\ lysate\ to\ load$$

Equation 3. Used to establish platelet lysate loading volume for SDS-PAGE

Used to calculate protein content, ensuring equal loading. The desired protein mass (e.g., 20 µg) is divided by the protein content calculated using a protein assay, resulting in the loading volume required per well.

2.5.1.3. Methodology for SDS-PAGE

For separation of proteins, pre-cast 4-20% gradient gels (Bio-Rad) were used to increase the range of molecular weights that can be separated on one gel. However, in some cases, 10% gels (Bio-Rad) were used to assess specific higher molecular weight proteins. Each gel was loaded with a protein standard (dual colour precision plus, Bio-Rad) before adding samples (20 µg). After loading, gels were subjected to a current of 120 V for 1 hour; in some cases, gels were run at 100 V for 3.5 hours on ice to assess higher molecular weight proteins (e.g., PDE3A; 100-120 kDa).

2.5.2. Immunoblotting

Western immunoblotting is a commonly used method to indirectly detect and quantify a protein or group of proteins within a cell mixture. The technique involves transferring proteins from a gel to an adhesive matrix such as a polyvinylidene difluoride (PVDF) membrane under an electric current. Once transferred, the membranes are then probed with specific primary antibodies against target proteins (e.g., p-VASP^{Ser157}). This is followed by a horseradish peroxidase (HRP) conjugated secondary antibody incubation. The detection of antigen-bearing proteins is facilitated by enhanced chemiluminescence (ECL), whereby a signal can be produced due to an interaction between hydrogen peroxide and luminol in the presence of HRP. This results in an excited product, which decays to a lower energy state and simultaneously luminesces at 425 nm that can be captured and visualised using a G:Box (Synegene) imaging system.

2.5.2.1. Immunoblotting methodology for detection of platelet proteins

After separating protein mixtures via SDS-PAGE, the separated proteins were transferred onto a methanol-pre-activated PVDF membrane at 25 V for 7 mins. The correct order of the gel and membrane and orientation in the transfer pack (Bio-Rad) ensure the migration of the negatively charged proteins on the gel towards the anode, resulting in their transfer and capture by the membrane. Once transferred, the membrane is blocked to inhibit non-

specific protein-membrane interactions by incubation with BSA (5-10%; w/v) or skimmed dry milk (5%; w/v) in Tris Buffered Saline with Triton X-100 (0.1%) (TBS-T) for 1 hr at RT with agitation. After blocking, the membranes were incubated with a primary antibody (1:1000 2% BSA/TBS-T or 1:1000 2% skimmed milk/TBS-T) overnight at 4˚C with agitation. After three TBS-T washing steps (5 min per wash), membranes were incubated for 1 hr at RT with a HRP-conjugated (anti-mouse or anti-rabbit) secondary antibody (1:10000 in 2% BSA/TBS-T or 2% skimmed milk/TBS-T), followed by another three washes with TBS-T. Membranes were then incubated with SuperSignal™ West Pico PLUS Chemiluminescent Substrate (ThermoFisher), and the produced signal was captured and visualised using a G:box (Figure 12).

In some cases, membranes were stripped of the bound antibody by using Restore ™ Western Blotting stripping buffer (ThermoFisher) with agitation. Membranes were incubated for 10 mins at RT followed by three wash steps with TBS and re- blocked and probed as previously described. In some cases, membranes were stripped and re-probed twice, first to assess another antibody where samples were precious and second to check for equal loading (anti-βeta-tubulin 1:1000 or anti-GAPDH 1:1000).

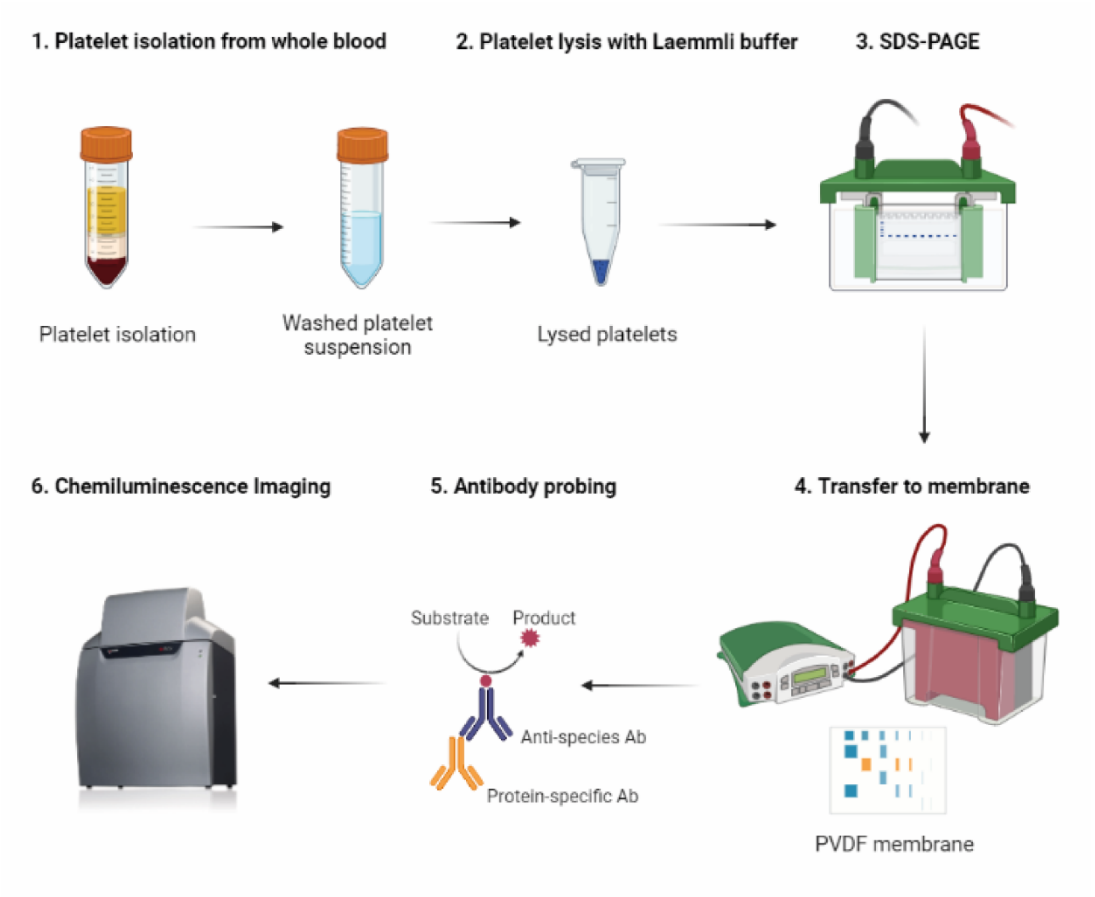

Figure 12. Schematic workflow for SDS-PAGE and immunoblotting

Washed platelets were isolated from whole blood, treated with desired cAMP-elevating, or inhibiting agents and lysed with Laemmli buffer. Samples were then boiled, and proteins were separated via SDS-PAGE. Gels were then transferred to a PVDF membrane and probed for specific proteins. Membranes were then imaged using a chemiluminescence imaging system (Created with BioRender.com).

2.5.3. Determination of platelet cAMP levels

The levels of cAMP were determined using a well-established cAMP direct Biotrak EIA kit (Cytiva) according to the manufacturer's protocol. This kit uses novel lysis reagents to facilitate rapid cAMP extraction from cell suspensions. The assay combines a peroxidase-labelled cAMP conjugate, a specific anti-serum immobilised onto pre-coated microplates and a stabilised substrate solution. Lysis reagent 1 is used to hydrolyse cell membranes to release intracellular cAMP, and lysis reagent 2 sequesters the critical component in lysis reagent 1 to ensure that cAMP is accessible for analysis. The assay is based on competition between unlabelled cAMP and a fixed quantity of peroxidase-labelled cAMP for a limited number of binding sites on a cAMP-specific antibody (Figure 13). The calculation for the amount of cAMP bound is displayed in Equation 4, additionally a new standard curve was generated for each new kit (Figure 14).

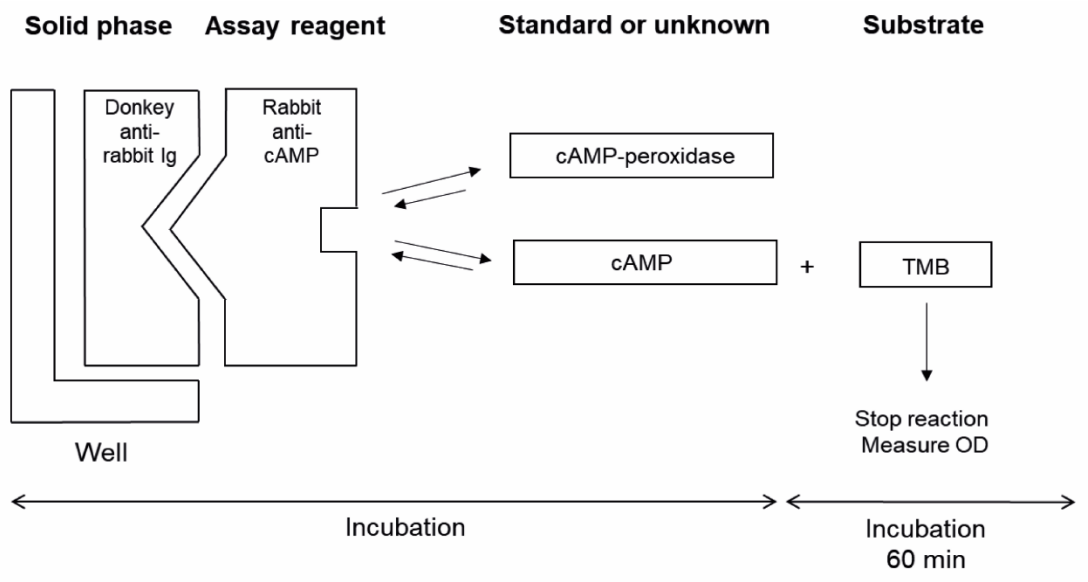

Figure 13. cAMP enzyme immunoassay (EIA) procedure

Schematical representation of the cAMP EIA procedure based on manufactures instructions.

2.5.3.1. Sample preparation and analysis

Washed platelets (180 µL; 2x10^8 platelets/ml) were treated with either PGI_2, forskolin, or adenosine. Following treatments, samples were lysed in 2.5% Dodecyltrimethylammonium Bromide per the manufacturer's instructions and incubated for 10 minutes at room temperature to achieve complete cell lysis. Following sample preparation, working cAMP standards (25-3200 fmol/well) were prepared following the manufacturer's protocol. All wells were read at 450 nm using a multiplate reader (Thermo Fisher Scientific). Data were analysed by calculating the average optical density (OD) for each set of replicates and the per cent bound for each standard and sample using the following equation.

$$\%\frac{B}{B0} = \left(\frac{standard\ or\ sample\ OD - NSB}{zero\ standard\ OD - NSB}\right) * 100$$

Equation 4. Calculation used to establish the percentage of cAMP bound

The calculation used to identify the percentage bound of cAMP to the plate in an unknown or standard sample.

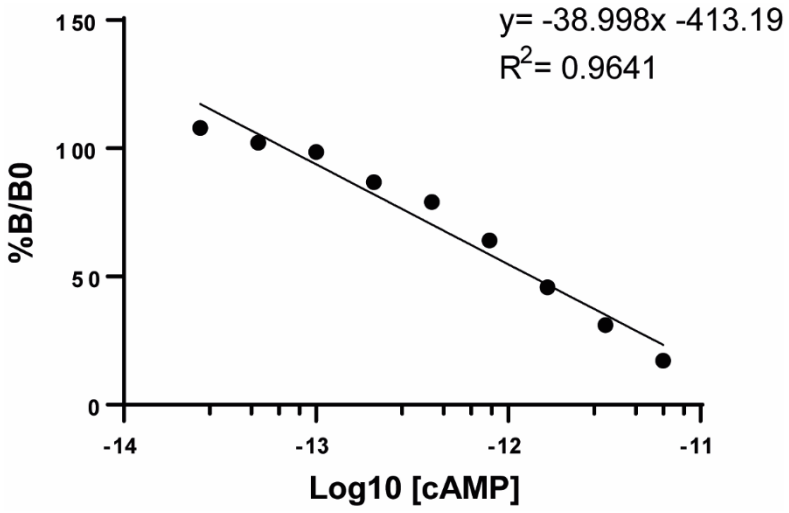

Figure 14. Example standard curve for the cAMP EIA

A representative standard curve used for determining levels of cAMP, generated for each new kit.

2.6. Generation of the platelet-specific AC6-KO mouse

2.6.1. Husbandry

All animal husbandry, housing and procedures were carried out in line with the regulations and guidelines of the University of Leeds Central Biological Services facility under the authority of a United Kingdom Home Office approved project licence (Professor Khalid Naseem – PP0499799 and Professor Robert Ariens – PP9539458) and my own personal licence (Miss Bethany Webb - I774212DC). Animals received standard rat and mouse no.1 maintenance diet (RM1, Special Diet Services) and water by Hydropac pouches. All mice were housed in individually ventilated cages (GM500, Techniplast), with 12-hour light/dark cycles, at 21˚C and 50-70% humidity.

2.6.2. Breeding

To induce a platelet specific deletion of *Adcy6*, we used cre-lox recombination methods, whereby *Adcy6* floxed mice were bred with iCre-recombinase mice under the control of the platelet factor 4 (PF4) promoter (Tiedt et al., 2007). Ludwig and Seuwen (2002) determined the *Adcy6* gene to contain 21 exons and span 17.9 kb, and the *Adcy6* floxed mice obtained from JAX (RRID: IMSR_JAX:022503) contained loxP sites at exons flanking 3-12 of the *Adcy6* gene, providing deletion of over half of the *Adcy6* gene by cre-recombinase. Lastly, the PF4-cre mice containing iCre-recombinase were kindly gifted by Dr Richard Pease (University of Leeds) and the gene constructs based on information provided by JAX and NCBI are shown in Figure 15.

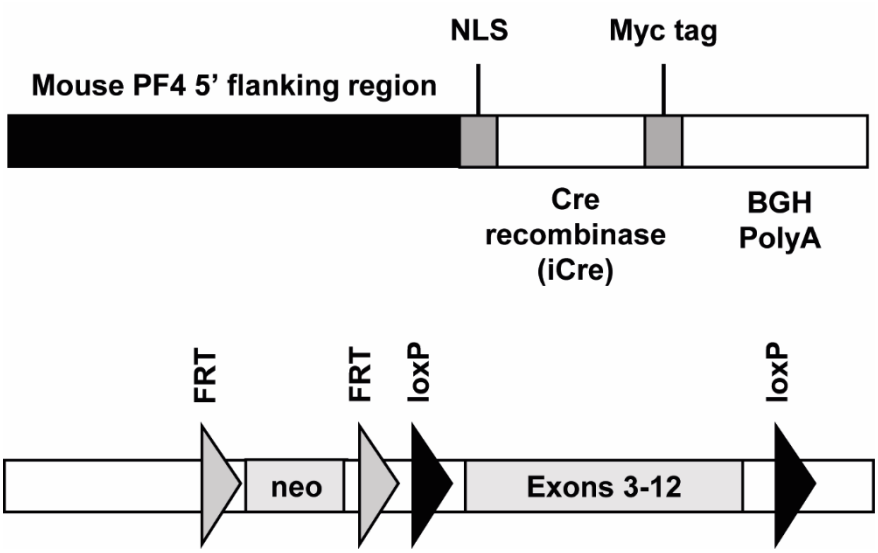

Figure 15. Gene constructs for PF4-cre and *Adcy6* floxed mice

Gene constructs used to generate a platelet specific knockout of the *Adcy6* gene. The top construct is Platelet Factor 4 (PF4)-cre containing a mouse PF4 promoter, an amino-terminal nuclear localisation sequence (NLS), a carboxy-terminal Myc epitope tag, iCre recombinase and a bovine growth hormone (BGH) PolyA sequence. The bottom construct is the floxed *Adcy6* gene with exons 3-12 flanked by loxP sites and an FRT-flanked neomycin resistance gene.

Homozygous *Adcy6* floxed ($Adcy^{fl/fl}$) female mice were bred with males expressing iCre-recombinase (PF4-cre^{+}). This yielded mice heterozygous for *Adcy6* and a carrier of PF4-Cre. Heterozygous *Adcy6* floxed ($Adcy^{fl/wt}$) female mice were then bred with male mice expressing PF4-cre and that were floxed for *Adcy6* (PF4-cre^{+}. $Adcy6^{fl/fl}$) to generate homozygous mice floxed for *Adcy6* with and without PF4-cre. Mice with PF4-cre expression have a PF4 specific knockout of *Adcy6* (PF4-cre^{+}. $Adcy6^{fl/fl}$), and mice without PF4-cre function are sibling controls (littermates). Throughout this study, PF4-cre^{+}. $Adcy6^{fl/fl}$ is denoted as 'AC6-KO', and littermate controls ($Adcy6^{fl/fl}$) are indicated as 'WT'. The breeding strategy is described in Figure 16.

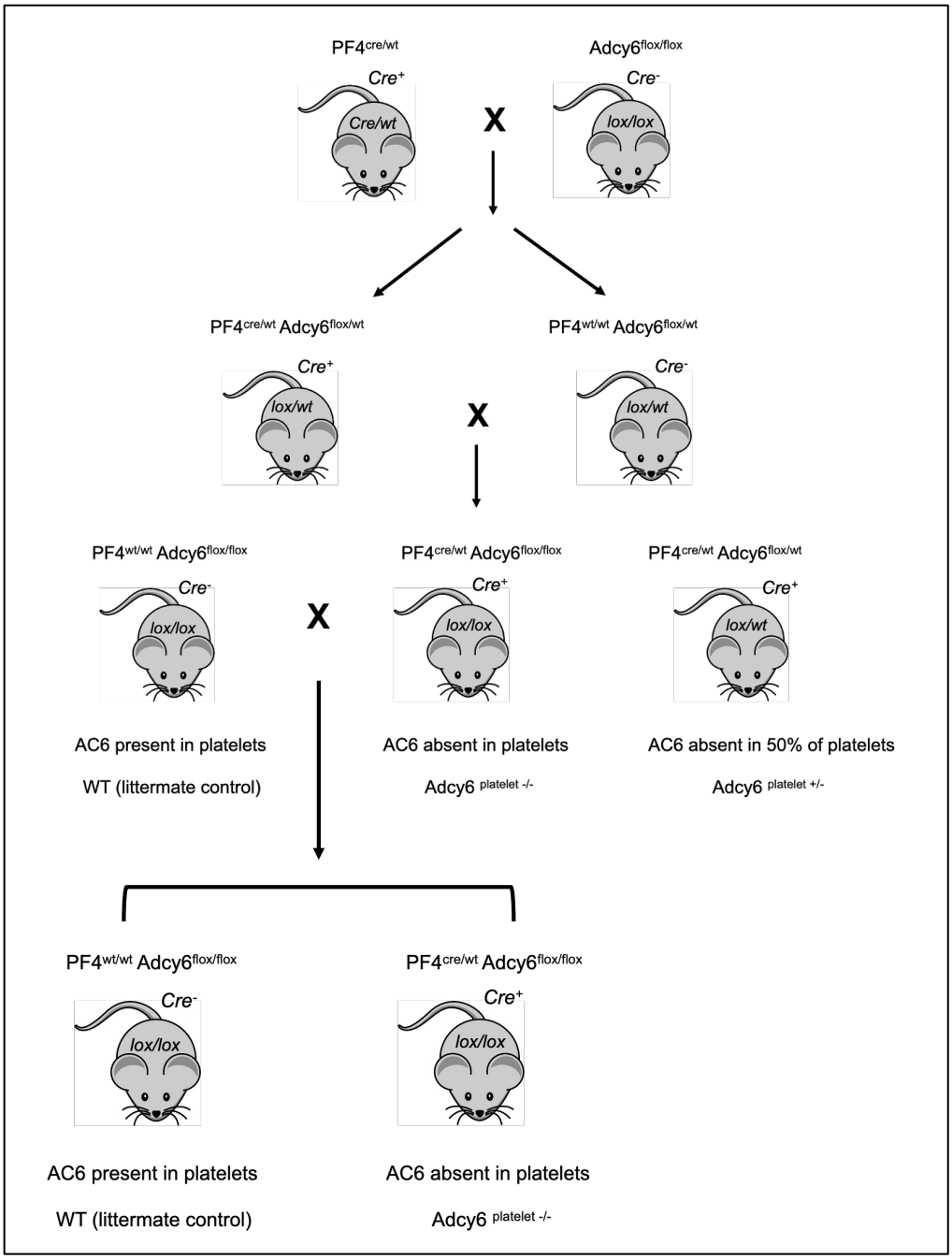

Figure 16. Breeding strategy for the platelet-specific AC6 knockout mouse

PF4-cre^{+}. *Adcyfl$^{/fl}$* and *Adcy$^{fl/fl}$* mice were produced by crossing PF4-cre mice with *Adcy$^{fl/fl}$* mice as per the diagram above.

2.6.3. Genotyping

Pups were ear notched at weaning (~3 weeks of age) to allow for identification and isolation of genomic DNA (gDNA) for genotyping. This process was critical for generating the platelet specific AC6 knockout mouse to ensure desired outcomes were reached at each breeding stage.

Genotyping and mRNA analysis was carried out by polymerase chain reaction (PCR). In the 1980s, Saiki and colleagues were the first to describe traditional PCR (Saiki et al., 1985; Saiki et al., 1988). The general concept of PCR includes primers, DNA polymerase, nucleotides, specific ions, and DNA templates. It consists of cycles that denature DNA, anneal primers, and extend DNA, and these critical steps have been unchanged since 1985. The development of real-time quantitative PCR (qPCR) was a substantial milestone in improving PCR methodologies; it allows for the monitoring of DNA amplification in real-time via monitoring fluorescence (Holland et al., 1991; Higuchi et al., 1992).

2.6.3.1. In-house genotyping

Genomic DNA was extracted from ear notches using a MyTaq™ extract PCR kit (Bioline). Extraction buffer mix was added to each ear notch and incubated at 75°C for 5 min. Samples were vortexed at least twice during incubation and then deactivated by heating for 95°C for 10 min. Samples were then centrifuged at high speed (12,000 *x g*) for 1 min to pellet any insoluble material and cell debris. The supernatant containing genomic DNA was then transferred to a fresh Eppendorf and diluted for PCR. PCR reactions were carried out in 50 µL total volumes containing 1 µL of gDNA template along with 25 µL of MyTaq™ Red master mix, 1 µL of each primer (forward, reverse and in some cases common) and the remaining volume adjusted with water. Reactions were performed using a touchdown PCR protocol as described in Table 6 and the primers and sequences recommended by JAX for each genotype are shown in Table 7.

Temperature (°C)	Time	Cycles
94	2 min	
94	20 sec	10 cycles (0.5°C drop per cycle)
65	15 sec	
68	10 sec	
94	15 sec	28 cycles
60	15 sec	
72	10 sec	
72	2 min	
10	hold	

Table 6. PCR conditions for ADCY6 and PF4-cre genotyping

Temperature, time, and cycle conditions for *ADCY6* and PF4-cre genotyping by touchdown PCR.

Primer	Sequence
ADCY6 F	5’-CAG CTC CTT GTG TTC CCA TAG
ADCY6 R	5’-AGC ACA GTG ACC AGC AAC AG
PF4-cre F	5’-TGG GCA GGC AGT GAA GAT AA
PF4-cre R1	5’-CAT GTC AAG AGG GTG CCA CTG GA
PF4-cre R2	5’-ATG TCC ATC AGG TTC TTC CTG AC

Table 7. Genotyping primers

Primer sequences used to identify genotypes for *ADCY6* and PF4-cre.

2.6.3.2. Agarose gel electrophoresis

For genotype determination of the PF4-cre/Adcy6-lox mouse line, PCR products were separated using agarose gel electrophoresis, whereby smaller DNA molecules migrate across the gel faster and further than larger ones. Gels were cast in 8 cm x 15 cm gel tanks with two 16 well combs inserted. For all in-house genotyping assays, 2% (2 g/100 mL) agarose gels in 100 mL of 1x TAE (40 mM Tris-HCl, 20 mM acetic acid, 1 mM EDTA, pH 7.6) were used. The agarose in TAE was mixed using a 500 mL conical flask and brought to melting in an 800 W microwave. Once heated and the agarose was dissolved 5 µL of ethidium bromide (10 mg/mL; Sigma-Aldrich) or GelRed® (Biotium) was added to the gel mix and the gel was left to set. Next, the gel was added to the tank and submerged in 1x TAE buffer. Next, 10 µL (0.5 µg/µL) of 50 bp GeneRuler Ladder (Thermo Fisher Scientific) was added to appropriate lanes, and a total of 12.5 µL PCR product was loaded to appropriate wells. Upon connection to a PowerPac Basic power supply (Bio-Rad), electrophoresis was carried out at 100V for 1.5 hrs.

Using UV illumination, gels were then imaged on a G:box (Syngene). Genotypes were determined manually based on base pair (bp) results, compared to expected primer bp, and verified by two independent parties. Figure 17 demonstrates the desired product sizes for each genotype after gel electrophoresis.

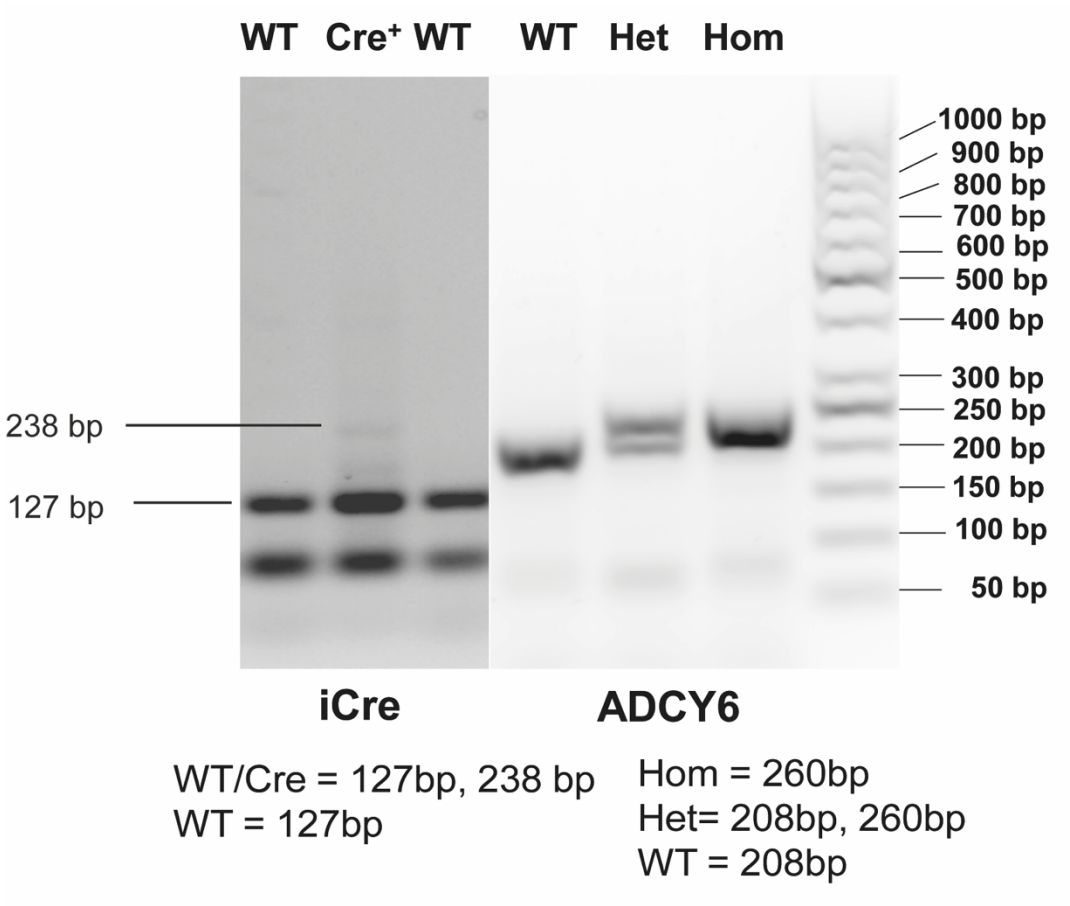

Figure 17. In-house genotyping results for PF4-cre and ADCY6

PCR analysis was performed on isolated genomic DNA from ear notches. The PCR product was measured by agarose gel electrophoresis and imaged via UV illumination. Bands were compared to desired base pair (bp), and genotypes were identified. The image represents 3 individual mice probed for both iCre and *ADCY6*.

2.6.3.3. Genotyping by Transnetyx

During the COVID-19 pandemic, whereby colony management was carried out remotely, we decided to outsource genotyping to Transnetyx. The genotyping was performed via Real-time PCR using a Taqman™ assay system, a high throughput system that allowed genotyping results within 72 hrs. Example amplification plots are shown in Figure 18.

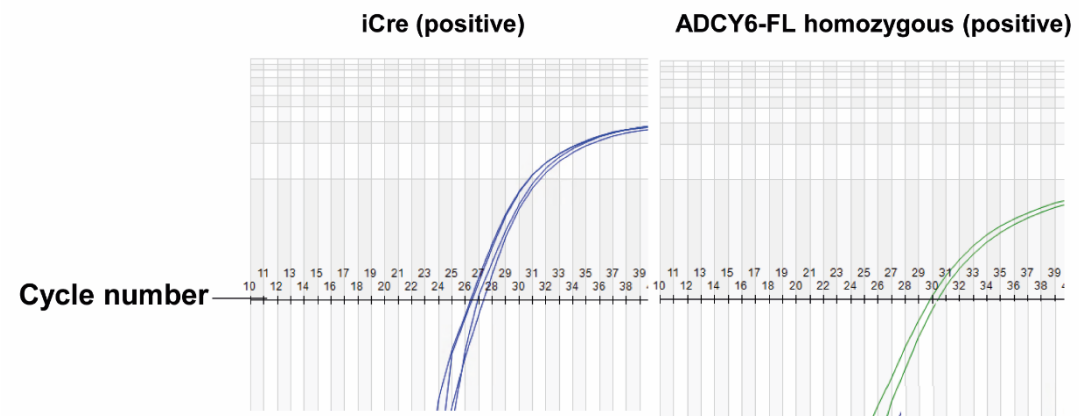

Figure 18. Example Real-Time PCR amplification plot from Transnetyx genotyping

Ear notches were collected and sent to Transnetyx, whereby the tissues were lysed, and DNA was purified. The isolated DNA was then analysed using a Taqman Real-time PCR assay system. The data presented is an amplification plot for iCre (left) and Adcy6-flox (right).

2.6.4. Assessment of mRNA levels

To assess the expression of our gene of interest in platelets and tissues, we used qPCR, which is widely considered to be the gold standard for gene expression as a result of its high assay specificity, sensitivity and wide linear dynamic range (Holland et al., 1991; Higuchi et al., 1992). Assessment of *ADCY6* expression from mRNA was critical to establishing the specificity of our AC6-KO mouse model.

2.6.4.1. Cell lysis of whole organs

Murine tissues (heart and kidneys) were initially added to an ice-cold cell extraction buffer (ThermoFisher) before being transferred to a new tube containing TRIzol. The sample was then lysed and homogenised using a TissueLyser II (Qiagen). The sample was then centrifuged at 17,000 *x g* for 10 minutes at 4°C. The supernatant was then transferred to a fresh RNase free tube for further isolation as described in 2.6.4.3.

2.6.4.2. Cell lysis of platelets

For cell lysis, washed platelets ($5x10^8$ platelets/mL) were pelleted, resuspended in TRIzol and incubated at RT for 5 minutes to ensure complete dissociation of nucleoprotein complexes. RNA isolation for both tissues and platelets was performed as described in 2.6.4.3.

2.6.4.3. RNA isolation

RNA was isolated from murine washed platelets and tissues using a combination of TRIzol Reagent (ThermoFisher) and the PureLink RNA mini kit (Invitrogen) following the manufacturer's protocol. TRIzol is composed of guanidium thiocyanate (chaotropic agent to assist in the denaturation of proteins) and phenol. TRIzol was used to lyse cells, releasing their cellular contents (Chomczynski and Sacchi, 1987).

Chloroform (0.2 mL per 1 mL of TRIzol) was added, shaken vigorously for 15 seconds, and then incubated for 2 mins at RT. The lysate was then centrifuged at 12,000 *x g* for 15 min at 4°C, causing phase separation. The upper colourless liquid phase containing RNA was removed and transferred to a fresh tube.

Ethanol (70%) at equal volume was added and vortexed. A volume of up to 700 µL of the RNA sample was transferred to the spin cartridge. The cartridge was centrifuged at 12,000 x *g* for 15 seconds at RT, and the flow-through was discarded. This was repeated until the entire sample had been processed. Once the sample had been processed, 700 µL of wash buffer 1 was added to the spin cartridge and centrifuged at 12,000 x *g* for 15 seconds. The flow-through was discarded, and 500 µL of wash buffer 2 (containing ethanol) was added to the cartridge. The sample was centrifuged at 12,000 x *g* for 15 seconds, and the flow-through was discarded. This was repeated once and then centrifuged further at 12,000 x *g* for 15 seconds to dry the membrane. Next, 20 µL of RNase-free water was added to the centre of the spin cartridge. The manufactures protocol suggests 30-100 µL, but it was found that 20 µL was optimum for platelet RNA isolation. The spin cartridge was then incubated for 1 min at RT and centrifuged with a recovery tube for 2 minutes at 12,000 x *g.*

2.6.4.4. Quantification of isolated RNA

Isolated RNA was quantified by ultraviolet (UV) absorbance using a DS-11 spectrophotometer (Denovix). An absorbance reading at 260nm (A_{260}) measures the nucleic acids, whereas an absorbance at 280nm (A_{280}) measures the amount of protein in the sample. The nucleic acid concentration can be calculated from the 260 nm reading using the Beer-Lamber Law based on the extinction coefficient for each nucleic acid (Grimsley and Pace, 2003).

RNA yields and $A_{260/280}$ were consistent between WT and AC6-KO platelets (Figure 19). The ratio of A_{260} and A_{280} is somewhat lower ($A_{260/280}$ = 1.4) than desired for downstream applications ($A_{260/280}$ = 1.8-2.0); though this may be attributed to the low levels of RNA present in platelets. The concentration of RNA isolated was close to the lower detection limit of 10 ng/µL of the spectrophotometer. However, we found that qPCR gene expression was successful, which, as the name suggests, is considered an alternative method of RNA quantification.

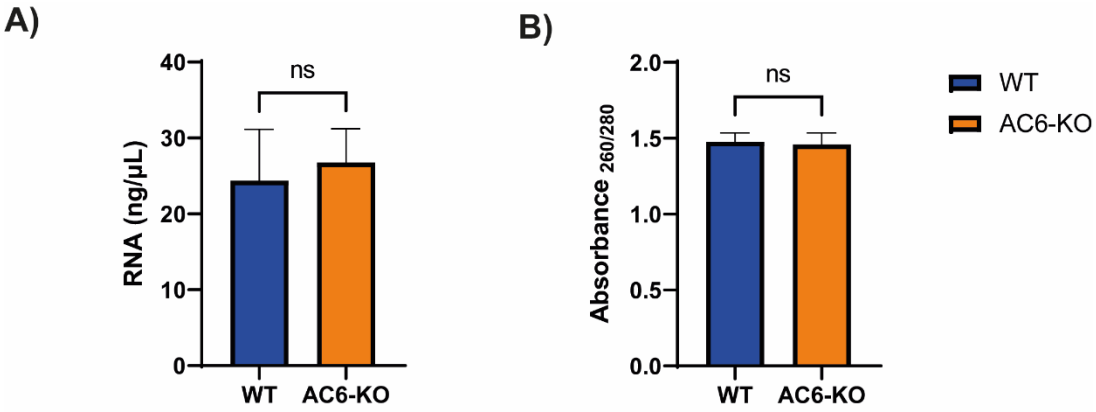

Figure 19. RNA yield and purity from murine platelets

RNA yield (A) and purity (B) from murine washed platelets ($5x10^8$ platelets/mL) isolated using TRIzol and the PureLink RNA mini kit according to the manufacturer's protocols. Platelet RNA samples were quantified by UV absorbance using a spectrophotometer. Data presented as means ± SD and compared between WT and AC6-KO by an unpaired students t-test with Welch's correction (n=4, ns=not significant).

2.6.4.5. Reverse transcription

Isolated mRNA was heated to 70°C for 10 minutes using a PCR heat cycler (Bio-Rad) and placed on ice. The mRNA was added to the reverse transcription master mix (Promega) containing Avian Myelobastosis Virus Reverse Transcriptase (AMV RT) (Kacian and Myers, 1976) and further incubated for 30 minutes using a reverse transcription protocol (Table 8), thus converting RNA to cDNA. After reverse transcription, cDNA samples were diluted in DNase/RNase free water to ensure sufficient cDNA for real-time qPCR.

Temperature (°C)	Time (minutes)
25	10
42	15
95	5
4	Holding

Table 8. Reverse Transcription PCR conditions

2.6.4.6. Real-time quantitative PCR

Real-time quantitative polymerase chain reaction (qPCR) is an exponential process that allows us to monitor the progress of PCR as it occurs in real-time (Holland et al., 1991; Higuchi et al., 1992). Data is collected throughout the PCR process, unlike other PCR methods where the data is collected at the end. This allows for reactions to be characterised by the point in time when amplification of a target is first detected rather than the amount of target accumulated after a fixed number of cycles. It works on the principle that the higher the starting copy, the sooner a significant increase in fluorescence is observed.

This study carried out qPCR analysis using the TaqMan® gene expression method. The TaqMan® assay uses the thermostable DNA polymerase isolated from the heat-tolerant bacterium *Thermus aquaticus* (Taq) (Chien et al., 1976). The TaqMan® Gene Expression assay is based on 5' nuclease

chemistry, whereby a fluorogenic probe is used to enable the detection of specific PCR products as it accumulates during PCR. The assay contains a pair of unlabelled primers and a TaqMan® probe with a FAM™ dye label on the 5' end and a minor groove binder (MGB), as well as a nonfluorescent quencher (NFQ) on the 3' end (Arikawa et al., 2008).

The cDNA was added to the TaqMan® gene expression PCR master mix, TaqMan primers (ThermoFisher) (Table 8), and H_2O in a 96-well plate. Samples were mixed using a plate spinner (Eppendorf) for 30 seconds before qPCR analysis using a QuantStudio Real-Time PCR system (ThermoFisher).

In the first step of real-time qPCR, the temperature is raised to denature double-stranded cDNA. During this stage, the signal from the fluorescent dye (5' end) of the TaqMan® probe is quenched by the NFQ (3' end). Next, the temperature is lowered, allowing the primers and the probe to anneal to their target sequences. Then the Taq DNA polymerase synthesises new strands using the unlabelled primers and the cDNA template. As the polymerase reaches the TaqMan® probe, the 5' endogenous nuclease activity cleaves the probe, separating the dye from the quencher. Meaning that with each PCR cycle, more dye molecules are released, leading to an increase in fluorescence intensity which is proportional to the amount of amplified product synthesised. Taqman® primers used throughout this study are displayed in Table 9 below.

Gene	TaqMan® primers	Exon boundary
ADCY6	Mm00475773_g1	10-12
ADCY5	Mm00674122_m1	20-21
ADCY3	Mm00460371_m1	11-12
GAPDH	Mm99999915_g1	2-3

Table 9. TaqMan® primers used for qPCR

The primers used and their exon boundary information for each gene of interest.

A threshold was set to determine quantities of the target gene within a sample. The general principle of using a threshold is to be able to visualise the fluorescent signal from qPCR amplification; the signal must increase so that it is above the detection limit of the machine and therefore is considered the baseline. The number of cycles required is proportional to the initial starting copy number of the target in the sample, meaning the more cycles needed for the signal to increase above the threshold suggests the original copy number is low. If few cycles are required, the copy number is high, which is essential when detecting the absence or presence of a target gene. qPCR was run for 50 cycles to ensure a large enough window to assess whether *ADCY6* was knocked out successfully, and the threshold was set to 0.1.

2.6.4.7. Quantitation of qPCR results

Quantitation of mRNA expression was carried out using the comparative threshold cycle (Ct) method, which uses the arithmetic formula $2^{-\Delta Ct}$ that compares the Ct value of one target gene to another, such as a reference house-keeping gene (e.g., *GAPDH*) in a single sample. This is known as relative quantification, as changes in expression of the target gene are compared to the endogenous control. Analysis of results involves normalising the determined Ct value for a target gene to the control.

Ct values were generated using the Livak method (Livak and Schmittgen, 2001). This calculates the exponential amount of product produced from the Ct value by subtracting the reference gene mean from the target gene Ct. This results in delta Ct (ΔCt); next, the normalised Ct is transformed using $2^{-\Delta Ct,}$ which converts the logarithmic ΔCt into a linear value. This value is then multiplied by 100 to result in the percentage expression of the target gene compared to *GAPDH*. Each sample was carried out in duplicate, and an average of ΔCt was calculated per sample. The average Ct for *GAPDH* was 24.4 ± 0.76 (mean ± SD).

2.6.5. *In vivo* methodologies

To translate *in vitro* findings into a more physiological setting, we performed well established *in vivo* techniques to explore the role of thrombosis in the AC6-KO mouse. Since platelet research is currently dependent on the use of gene manipulation via transgenic mouse models, we employed the use of a

well-characterised thrombosis injury model. This allows us to assess thrombus formation in response to injury in real-time.

2.6.5.1. Thrombosis injury model using $FeCl_3$

Many models studying real-time thrombus formation in mice have been established since the model was first developed in the early 2000s (Falati et al., 2002). Models including mechanical, laser, photoreactive and ferric chloride ($FeCl_3$) injury are now commonplace in studying thrombosis in mice (Rosen et al., 2001; Celi et al., 2003; Li et al., 2013; Darbousset et al., 2014). $FeCl_3$ induced thrombosis is one of the most widely used procedures to assess murine thrombosis in real-time. In principle, it utilises the topical application of $FeCl_3$ to a vessel to induce a thrombotic injury (Kurz et al., 1990).

$FeCl_3$ is a chemical injury that causes significant oxidative stress, generating free radicals leading to lipid peroxidation and destruction of endothelial cells, ultimately resulting in occlusive thrombus formation (Eckly et al., 2011; Li et al., 2013; Bonnard and Hagemeyer, 2015). The injury triggers platelet adhesion and aggregation, and leukocyte recruitment through the expression of several adhesion molecules. Thrombus formation can be directly observed by intravital microscopy via fluorescent labelling of platelets and leukocytes, allowing for several parameters including occlusion, thrombus formation over time and size to be investigated (Celi et al., 2003). It's been reported that this method is well suited to reproduce the coagulation cascade (Darbousset et al., 2014).

Mesenteric vessels were chosen based on their ease of access, allowing us to study the dynamics of thrombus formation while also allowing for multiple vessels to be assessed per mouse, in line with the NC3Rs (replacement, reduction and refinement) (Burden et al., 2015). Typically, the carotid artery is used in this model; while the vessel is much larger and provides a solid model to study occlusive thrombosis, we decided not to go ahead due to limited ease of access and limited vessel number.

Mice were injected intraperitoneally with Ketamine and Medetomidine (2.5 µL/g body weight) (Table 10) and left until unconscious. Depth of anaesthesia was assessed via withdrawal response before performing surgery. Once

confirmed, the mouse was injected with Rhodamine 6G (0.25 mg/mL; 50 µL) via the tail vein using a 30 G needle. A vertical incision was made on the abdomen, and the abdominal viscera were gently squeezed out to expose the intestine. The mouse was repositioned on its side whilst mesenteric vessels were located. Once a vessel was located, the tissue was pinned, and black plastic (3mm x 8mm) was placed under the vessel to reduce autofluorescence. The mouse was then brought to the microscope stage, and PBS was pipetted over the vessel to prevent drying. Once the vessel was lined up under the microscope, the fluorescent (540 nm) light was turned on, and a baseline image and video were captured. Once baseline imaging was complete, the cross-section of the vessel was measured. Next, filter paper (1mm x 1mm) was soaked in $FeCl_3$ (7.5%) and placed onto the exposed vessel for 30 seconds before images were taken sequentially every minute up to 5 minutes, then every 5 minutes up to 30 minutes. Time for vessel occlusion was recorded based on whether two independent parties still observed blood flow. After 30 minutes, the mouse was subjected to schedule 1 via cervical dislocation.

Ketamine (100 mg/mL)	**Medetomidine (1 mg/mL)**	**H_2O**
50µL	100µL	50µL

Table 10. Components of injectable anaesthetic for murine surgeries

The components and concentrations of anaesthetics that were administered via IP injection at 2.5 µL / g body weight.

2.7. Data presentation and statistical analyses

2.7.1. Data presentation

Where flow cytometry data was presented as histograms or scatter plots, CytExpert (v.2) was used for analysis and graphics. Where raw values were presented, GraphPad Prism (v.9) and/or Microsoft Excel (Office 365) were used. Throughout this study, data are presented as XX ± standard deviation.

2.7.2. Statistical analysis

Statistical analysis was performed using GraphPad Prism (v.9). In cases of single comparison, Student T-tests with Welch's correction were performed. Whereas in cases whereby multiple parameters were compared, One-way ANOVA with Dunnett's multiple comparisons test or Two-way ANOVA with Šídák's multiple comparison test were carried out (unless otherwise stated).

Chapter 3
Cyclic-AMP signalling in human and murine platelets

3.1. Introduction

Blood platelets play a key role in haemostasis by adhering to sites of vascular injury. Under normal physiological conditions, platelets circulate in a quiescent state. This is maintained by the constant exposure of endothelial-derived platelet inhibitors prostacyclin (PGI_2) and nitric oxide (NO). PGI_2 and NO act to control platelet activation and extent of activation upon vascular injury by activating cyclic nucleotide signalling pathways that ultimately lead to inhibition of platelet function. NO is the major endothelial-derived activator of 3',5'-cyclic guanosine monophosphate (cGMP) signalling (Mellion et al., 1981) while PGI_2 is the main physiological activator of 3',5'-cyclic adenosine monophosphate (cAMP) (Moncada et al., 1976). This study will primarily focus on cAMP-mediated platelet inhibitory signalling stimulated by endogenous PGI_2 and in particular the role of adenylyl cyclase (AC) in the process.

To first characterise cAMP signalling in human and murine platelets, several different tools were used that target different elements of the pathway. These include a variety of cAMP-elevating agents such as PGI_2, forskolin, adenosine and 8-CPT-cAMP, along with agents such as SQ22536, H89, KT-5720 and RP-8-CPT-cAMP, that target AC and PKA isoforms respectively. Throughout this chapter, each of these agents has been characterised in their ability to target different aspects of cAMP signalling, along with the inhibition of platelet function before they were used to characterise the AC6-KO mouse in subsequent chapters.

3.1.1. Aims of chapter

- To characterise platelet cyclic-AMP signalling in human and murine wild-type platelets
- To optimise cAMP-elevating and inhibiting agents in human and murine wild-type platelets
- To assess platelet activation and inhibition by PGI_2 in patients with acute coronary syndrome (ACS)

3.2. Isolation of human washed platelets

Many platelet studies use isolated platelets using the well-established prostaglandin method of isolation, whereby platelets are inhibited with either PGE_1 or PGI_2 (Vargas et al., 1982). This method produces isolated, also known as washed platelets, that are highly sensitive to platelet activation, likely due to the inhibition of physiologically relevant cyclic-nucleotide inhibitory pathways. As this method relies on the activation of cAMP to prevent residual platelet activation during the isolation process, it was not suitable for studying cAMP signalling. Here an alternative method that reduces the pH of using the buffers, established by Mustard and colleagues (Mustard et al., 1989), was used. This method relies on lowering the pH of PRP to 6.4 to prevent platelet activation. Washed platelets isolated via the pH method were functionally compared to the PGI_2 method of isolation using light transmission aggregometry.

3.2.1. Assessment of functional response in human washed platelets

Platelets were treated with collagen or thrombin and aggregation was assessed for up to 5 minutes. Platelets isolated by either method were found to be functionally responsive, and aggregation increased in an agonist concentration-dependent manner. In platelets isolated by the PGI_2 method (Figure 20 A-B) maximal percentage aggregation in response to thrombin (0.1 U/mL) and collagen (10 µg/mL) were 79.0 ± 2.83% and 76.3 ± 5.5% respectively. While using, the pH method (Figure 20 C-D) of isolation we observed no difference in maximal aggregation in response to thrombin (0.1 U/mL) and collagen (10 µg/mL), 73.7 ± 3.7% and 77.3 ± 3.7% respectively. EC_{50} analysis of the pH method identified as 3.9 µg/mL for collagen and 0.02 U/mL for thrombin, however at this concentration of thrombin aggregation responses were variable so we opted for 0.05 U/mL for human platelet aggregation studies (Figure 20 G-H). While the PGI_2 method, identified EC_{50} values of 2.7 µg/mL for collagen and 0.01 U/mL for thrombin although we found that thrombin exhibited an “all or nothing” response to activation (Figure 20 C-D).

Based on EC_{50} analysis we then compared isolation methods at collagen (5 µg/mL) (60.3 ± 4.5 % pH method vs 68 ± 10% PGI_2 method) and thrombin (0.05 U/mL) (67.7 ± 6.0 % pH method vs 77.0 ± 2.8% PG_2 method). We found no significant differences between the pH and PGI_2 method of platelet isolation, therefore we opted for the pH method throughout this study to preserve cyclic nucleotide signalling pathways.

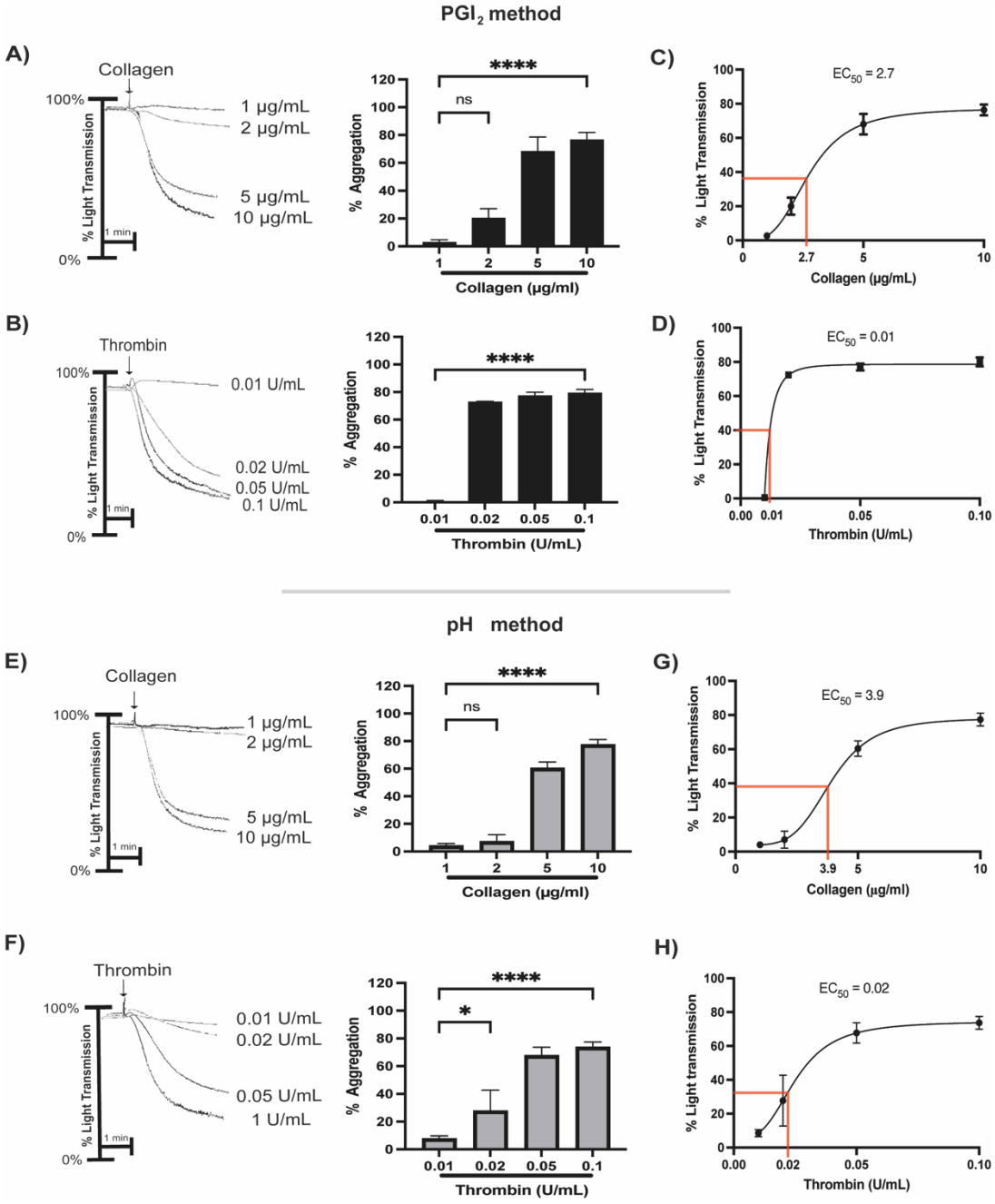

Figure 20. Validation of human platelet isolation method

Human washed platelets ($2.5x10^8$ platelets/mL) were isolated via the prostacyclin method (A-D) or the pH method (E-H) and treated with either collagen or thrombin at marked concentrations under constant stirring (1000 rpm) at 37°C for up to 5 minutes. Representative aggregation traces were generated by AggroLink Software (Chronolog, USA). Bar graphs represent percentage light transmission at 5 mins presented as means ± SD compared to the lowest concentration (One-way ANOVA with Dunnets multiple comparisons test, n=3 for all experiments, ns= not significant, *≤0.05, and ****≤0.0001). Line graphs represent EC_{50} calculated by non-linear regression as means ± SD.

3.2.2. Assessment of sensitivity to prostacyclin in human washed platelets

Next the sensitivity of isolated platelets to PGI_2 was established. Washed platelets were treated with PGI_2 (1-1000 nM) for 1 min prior to stimulation with collagen (5 µg/mL) or thrombin (0.05 U/mL). Inhibition of agonist induced aggregation occurred in a concentration-dependent manner, reaching near maximal inhibition with PGI_2 (100 nM) for thrombin (12.1 ± 4.9%) and PGI_2 (1000 nM) for collagen (13.3 ± 7.2%). The concentration of PGI_2 that caused 50% inhibition (IC_{50}) of aggregation upon stimulation with collagen (5 µg/mL) was 2.6 nM and 2.8 nM for thrombin (0.05 U/mL) (Figure 21 C-D).

These data confirm the ability of PGI_2 to inhibit GPVI-mediated aggregation by collagen and PAR-mediated aggregation by thrombin, suggesting that PGI_2 targets aspects of platelet function that are common between different agonists.

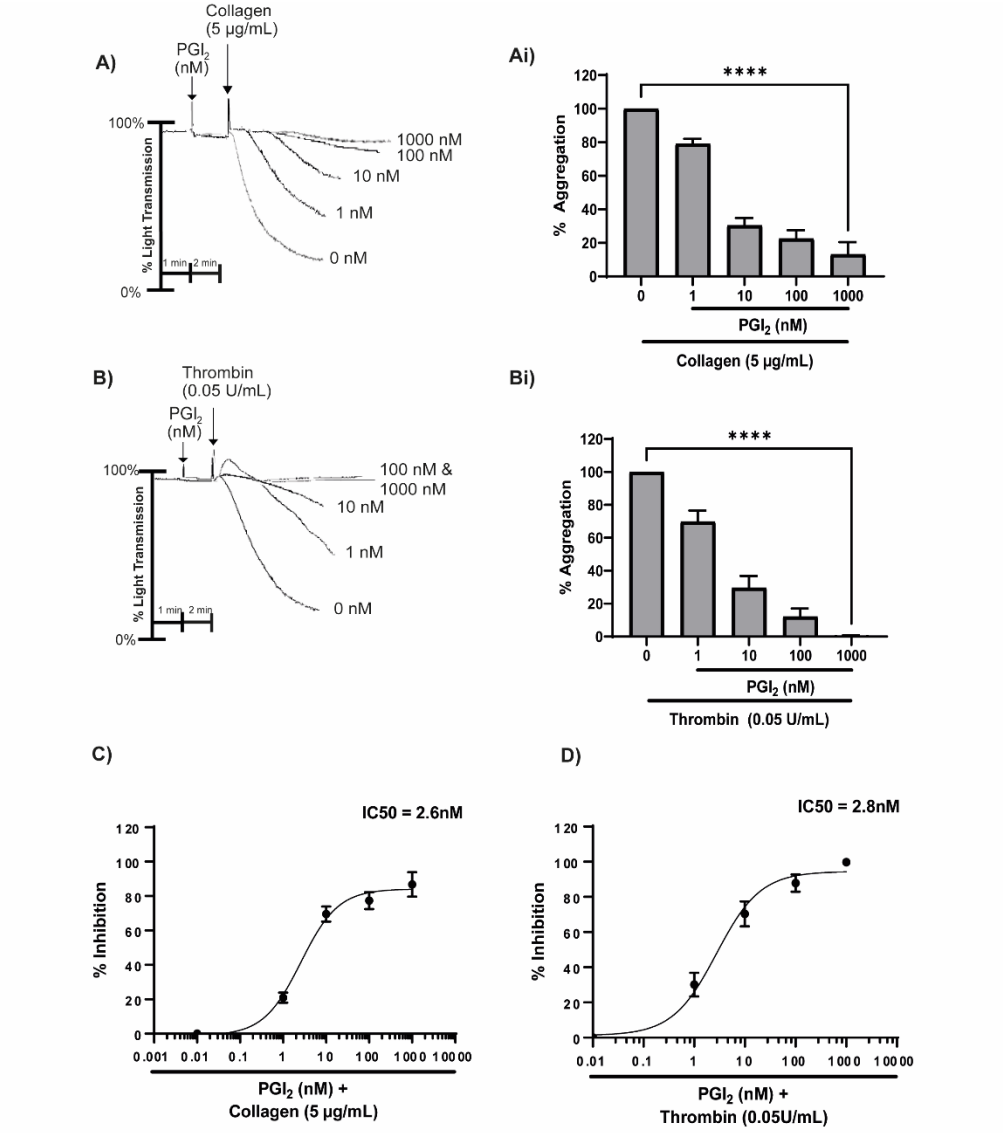

Figure 21. Inhibition of human washed platelets by PGI_2

Human washed platelets ($2.5x10^8$ platelets/mL) were treated with increasing concentrations of PGI_2 (1-1000 nM) and stimulated with either collagen (A) or thrombin (B) under constant stirring (800 rpm) at 37°C for up to 5 minutes. Representative aggregation traces were generated by AggroLink Software (Chronolog, USA). Bar graphs represent percent aggregation at 5 minutes. Data presented as means ± SD and compared to agonist alone by one-way ANOVA with Dunnett's multiple comparisons test (n=4, ****≤0.0001). IC_{50} was determined using a modified Hill equation (C-D).

3.3. Assessment of spreading of human washed platelets on immobilised proteins

Having confirmed that washed platelets respond functionally to both stimulators and inhibitors, we next sought to assess adhesion and spreading. During injury platelets adhere and spread across the site of injury and undergo cytoskeletal rearrangement (Aslan and Mccarty, 2013). Finger-like projections known as filipodia and actin-rich sheets of lamellipodia allow for platelets to significantly increase their surface area and stabilise platelet aggregates to form a thrombus.

3.3.1. Optimisation of human platelet spreading conditions

In the first instance the conditions for assessment of platelet spreading were optimised by examining the immobilised protein and platelet concentration. Platelets ($5x10^6$ - $1x10^8$ platelets/mL) were adhered on the surface of immobilised fibrinogen (100 µg/mL) (Yusuf et al., 2017; Atkinson et al., 2018) or collagen (50 µg/mL) (Mangin et al., 2018) for 45 mins prior to fixation, permeabilization, staining with either FITC- or TRITC-phalloidin (Figure 22) and visualised using fluorescence microscopy.

The number of adhered platelets decreased with diminishing platelet count for when using either collagen (50 µg/mL) or fibrinogen (100 µg/mL). The total area covered also decreased with platelet concentration and was consistent between collagen and fibrinogen, apart from at $5x10^7$ and $5x10^6$ platelets/mL, though likely an experimental error given it is an n=1 (Figure 22 A-B). Based on the representative images and analysis, concentrations between 1 $x10^7$ - $2x10^7$ platelets/mL were optimal for our spreading assay and are consistent with previous studies (Yusuf et al., 2017; Atkinson et al., 2018; Khan et al., 2020).

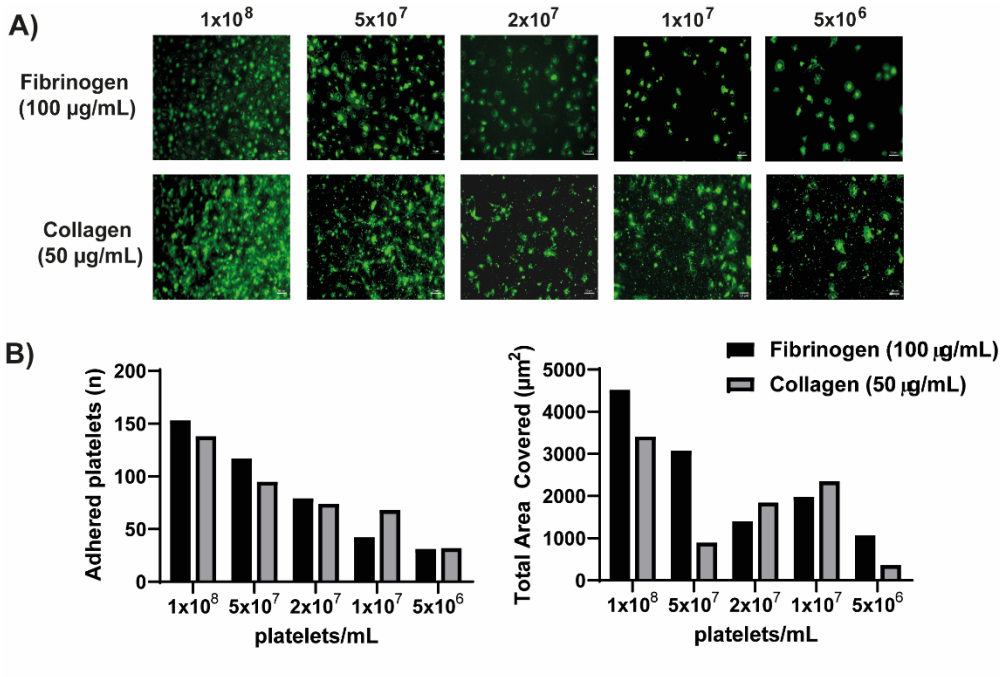

Figure 22. Optimisation of the platelet spreading protocol in human washed platelets

Washed platelets at different concentrations were spread on either fibrinogen (100 µg/mL) or collagen (50 µg/mL) for 45 mins, then fixed and stained with FITC-phalloidin. Representative images taken using a Zeiss AX10 microscope with 63x oil emersion (A). Bar graphs indicate number of adhered platelets and total area covered from an average of 5 images (B) (n=1, scale bar =10 µm).

3.3.2. Human platelet spreading on the surface of fibrinogen in response to PGI_2

After establishing conditions for platelets adhesion and spreading, the effects of PGI_2 on platelet spreading on immobilised fibrinogen was tested. Washed platelets ($2x10^7$ platelets/mL) were treated with and without PGI_2 (10 nM) and adhered to fibrinogen (100 µg/mL) over time.

We found no significant difference for number of platelets adhered per field of view (FoV) and percentage surface area covered compared between platelets treated with and without PGI_2. For example, at 45 minutes the number of platelets adhered per FoV was 55.5 ± 3.2 without PGI_2 vs 39.3 ± 15.7 with PGI_2 and the percentage surface area covered was 9.9 ± 0.4% without PGI_2 vs 5.7 ± 1.8% with PGI_2 (Figure 23).

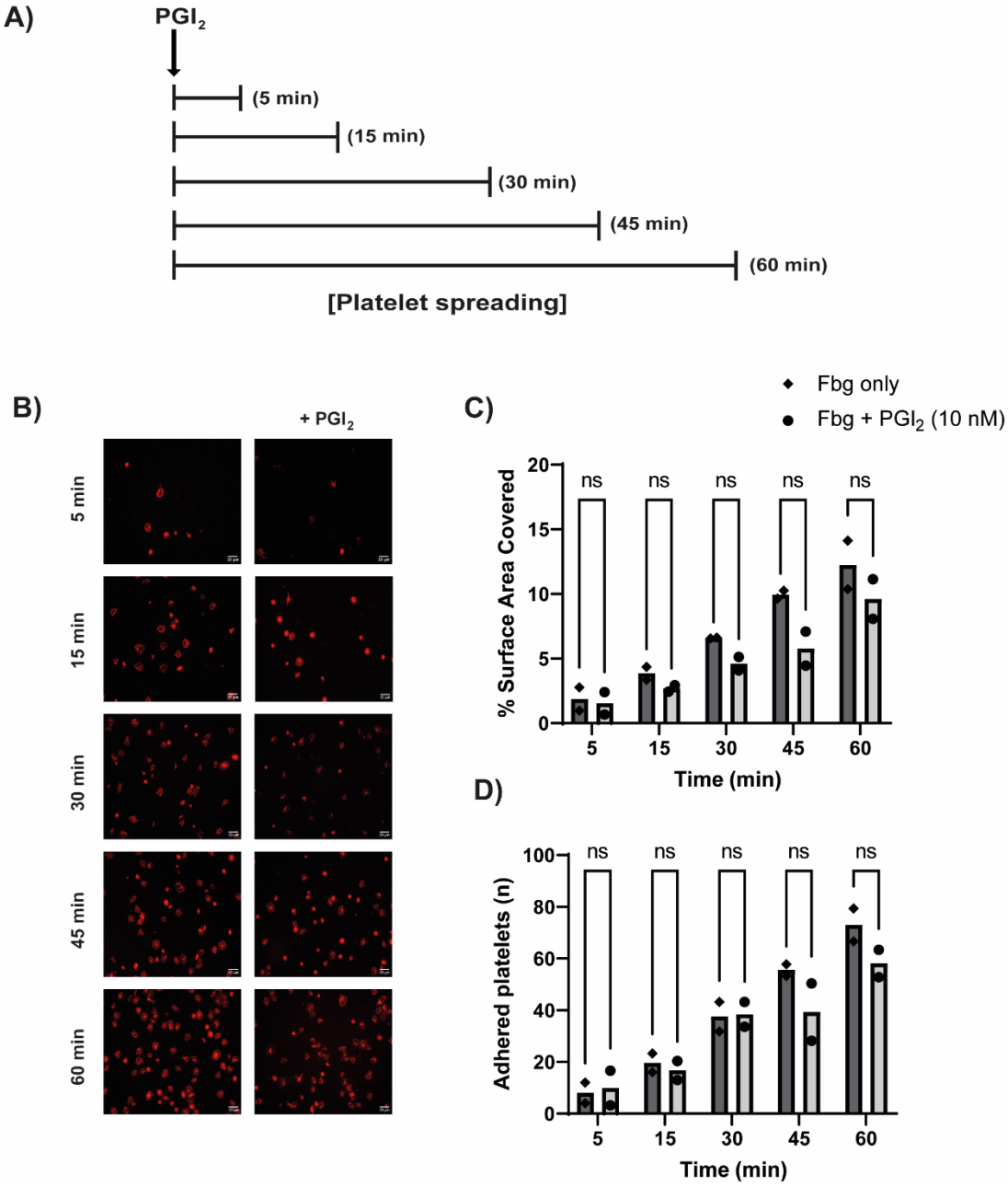

Figure 23. Human platelet spreading in response to PGI_2

Washed platelets ($2x10^7$ platelets/mL) were spread on fibrinogen (100 µg/mL) and treated with PGI_2 (10 nM) at increasing time points up to 60 minutes. Platelets were then fixed and stained with TRITC-phalloidin. Experimental design shown in (A). Representative images taken using a Zeiss AX10 microscope (Zeiss, Cambridge, UK) with 63x oil immersion objective (1.4 NA) and Zen Pro software (Zeiss, Cambridge, UK) (B). Bar graphs indicate percentage surface area coverage (C) and number of adhered platelets from an average of 5 images (D). Data presented as individual values and compared between with and without PGI_2 by two-way ANOVA with Šidák multiple comparisons test (Fbg = fibrinogen, n=2, ns = not significant, scale = 10 µm).

3.3.3. Adaptation of platelet spreading on fibrinogen in response to PGI_2

After finding no significant difference between platelets treated with and without PGI_2, the spreading protocol was adapted to use the method described by Yusuf and colleagues (Yusuf et al., 2017). In this experimental design, washed platelets ($2x10^7$ platelets/mL) were spread on fibrinogen (100 µg/mL) for 25 min, washed twice with PBS to remove non-adherent platelets and then treated with PGI_2 (10 nM) at increasing time points prior to fixation. The method continued as described in 3.3.2.

We found a clear reduction in the number of adhered platelets in the presence of PGI_2 at shorter incubation times (2-5 mins). At 2 mins the number of adhered platelets per FoV reduced from 7.4 ± 0.6 to 4.7 ± 0.2 in the presence of PGI_2 (10 nM) ($p<0.005$). Following the same trend, percentage area covered also displayed a reduction in response to PGI_2. At 2 mins the area covered reduced from 1.7 ± 0.2% to 0.8 ± 0.0% in the presence of PGI_2 ($p=0.004$) (Figure 24).

Given the lack of response after a 10 min PGI_2 incubation, it's likely that PGI_2 has degraded over time, suggesting that the longer incubation times are not suitable. Due to the success of this method of assessing sensitivity to PGI_2 on spread platelets, we decided to use this method throughout the study.

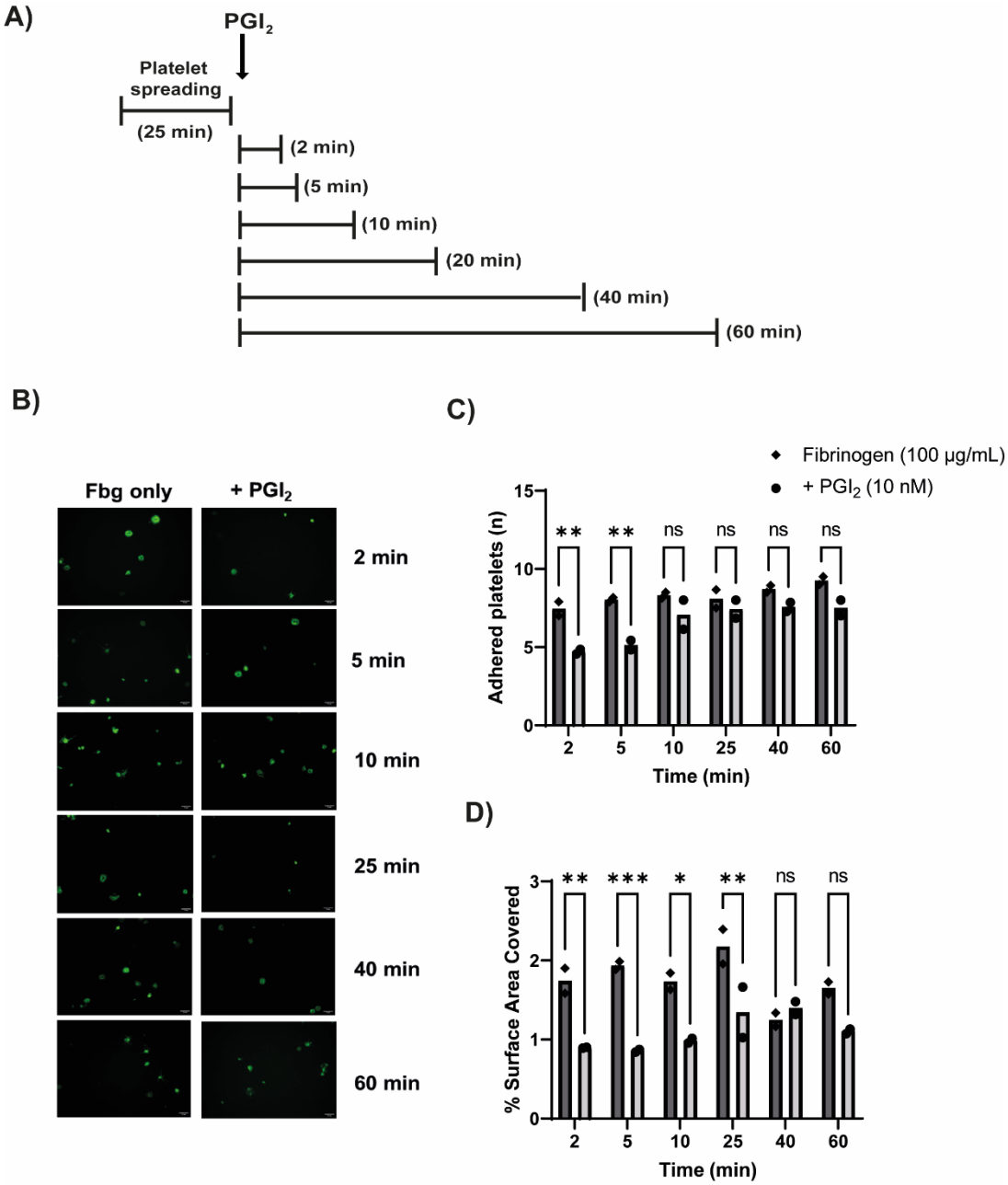

Figure 24. Inhibition of human platelet spreading by PGI_2

Washed platelets ($2x10^7$ platelets/mL) were spread on fibrinogen (100 µg/mL) for 25 minutes, washed with PBS and then treated with PGI_2 (10 nM) at increasing time points up to 60 minutes. Platelets were then fixed and stained with FITC-phalloidin. Experimental design shown in (A). Representative images (B) and bar graphs indicate percentage number of adhered platelets (C) and percentage area covered (D) from an average of 5 images. Data presented as individual values and compared between with and without PGI_2 by two-way ANOVA with Šidák multiple comparisons test (Fbg = fibrinogen, n=2, ns = not significant, *≤0.05, **≤0.01 and ***≤0.001, scale = 10 µm).

3.4. Expression of platelet surface markers in response to agonists in human whole blood

Platelet activation was examined using fluorescent flow cytometry (FFC) in whole blood. FFC is an attractive method for analysing platelet function as the sample requirements are low (5 – 10 µL of whole blood) but its output is data-rich. In this case, several surface markers were measured, the expression of which have previously been shown to link to the extent of platelet activation (Adelman, B. et al., 1985; Shattil, S.J. et al., 1985; Kennedy et al., 1997).

3.4.1. Activation induced platelet markers by three-parameter flow cytometry

In the first instance, a three-parameter flow cytometry panel was used to assess platelet activation which targeted CD62P (P-selectin), PAC1 (active $\alpha_{IIb}\beta_3$) and CD42b (Adelman et al., 1985; Shattil et al., 1985; Kennedy et al., 1997). This combination of markers allows us to measure two distinct aspects of platelet activation, integrin activation and α-granule secretion, along with a constitutively expressed platelet marker. Platelet activation was a determined by changes in the surface protein expression in response to the potent platelet agonist PAR1 peptide to mimic thrombin activation of the PAR1 receptor. Antibodies were tagged with fluorescent conjugates; CD62P-PE, PAC1-FITC and CD42b-APC.

Whole blood was stimulated with increasing concentrations of PAR1 peptide (0.5 – 20 µM) and stained with fluorescent conjugates prior to analysis by flow cytometry. The thrombin mimetic, PAR1 peptide generated a concentration-dependent increase in both PAC1 and CD62P expression (Figure 25). In data expressed as percentage of platelets positive, each marker reached near 100% expression at PAR1 (2 µM) and did not increase significantly beyond this concentration of agonist. The percentage of PAC1 positive cells increased from 45 ± 7.9 % (basal) to a maximal of 98.2 ± 1.9% (PAR1; 2 µM), while CD62P positive cells increased from 10.6 ± 6.3 % (basal) to a maximal of 98.4 ± 0.4 % (PAR1; 2 µM) ($p<0.0001$).

In contrast, MedianFI continued to increase beyond PAR1 (2 µM) for CD62P, but not PAC1. CD62P expression increased from 425 ± 15.1 (basal), to 24822.9 ± 6842.0 (2 µM) and then a maximal of 39050.8 ± 9594.6 (10 µM)

($p<0.0001$). While PAC1 binding this increased from 2227.6 ± 1628.5 (basal) to 37254.6 ± 6396.7 (2 μM) without further significant elevation ($p=0.0009$). In addition, we found that percent positive at basal for the PAC1-FITC antibody was unusually high (45.6 ± 7.9%) however, this has also been observed in studies by Frelinger et al (2015) and Michelson et al (2018). Overall, these data demonstrate that platelets in whole blood are functional and respond to agonist stimulation using three-parameter flow cytometry.

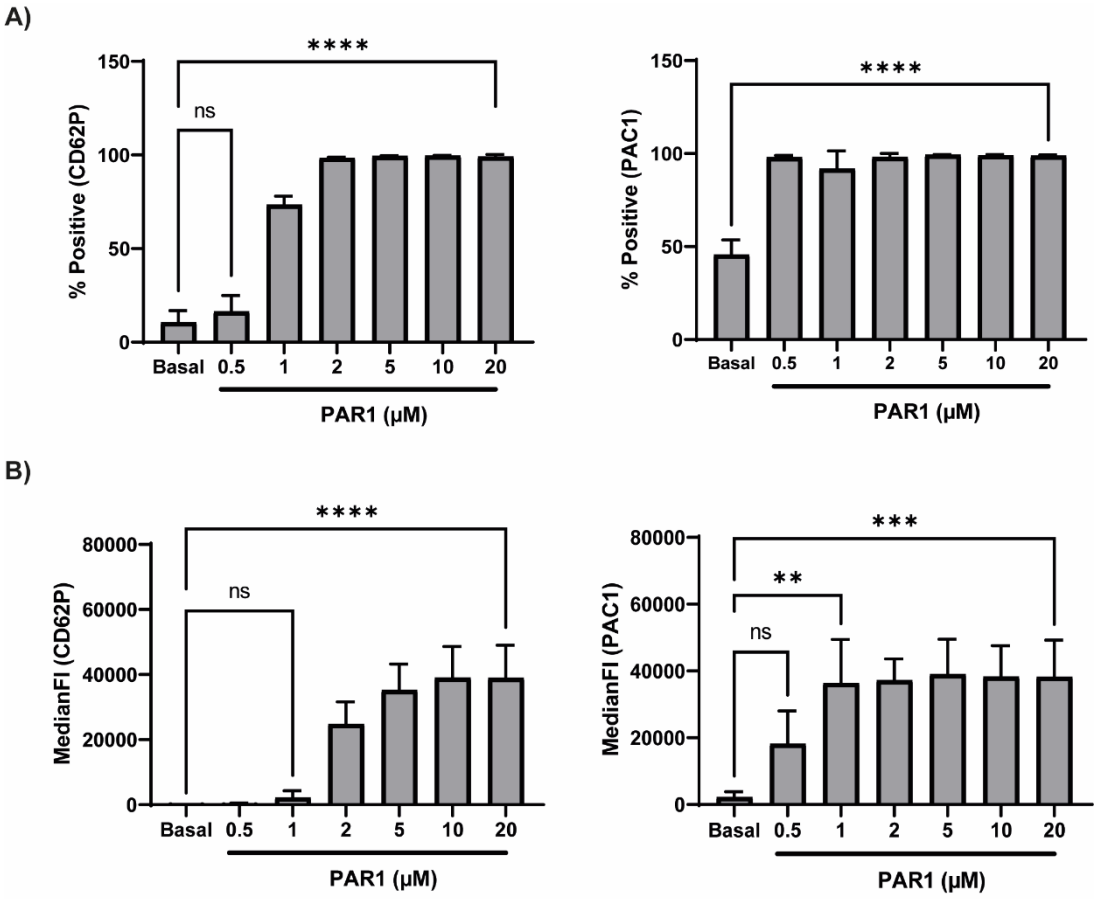

Figure 25. Human platelet activation in response to PAR1 peptide by three-parameter flow cytometry

Human whole blood was stimulated with PAR1 peptide (0.5-20 μM) and probed with either CD62P (left) or PAC1 (right) for 20 minutes prior to fixation in 1% PFA/PBS. CD42b-APC was used as a platelet marker and samples were analysed for 10,000 platelet positive events. Bar graphs represent percent positive (A) and Median Fluorescence Intensity (MedianFI) (B). Data presented as means ± SD and compared to basal by one-way ANOVA with Dunnett's multiple comparisons test (n=3, **≤0.01, ***≤0.001, and ****≤0.0001).

3.4.2. Assessment of PGI_2 sensitivity in human whole blood using three-parameter flow cytometry

After establishing platelet activation by three-parameter flow cytometry in response to PAR1 peptide the effects of PGI_2 were tested (Figure 26).

Human whole blood was treated with PGI_2 (0.1-1000 nM) for 2 mins prior to stimulation with PAR1 peptide (5 μM). This concentration of PAR1 was chosen based on the extent of platelet activation as shown in Figure 25. Binding of PAC1 and CD62P was inhibited in a concentration-dependent manner by the presence of PGI_2 (0.1 – 1000 nM). PAC1 binding, and therefore integrin activation was returned to basal (45.6 ± 7.9 %) with maximal effects observed at 100nM of PGI_2 whereby antibody binding reduced from 98.9 ± 0.7% to 42.7 ± 9.6 % ($p<0.0001$). For, CD62P expression the effects of PAR1 peptide were reduced at 10 nM PGI_2, with maximal effects observed at 100 nM where the level of surface marker was reduced from 98.9 ± 0.3% to 8.3 ± 1.9 % ($p<0.0001$) (Figure 26). These data confirm that the expression of key platelet activation markers in whole blood can be inhibited by PGI_2.

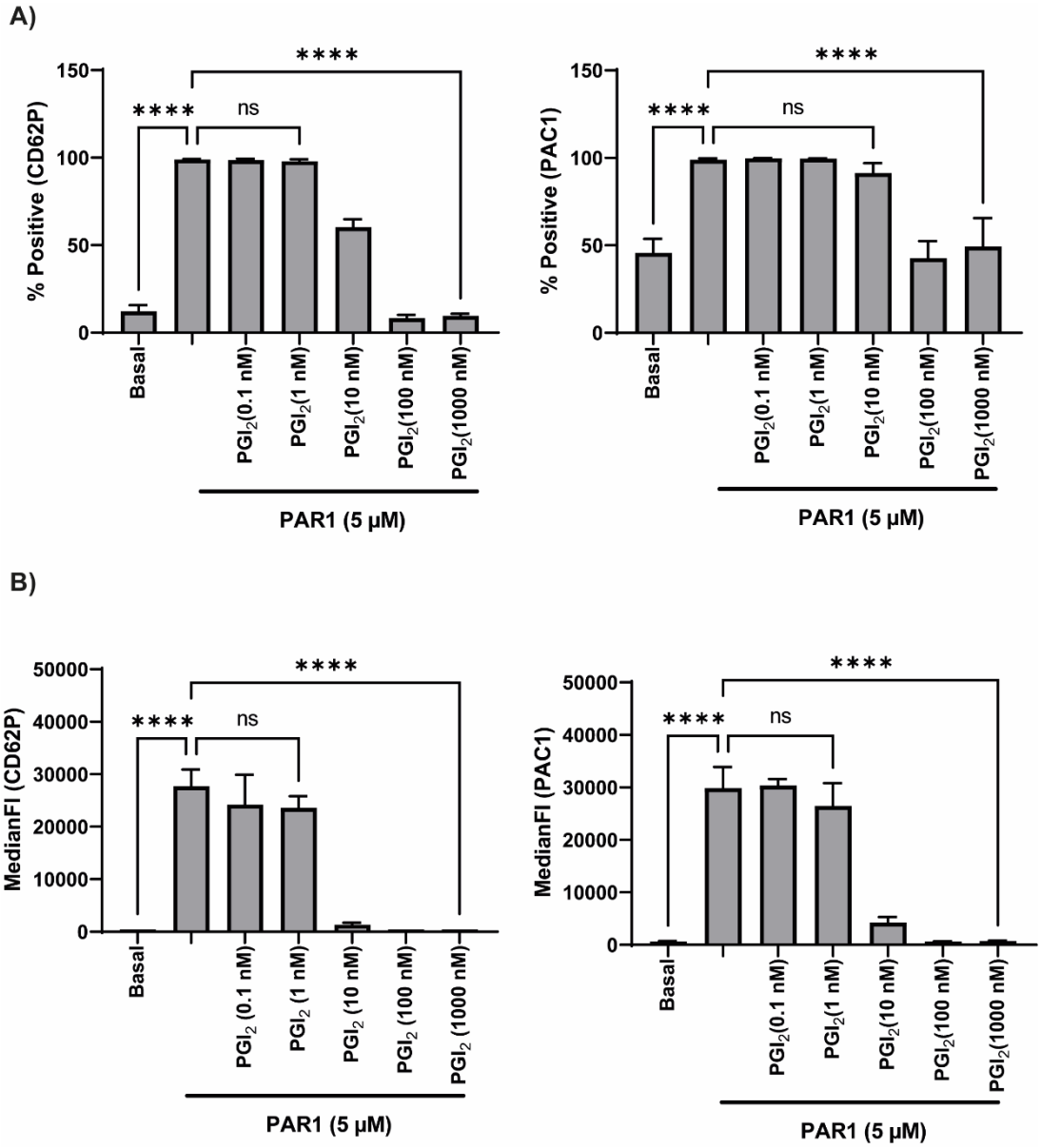

Figure 26. Inhibition by PGI_2 in human whole blood using three-parameter flow cytometry

Human whole blood was pre-treated with PGI_2 (0.1-1000 nM) for 2 mins and stimulated with PAR1 peptide (5 µM). Platelets were then probed with either CD62P (left) or PAC1 (right) for 20 minutes prior to fixation in 1% PFA/PBS. CD42b-APC was used as a platelet marker and samples were analysed for 10,000 platelet positive events. Bar graphs represent percent positive (A) and Median Fluorescence Intensity (MedianFI) (B). Data presented as mean ± SD and compared to basal and agonist alone by one-way ANOVA with Dunnett's multiple comparisons test (n=3, ****≤0.0001).

3.4.3. Comparison between human platelet preparation methods by four-parameter flow cytometry

After establishing various antibodies for specific characteristics of platelet activation can be used via a three-parameter flow cytometry assay, we decided to apply this method further by using a high throughput four-parameter platelet activation panel. Initially, it was important to assess whether the platelet preparation affected antibody binding in this assay before translating this into murine platelets (Metcalfe et al., 1997).

Whole blood, in many cases, is the ideal platelet preparation as it is the most physiologically relevant environment to assess platelet activation. However, the use of whole blood in certain experimental conditions is not always feasible. In cases where chemical reagents lose their specificity or activity in whole blood, preparations such as platelet-rich plasma (PRP) and washed platelets are used instead.

In this assay, four fluorescently labelled conjugates were used to assess four different aspects of platelet activation in each sample (Table 11).

Name	**Antibody Binding**	**Type of marker**
CD42b	Binds to CD42b expressed on the surface of platelets	Constitutive
PAC1	Binds to the activated form of the $\alpha_{IIb}\beta_3$ receptor complex on the surface of platelets	Activation-dependent
CD62p	Binds to P-selectin expressed on the surface of platelets after α-granule secretion	Activation-dependent
Annexin V	Binds to Annexin V which binds to platelets that express phosphatidylserine on their surface	Activation-dependent

Table 11. Platelet specific fluorescent antibodies used in the four-parameter flow cytometric assay

Human whole blood and PRP from sodium citrate vacutainers were compared with ACD-A vacutainer washed platelets from matched donors. Each platelet preparation was stimulated with PAR1 peptide (10 μM) or CRP-XL (10 μg/mL) to assess PAR1-mediated and GPVI-mediated activation, respectively. A combination of PAR1 and CRP-XL was also used since this has been shown to generate a specific pro-coagulant subpopulation of platelets as measured by Annexin V (AnnV) binding (Tait et al., 1999; Munnix et al., 2003).

All platelet preparations displayed a concentration-dependent increase upon stimulation with PAR1 peptide and CRP-XL (Figure 27). Whole blood and PRP demonstrated a clear increase in CD62P binding upon agonist stimulation and did not increase further upon dual agonist stimulation. Whole blood displayed an increase in CD62P binding from 15.9 ± 7.8 % positive (basal) to 97.9 ± 0.8 % positive (dual agonist), while PRP increased from 16.4 ± 9.5 % positive (basal) to 82.4± 28.6 positive (dual agonist). However, CD62P binding at basal was highly elevated in washed platelets (58.9 ± 24.1 % positive) whereas whole blood and PRP remained consistently low. This is likely a result of stress from the process of platelet isolation resulting in ~60% of washed platelets being pre-activated (Figure 27 A). We also found that upon stimulation with dual agonists, expression of CD62P was more sensitive in washed platelets compared to whole blood (whole blood: 61169.5 ± 21980 MFI vs washed platelets:115289.8 ± 23701.1 MFI, p=0.01).

PAC1 binding was robust across each of the platelet preparations and demonstrated a clear increase upon agonist stimulation (Figure 27 B). Whole blood increased from 8.1 ± 10.1 % positive (basal) to 70.1 ± 31.3 % positive (dual agonist), while PRP increased from 13.0 ± 17.4 % positive (basal) to 88.3 ± 10.8 % positive (dual agonist) and washed platelets increased from 7.0 ± 5.5 % positive (basal) to 93.3 ± 8.8 % positive (dual agonist). The percentage of PAC1 binding displayed no difference between platelet preparations, while MFI demonstrated that washed platelets were more sensitive to activation by dual agonists compared to whole blood (washed platelets: 149167.7 ± 22105.1 MFI vs whole blood: 76746.9 ± 33315.7, p=0.005)

Binding of AnnV displayed a subtle increase upon stimulation and showed no significant differences between platelet preparation. While AnnV expression upon dual agonist stimulation was the most sensitive in whole blood (8880.4 ± 451.3 MFI) compared to PRP (3174.2 ± 2488.1 MF) and washed platelets (4107.0 ± 1518.2 MFI). The degree of activation by dual agonist stimulation was significantly higher in whole blood ($p<0.0001$) compared to PRP and washed platelets. Basal AnnV in PRP was 918.6 ± 252.9 (MFI), along with washed platelets at 1650.4 ± 116.8 (MFI), while whole blood was 281.8 ± 130.5 (MFI). This may be due increased basal AnnV binding in PRP and washed platelet preparations, which could affect the capacity for activation (Figure 27 C). Where possible, and assay reagents do not require PRP or washed platelets, whole blood should be used to assess PAC1, CD62P and AnnV binding. Though, PAC1 and CD62P binding remain strong in other platelet preparations.

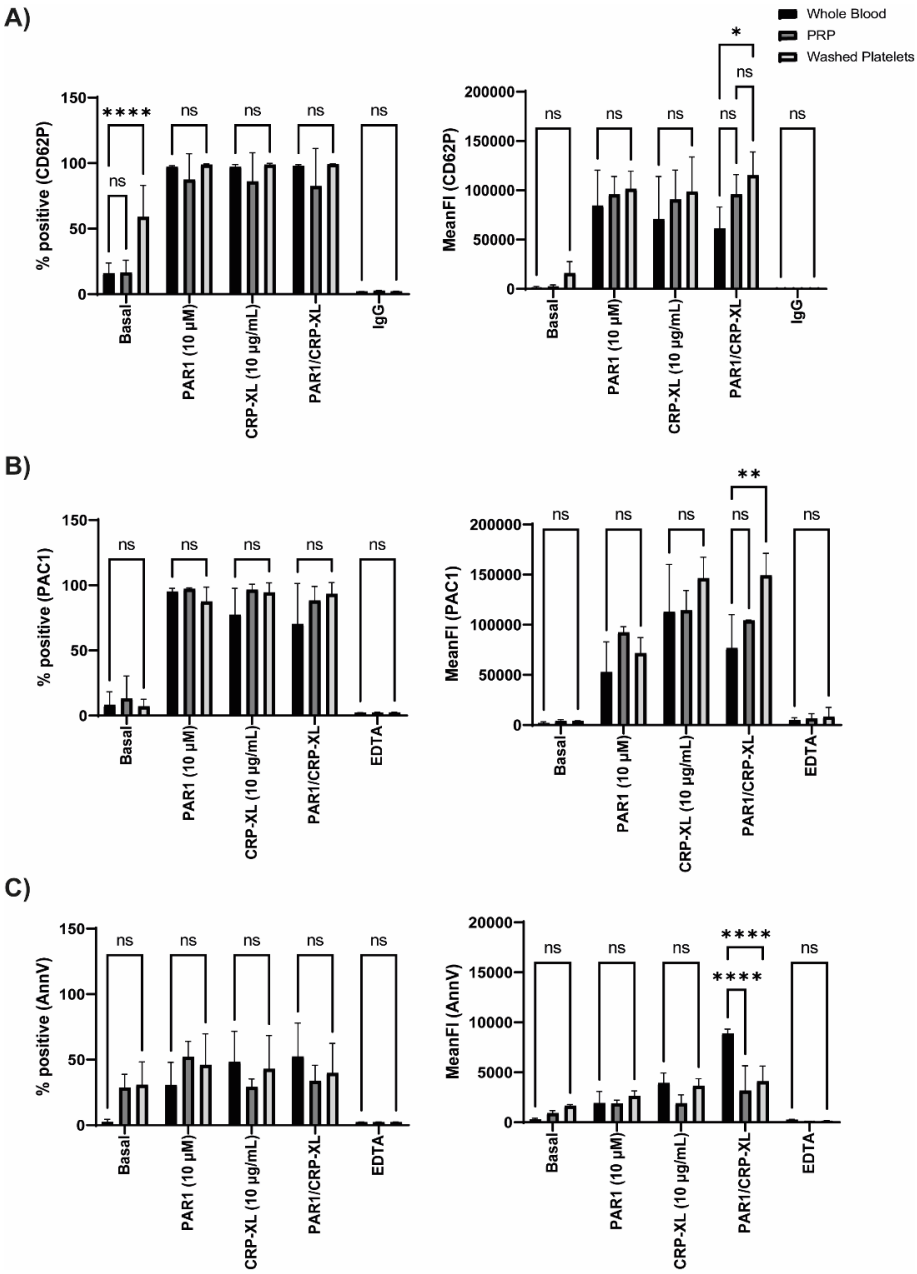

Figure 27. Comparison of human platelet preparation by four-parameter flow cytometry

Human washed platelets (5x10^8 platelets/mL), platelet rich plasma and whole blood were stimulated with PAR1 peptide (10 µM) or CRP-XL (1 µg/mL) and probed with either CD62P (A), PAC1 (B) or AnnV (C) for 20 minutes prior to fixation in 1% PFA/PBS. CD42b was used as a platelet marker and samples were analysed for 10,000 platelet positive events. Bar graphs represent percent positive (left) and Mean Fluorescence Intensity (MeanFI) (right) over control. Data presented as means ± SD and compared between platelet preparation groups by two-way ANOVA with Šídák's multiple comparisons test (n=3, ns = not significant, *≤0.05, ***≤0.001, and ****≤0.0001).

3.4.4. Optimisation of the four-parameter activation panel assay in human whole blood

After establishing that whole blood was the preferred platelet preparation for the four-parameter activation panel, platelet activation in response to PAR1 and CRP-XL was assessed in more detail. Citrated whole blood was stimulated with PAR1 (1 – 10 µM), CRP-XL (0.1 – 10 µg/mL) or a combination of PAR1 (10 µM) and CRP-XL (10 µg/mL), and probed with CD62P, PAC1 and AnnV for 20 minutes before fixation with PFA.

All antibody binding increased in a concentration-dependent manner in response to PAR1 (1-10 µM) and CRP-XL (0.1-10 µg/mL) (Figure 28). CD62P binding increases from 12.2 ± 3.2% positive (basal) to near maximal 97.1 ± 0.2 % positive (PAR1; 5 µM) ($p<0.0001$) and does not increase further (Figure 28 A). While CD62P expression increases from 517.6 ± 152.7 MFI (basal) to a maximal of 42215.3 ± 17964.7 MFI (PAR1; 10 µM) ($p=0.0006$). CRP-XL-induced (1 µg/mL) CD62P binding increased to near maximal 96.7 ± 1.5 % positive and did not increase any further ($p<0.0001$). Expression of CD62P in response to CRP-XL (1 µg/mL) was also maximal with an MFI of 31849.1 ± 2775.9.

Next, PAC1 binding in response to PAR1 peptide increased from 2.4 ± 1.8 % positive (basal) to a maximal of 95.4 ± 4.2 % positive (1 µM) ($p=0.0001$), with expression increasing from 1368.4 ± 394.2 MFI (basal) to 36274.6 ± 1344.8.1 MFI (10 µM) ($p=0.0007$). PAC1 binding also increased in response to CRP-XL (1 µg/mL), reaching 82.1 ± 11.28 % positive with PAC1 expression also reaching maximal of 24035.5 ± 7409.9 MFI (Figure 28 B).

AnnV binding was lower compared to CD62P and PAC1 as it requires both PAR and GPVI signalling for PS to be exposed on the platelet surface. The combination of PAR1 and CRP-XL caused an increase in AnnV binding from 1.5 ± 0.6% (basal) to 65.2 ± 18.8% (dual agonist) ($p<0.0001$) (Figure 28 C). Lastly, AnnV expression increased from 285.3 ± 159.5 MFI (basal) to 11906.9 ± 1913.5 MFI (dual agonist) ($p<0.0001$). The dual agonist approach did not significantly increase CD62P and PAC1 expression over maximal PAR1 and CRP-XL.

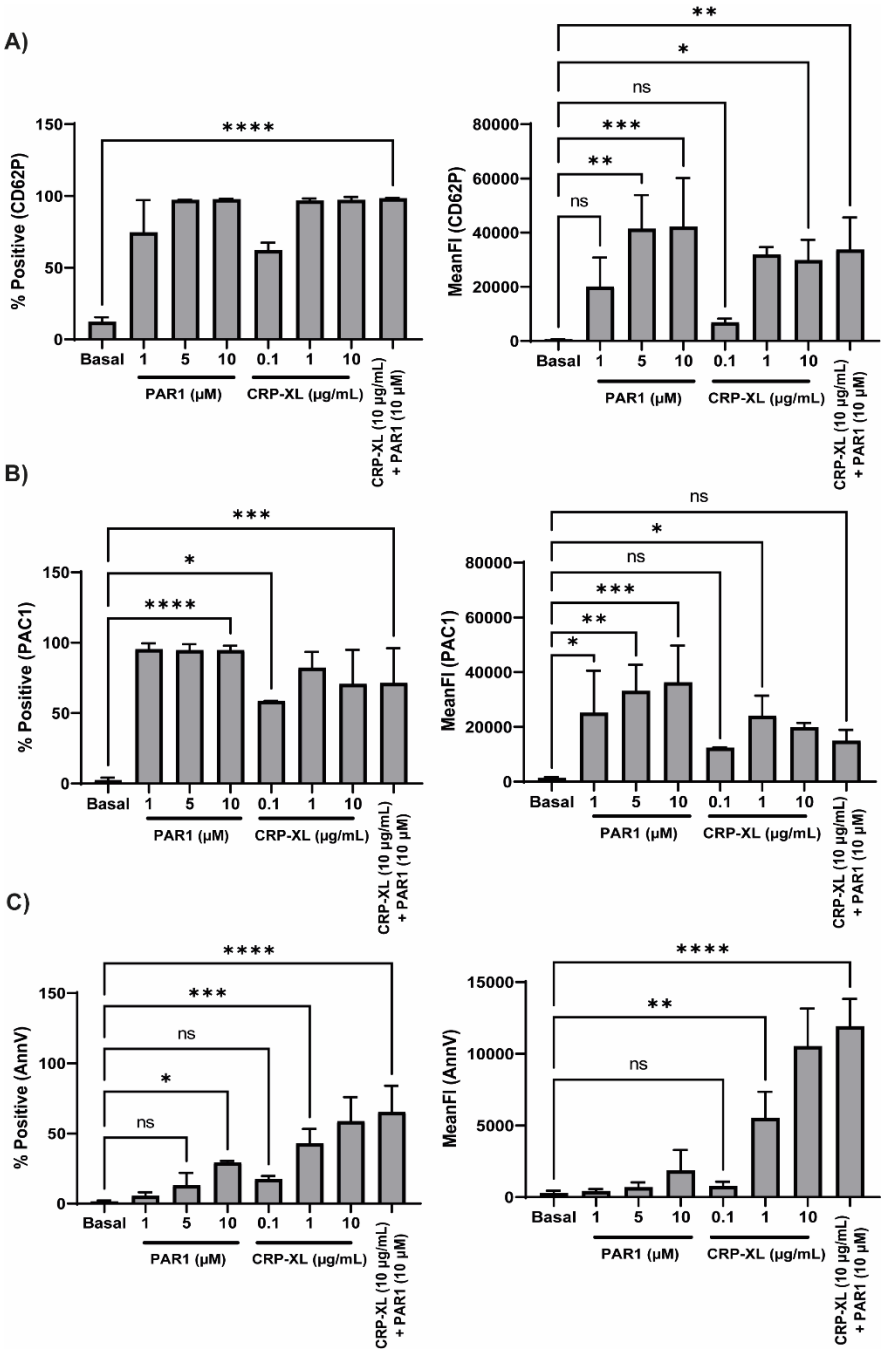

Figure 28. Optimisation of a four-parameter activation panel in human whole blood by flow cytometry

Human whole blood was stimulated with either PAR1 peptide (1-10 μM) or CRP-XL (0.1-10 μg/mL) and probed with CD62P (A), PAC1 (B) and AnnV (C) for 20 minutes prior to fixation in 1% PFA/PBS. CD42b was used as a platelet marker and samples were analysed for 10,000 platelet positive events. Bar graphs represent percent positive (left) and Mean Fluorescence Intensity (MeanFl) (right) over control. Data presented as mean ± SD and compared to basal by one-way ANOVA with Dunnett's multiple comparisons test (n=3, *≤0.05, **≤0.01, ***≤0.001, and ****≤0.0001).

3.4.5. Impaired sensitivity to PGI_2 in ACS patients' post-MI by four-parameter flow cytometry

Acute coronary syndrome (ACS) describes a range of conditions linked to sudden and reduced blood flow to the heart (Libby, 2001). One of the main conditions associated with ACS is myocardial infarction (MI) which is characterised by platelet-driven atherothrombotic events which ultimately lead to acute occlusion of a coronary vessel (Mitchell et al., 2008). Excessive platelet activation is typically regulated by PGI_2 and NO, but these protective mechanisms are overcome during MI.

After optimising the four-parameter flow cytometry activation panel we sought to assess the effect of PGI_2 on platelet activation in a "real world" scenario using patient cohort of post-MI individuals (n=7) and comparing these to healthy age-matched controls (n=15). Data from these patients were invaluable, allowing us to compare phenotypic characteristics of the AC6-KO mouse. Due to supply issues of CRP-XL, the assay used Convulxin (CVX), a snake venom known to activate GPVI signalling pathways (Jandrot-Perrus et al., 1997; Polgár et al., 1997). Whole blood was activated with PAR1 peptide (20 μM) and Convulxin (500 ng/mL), in the presence or absence of PGI_2 (100 nM) for 2 mins, and stained for PAC1, CD62P and AnnV (Figure 29).

Measurement of CD62P demonstrated that under basal conditions the expression of the α-granule marker was increased in the subjects with ACS (Figure 29 A). Here the level of CD62P 9.5 ± 4.4 % positive (healthy) compared to 23.0 ± 15.3 % positive (acute) ($p=0.02$). No difference in the levels of CD62P expression was observed at any of the agonists used. However, it was noticeable that MFI were elevated for each agonist concentration although this was only significant with PAR1 peptide alone. Interestingly, CD62P binding appeared to be unaffected by the presence of PGI_2 in both cohorts and is consistent with previous studies (Hindle et al., 2021).

Next, PAC1 binding at basal was unchanged between ACS patients and healthy controls. PAC1 binding displayed a defect in PGI_2 sensitivity in acute platelets (90.8 ± 12.4% positive) compared to control (68.1 ± 17.0% positive; $p<0.0001$) (Figure 29 B). This was also confirmed by MFI values;

12662.5±3989.1 (healthy) versus 26435.8±11100.7 (acute) (p=0.01), as well displaying a similar elevated response to PAR1 peptide in ACS patients compared to control (58410.3 ± 19696.6 MFI vs 36690.7 ± 7491.1 MFI, p=0.03).

Finally, AnnV binding, and expression revealed the most difference between the two cohorts. Basal AnnV binding was significantly elevated in platelets taken from subjects with ACS compared to controls (70.3 ± 20.5 % positive, vs 8.9 ± 1.9 % positive, p<0.0001) (Figure 29 C). Elevated AnnV expression at basal was also observed (138.9 ± 56.6 MFI vs 1577.6 ± 1096.6 MFI, p=0.008). The extent of AnnV binding upon agonist stimulation was significantly higher in ACS compared to control, in particular with PAR1 peptide (86.3 ± 14.2 % positive vs 23.5 ± 3.9 % positive, p=0.005). While MFI values only observed significance for platelets treated with PAR1 peptide alone 2756.3 ± 1170.2 MFI (acute) vs 522.1 ± 160.7 MFI (healthy) (p<0.0001). In addition to elevated basal and agonist stimulation, diminished sensitivity to PGI_2 was observed in ACS patients compared to controls (72.6 ± 17.5 % positive vs 23.6 ± 7.8 % positive, p=0.003) suggesting that platelets from subjects with ACS may be pre-activated and therefore insensitive to the effects of PGI_2. This observed inability of PGI_2 to inhibit AnnV expression was also demonstrated by MFI values in ACS patients compared to control (1915.3 ± 113.7 MFI vs 525.3 ± 205.6 MFI, p=0.01).

Altogether, these data demonstrate a defect in PGI_2 sensitivity in patients post-MI. Exposure of PS and integrin activation are largely affected in this patient cohort, whereas expression of CD62P is less so. The capacity for CD62P expression to be inhibited by PGI_2 even in healthy controls was weaker compared to AnnV and PAC1 expression (Hindle et al., 2021). While this defect in PGI_2 sensitivity could be due to pre-activated platelets present in platelets post-MI, impaired cAMP signalling could also be at play here. Faults in cAMP signalling could be attributed to activation of PDEs, IP receptor desensitisation or perhaps a fault in adenylyl cyclase activation in post-MI platelets (Fisch et al., 1997; Berger et al., 2018a; Bunting et al., 1983).

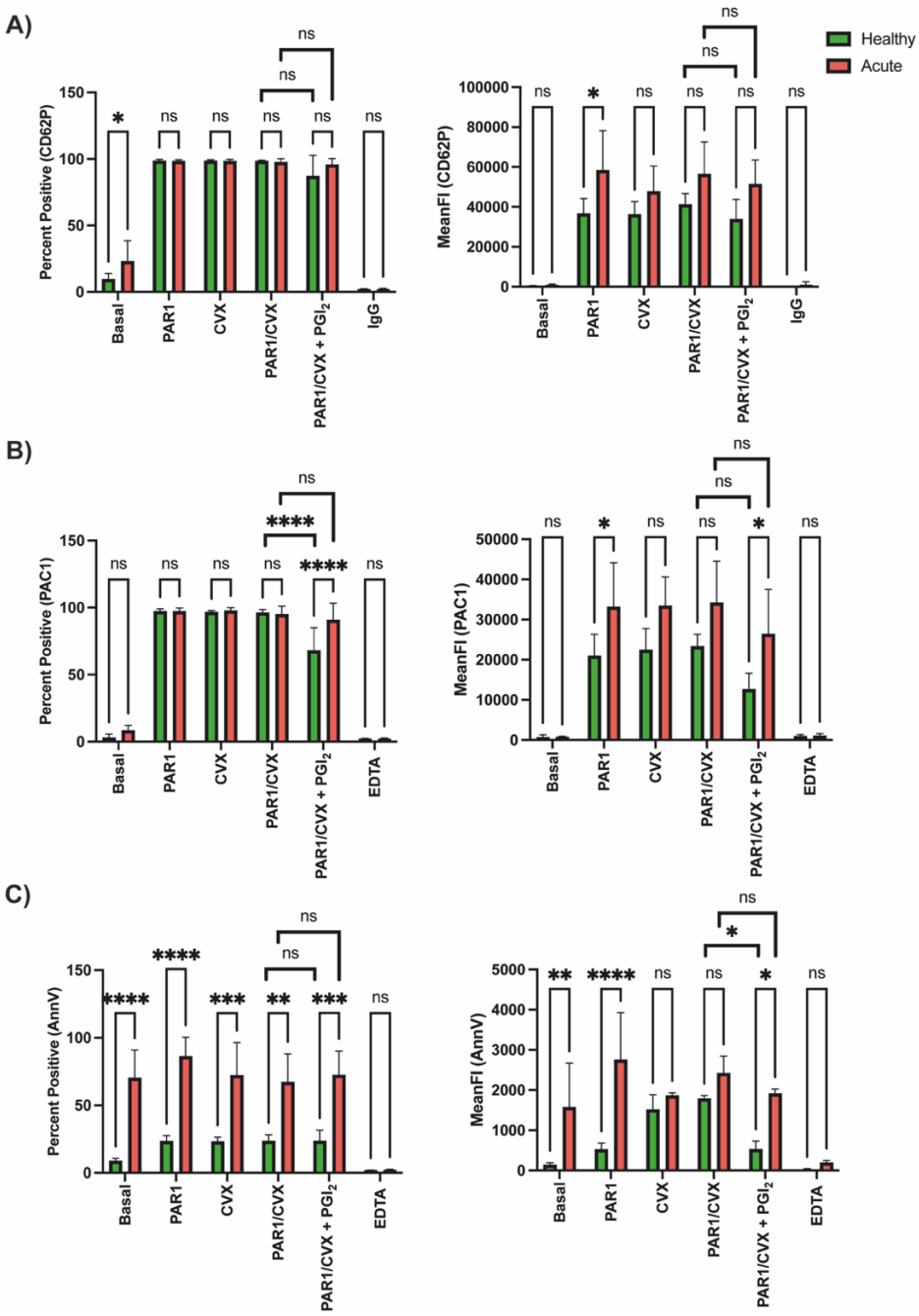

Figure 29. Elevated platelet activation and impaired sensitivity to PGI_2 in ACS patients' post-MI

Human whole blood was stimulated with either PAR1 peptide (20 μM) or CVX (500 ng/mL) and probed with CD62P (A), PAC1 (B) and Annexin V (C) for 20 minutes prior to fixation in 1% PFA/PBS. CD42b-BB700 was used as a platelet marker and samples were analysed for 10,000 platelet positive events. Bar graphs represent percent positive (left) and Mean Fluorescence Intensity (MeanFI) (right) over control. Data presented as mean ± SD and compared between healthy and acute as well as with and without PGI_2 by two-way ANOVA with Šídák's multiple comparisons test, n=5, *≤0.05, **≤0.01, ***≤0.001, and ****≤0.0001).

3.5. Optimisation of cAMP-elevating agents human washed platelets

To understand different aspects of cAMP signalling the use of several pharmacological tools that target different aspects of cAMP signalling were employed. PGI_2 was used to assess IP receptor-mediated cAMP production, whereas forskolin, a diterpene isolated from the Indian plant called *Forskohlii* (Seamon and Daly, 1981; Seamon et al., 1981), was used to examine cAMP production via activating all AC isoforms, except AC9. Forskolin is a direct AC activator and therefore allows us to assess cAMP signalling in a receptor-independent fashion. Alternatively, adenosine increases cAMP production by the G-protein-coupled A_2 receptor, providing another signalling pathway for assessing receptor-mediated cAMP production (Fredholm et al., 2001; Johnston-Cox and Ravid, 2011). Lastly, 8-CPT-cAMP is a direct lipophilic activator of cAMP leading to activation of PKA (Geiger et al., 1992).

3.5.1. Measurement of cAMP synthesis in human washed platelets

Washed platelets ($2x10^8$ platelets/mL) were incubated with increasing concentrations of PGI_2 (1-100 nM), forskolin (1-20 μM) or adenosine (10-100 μM) and reactions were terminated by a lysis buffer containing 2.5% dodecyltrimethylammonium bromide. Intracellular cAMP was measured using a commercially available cAMP enzyme immunoassay system (Cytiva).

All cAMP-elevating agents increased production of cAMP in a concentration dependent manner. Interestingly, forskolin (20 μM) displayed a 5-fold higher production of cAMP, while adenosine (100 μM) demonstrated a 3-fold higher cAMP production compared to PGI_2 (100 nM) (Figure 30). Levels of cAMP were elevated in response at to PGI_2 at 2 mins and was sustained for up to 20 mins (5250.4 ± 1284.9 fmol/10^7 platelets at 100 nM and 5250.4 ± 1284.9 fmol/10^7 platelets, at 1000 nM). At 60 mins the levels of cAMP began to drop, for platelets treated with PGI_2 at 100nM, cAMP returned to levels near basal (1185.4 ± 850.1 fmol/10^7 platelets at basal vs 1783.9 ± 1112.0 fmol/10^7 platelets at 60 mins). However, for PGI_2 at 1000 nM, the decline in cAMP levels was more subtle (4177.5 ± 971.2 fmol/10^7 platelets) likely due to saturating the system with such a high concentration of PGI_2.

Forskolin treated platelets increased from 46.5 ± 38.2 fmol/10^7 platelets (basal) to 22592.0 ± 5605.4 fmol/10^7 platelets (20 µM), while adenosine treated platelets increased from 1042 ± 67.8 fmol/10^7 platelets (basal) to 13982.0 ± 822.4 fmol/10^7 platelets (100 µM).

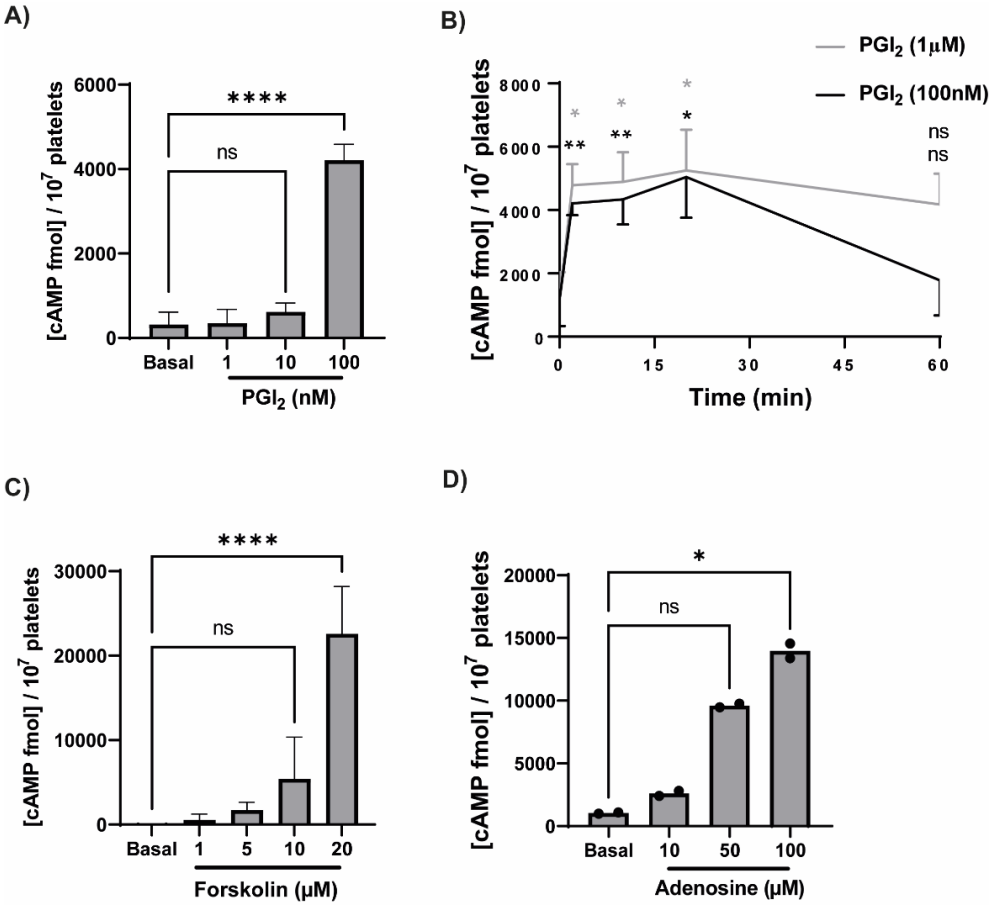

Figure 30. Optimisation of cAMP-elevating agents on cAMP production in human washed platelets

Human washed platelets (2x10^8 platelets/mL) were incubated with increasing concentrations of PGI_2 (1-100 nM; n=5) (A) for 2 mins, PGI_2 at (100-1000nM; n=4) over time (B), increasing concentrations of forskolin (1-20µM; n=3) (C) or Adenosine (10-100 µM; n=2) (D) for 5 mins. Reactions were terminated by the addition of lysis buffer containing 2.5% dodecyltrimethylammonium bromide and cAMP levels were assayed with a commercially available enzyme immunoassay system (GE Healthcare) and expressed as fmol cAMP/10^7 platelets. All assays were carried out in duplicate with independent platelet donors. Data presented as means ± SD and compared to basal by one-way ANOVA with Dunnett's multiple comparisons test (*≤0.05, **≤0.01, and ****≤0.0001)

3.5.2. PKA substrate phosphorylation in response to cAMP-elevating agents in human washed platelets

Since establishing the effect of AC-activating agents on cAMP production, the next series of experiments examined their ability to activate downstream PKA signalling events. We used immunoblotting to measure phospho-VASP^{Ser157}, a key PKA substrate in response to PGI_2, forskolin and 8-CPT-cAMP (a direct PKA agonist). Washed platelets ($5x10^8$ platelets/mL) were treated with increasing concentrations of PGI_2 (1-1000 nM) for 2 mins, forskolin (1-20 µM) and 8-CPT-cAMP (5-100 µM) for 5 mins, as well as PGI_2 (100 nM), forskolin (10 µM) and 8-CPT-cAMP (100 µM) for increasing periods of time (Figure 31). Reactions were terminated by the addition of Laemmli buffer and separated via SDS-PAGE to be analysed via immunoblotting.

Consistent with cAMP production, all cAMP-elevating agents increased phospho-VASP^{Ser157} in a concentration-dependent manner. Treatment with forskolin and 8-CPT-cAMP increased VASP^{Ser157} phosphorylation consistently over time (Figure 31 C-D), while PGI_2 peaked at 2 minutes (93.7 ± 25.2% p-VASP^{Ser157} expression over control) before declining (Figure 31 B) . Forskolin and 8-CPT-cAMP are both strong activators of PKA compared to PGI_2. Understandably, as PGI_2 acts through the IP receptor whereas forskolin and 8-CPT-cAMP take effect in a more direct fashion. Optimal incubation time for PGI_2 for immunoblot analysis was observed at 2 mins and was therefore the chosen incubation time throughout this study. Altogether these data demonstrate that platelets are responsive to different cAMP-elevating agents.

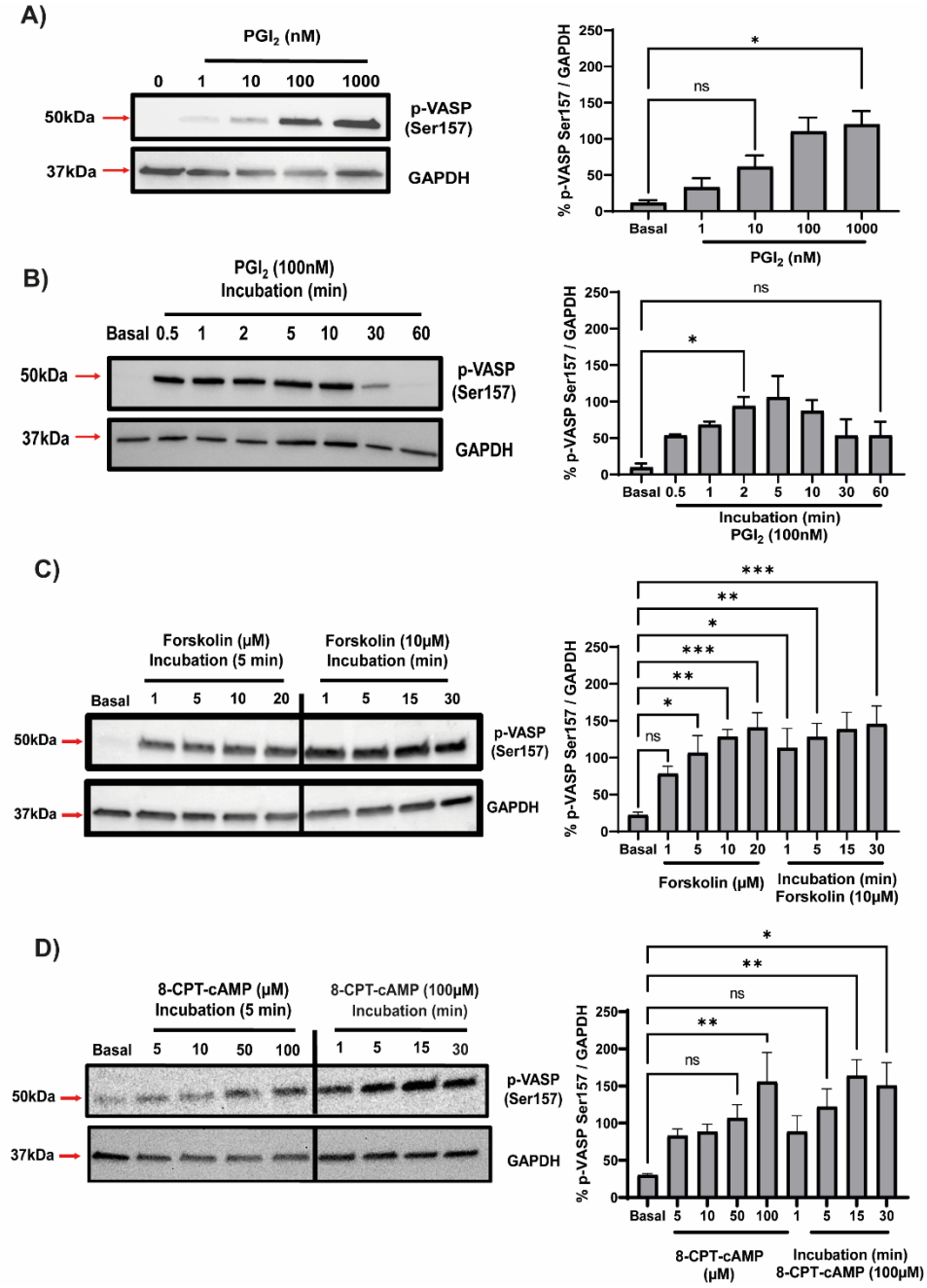

Figure 31. Optimisation of VASP phosphorylation in response to cAMP-elevating agents in human washed platelets

Human washed platelets ($5x10^8$ platelets/ml) were lysed in 2x Laemmli buffer, separated via SDS-PAGE and immunoblotted for p-$VASP^{Ser157}$ with a GAPDH loading control. Platelets were stimulated with increasing concentrations of prostacyclin for 2 min (A) or PGI_2 (100 nM) over time (B) or forskolin (C) or 8-CPT-cAMP (D) under constant stirring (1000 rpm) at 37˚C. Bar graphs represent densitometry analysis carried out using ImageJ software. Data presented as mean ± SD and compared to basal by one-way ANOVA with Dunnett's multiple comparisons test (n=4, ns = not significant, *≤0.05, **≤0.01, ***≤0.001, and ****≤0.0001).

3.5.3. Assessment of VASP phosphorylation in response to PGI_2 in human whole blood

To cross-validate responses to PGI_2 on PKA phosphorylation, we used a phosphoflow assay, whereby assessment of intracellular phosphorylation can be carried out in whole blood and analysed by flow cytometry (Spurgeon et al., 2014). There are two phosphorylation sites of VASP, Ser157 and Ser239. It is proposed that the former is preferential to PKA, while the latter is preferential to PKG (Waldmann et al., 1987). However, cross-talk between cAMP and cGMP is widely accepted and an elegant study by Spurgeon and colleagues have shown that PGI_2 can phosphorylate VASP at both sites (Spurgeon et al., 2014) as measured by phosphoflow cytometry and immunoblotting. Based on this we decided to measure both sites of VASP in response to PGI_2 in this assay.

Whole blood was treated with increasing concentrations of PGI_2 (1-100 nM) for 2 mins before cells were fixed, permeabilised and stained for phospho-$VASP^{Ser157}$ and phospho-$VASP^{Ser239}$ prior to analysis by flow cytometry. Phosphorylation of VASP at both sites increased in a concentration-dependent manner in response to PGI_2 (Figure 32). Interestingly, at 100 nM of PGI_2, phosphorylation of $VASP^{Ser239}$ appeared to be more profound compared to phosphorylation of $VASP^{Ser157}$ (30.6 ± 6.5-fold over basal vs 11.8±6.1 fold over basal, respectively). While phosphorylation of VASP at 10 nM of PGI_2 was consistent between the two phosphorylation sites (9.7 ± 5.3-fold over basal $VASP^{Ser157}$ vs 6.7 ± 2.5-fold over basal $VASP^{Ser239}$).

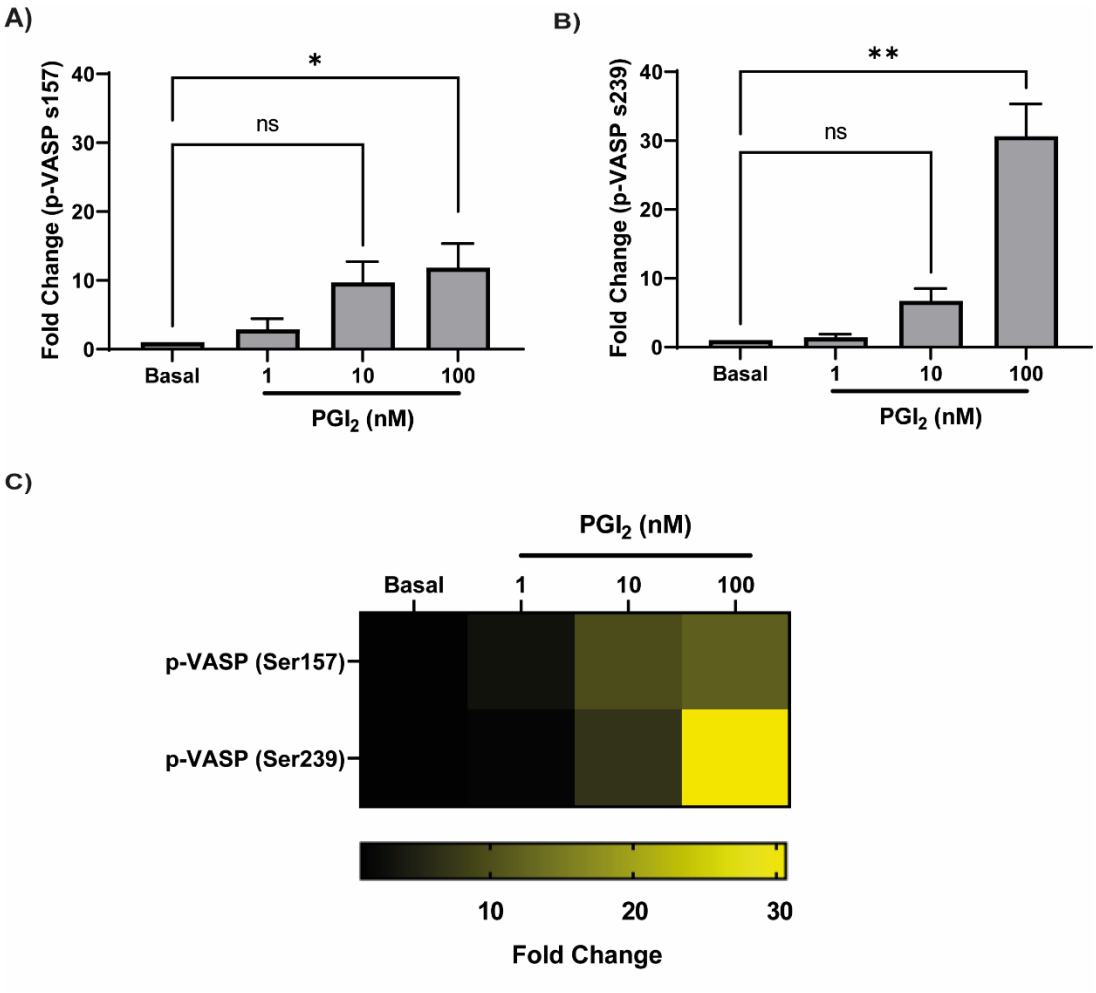

Figure 32. Assessment of VASP phosphorylation in human whole blood via phosphoflow cytometry

Human whole blood was treated with increasing PGI_2 concentrations for 2 mins. Cells were fixed, permeabilised, stained for desired phospho-protein and then analysed by flow cytometry. Measuring for p-VASP^{Ser157} (A) and p-VASP^{Ser239} (B). Bar graphs represent fold change over basal and heatmap represents mean fold change over basal whereby an increase in fold change is indicated by a colour change to yellow (C). Data presented as means ± SD and compared to basal by one-way ANOVA with Dunnett's multiple comparisons tests (n=3, ns = not significant, *≤0.05, and **≤0.01)

3.5.4. Phosphorylation of multiple PKA substrates in human washed platelets

To cross-validate phospho-VASP data, we assessed PKA substrate phosphorylation in response to cAMP-elevating agents using a pan phospho-PKA substrates antibody. Washed platelets $5x10^8$ platelets/mL were treated with increasing concentrations of PGI_2 (1-1000 nM) for 2 mins, forskolin (1-20 µM) and 8-CPT-cAMP (5-100 µM) for 5 mins (Figure 33). Reactions were terminated by the addition of Laemmli buffer and separated via SDS-PAGE to be analysed by immunoblotting.

Consistent with phosphorylation of VASP, the extent of general PKA substrate phosphorylation increased in a concentration-dependent manner upon treatment with cAMP-elevating agents. Whole-lane densitometry analysis displayed a subtle increase in PKA substrate phosphorylation in platelets stimulated with PGI_2 (1-100 nM), while the phosphorylation at 1000 nM of PGI_2 was much more profound (Figure 33 A). In addition, the extent of PKA substrate phosphorylation was more intense in platelets incubated with forskolin and 8-CPT-cAMP compared to PGI_2 (Figure 33 B-C). Interestingly, the band are ~150 kDa reduced with increasing PGI_2 concentrations, whereas upon treatment with forskolin and 8-CPT-cAMP an increase was observed. The variations observed are likely due to the differences in target. Forskolin and 8-CPT-cAMP are direct cAMP-elevating agents, whereas PGI_2 is dependent on the IP receptor.

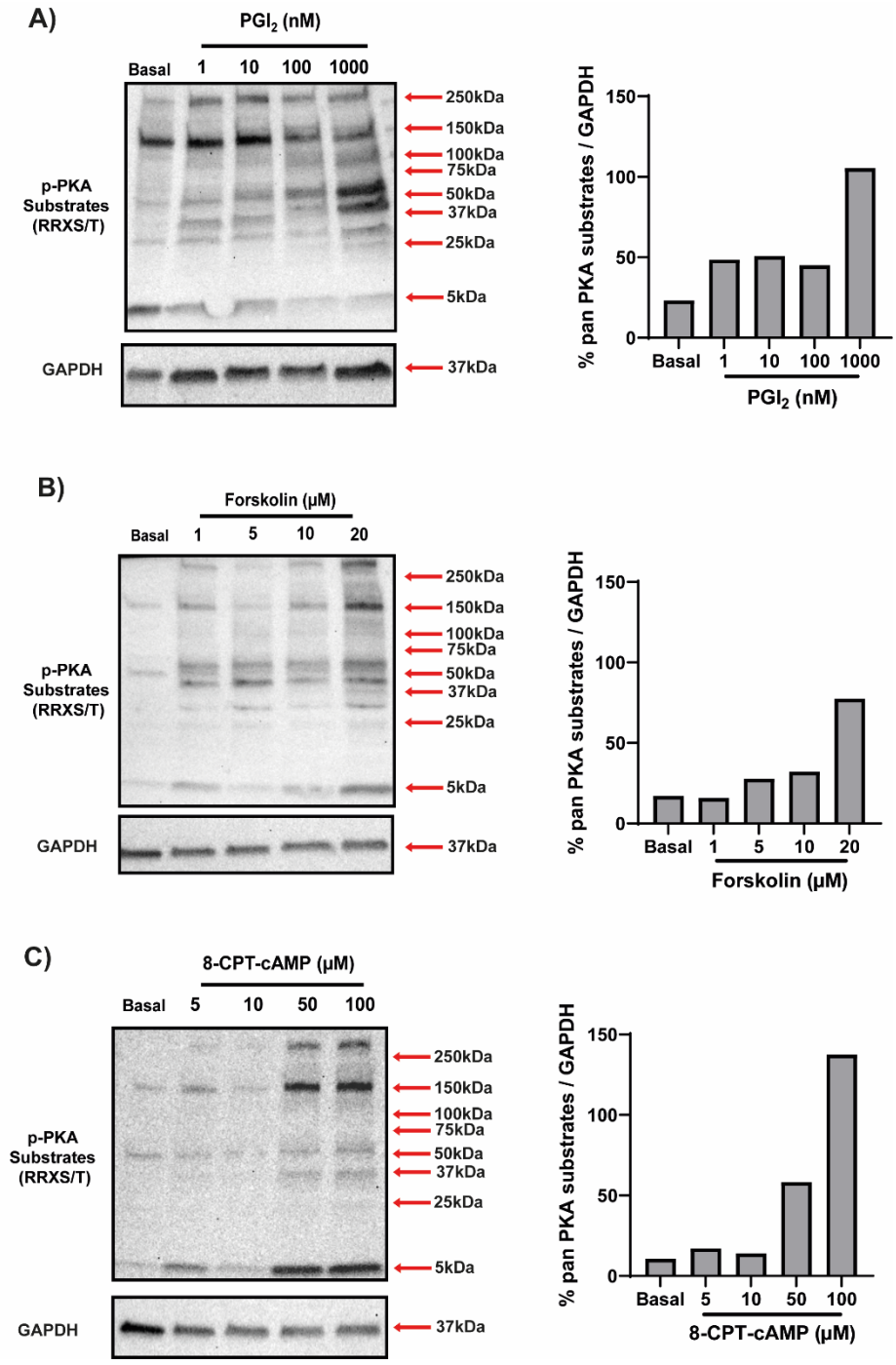

Figure 33. Phosphorylation of PKA substrates in response to cAMP-elevating agents in human washed platelets

Human washed platelets ($5x10^8$ platelets/mL) were lysed in 2x Laemmli buffer, separated via SDS-PAGE and immunoblotted for p-PKA Substrates (RRXS/T) with a GAPDH loading control. Platelets were stimulated with increasing concentrations of PGI_2 for 2 min (A) or forskolin for 5 mins (B) or 8-CPT-cAMP for 5 mins (C) under constant stirring (1000 rpm) at 37˚C. Representative images (left) and whole lane densitometry analysis (right) (n=1).

Another key aspect of cAMP signalling are phosphodiesterase's (PDEs), in particular PDE3A which hydrolyses the second messenger and can be phosphorylated by PKA (Murthy et al., 2002).

PGI_2 and forskolin induced a concentration-dependent increase in $PDE3A^{Ser312}$ phosphorylation (Figure 34). Platelets treated with forskolin reached maximal $PDE3A^{Ser312}$ phosphorylation at 1 µM (174.1±28.5 % p-$PDE3A^{Ser312}$) with no significant increase at the higher concentrations (10-20 µM) whereas PGI_2 reached maximal at 100 nM (143.3± 14.4 % p-$PDE3A^{Ser312}$).

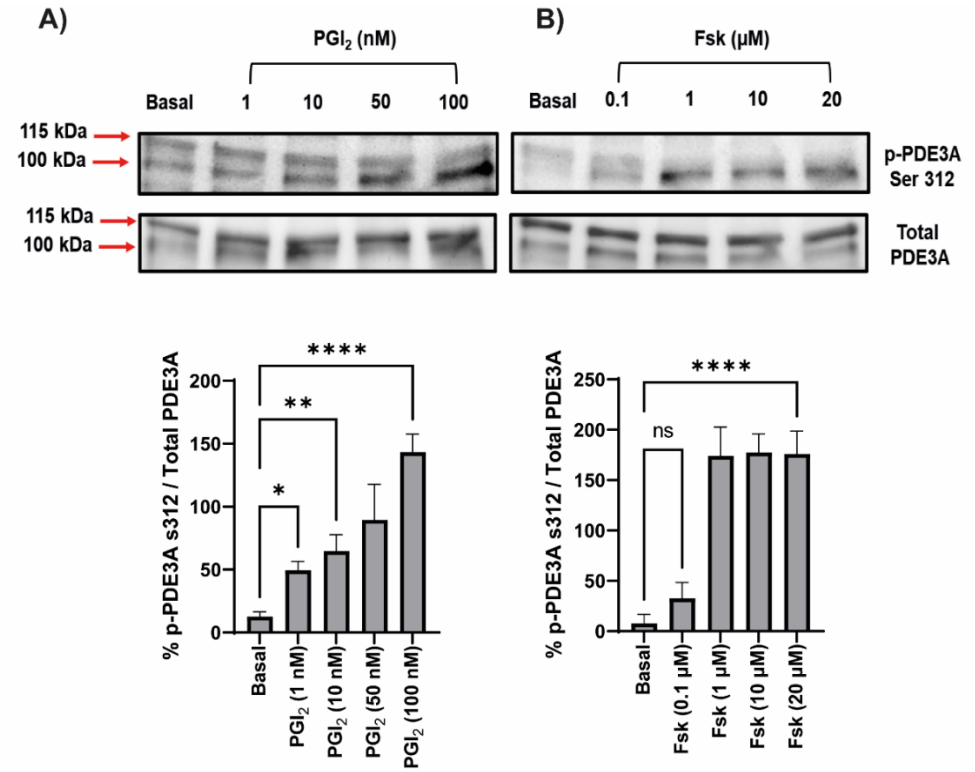

Figure 34. Measurement of PDE3A phosphorylation by cAMP-elevating agents

Human washed platelets ($5x10^8$ platelets/mL) were lysed in 2x Laemmli buffer, separated via SDS-PAGE and immunoblotted for phospho-$PDE3A^{Ser312}$ with a total PDE3A loading control. Platelets were stimulated with increasing concentrations of PGI_2 for 2 min (A) or forskolin for 5 mins (B) under constant stirring (800 rpm) at 37˚C. Data presented as means ± SD and compared to basal by one-way ANOVA with Dunnett's multiple comparisons test (n=3, ns = not significant, *≤0.05, **≤0.01 and ****≤0.0001).

3.6. Optimisation of PKA inhibitors in human washed platelets

Since establishing how cAMP-elevating agents affect cAMP production and subsequent PKA substrate phosphorylation, the effect of different PKA inhibitors on PGI_2 treated platelets were also assessed. Initial characterisation of PKA inhibitors was performed in human washed platelets before assessment in murine platelets and eventually AC6-KO platelets.

3.6.1. Inhibition of PGI_2-induced VASP phosphorylation using PKA inhibitors in human washed platelets

It was important to characterise and optimise the PKA inhibitors before translating them into murine platelets. RP-8-CPT-cAMP, H89 and KT-5720 are direct PKA inhibitors (Dostmann et al., 1990; Bain et al., 2003; Gambaryan et al., 2004; Lochner and Moolman, 2006) and SQ22536 is a direct AC inhibitor (Emery et al., 2013). Washed platelets ($5x10^8$ platelets/mL) were treated with increasing concentrations of RP-8-CPT-cAMP (50-250 µM), SQ22536 (1-50 µM) and H89/KT-5720 (1-20 µM) for 25 mins at 37°C before addition of PGI_2 (100 nM) for a further 2 mins and VASP phosphorylation was evaluated.

Each PKA inhibitor prevented phosphorylation of $VASP^{Ser157}$ in the presence of PGI_2 in a concentration dependent manner. Treatment with H89 and KT-5720 (20 µM) combined reduced from 1.80 $p\text{-}VASP^{Ser157}$ fold over basal (PGI_2, 100 nM) to 0.40 $p\text{-}VASP^{Ser157}$ fold over basal (Figure 35). While platelets treated with RP-8-CPT-cAMP (50 µM) reduced VASP phosphorylation to below basal (0.70-fold over basal: PGI_2 100 nM). Lastly, the direct AC inhibitor SQ22356 reduced PGI_2-mediated VASP phosphorylation from 1.70-fold over basal (PGI_2,100 nM) to 0.06-fold over basal (SQ22536, 50 µM).

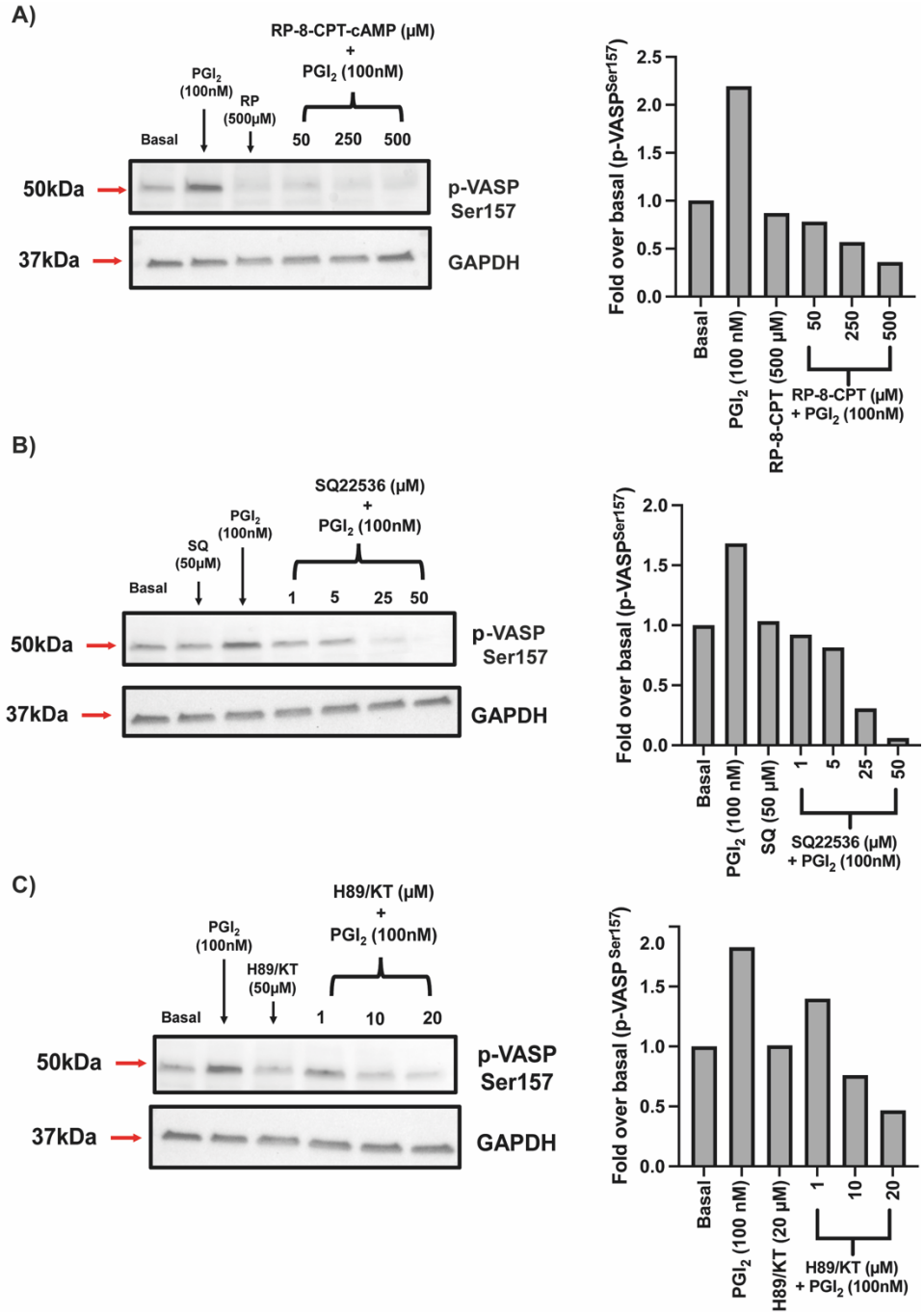

Figure 35. Optimisation of commercially available inhibitors of cAMP signalling in human washed platelets

Human washed platelets ($5x10^8$ platelets/ml) were lysed in 2x Laemmli buffer, separated via SDS-PAGE and immunoblotted for p-PKA Substrates (RRXS/T) with a GAPDH loading control. Platelets were pre-treated with RP-8-CPT-cAMPs (A) or SQ22536 (B) or H89 & KT-5720 (C) then stimulated with prostacyclin (100nM) for 2 min under constant stirring (00 rpm) at 37˚C. Bar graphs represent densitometry analysis carried out using ImageJ software, displayed as fold over basal (n=1).

3.7. Validation of platelet isolation method for murine wild-type washed platelets

As described in 3.2, it was important to establish an appropriate platelet isolation method for murine platelets. The PGI_2 method was compared with an adapted version of the pH method (Cazenave et al., 2004; Aurbach et al., 2019). Murine whole blood was collected from the inferior vena cava under inhalation anaesthetic into syringes containing ACD using a 25-G needle. The quantity of blood obtained from a mouse at ~8 weeks of age is ~1 mL. The method of isolation uses 1 volume of ACD for 5 volumes of murine whole blood. Murine washed platelets were then isolated as described in 2.3.2. It was important to assess whether this method was viable for the rest of the study, so we compared it to the well-known PGI_2 method of isolation using C57BL/6 (wild type) mice.

3.7.1. Assessment of platelet function in murine platelets

Washed platelets isolated via the PGI_2 method, or the adapted pH method (denoted as pH) were stimulated with thrombin (0.05-0.1 U/mL), or collagen (5-10 µg/mL) and aggregation was assessed for up to 5 minutes (Figure 36). Comparison of the data shows no significant difference in percentage maximal aggregation when stimulated with either thrombin or collagen. At 0.05 U/mL of thrombin percentage max aggregation was near the same (58.6±15.9% adapted pH method vs 54.0% PGI_2 method), similarly collagen at 5 µg/mL displayed no differences (47.5 ± 0.7% adapted pH method vs 52.0% PGI_2 method). Confirming that platelets isolated via the adapted pH method are functional and is a viable method for isolating murine platelets without affecting cAMP signalling.

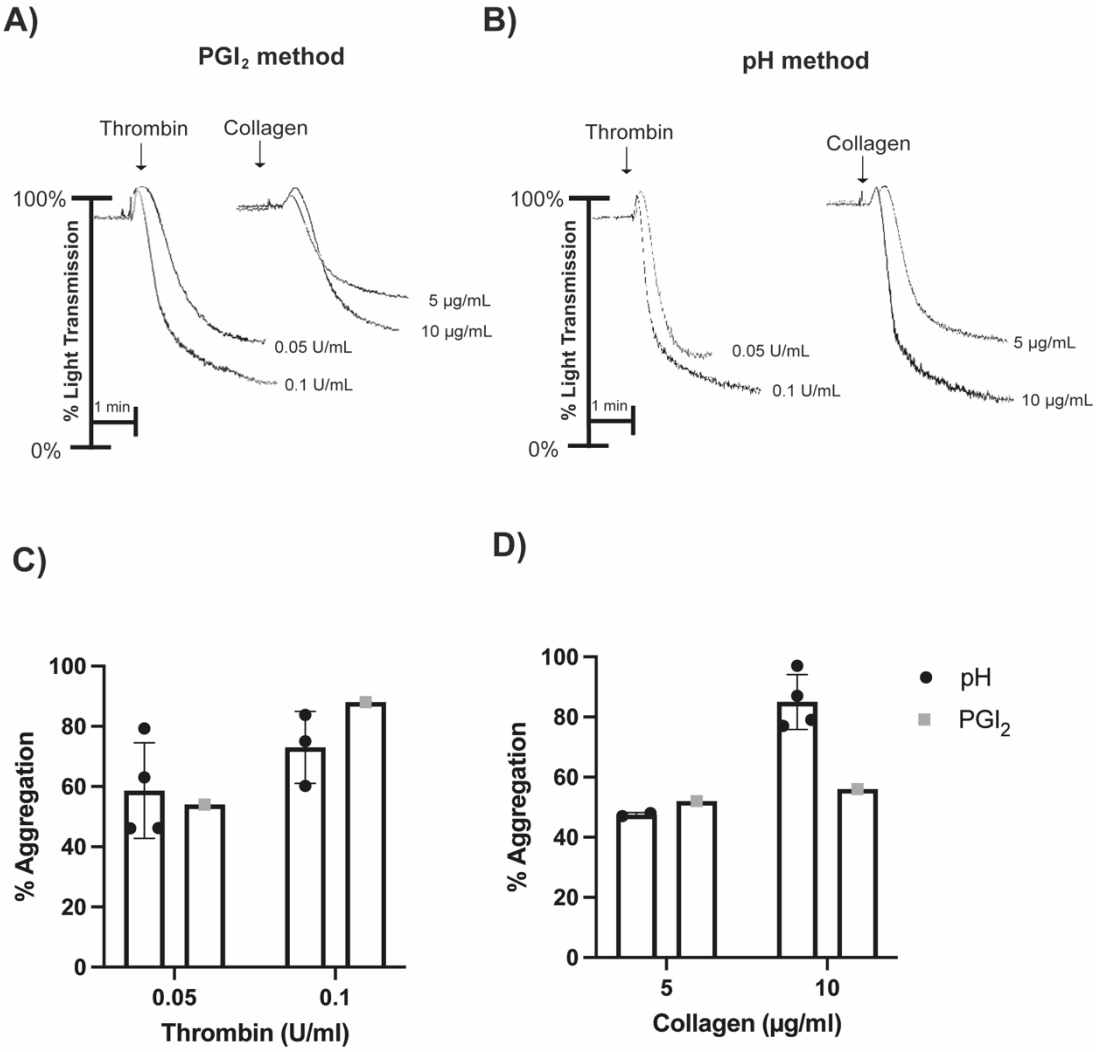

Figure 36. Validation of murine platelet isolation method

Murine washed platelets ($2x10^8$ platelets/mL) were isolated via the PGI_2 method (A) or the pH method (B) and treated with either collagen or thrombin at marked concentrations under constant stirring (100 rpm) at 37°C for up to 10 minutes. Representative aggregation traces were generated by AggroLink Software (Chronolog, USA). Bar graphs represent percentage aggregation at 5 minutes presented as individual values, pH method (●) and PGI_2 method (▪).

3.7.2. Response to PGI_2 in murine washed platelets

The sensitivity to the inhibitory effects of PGI_2 in murine platelets was then tested. Washed platelets ($2x10^8$ platelets/mL) were pre-treated with PGI_2 (1-100 nM) for 2 mins prior to stimulation with thrombin (0.05 U/mL) or collagen (5 µg/mL), while aggregation was observed for up to 10 minutes. The response to PGI_2 in both thrombin and collagen treated platelets was subtle between 1-10 nM PGI_2, while 100 nM of PGI_2 significantly inhibited platelet aggregation (Figure 37). Thrombin (0.05 U/mL) aggregation alone generated 86.7 ± 5.9 % aggregation, while in the presence of PGI_2 (100 nM) aggregation reached only 6.6 ± 2.8% aggregation ($p<0.0001$). Collagen (5 µg/mL) alone reached 82.9 ± 2.4 % aggregation which was then reduced to 15.7 ± 3.0 % aggregation by PGI_2 (100 nM) ($p<0.0001$).

Murine platelets appear to be less sensitive to PGI_2 than human platelets, however this could be due to the concentration of agonists used in this assay. Based on the lack of clear dose response to PGI_2, we decided to reduce the agonist concentrations to 0.035 U/mL for thrombin and 2 µg/mL for collagen to allow us to observe subtle changes in cAMP signalling in the AC6-KO.

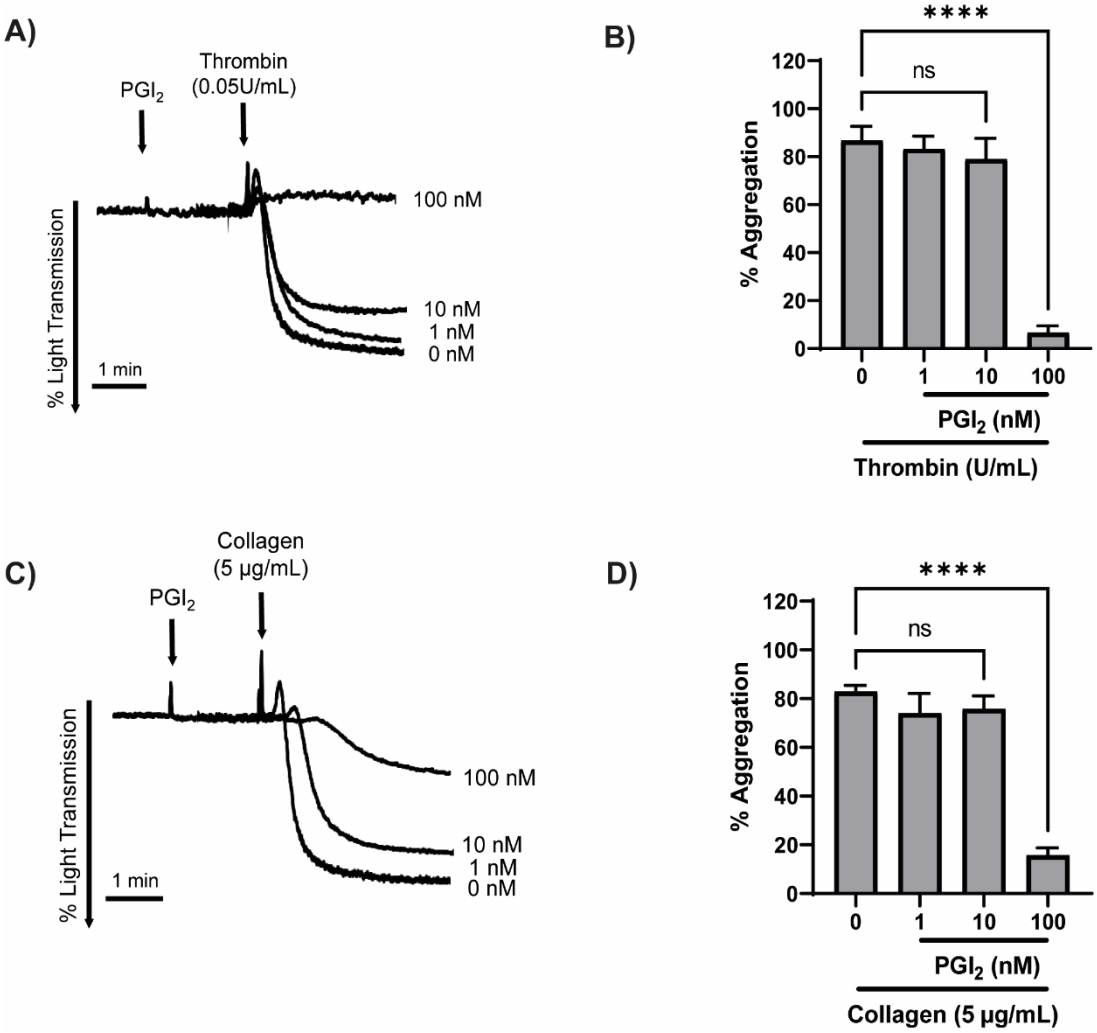

Figure 37. Sensitivity to PGI_2 in wild-type murine platelets

Murine washed platelets ($2x10^8$ platelets/ml) were treated pre-incubated with increasing concentrations of PGI_2 (1-100 nM) for 2 mins and then stimulated with either thrombin (0.05 U/mL) (A-B) or collagen (5 µg/mL) (C-D) under constant stirring (800 rpm) at 37°C for up to 10 minutes. Representative aggregation traces were generated by AggRAM software (Helena Biosciences, UK). Bar graphs represent percentage aggregation at 10 minutes presented as means ± SD and compared to agonist alone by one-way ANOVA with Dunnett's multiple comparisons test (n=3, ns= not significant, ****≤0.0001).

3.8. Validation of cAMP-elevating agents on cAMP signalling in murine washed platelets.

After establishing cAMP-elevating agents in human platelets, we decided to assess whether these tools were as equally effective in murine platelets.

3.8.1. Assessment of cAMP production in murine platelets

To establish whether the commercially available cAMP assay was viable to use in murine platelets, we tested the effect of PGI_2 as either a function of concentration or a function of time on cAMP production. Synthesis of cAMP in response to PGI_2 increased over time, peaking at 30 secs (8167.6 ± 2603.4 fmol/10^7 platelets) (Figure 38 A). In addition, production of cAMP increased in a concentration-dependent fashion in the presence of PGI_2 (Figure 38 B). These data confirm that the cAMP EIA kit is sufficient to assess production of cAMP in murine platelets.

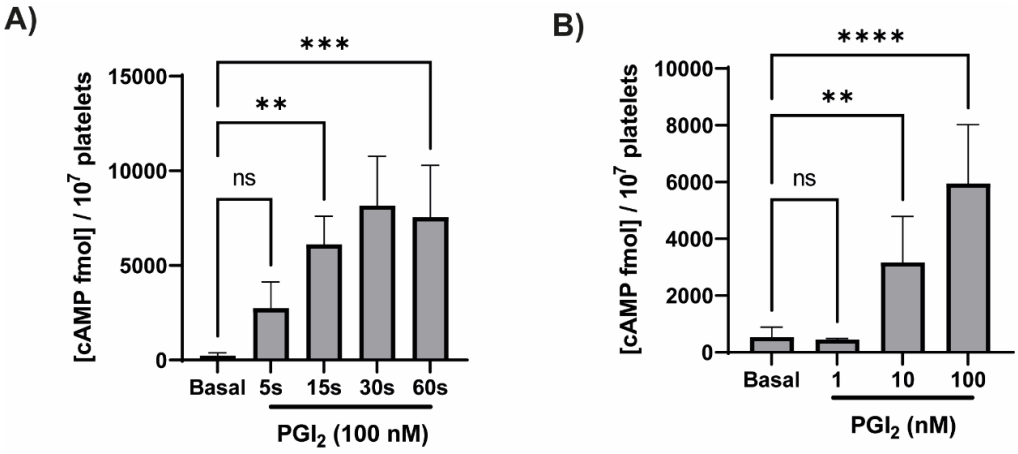

Figure 38. Measurement of cAMP production in response to PGI_2 in murine platelets

Murine washed platelets (2x10^8 platelets/mL) were treated with PGI_2 (100 nM) over time (A) or increasing concentrations of PGI_2 (1-100 nM) at 30 secs (B) at RT. Reactions were terminated by the addition of lysis buffer containing 2.5% dodecyltrimethylammonium bromide and cAMP levels were assayed with a commercially available enzyme immunoassay system (Cytiva) and expressed as fmol cAMP/10^7 platelets. All assays were carried out in duplicate. Data presented as means ± SD and compared to basal by one-way ANOVA with Dunnett's multiple comparisons test (n=3, **≤0.01, ***≤0.001, and ****≤0.0001).

3.8.2. Assessment of VASP phosphorylation via immunoblot in murine platelets

Since establishing that cAMP production in murine platelets in response to PGI_2, is comparable to human platelets, VASP phosphorylation in response to different cAMP-elevating agents was also examined.

Phosphorylation of $VASP^{Ser157}$ increased over time in response to PGI_2 peaking at 2 mins (197.4 ± 54.1 % p-$VASP^{Ser157}$) before returning to near basal at 60 mins (50.9 ± 44.5 % p-$VASP^{Ser157}$) (Figure 39 B). In response increasing concentrations of PGI_2, phosphorylation of $VASP^{Ser157}$ phosphorylation increased peaking at 100 nM (96.5 ± 33.5 % p-$VASP^{Ser157}$) and maintaining high levels of phosphorylation. We observed a similar trend in response to increasing forskolin and 8-CPT-cAMP concentrations. Forskolin-mediated Phosphorylation of $VASP^{Ser157}$ increased with concentration, peaking at 10 µM (70.1 ± 15.3 % p-$VASP^{Ser157}$) and 8-CPT-cAMP-mediated phosphorylation of $VASP^{Ser157}$ reached 153.2 ± 43.5 % at 1000 µM.

While $VASP^{Ser157}$ phosphorylation increased in response to PGI_2, forskolin and 8-CPT-cAMP with rising concentrations (Figure 39), forskolin displayed a weaker response compared to platelets treated with PGI_2 and 8-CPT-cAMP. This could suggest that murine platelets are more sensitive to inhibition by PGI_2 than human platelets, while human platelets could be more responsive to inhibition by forskolin (Figure 31 & Figure 39). These data demonstrate that murine platelets are responsive to cAMP-elevating agents as shown by a concentration-dependent increase in $VASP^{Ser157}$ phosphorylation.

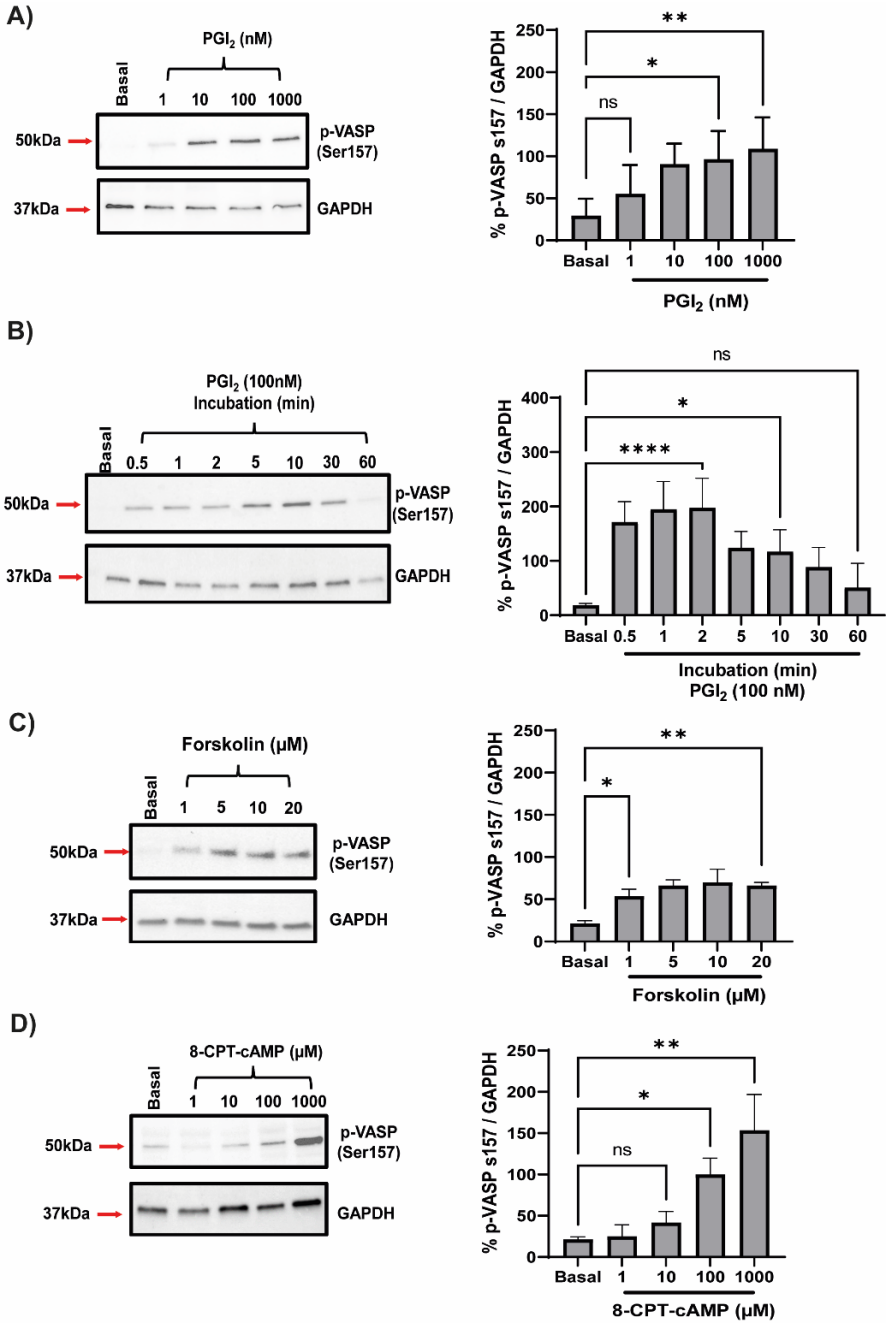

Figure 39. Validation of cAMP-elevating agents in murine platelets by measurement of p-VASP^{Ser157}

Murine washed platelets (5x10^8 platelets/mL) were lysed in 2x Laemmli buffer, separated via SDS-PAGE and immunoblotted for p-VASP^{Ser157} with a GAPDH loading control. Platelets were stimulated with increasing concentrations of PGI_2 for 2 min (A) or PGI_2 (100 nM) over time (B) or forskolin (C) or 8-CPT-cAMP (D) under constant stirring (800 rpm) at 37˚C. Bar graphs represent densitometry analysis carried out using ImageJ software. Data presented as means ± SD and compared to basal by one-way ANOVA with Dunnett's multiple comparisons test (n=3, ns = not significant, *≤0.05, **≤0.01 ***≤0.001 and ****≤0.0001).

3.8.3. Measurement of VASP phosphorylation in murine whole blood by phosphoflow

After confirming that VASP phosphorylation was consistent in murine platelets and human platelets, VASP phosphorylation in murine whole blood was assessed by phosphoflow cytometry. Murine whole blood was treated with increasing concentrations of PGI_2 (0.1-100 nM) for 2 mins before cells were fixed, permeabilised and stained for phospho-$VASP^{Ser157}$ and phospho-$VASP^{Ser239}$ prior to analysis by flow cytometry.

Phosphorylation of VASP at both sites increased in a concentration-dependent manner in response to PGI_2 (Figure 40). Consistent with human VASP phosphorylation, at 100 nM of PGI_2, phosphorylation of $VASP^{Ser239}$ appeared to be even more profound compared to $VASP^{Ser157}$ (13.8 ± 3.7-fold over basal vs 3.5 ± 0.4-fold over basal, respectively). While phosphorylation of VASP at 10 nM of PGI_2 was consistent between the two phosphorylation sites (1.8 ± 0.8-fold over basal $VASP^{Ser157}$ vs 2.0 ± 1.4-fold over basal $VASP^{Ser239}$). These data confirm that phosphoflow assessment of VASP phosphorylation is applicable in murine platelets.

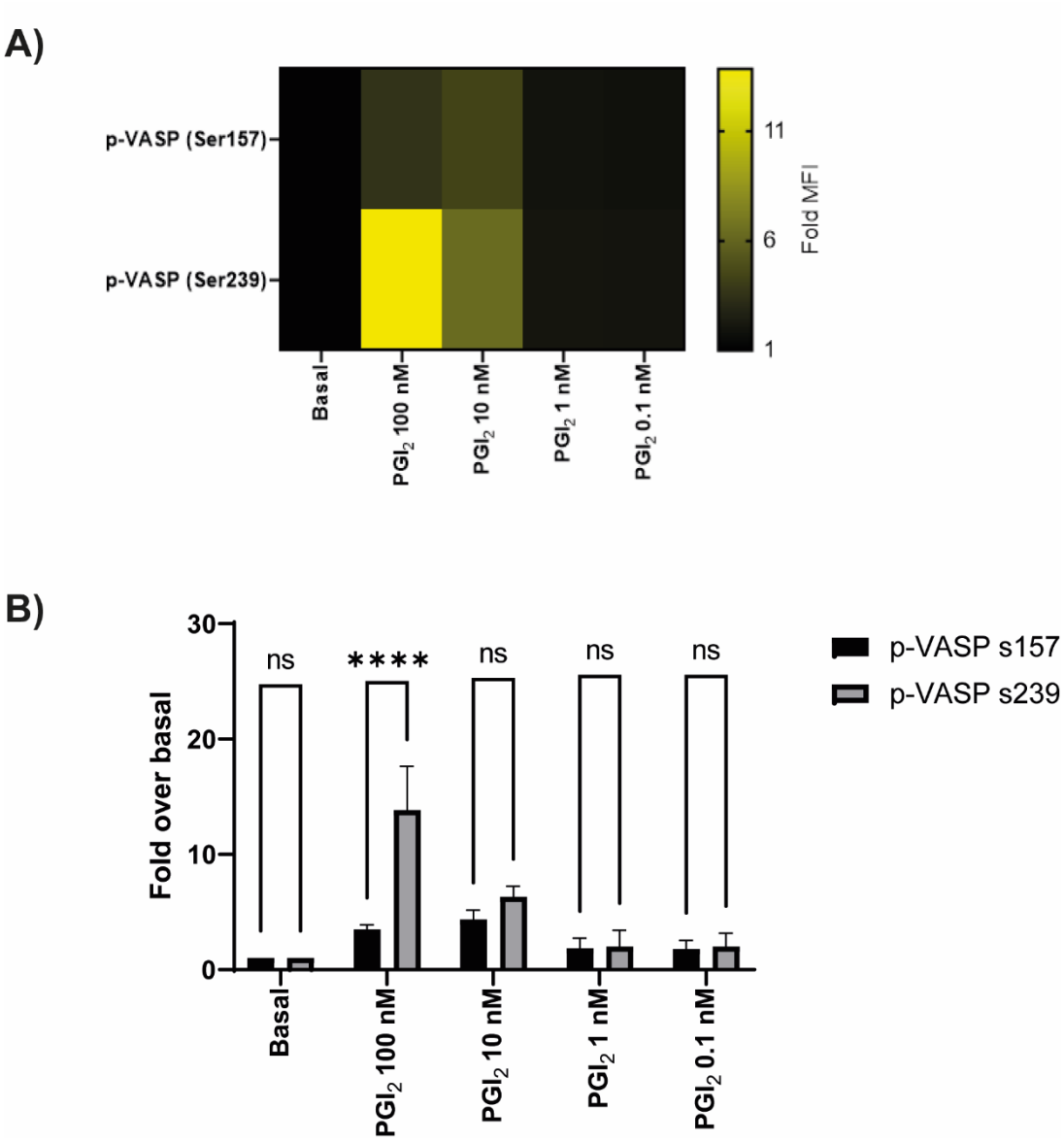

Figure 40. Measurement of VASP phosphorylation by phosphoflow cytometry in murine whole blood

Murine whole blood was treated with increasing concentrations of PGI_2 for 2 min, fixed using PhosFlow Fix/Lyse buffer (BD Biosciences), permeabilised and incubated with phospho-specific antibodies (p-VASP^{ser157}, p-VASP^{ser239} and CD41; 1 µg/mL). Cells were gated on platelet physical properties at 10k and then analysed for p-VASP expression in CD41 positive cells. Data presented as means ± SD fold over basal in heatmap (A) and bar chart (B). Data were compared by phosphorylation site using two-way ANOVA with Šídák's multiple comparisons test (n=3, ns = not significant, ****≤0.0001).

3.8.4. Phosphorylation of PKA substrates in response to cAMP-elevating agents in murine platelets

To cross-reference murine phospho-VASP data demonstrated immunoblotting and phosphoflow techniques, we evaluated PKA substrate phosphorylation in response to cAMP-elevating agents, PGI_2 (1-100 nM) and forskolin (1-10 µM), using a pan phospho-PKA substrates antibody. Consistent with VASP phosphorylation, the extent of PKA substrate phosphorylation increased in a concentration-dependent manner upon treatment with PGI_2 and forskolin. Whole-lane densitometry showed a subtle increase in PKA substrate phosphorylation in response to PGI_2 (1-10 nM), while phosphorylation at 100 nM was much clearer (Figure 41 B). However, consistent with phospho-VASP blots, the response to forskolin was less profound than PGI_2 (Figure 41 B). These data confirm that PGI_2 and forskolin are responsive in murine platelets upon assessment of PKA substrate phosphorylation. This provides a useful method to assess potential changes in various PKA substrates in the AC6-KO at the same time.

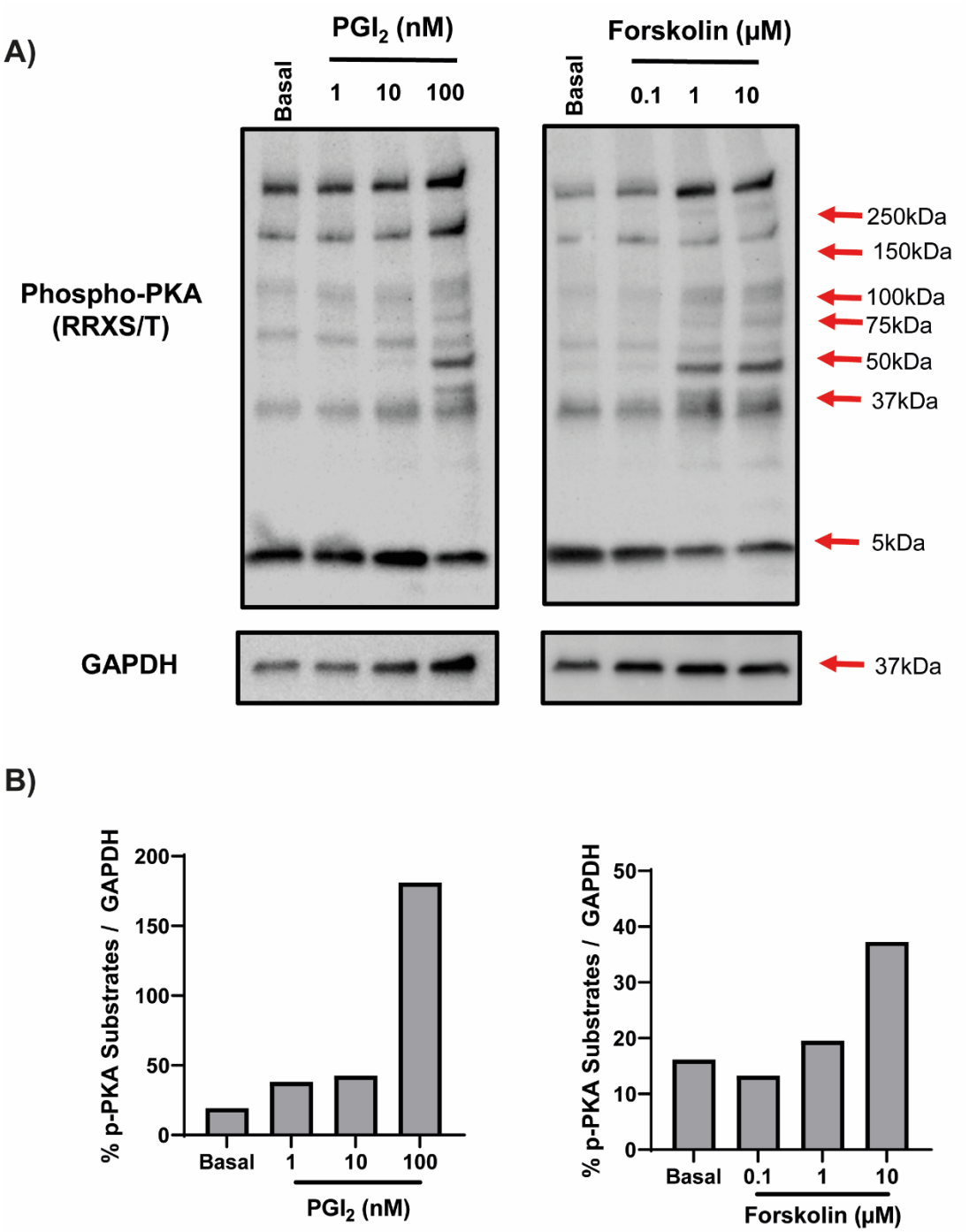

Figure 41. Assessment of phospho-PKA substrates in murine platelets

Murine washed platelets ($5x10^8$ platelets/mL) were lysed in 2x Laemmli buffer, separated via SDS-PAGE and immunoblotted for pan phospho-PKA substrates with a GAPDH loading control. Platelets were stimulated with increasing concentrations of PGI_2 for 2 min (right) or forskolin (left) under constant stirring (800 rpm) at 37˚C. Data presented as images (A) and whole lane densitometry bar graphs (B) analysed using ImageJ software (n=1).

3.9. Validation of PKA inhibitors in murine wild-type platelets

After confirming that phopsho-VASP^{Ser157} and phospho-PKA substrate antibodies are applicable for murine platelets in response to cAMP-elevating agents, we decided to assess the effect of PKA inhibitors in murine platelets.

3.9.1. Inhibition of PKA in murine platelets measured by VASP phosphorylation

Washed platelets 5x10^8 platelets/mL were treated with increasing concentrations of RP-8-CPT-cAMP (50 - 250 µM), H89/KT-5720 (1 - 20 µM) and SQ22536 (1 - 50 µM) and PGI_2 (100 nM) induced VASP phosphorylation measured. Each PKA inhibitor, except RP-8-CPT-cAMP, caused a significant reduction in PGI_2-mediated VASP phosphorylation (Figure 42). The RP-8-CPT-cAMP compound reduced VASP phosphorylation from 132.8 ± 34.6 % p-VASP^{Ser157} (PGI_2, 100nM) to 83.2 ± 29.0 % p-VASP^{Ser157} (RP-8-CPT-cAMP, 500 µM). While H89/KT-5720 reduced VASP phosphorylation from 151.9 ± 27.1% p-VASP^{Ser157} (PGI_2, 100nM) to 84.0 ± 27.2% p-VASP^{Ser157} (H89/KT-5720, 20 µM). The direct AC inhibitor caused the largest reduction in PGI_2-mediated VASP phosphorylation from 113.1 ± 15.5% p-VASP^{Ser157} (PGI_2, 100nM) to 39.9 ± 9.8% p-VASP^{Ser157} (SQ22536 1 µM), and then further to 21.4 ± 7.8% p-VASP^{Ser157} (SQ22536, 50 µM) ($P<0.0001$).

Excluding RP-8-CPT-cAMP, the PKA inhibitors successfully inhibited PGI_2-mediated VASP phosphorylation in murine platelets. In terms of the response from RP-8-CPT-cAMP, perhaps a lower concentration of PGI_2 would allow for further inhibition.

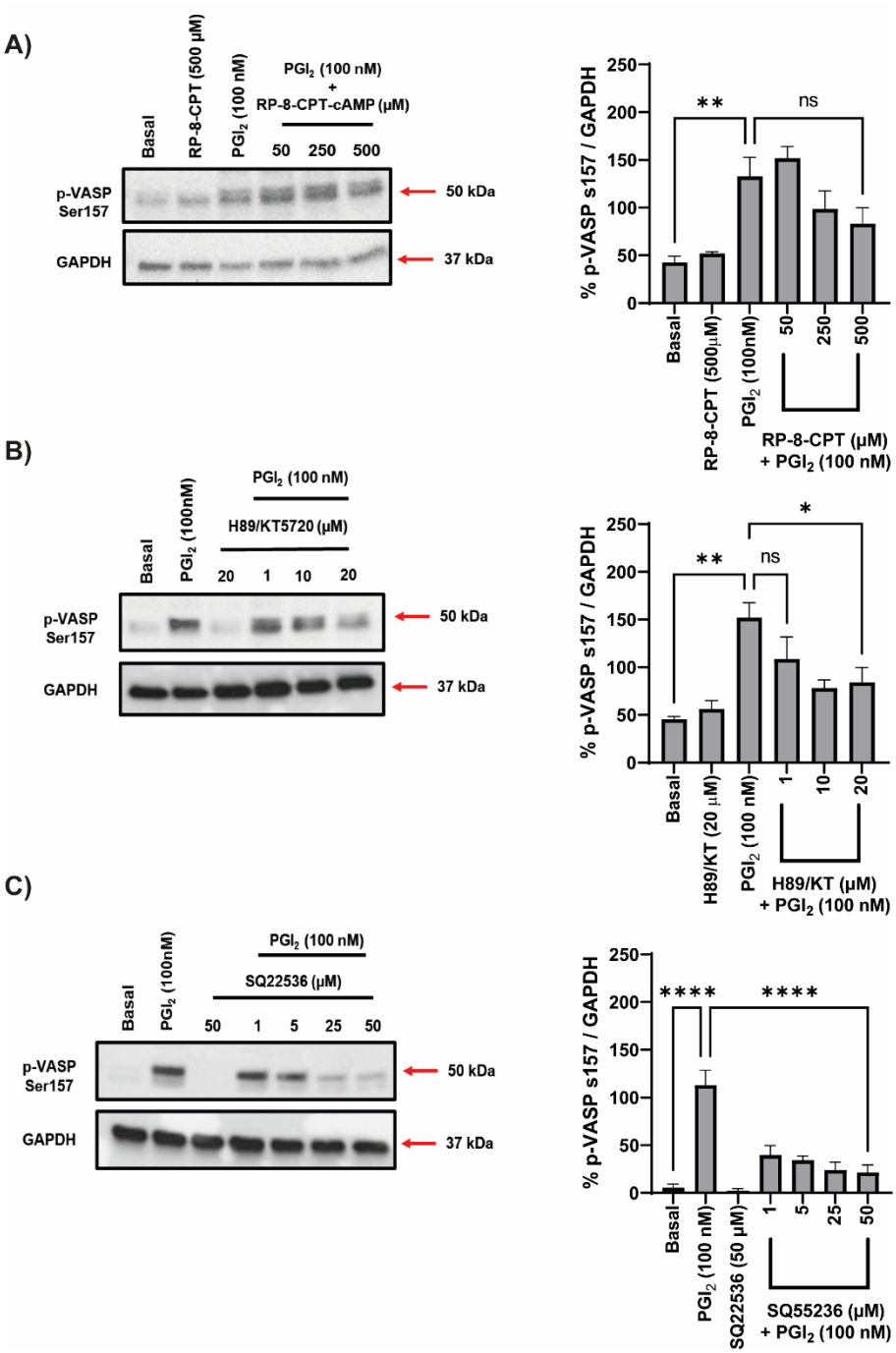

Figure 42. Optimisation of cAMP signalling inhibitors in murine platelets

Murine washed platelets ($5x10^8$ platelets/mL) were pre-treated with PKA inhibitors for 25 mins under constant stirring (800rpm) at 37°C prior to the addition of PGI_2 (100nM; 2 mins). (A) Direct PKA inhibitors RP-8-CPT-cAMP (B) and combination of H89 and KT5720 and (C) AC inhibitor SQ22536. Representative images (left) and densitometry bar graphs (right) carried out using ImageJ software. Data presented as means ± SD and compared to PGI_2 alone by one-way ANOVA with Dunnett's multiple comparisons test (n=3, ns = not significant, *≤0.05, **≤0.01 and ****≤0.0001).

3.10. Optimisation of spreading in murine platelets

Using methods established by Yusuf et al., (2017) we decided to assess platelet adhesion in murine washed platelets in the presence and absence of PGI_2 (10 nM). Washed platelets ($1x10^7$ platelets/mL) treated with thrombin (0.05 U/mL) were spread on the surface of fibrinogen (100 µg/mL) for 25 mins (Mazharian et al., 2007; Pleines et al., 2010), washed to remove non-adherent cells, and then treated with PGI_2 (10 nM) for 2 minutes before fixation.

In the presence of PGI_2, the number of adhered reduced platelets from 44.7 ± 3.9 (fibrinogen only) to 11.8 ± 8.0, while the total area (μm^2) per FoV reduced from 602.9 ± 57.0 (fibrinogen only) to 97.7 ± 67 (PGI_2; 10 nM) (Figure 43).

These data confirm that spreading and adhesion is inhibited by PGI_2, and this method is applicable in murine platelets.

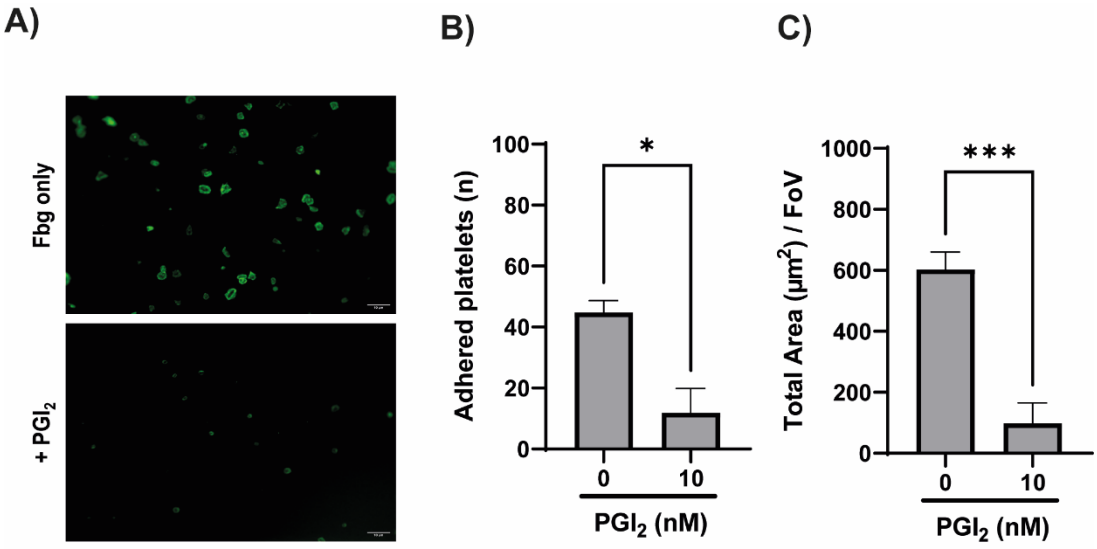

Figure 43. PGI_2 inhibits spreading and adhesion in murine platelets

Washed platelets ($1x10^7$ platelets/mL) were spread on the surface of fibrinogen (100 µg/mL) for 25 minutes before washing in PBS and then incubated with PGI_2 (10 nM) for 2 mins prior to fixation. Data presented as representative images (A), average number of adhered platelets per FoV (FoV = 5) (B) and total area μm^2 per FoV (C). Data presented as means ± SD data compared with and without PGI_2 two-way ANOVA with Tukey's multiple comparisons test (n=3, ns = not significant, *p≤0.01 and ***≤0.001, scale bar = 10 µm).

3.11. Expression of surface markers on murine platelets

To further establish platelet function and morphology, we employed the use of FFC in murine whole blood. A key part of this project is to establish a phenotype in the AC6-KO mouse; therefore, it was important to assess surface receptor expression in resting and activated murine whole blood using FFC.

3.11.1. Expression of surface markers on murine platelets by flow cytometry

Murine whole blood was pre-incubated with fluorescently conjugated antibodies at saturating concentrations for 10 mins prior to fixation with 1% PFA. Cells were then analysed for 10,000 platelet positive events characterised by physical properties. The antibodies used and the extent of expression for each receptor was consistent with the literature (Pleines et al., 2010; Nieswandt et al., 2004). Confirming that this method of surface receptor expression is viable in murine whole blood (Figure 44).

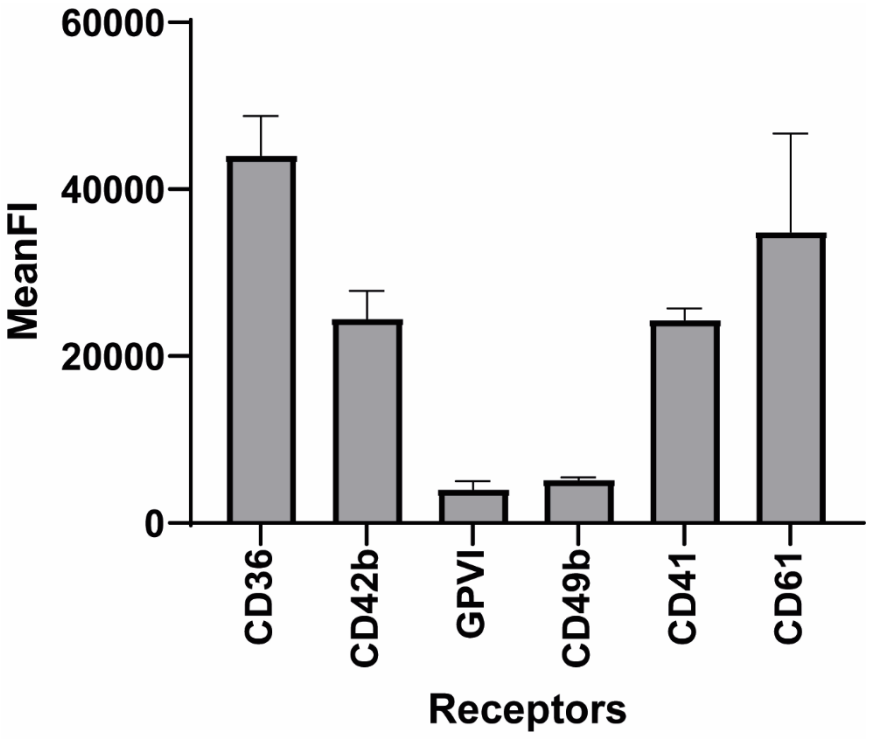

Figure 44. Surface receptor expression in murine whole blood by flow cytometry

Murine whole blood was pre-incubated with fluorescently conjugated antibodies at saturating concentrations for 10 mins at RT prior to fixation with 1% PFA/PBS. Samples were analysed for 10,000 platelet positive events based on physical platelet characteristics. Data presented as Mean Fluorescence Intensity (MeanFI) and expressed as means ± SD (n=3). GP refers to glycoprotein.

3.11.2. CRP-XL-mediated platelet activation in the presence of PGI_2 in murine whole blood

Murine whole blood was pre-treated with and without PGI_2 (0.1 - 100 nM) for 2 mins before stimulation with CRP-XL (1 µg/mL) and probed with CD62P or JON/A (activated $\alpha_{IIb}\beta_3$) for 20 mins.

Platelets demonstrated activation in response to CRP-XL (1 µg/mL) as demonstrated by an increase in CD62P expression and JON/A binding compared to basal, while PGI_2 inhibited CRP-XL-mediated platelet activation in a concentration-dependent manner (Figure 45).

CD62P binding went from 13.5 ± 10.2% (basal) to 68.3 ± 24.0% (CRP-XL, 1 µg/mL) ($p=0.0001$) and was inhibited by PGI_2 at 100 nM (20.0 ± 6.3% positive), returning CD62P binding to near basal levels ($p=0.0003$). While CD62 expression was inhibited in the presence of PGI_2 (5 nM) with no further significant inhibition despite increases in PGI_2 concentration. CD62P expression went from 3107.3 ± 989.8 MedianFI (CRP-XL, 1 µg/mL) to 297.2 ± 97.7 MedianFI (PGI_2, 5 nM) ($p<0.0001$).

JON/A binding appeared to be more sensitive to CRP-XL stimulation and inhibition by PGI_2, compared to CD62P. Binding of JON/A went from 10.5 ± 12.1% (basal), to 75.5 ± 21.5% (CRP-XL, 1 µg/mL) ($p<0.0001$). JON/A binding showed clear inhibition by PGI_2 at 10 nM (21.5 ± 11.4%) ($p=0.0001$) and was inhibited further at 100 nM (10.7 ± 5.5%) ($p<0.0001$). While, integrin activation was inhibited at PGI_2 (10 nM), starting from 2126.1 ± 432.1 MedianFI (CRP-XL, 1 µg/mL) reducing to 316.6 ± 27.9 MedianFI (PGI_2, 10 nM) ($p<0.0001$). These data confirm that murine platelets can be activated by CRP-XL (1 µg/mL) as well as inhibit CRP-XL-mediated platelet activation by PGI_2.

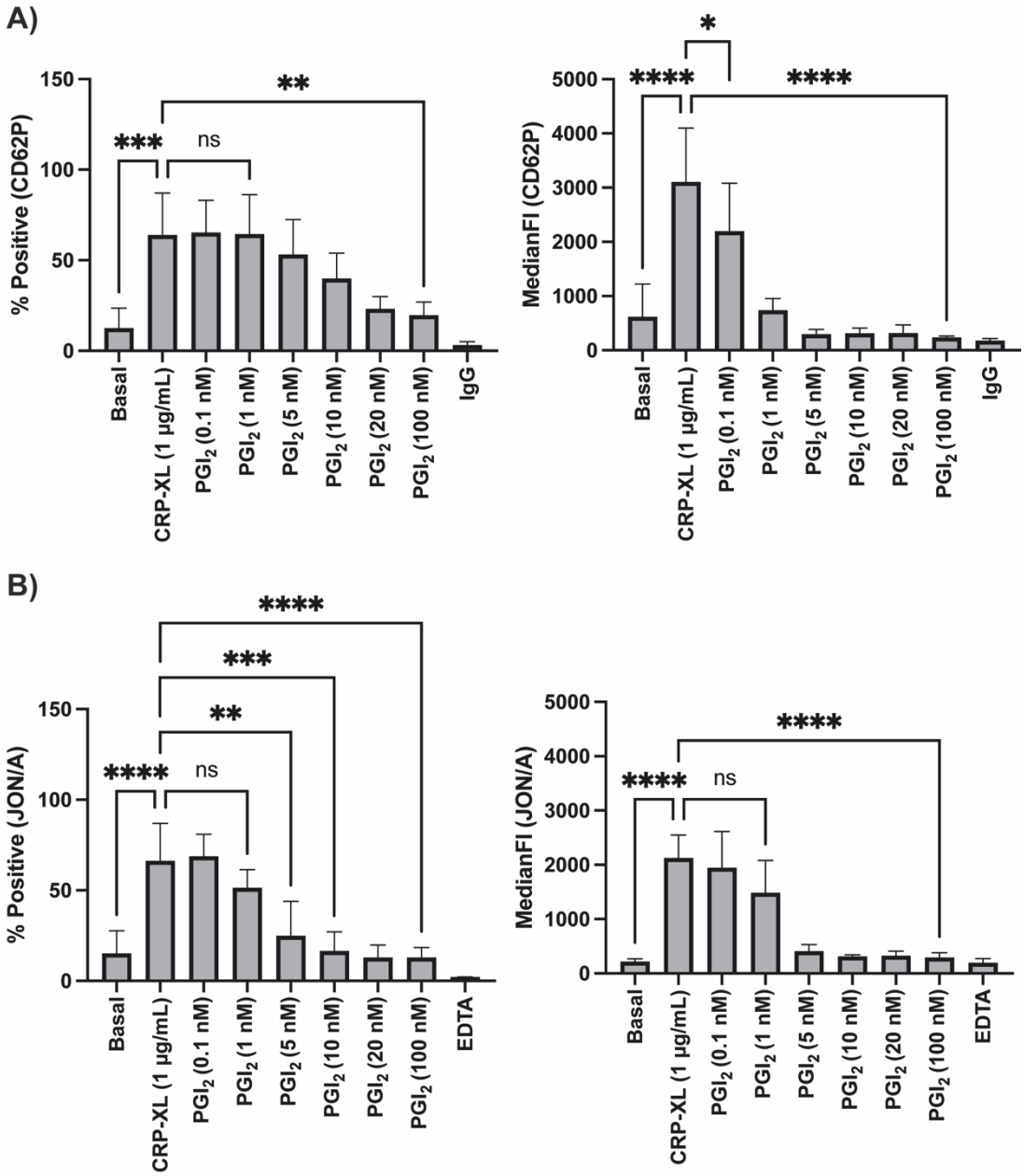

Figure 45. Expression of P-selectin and integrin activation by CRP-XL in the presence of PGI_2 in murine whole blood

Murine whole blood was pre-treated with and without PGI_2 (0.1-100 nM) for 2 mins before stimulation with CRP-XL (1 µg/mL) and probed for CD62P (A) and JON/A (B) for 20 mins prior to fixation. CD41-BB700 was used to identify platelets, and samples were analysed for 10,000 platelet positive events. Bar graphs represent percent positive (left) and Median Fluorescence Intensity (MedianFI) (right). Data presented as means ± SD and compared to basal and agonist alone by one-way ANOVA Tukey's multiple comparisons tests (n=3, ns = not significant, *≤0.05, **≤0.01, ***≤0.001 and ****≤0.0001).

3.11.3. PAR4 peptide-mediated platelet activation in the presence of PGI_2 in murine whole blood

Since murine platelets do not express the PAR1 receptor (Kahn et al., 1998) the PAR1 peptide could not be used for murine FFC experiments. They do however express a PAR4 receptor, therefore a PAR4 peptide (Connolly et al., 1994) was used to mimic thrombin mediated signalling pathways by cleavage of the PAR4 receptor. Murine whole blood was pre-treated with and without PGI_2 (0.1-100 nM) for 2 mins before stimulation with PAR4 peptide (100 µM) and probed with CD62P or JON/A (activated $\alpha_{IIb}\beta_3$) for 20 mins. Samples were fixed using Fix/Lyse and then analysed by flow cytometry. A marker for CD41 was used to identify platelets and samples were gated for 10,000 CD41-positive events (Figure 46).

CD62P binding went from 30.9 ± 10.7% (basal) to 72.7 ± 16.9% (PAR4, 100 µM) and was reduced to 28.2 ± 11.5% (PGI_2, 20 nM) ($p<0.0001$) without further inhibition. While CD62P expression, demonstrated maximal inhibition at PGI_2 (10 nM), with expression going from 1447.9 ± 334.5 MedianFI (PAR4, 100 µM) reducing to 269.3 ± 82.7 MedianFI (PGI_2, 10 nM).

JON/A binding, upon PAR4 stimulation and inhibition by PGI_2 appeared to be more sensitive compared to CD62P binding. JON/A binding went from 10.4 ± 4.5% (basal) to 90.2 ± 10.8% (PAR4, 100 µM) ($p<0.0001$) and was reduced to 12.9 ± 4.7% (PGI_2, 10 nM) ($p<0.0001$) near to basal. Extent of JON/A binding displayed maximal inhibition at PGI_2 (20 nM), with integrin activation going from 2344.7 ± 860.1 MedianFI (PAR4, 100 µM) reducing to 273.6 ± 67.7 MedianFI (PGI_2, 20 nM) ($p<0.0001$). Altogether, these data confirm that CD62P expression and integrin activation are sensitive to PAR4 stimulation, as well as inhibition by PGI_2.

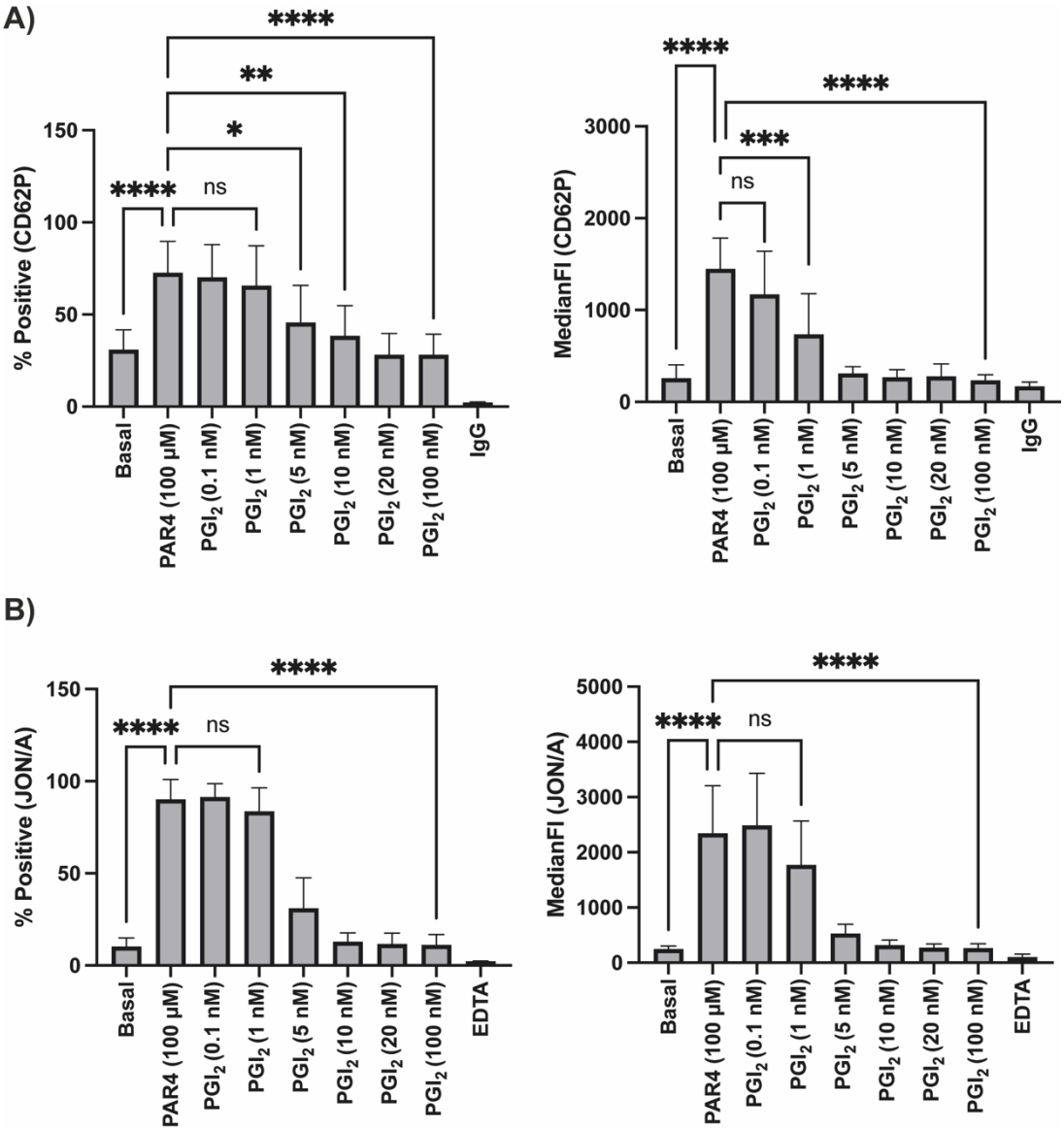

Figure 46. Expression of P-selectin and integrin activation by PAR4 in the presence of PGI_2

Murine whole blood was pre-treated with and without PGI_2 (0.1-100 nM) for 2 mins before stimulation with PAR4 (100 µM) and probed for CD62P (A) and JON/A (B) for 20 mins prior to fixation. CD41-BB700 was used to identify platelets, and samples were analysed for 10,000 platelet positive events. Bar graphs represent percent positive (left) and Median Fluorescence Intensity (MedianFI) (right) over control. Data presented as means ± SD and compared to basal and agonist alone by one-way ANOVA with Tukey's multiple comparisons tests (n=3, ns = not significant, *≤0.05, **≤0.01, ***≤0.001 and ****≤0.0001).

3.12. Discussion

Work presented in this chapter aimed to characterise the cAMP signalling pathway in both human and murine platelets, as well as the pharmacological tools to study the pathway under our own experimental conditions.

3.12.1. Validation of platelet isolation in human and murine platelets

The use of the classic prostaglandin method (Vargas et al., 1982) was inappropriate for this study as it would lead to activation of the cAMP signalling pathway, which could cofound the data and potentially be ineffective in our AC6-KO mouse. An alternative method which relies on lowering the pH of plasma to 6.4 without adding inhibitors was chosen for the isolation of human platelets (Mustard et al., 1989) and an adapted pH method was used to isolate murine platelets (Cazenave et al., 2004; Aurbach et al., 2019).

It was, therefore, important to validate these methods under our experimental conditions. We found little difference in response to platelet agonists or the sensitivity to the inhibitory actions of PGI_2 between the two platelet preparations. This was consistent between platelet prepared from human or murine blood. Data from Figure 21 and Figure 37 showed that PGI_2 can inhibit both collagen and thrombin-induced aggregation in a concentration-dependent manner in both human and murine platelets, respectively. The concentration of PGI_2 required to achieve 50% inhibition (IC_{50}) for human platelets stimulated with collagen (5 µg/mL) was 2.6 nM and 2.8 nM for thrombin (0.05 U/mL) (Figure 21). IC_{50} values generated were consistent with two studies by Radomski and colleagues (Radomski, M.W. et al., 1987; Radomski, M. W. et al., 1987). Interestingly, murine platelets displayed a stronger response to agonists, which may account for the potential weaker response to PGI_2 (Figure 37) compared to human platelets. Murine platelets could be more sensitive to activation, and therefore a lower concentration of each agonist may be required. Though evidence of this is lacking, it has been reported that female mice are more sensitive to agonists than males (Leng et al., 2004). However, this was not assessed as part of this study. Furthermore, in subsequent chapters we decided to reduce agonist concentrations to 0.035 U/mL and 2 µg/mL for thrombin and collagen, respectively.

3.12.2. Optimisation of methods to assess human and murine platelet function

Upon activation, platelets adhere and spread across the injury site and undergo profound changes to their morphology, release granule contents and express surface receptors required for their function (Aslan and Mccarty, 2013; Raslan and Naseem, 2014). The aim of these experiments was to establish that human and murine platelets were sensitive to agonists, and antagonists in functional assays beyond aggregation.

Data presented in Figure 22 demonstrates that isolated human platelets were able to adhere and spread on the surface of immobilised fibrinogen (100 µg/mL) and collagen (50 µg/mL) with increasing platelet concentrations. Translating this assay into murine platelets, we used the same conditions, however murine platelets were much smaller and therefore more challenging to identify. Hence, we decided to use 0.05 U/mL of thrombin to ensure that murine platelets adhere and spread on the surface of fibrinogen (Figure 43) (Hughan et al., 2007).

In addition, we also assessed the effect of PGI_2 on platelet spreading and optimised conditions before moving into murine platelets. Initially, human platelets were spread on fibrinogen with and without PGI_2 (10 nM) over time (up to 60 minutes), however we found little to no effect from PGI_2 (Figure 23). As the differences were so subtle and not significant, we thought this might be due to possible degradation of PGI_2 over the time course. Therefore we used methods described by Yusuf and colleagues (2017) whereby platelets were spread for 25 mins, washed with PBS and then treated with PGI_2 (10 nM) for 2 mins prior to fixation. This displayed a clear inhibitory response from PGI_2 which we didn't observe previously (Figure 24). Based on the success of this method we decided to apply this to murine platelets (Figure 43). As in human platelets, murine platelets exhibited a clear inhibitory response to PGI_2. We demonstrated that the number of adhered murine platelets in the presence of PGI_2 (10 nM) was significantly reduced along with the percentage surface area covered (Figure 43).

To further assess platelet function, we employed the use of fluorescent flow cytometry. In the first instance, to ensure that the appropriate platelet preparation is used throughout this study we compared human washed platelets, PRP and whole blood using a four-parameter activation panel (Figure 27). Data presented in Figure 27 shows that in platelet activation assays, whole blood was the optimal platelet preparation, especially upon assessment of AnnV (Figure 27 C). Based on this, whole blood was also chosen as the optimal platelet preparation for murine FFC assays. The low sample volume allows us to undergo multiple experiments from one mouse which is attractive for this study. Murine whole blood also demonstrated clear platelet activation by PAR4 peptide and CRP-XL, as well as inhibition by PGI_2 in a three-parameter FFC assay (Figure 45). Observed binding for both CD62P and PAC1 were inhibited by PGI_2 in PAR4 peptide and CRP-XL stimulated platelets.

We also assessed murine receptor expression at rest to establish the protocol before moving onto the AC6-KO mouse (Figure 44). Expression of murine platelet surface receptors were consistent with studies by Pleines et al., (2010) and Nieswandt et al., (2004).

Altogether, these experiments demonstrate that human and murine platelets are responsive to activation by different agonists and exhibit inhibition of platelet activation by PGI_2.

3.12.3. Elevated platelet activation and reduced PGI_2 sensitivity in ACS patients post-MI

Platelet hyperactivity is a key characteristic of atherothrombosis, yet the distinct mechanisms remain unclear. Some arguments suggest that platelet hyperactivity is a result of dyslipidaemia, which is a key risk factor for myocardial infarction (MI) (Davì et al., 1998; Jackson, 2011), while others suggest an impairment in platelet inhibitory mechanisms (Bunting et al., 1983; Fisch et al., 1997; Van Geet et al., 2009; Berger et al., 2020). Though it is likely multifactorial, perturbations in platelet cAMP signalling are possible to play a key part in platelet hyperactivity. Some studies suggest that breakdown of cAMP by PDEs is accelerated in cardiovascular disease (Berger et al., 2020), while other studies have demonstrated reduced sensitivity to PGI_2

(Bunting et al., 1983; Akai et al., 1983; Burghuber et al., 1986). We, therefore, decided to apply the four-parameter FFC activation panel to platelets from patients' post-MI and compared with age-matched healthy controls.

In data presented in Figure 29 we observed impaired sensitivity to PGI_2 in ACS patients' post-MI across all the platelet markers. Consistent with other studies we found that basal CD62P binding was significantly elevated in subjects with ACS compared to controls (Tschoepe et al., 1993; Itoh et al., 1995; Minamino et al., 1998; Bath et al., 1998; Serebruany and Gurbel, 1999).

We also observed elevated CD62P expression in response to PAR1 peptide in ACS patients, suggesting that these platelets could be more sensitive to activation (Ault et al., 1999) (Figure 29 A). Though there was no difference in CD62P expression between healthy and acute platelets upon treatment with CVX or PAR1/CVX combined, healthy platelets demonstrated only a subtle reduction in CD62P expression upon PGI_2 treatment. Consistent with a study by Hindle and colleagues (2021), whereby they observed a subtle and non-significant reduction in CD62P expression upon PGI_2 treatment, suggesting that the control of CD62P expression is not linked to PGI_2.

PAC1 binding was elevated upon treatment with agonists in both healthy and acute platelets, while platelets from ACS patients remained elevated even in the presence of PGI_2 compared to control. Expression of PAC1, like CD62P, was also elevated in ACS patients upon PAR1 peptide stimulation, while inhibition by PGI_2 was significantly impaired compared to control (Figure 29 B)

Finally, ACS platelets displayed markedly elevated AnnV binding at basal, and remained elevated upon agonist treatment and even in the presence of PGI_2 compared to control. In addition, basal AnnV expression was elevated and remained elevated upon treatment with PAR1 peptide compared to control, while CVX and PAR/CVX combined demonstrated no difference in AnnV expression between healthy and acute platelets. However, a clear defect was observed in response to PGI_2 as AnnV was significantly elevated in ACS patients compared to control (Figure 29 C).

It's been well documented that levels of P-selectin (CD62P) are elevated in patients with ACS (Tschoepe et al., 1993; Itoh et al., 1995; Minamino et al.,

1998; Bath et al., 1998; Serebruany and Gurbel, 1999), while our data are consistent with these reports, we have also reported the first evidence of significantly elevated PAR-mediated platelet activation in ACS patients, demonstrated by elevated P-selectin, $\alpha_{IIb}\beta_3$ activation and PS exposure.

In addition, we have shown that basal PS exposure is elevated in ACS patients compared to controls. While this may be indicative of platelets that are activated because of a cardiovascular event, these platelets could also be due to micro-emboli that have left the occlusion site or a potential predicator of future cardiovascular events. Elevated PS exposure has been demonstrated in hospitalised patients with acute medical illnesses and is associated with increased pro-coagulant platelet activity (Porreca et al., 2009). Interestingly, in these studies, levels of PS remained elevated upon hospital discharge, despite antiplatelet treatment. In comparison to our data, this suggests that elevated CD62P and PS exposure could be linked to PAR-mediated platelet activity.

Current antiplatelet therapeutics target platelet secondary signalling events, which include aspirin that targets TxA_2-mediated platelet activity, and $P2Y_{12}$ receptor antagonists which target ADP-mediated platelet activity (Warner et al., 2011). Though, PAR-mediated platelet activation presents the most potent secondary signalling cascade aiding amplification of platelet activity (Heemskerk et al., 2002). Given that our data demonstrates ACS platelets are hyperresponsive to PAR signalling, this suggests that upon vascular injury, patients post-MI, are more likely to display accelerated platelet activation, which in turn may lead to recurrent cardiovascular events. Not only are ACS platelets hyperresponsive to PAR1 peptide, but they also demonstrate elevated PS exposure which can subsequently initiate thrombin activation, supporting coagulation (Hoffman and Monroe, 2001; Monroe et al., 2002).

Though, pre-activated platelets post-MI could be a work here, impaired cAMP signalling events are likely to also contribute. In addition to elevated platelet activity at basal and in response to PAR1 peptide, we have also demonstrated impaired sensitivity to PGI_2 as shown by reduced inhibition of integrin activation and PS exposure (Figure 29). You could argue that elevated response to PAR1 peptide, outweighs inhibitory mechanisms by PGI_2 in ACS.

However, impaired PGI_2 sensitivity in cardiovascular disease has been well reported, some attribute this to IP receptor desensitisation (Bunting et al., 1983; Fisch et al., 1997) or endothelial dysfunction (Gryglewski et al., 2001), while others suggest accelerated PDE3A activity (Berger et al., 2020; Aburima et al., 2021). Though the precise mechanisms involved are yet to be elucidated.

3.12.4. Validation of methods to assess activation of cAMP signalling pathway in human and murine platelets

After establishing the effect of PGI_2 on platelet function we decided to assess the effect of different cAMP-elevating agents on the cAMP signalling pathway itself. First, through the production of cAMP and then via assessment of downstream PKA signalling. Strategically, it was important to ensure that isolated human and murine platelets were responsive to activation and inhibition before assessing the signalling events associated. Importantly, we wanted to characterise normal cAMP signalling events before exploring the AC6-KO mouse.

We used PGI_2, forskolin, adenosine and 8-CPT-cAMP to initiate cAMP signalling in both human and murine platelets. PGI_2 was used to assess IP-receptor-mediated cAMP production, whereas forskolin allows us to assess AC-mediated cAMP production directly (Seamon and Daly, 1981; Seamon et al., 1981). The use of adenosine provides an alternative pathway for assessing receptor-mediated cAMP production via the A_2 receptor (Fredholm et al., 2001; Johnston-Cox and Ravid, 2011), while 8-CPT-cAMP is a direct cAMP activator (Geiger et al., 1992).

Our assessment of cAMP production demonstrated that PGI_2 and forskolin, as well as adenosine, could trigger cAMP production in a concentration-dependent manner in human platelets (Figure 30). We also assessed the temporal dynamics of PGI_2, and we showed that after 20 mins the extent of PGI_2-mediated cAMP production started to decline (Figure 30 B). We also showed that with high concentrations of PGI_2 (1 μM), cAMP levels remained elevated after 20 mins. This was also consistent with time-course experiments on PGI_2-induced PKA phosphorylation events (Figure 31).

Murine platelets also exhibited a concentration-dependent increase in cAMP production in response to PGI_2 (Figure 38). We also decided to assess the production of cAMP in murine platelets at shorter time points to ensure peak cAMP production was captured (Gorman et al., 1977). Downstream PKA phosphorylation analysis by western blotting peaked at 2 mins PGI_2 (Figure 39), therefore we hypothesised that peak production of cAMP would occur more quickly. Consistent with our theory, the production of cAMP in murine platelets peaked at 30 secs (8167.6 ± 2603.4 fmol/10^7 platelets) and was chosen as the optimal incubation time for PGI_2 for cAMP analysis.

To cross-validate cAMP signalling events in both human and murine platelets, we assessed PKA substrate phosphorylation in response to cAMP-elevating agents. To measure downstream PKA activity we assessed PKA phosphorylation events via immunoblotting and phosphoflow (Spurgeon et al., 2014). In the first instance, we used an antibody for the well-established phosphorylation of $VASP^{Ser157}$ (Halbrügge et al., 1990; Horstrup et al., 1994) and a PKA substrate profile antibody. Using the PKA substrate profile antibody allowed us to confirm p-$VASP^{Ser157}$ as well as simultaneously assess multiple PKA substrates (Raslan et al., 2015a).

Data in Figure 31 showed that PGI_2, forskolin and 8-CPT-cAMP were able to induce phosphorylation of $VASP^{Ser157}$ in a concentration-dependent manner, which was consistent with the PKA substrate profile presented in Figure 33. Temporal regulation of $VASP^{Ser157}$ by PGI_2 was consistent with cAMP production, peaking at 2 minutes in human platelets and declining after 20 minutes. To cross-examine phosphorylation of $VASP^{Ser157}$ and $VASP^{Ser239}$ we used whole blood phosphoflow cytometry. Phosphorylation of VASP at both sites increased with PGI_2 concentration, interestingly $VASP^{Ser239}$ exhibited greater phosphorylation at higher PGI_2 concentrations compared to $VASP^{Ser157}$, though this hasn't been previously reported. Additionally, phosphoflow analysis of murine VASP phosphorylation has not previously been assessed.

Here we show that murine platelets also demonstrate concentration-dependent $VASP^{Ser157}$ phosphorylation in response to PGI_2, forskolin and 8-CPT-cAMP (Figure 39). While differences between the two phosphorylation

sites were more profound in murine platelets (Figure 40). Consistent with human data, PGI_2 induced VASP phosphorylation in a concentration-dependent manner in murine platelets and therefore, these conditions were used in subsequent chapters.

In addition, we also assessed the phosphorylation of PDE3A^{Ser312} by PGI_2 and forskolin in human platelets (Figure 34). The role of PDE3A within cAMP signalling is to hydrolyse cAMP, ensuring that levels of cAMP do not exceed the limit for platelet activation (Sim et al., 2004). Our results demonstrate that PGI_2 induced a concentration-dependent increase in PDE3A^{Ser312} phosphorylation. Forskolin, however, elevated PDE3A^{Ser312} phosphorylation at 1 μM were maintained even as concentration increased.

Altogether these experiments confirm that human and murine platelets are responsive to various cAMP-elevating agents. We have also shown the methods used to assess cAMP production and downstream PKA phosphorylation events are applicable in murine platelets.

3.12.5. Validation of methods to assess inhibition of cAMP signalling in human and murine platelets

Since establishing that cAMP-elevating agents are appropriate in both human and murine platelets, we set out to characterise inhibitors of the cAMP signalling pathway in the presence or absence of PGI_2. We used a variety of commercially available inhibitors including RP-8-CPT-cAMP, H89 and KT-5720 (Dostmann et al., 1990; Bain et al., 2003; Gambaryan et al., 2004; Lochner and Moolman, 2006) to assess direct PKA inhibition and SQ22536 to assess direct AC inhibition (Emery et al., 2013).

Human and murine platelets displayed inhibition of p-VASP^{Ser157} in the presence of each inhibitor in a concentration-dependent manner (Figure 35 and Figure 42). Murine platelets appeared to be more sensitive to inhibition by SQ22536 compared to human, while H89/KT5720 and RP-8-CPT-cAMP were comparable between species. Although, reports have shown that H89, KT5720 and RP-8-CPT-cAMP are not specific PKA inhibitors. It was found that H89 and KT5720 target multiple protein kinases, which may account for the weak response observed (Davies et al., 2000). H89 has been shown to target PKBα, PKA and ROCK-II, while KT-5720 targets GSK3β, PDK1, AMPK

and PKA, which may lead to misinterpretation of results. Moving forward, SQ22536 appears to be an appropriate inhibitor of cAMP signalling as it specifically targets all ACs. Given the nature of the project, assessment of AC inhibition is vital and allows us to demonstrate the role of ACs in platelet cAMP signalling. These experiments demonstrate that human and murine platelets are responsive to cAMP-inhibiting agents, in particular the AC inhibitor, SQ22536.

In conclusion, data presented in this chapter demonstrate that isolated platelets and whole blood are both functional and responsive to activation and inhibition. We have optimised the conditions required for different cAMP-elevating agents to inhibit platelet activation, produce cAMP, and initiate downstream PKA signalling events. We have also characterised cAMP-inhibiting agents via immunoblotting in human and murine platelets, as well as establishing appropriate conditions to assess PKA phosphorylation events in washed platelets and whole blood. We have also shown that cAMP signalling is impaired in patients post-MI, confirming that exploring different aspects of cAMP is clinically relevant. Data from these patients were invaluable, allowing us to compare phenotypic characteristics of the AC6-KO mouse in subsequent chapters. Lastly, we've shown that all methods established and characterised in this chapter are viable in both human and murine platelets which is relevant for subsequent chapters.

Chapter 4
Functional characterisation of the platelet specific AC6-KO mouse

4.1. Introduction

Adenylyl cyclases (ACs) are key signal transducers of the platelet cAMP signalling pathway. They couple endothelial-derived PGI_2, PGE_1 and adenosine to the production of cAMP which in turn maintains platelets in a resting state while also leading to reduced platelet accrual at sites of vascular injury (Cheng et al., 2003; Sim et al., 2004). Understanding the mechanisms that influence platelet sensitivity to cAMP signalling is important in understanding how platelet hyperactivity occurs during disease. PGI_2 binds to its IP receptor, which activates AC via $G\alpha_s$ to elevate cAMP levels. The binding of cAMP to the regulatory subunits of PKA leads to its activation and to the phosphorylation of several signalling proteins that are associated with inhibition of platelet function. AC activity is inhibited by ADP and potentially thrombin which acts through GPCRs linked to $G\alpha_i$, preventing cAMP synthesis and breakdown, respectively (Zhang and Colman, 2007; Godinho et al., 2015). Given that AC6 is the major isoform in both human and murine studies, we hypothesised that AC6 is a critical node whereby cAMP controls platelet function and thrombosis.

Since we have demonstrated a plethora of appropriate techniques to explore platelet function in murine platelets as described in Chapter 3, this chapter aims to demonstrate the functional characterisation of a novel platelet-specific AC6-KO mouse. In this chapter we assessed platelet morphology, function, and thrombosis in WT versus AC6-KO platelets.

4.1.1. Aims of chapter

- Assess platelet function in AC6-KO mouse
- Establish phenotype of AC6-KO mouse
- Understand the role of AC6 physiologically

4.2. Expression of AC6 in mice

According to proteomic and transcriptomic studies, AC6 is the predominant AC isoform in human and murine platelets (Hanoune and Defer, 2001; Rowley et al., 2011; Burkhart et al., 2012). While, chromosomal locations differ between human and mouse ACs (Edelhoff et al., 1995), using a platelet-specific AC6-KO mouse model allows us to explore the role of AC6 in platelet function and thrombosis. Confirmation of the AC6-KO mouse was vital for the progression of this study, in order to establish an appropriate breeding strategy, mice were genotyped as described in 2.6.3.3. While assessment of the platelet-specific AC6 deletion was carried out by qPCR and immunoblotting techniques.

4.2.1. Confirmation of the platelet-specific AC6-KO mouse by qPCR

The novel platelet specific AC6-KO mouse was generated via the cre-lox system using the PF4 promotor to ensure that the AC6 gene was deleted in cells of the megakaryocyte lineage only (Tiedt et al., 2007). To assess platelet specificity of the AC6-KO mouse we tested for the presence or absence of AC6 gene (*ADCY6*) in WT compared to AC6-KO platelets, kidney and heart tissues using qPCR.

We found that AC6 was knocked out in platelets but the other tissues tested, confirming that the deletion of AC6 was restricted to platelets (1.86 ± 0.28% *ADCY6* expression in WT vs 0.02 ± 0.01% *ADCY6* expression in AC6-KO). We also tested for the presence and absence of the other ACs in platelets (AC5 and AC3) (Figure 47). AC5 was expressed in both WT and AC6-KO platelets, whereas AC3 was not present in WT and AC6-KO platelets, consistent with the work of Rowley and colleagues (Rowley et al., 2011; Burkhart et al., 2012; Zeiler et al., 2014).

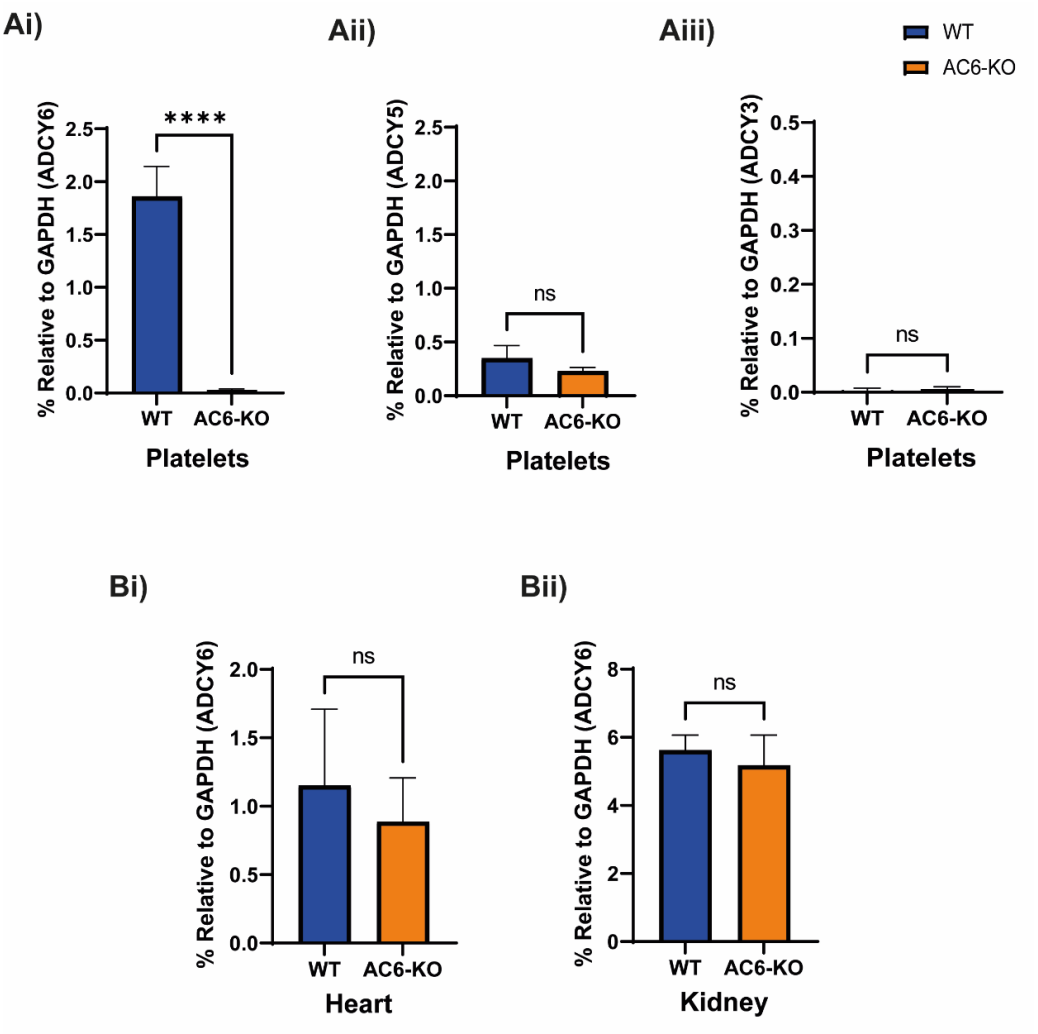

Figure 47. Confirmation of platelet-specific AC6 knockout mouse by qPCR

RNA was isolated from murine washed platelets ($5x10^8$ platelets/mL) and tissues using Trizol Reagent (Thermo Fisher) and the PureLink RNA mini kit (Invitrogen) following manufacturers protocol. Reverse transcription was performed using a Reverse Transcription System (Promega) following manufactures protocol and qPCR was carried out using the Taqman® gene expression system (Thermo Fisher). Gene expression was compared to a *GAPDH* control and bar graphs represent % expression relative to *GAPDH*. *ADCY* expression in platelets (A) and tissues (B). Data presented as means ± SD and compared between the two groups using an unpaired students t-test (n=3, ns = not significant, ****≤0.0001).

To cross-validate our qPCR data we assessed the total AC expression via immunoblotting. Levels of AC protein expression were significantly reduced in the AC6-KO compared to WT (107.6 ± 35.9 % WT vs 37.1 ± 3.2 % AC6-KO, p=0.009) (Figure 48). These data confirm that AC6 is knocked out in platelets and that the other AC is still present, AC5, though expressed to a much lower extent.

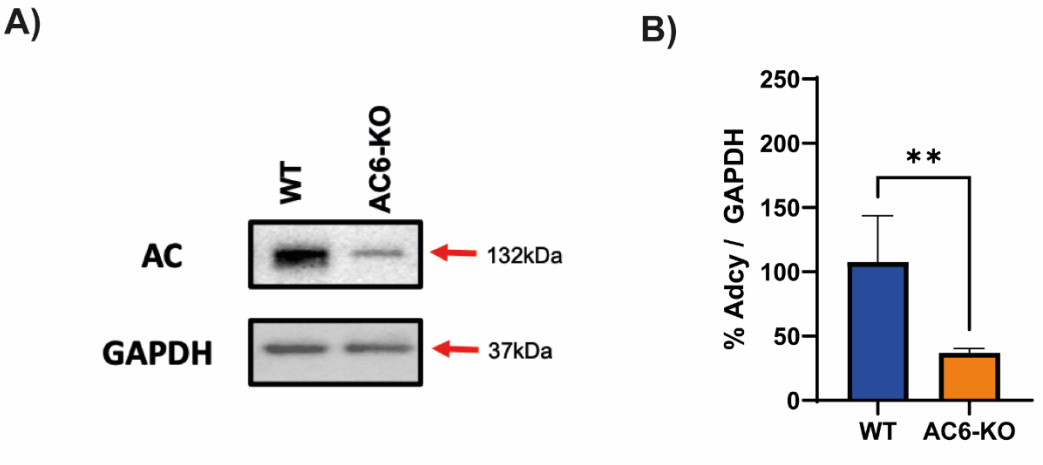

Figure 48. Confirmation of the AC6-KO mouse by immunoblotting

Murine washed platelets ($5x10^8$ platelets/mL) were lysed in 2x Laemmli buffer, separated via SDS-PAGE and assessed for total Adenylate Cyclase (AC) with a GAPDH loading control. Bar graph represents densitometry analysis carried out using ImageJ software. Data presented as means ± SD compared between the two groups using an unpaired students t-test (n=3, **≤0.01).

4.3. Assessment of basic characteristics in the AC6-KO mouse

Since establishing that our AC6-KO mouse model was specific to platelets, we decided to assess basic characteristics of the AC6-KO mouse compared to WT including weights, platelet counts, lifespan, and yield.

4.3.1. Assessment of mouse weights and isolated platelet yields

To confirm that AC6-KO mice were comparable to WT mice we assessed mouse weights at varying ages along with the yield of washed platelets isolated from 1 mL of whole blood containing ACD. Prior to blood collection, mice were weighed under anaesthesia and their weights were recorded against their age and sex. Isolated platelets were then counted and, plotted against sex and genotype (Figure 49). Bodyweights of WT and AC6-KO were comparable between both sexes, and we found no differences in mouse weight and platelet counts between WT and AC6-KO platelets, suggesting that deletion of AC6 in platelets does not affect mouse weight or isolated platelet yield (Figure 49).

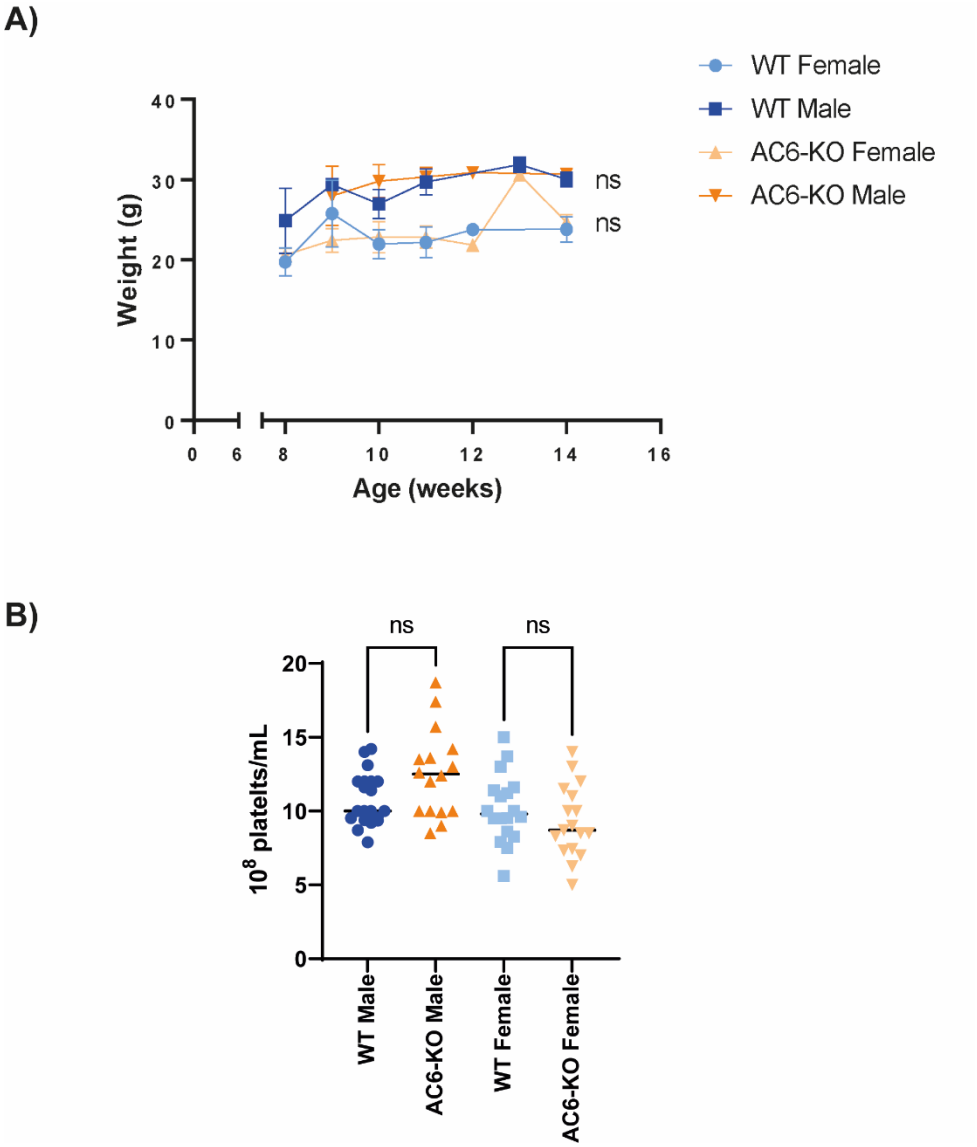

Figure 49. Assessment of physical characteristics of the AC6-KO mouse

Mouse weights and platelet yields were measured upon collection of blood. Anesthetised mice were weighed and compared to their age (weeks). Platelet yields were assessed via washed platelets isolated from 1 mL of whole blood collected in ACD. Platelet pellets were resuspended in 250 µL of Modified Tyrode's buffer and were counted using a Coulter particle counter (Beckmann Coulter). Data presented as means ± SD (A) and individual values and means (B) were compared between WT and AC6-KO by two-way ANOVA with Tukey's multiple comparisons test (n=16, ns = not significant).

4.4. Assessment of platelet counts by flow cytometry in the AC6-KO mouse

To cross-validate platelet yields, platelet numbers were counted by whole blood flow cytometry in WT and AC6-KO.

No difference in CD41 positive events between WT and AC6-KO mice was observed as shown by 336805 ± 83260 platelets/µL (WT) vs 328497 ± 99370 platelets/µL (AC6-KO), further confirming that a deletion of platelet-specific AC6 does not affect platelet count (Figure 50).

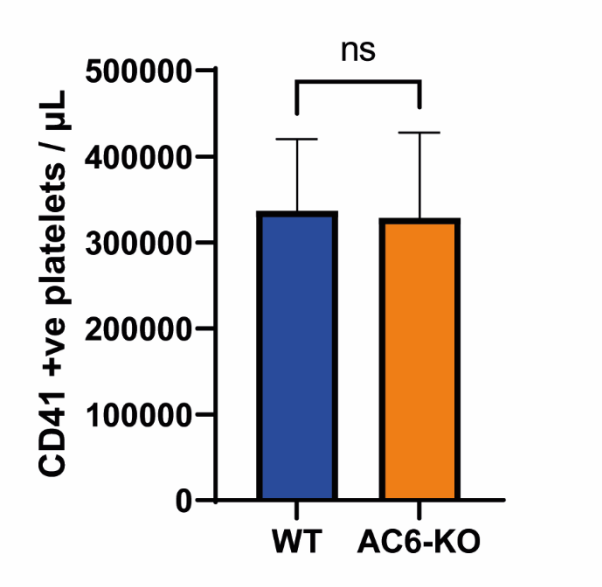

Figure 50. Assessment of platelet counts by flow cytometry in the AC6-KO mouse

Murine whole blood was incubated with CD41-BB700 for 20 minutes in the dark at RT prior to fixation with 1% PFA/PBS. Platelets were gated first on physical properties, then on CD41 positive events. Events were recorded for 2.5 minutes and analysed by CD41 positive events per µL of whole blood. Data presented as means ± SD and compared between the two groups using an unpaired students t-test (n=6, ns = not significant).

4.4.1. Assessment of reticulated platelets by flow cytometry in AC6-KO platelets

To determine whether a deletion of AC6 affected the presence of reticulated (immature) platelets, we measured reticulated platelets by whole blood flow cytometry using Thiazole Orange (TO). We observed no differences in the presence of reticulated platelets between WT and AC6-KO platelets as demonstrated (1313.9 ± 20.8 MFI; WT vs 1260.3 ± 165.2 MFI; AC6-KO), suggesting that AC6 deletion in platelets does not affect platelet lifespan (Figure 51).

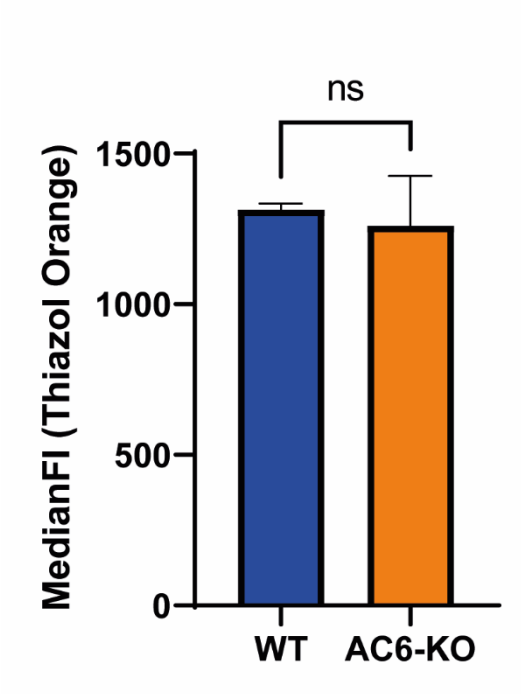

Figure 51. Assessment of reticulated platelets by flow cytometry

Murine whole blood was added to 1 mL of Retic-Count reagent (BD) and incubated for 30 minutes in the dark at RT. Platelets were gated by physical properties and analysed at 10,000 events. Bar graph represents median fluorescence intensity (MedianFI) of Thiazole Orange. Data presented as means ± SD and compared between the two groups using an unpaired students t-test (n=3, ns = not significant).

4.4.2. Assessment of platelet surface receptor expression by flow cytometry in AC6-KO platelets

To further explore platelet morphology, we assessed the expression of platelet surface receptors. We found no significant differences in platelet surface receptor expression of CD36, CD42b, CD49, GPVI, CD49b, CD41 and CD61 between WT and AC6-KO platelets (Figure 52). Expression of these receptors remains consistent between WT and AC6-KO platelets, confirming that the removal of AC6-KO does not subsequently cause a reduction in other surface receptors.

Overall, this series of experiments confirmed that the AC6-KO mouse model is comparable to WT in terms of mouse weights, platelet yield, blood counts, platelet lifespan and expression of surface receptors.

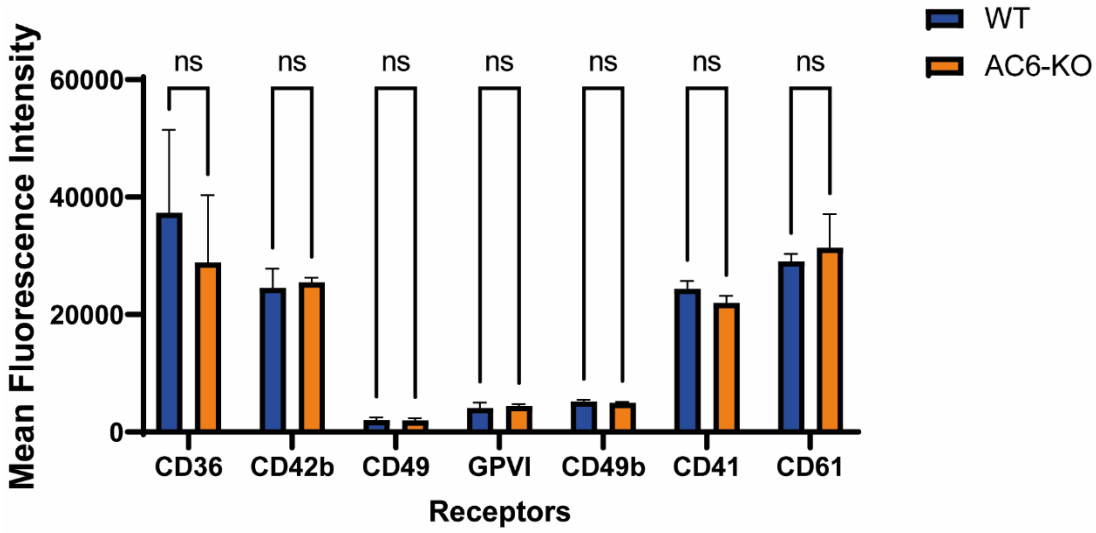

Figure 52. Assessment of platelet surface receptor expression in AC6-KO platelets

Murine whole blood was probed with fluorescently conjugated antibodies for platelet surface receptors for 20 minutes prior to fixation in 1% PFA/PBS. Platelets were gated by physical properties at 10,000 events. Bar graphs represent Mean Fluorescence Intensity (MFI). Data presented as means ± SD and compared between each group by two-way ANOVA with Šídák's multiple comparisons test (n=4, ns = not significant).

4.5. Assessment of platelet spreading adhesion to fibrinogen in the AC6-KO mouse

To further characterise morphology or AC6-KO platelets, we assessed platelet spreading and adhesion to fibrinogen in the presence and absence of PGI_2. We wanted to assess whether PGI_2 could prevent or reduce platelet spreading and adhesion in WT and AC6-KO platelets.

4.5.1. Platelet adhesion on fibrinogen in AC6-KO platelets

Using methods established by Yusuf et al., (2017) we first assessed platelet adhesion on the surface of fibrinogen alone in the AC6-KO compared to WT.

Washed platelets ($1x10^7$ platelets/mL) treated with thrombin (0.05 U/mL) were adhered to a surface of fibrinogen (100 µg/mL) for 25 mins (Mazharian et al., 2007; Pleines et al., 2010) (Figure 53). No difference in platelet adhesion was observed between WT and AC6-KO platelets. The number of platelets adhered observed per FoV was 44.7 ± 4.0 (WT) versus 45.4 ± 13.3 (AC6-KO), while percentage area per FoV was 3.9 ± 0.4 % (WT) versus 3.6 ± 0.5 % (AC6-KO). These data suggest that AC6 does not play a role in platelet spreading and adhesion to fibrinogen.

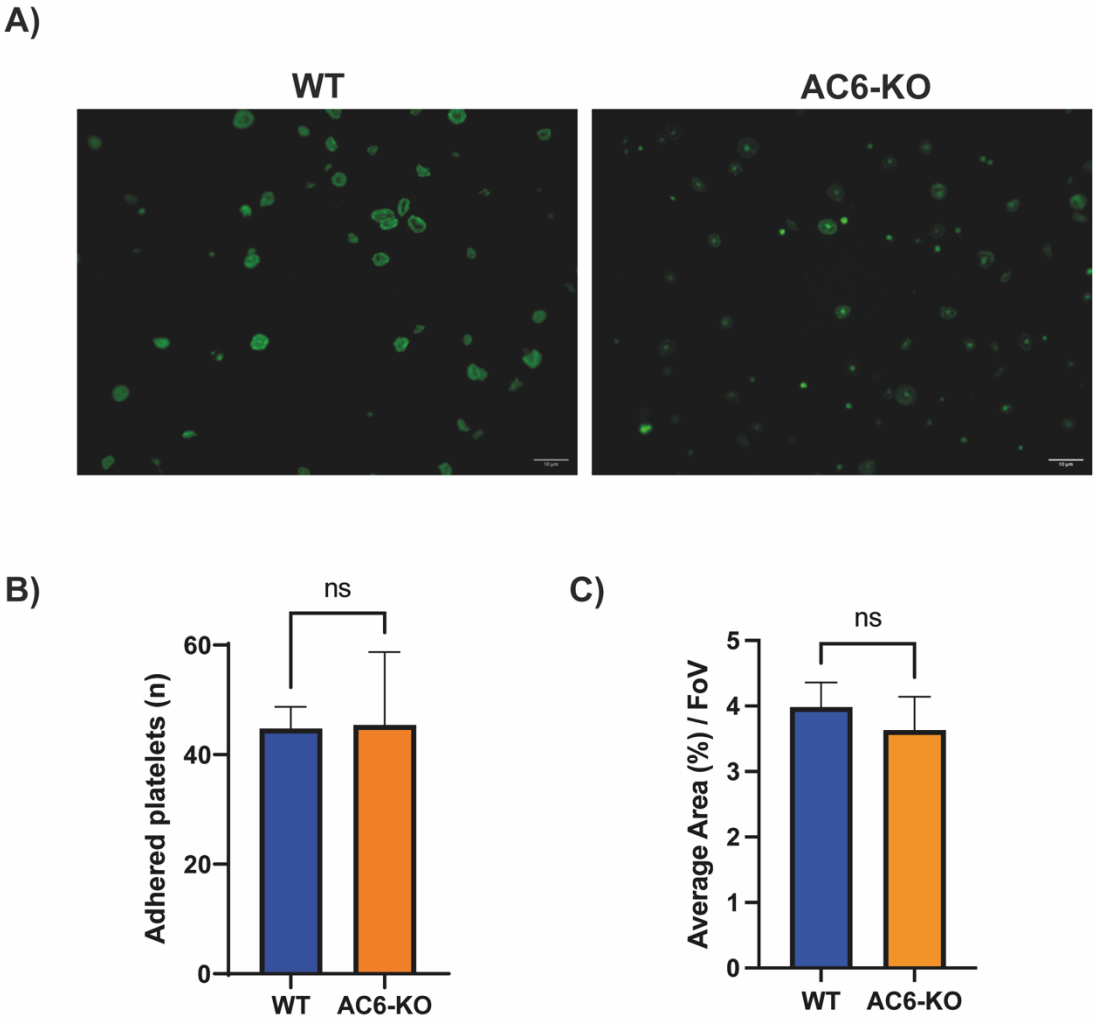

Figure 53. Assessment platelet spreading in the AC6-KO mouse

Washed platelets ($1x10^7$ platelets/mL) were spread on the surface of fibrinogen (100 µg/mL) for 25 minutes prior to fixation. Data presented as representative images (A), average number of adhered platelets per FoV (B) and average percentage area per FoV (C). Data presented as means ± SD and compared between WT and AC6-KO using an unpaired students t-test with Welch's correction (n=3, ns = not significant, scale bar = 10 µm).

4.5.2. The influence of PGI_2 on platelet adhesion to fibrinogen in the AC6-KO mouse

Next, we decided to assess whether inhibition of spreading and adhesion of platelets by PGI_2 was affected in the AC6-KO. Washed platelets ($1x10^7$ platelets/mL) treated with thrombin (0.05 U/mL) were spread on the surface of fibrinogen (100 µg/mL) for 25 mins before washing with PBS to remove non-adherent cells. PGI_2 (10 nM) was then added and after 2 minutes, cells were fixed and stained (Figure 54).

In WT platelets, there was a reduction in the number of adherent platelets in the presence of PGI_2 from 44.7 ± 4.0 (fibrinogen alone) to 11.8 ± 8.0 (PGI_2; 10 nM) (p=0.01). While the average percentage area per FoV was also significantly reduced from 3.9 ± 0.4 % (fibrinogen alone) to 0.6 ± 0.4 % (PGI_2; 10 nM) (p=0.0001). The number of platelets adhered to fibrinogen in the presence of PGI_2 in the AC6-KO displayed a subtle reduction, however it was not significant. Interestingly, the average percentage area per FoV showed a decrease upon PGI_2 treatment from 3.6 ± 0.5 % (fibrinogen alone) to 1.5 ± 0.0 % (PGI_2; 10 nM).

While PGI_2 had no effect on the number of platelets adhered to immobilised fibrinogen in the AC6-KO. There seemed to be a significant reduction in platelet spreading as the average percentage area per FoV was reduced.
Upon comparison between WT and AC6-KO platelets, in the presence of PGI_2 we observed a less pronounced effect from PGI_2 in AC6-KO platelets compared to WT, though this was not significant. The number of adhered platelets in the presence of PGI_2 was 11.8 ± 8.0 (WT) compared to 24.3 ± 10.4 (AC6-KO). While the average percentage area per FoV was 0.6 ± 0.4 % (WT) compared to 1.2 ± 0.5 % (AC6-KO). Suggesting a potential role for AC6 in PGI_2-mediated inhibition of platelet adhesion and spreading.

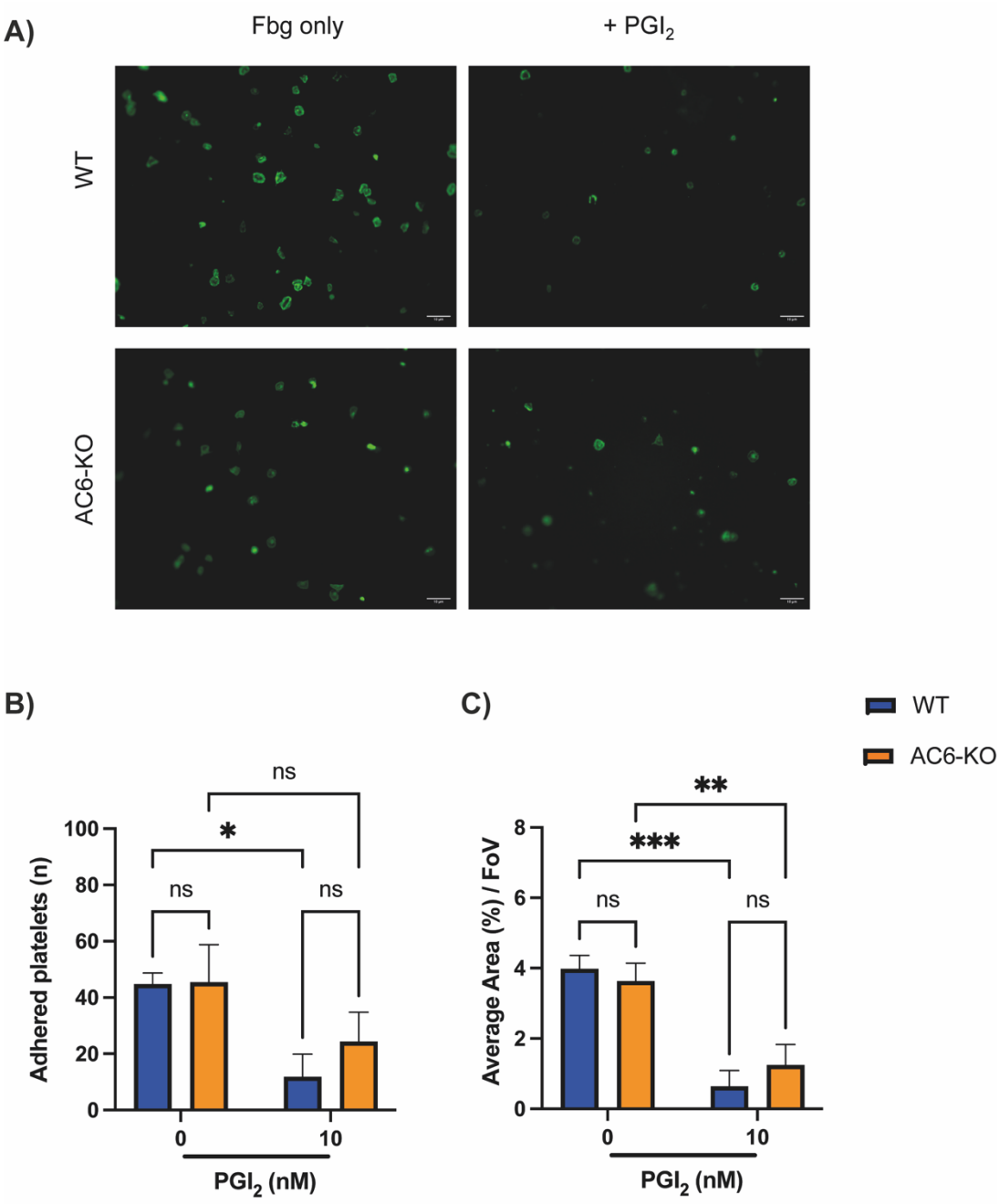

Figure 54. Platelet spreading in response to PGI_2 in AC6-KO platelets

Washed platelets ($1x10^7$ platelets/mL) were spread on the surface of fibrinogen (100 µg/mL) for 25 minutes before washing in PBS and then incubated with PGI_2 (10 nM) for 2 mins prior to fixation. Data presented as representative images (A), average number of adhered platelets per FoV (FoV=5) (B) and average percentage area per FoV (C). Data presented as means ± SD and first compared between WT and AC6-KO using an unpaired students t-test with Welch's correction. Then compared between the absence and presence of PGI_2 for each group by two-way ANOVA with Tukey's multiple comparisons test (n=3, ns = not significant, *≤0.05 **≤0.01 and ***≤0.001, scale bar = 10 µm).

4.6. Assessment of platelet aggregation in the AC6-KO mouse

Next, we assessed platelet aggregation, as means of platelet function in WT and AC6-KO platelets. We assessed platelet aggregation in response to collagen, thrombin and U46619 and inhibition of platelet aggregation by PGI_2 and GSNO.

4.6.1. AC6-KO mouse displays normal inhibition by PGI_2 in collagen-stimulated platelets

In first instance, we wanted to assess whether GPVI signalling was intact as well as sensitivity to PGI_2 in the AC6-KO by treating washed platelets with and without PGI_2 prior to stimulation with collagen (Figure 55).

We found no difference in platelet aggregation between WT and AC6-KO platelets upon stimulation with collagen (2 µg/mL) with and without PGI_2 (0.1-100 nM). We also found that both groups also displayed a concentration-dependent inhibition of aggregation by PGI_2. In WT platelets, aggregation was reduced from 74.4 ± 11.4 % aggregation (collagen alone; 2 µg/mL) to 9.8 ± 4.87 % aggregation (PGI_2; 100 nM). While AC6-KO platelets displayed a similar level of inhibition whereby aggregation went from 81.3 ± 6.6 % aggregation (collagen alone; 2 µg/mL) to 7.6 ± 4.2 % aggregation (PGI_2; 100 nM). These data indicate that AC6 does not play a role in PGI_2-mediated inhibition of collagen-stimulated platelet aggregation.

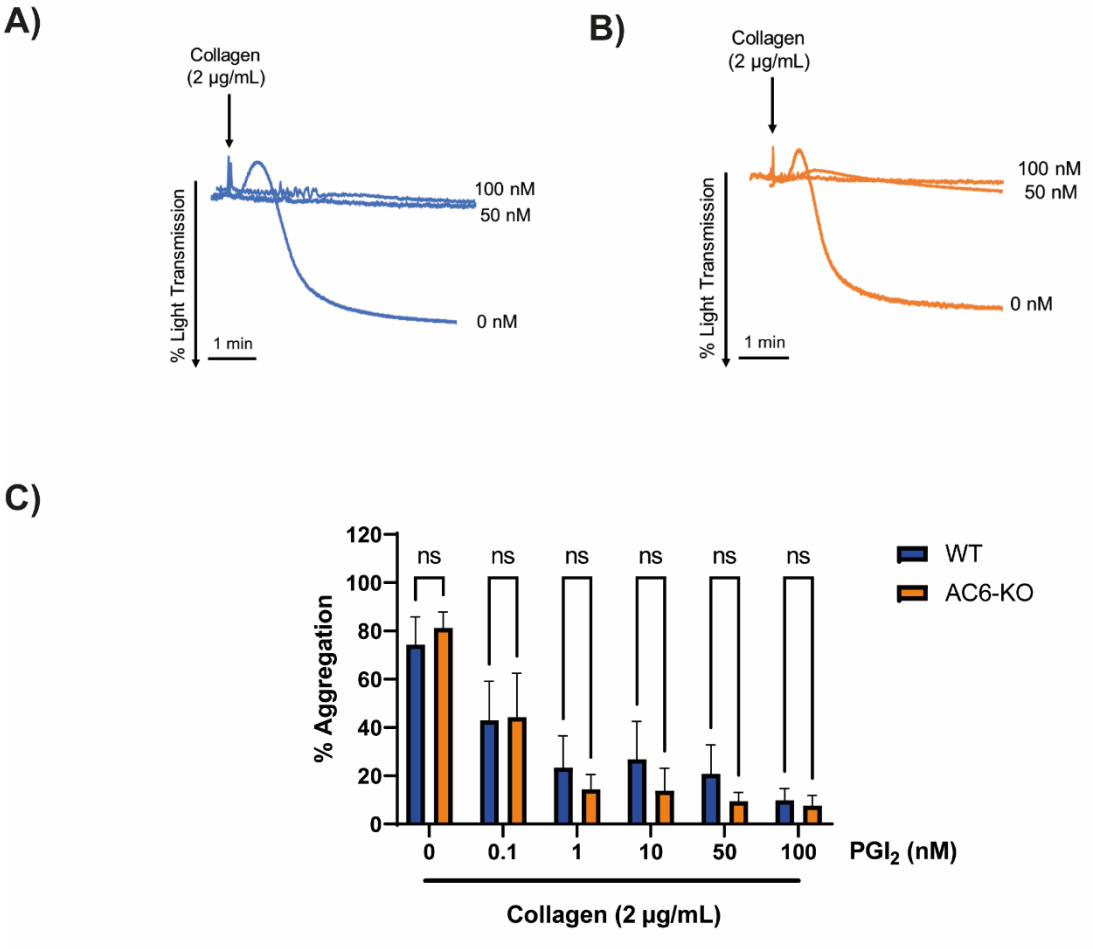

Figure 55. Inhibition of collagen-mediated platelet aggregation by PGI_2 is unaffected in AC6-KO platelets

Washed platelets ($2x10^8$ platelets/mL) were stimulated with PGI_2 (0.1 – 100 nM) for 2 minutes prior to addition of collagen (2 µg/mL) and aggregation was assessed for up to 10 minutes under constant stirring (800 rpm). Data presented as means ± SD shown by representative traces; WT (A) and AC6-KO (B), and percentage max aggregation (C). Comparisons were made between WT and AC6-KO by two-way ANOVA with Šídák's multiple comparisons test (n=5, ns=not significant).

4.6.2. AC6-KO mouse show impaired response to PGI_2 in thrombin-stimulated platelet aggregation

We next decided to assess PAR-mediated platelet aggregation in the AC6-KO in the absence and presence of PGI_2 (0.1-100 nM), prior to stimulation by thrombin (0.035 U/mL) (Figure 56).

Interestingly we found that inhibition of thrombin-stimulated platelet aggregation was significantly impaired in AC6-KO platelets compared to WT. While treatment with thrombin alone displayed no difference between AC6-KO and WT platelets (WT: 81.5 ± 11.5 % aggregation vs AC6-KO: 81.1 ± 7.9 % aggregation). We found that WT platelets demonstrated a clear concentration-dependent inhibition of thrombin-mediated platelet aggregation, whereas AC6-KO only displayed a subtle reduction upon treatment with PGI_2. Platelet aggregation in WT platelets was reduced from 81.5 ± 11.5 % aggregation (thrombin alone) to 8.3 ± 3.9 % aggregation (PGI_2; 100 nM), whereas AC6-KO platelets fell from 81.1 ± 7.9 % aggregation (thrombin alone) to 40.0 ± 23.7 % aggregation (PGI_2; 100 nM). These data demonstrate that AC6 is likely involved in PGI_2-mediated inhibition of PAR-stimulated platelet aggregation.

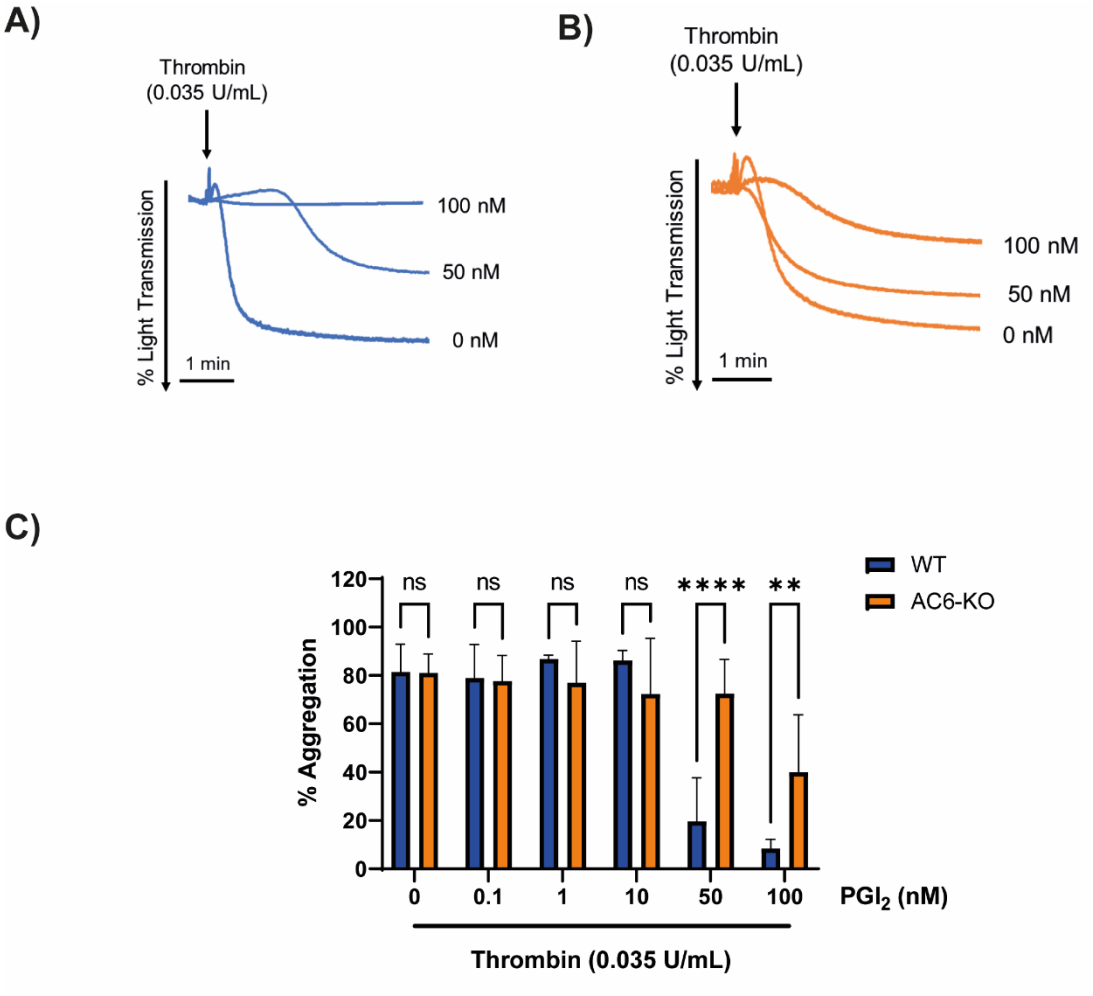

Figure 56. Impaired sensitivity to PGI_2 in AC6-KO platelets upon PAR-mediated platelet aggregation

Washed platelets ($2x10^8$ platelets/mL) were stimulated with PGI_2 (0.1 – 100 nM) for 2 minutes prior to addition of thrombin (0.035 U/mL) and aggregation was assessed for up to 10 minutes under constant stirring. Data presented as means ± SD shown by representative traces; WT (A) and AC6-KO (B), and percentage aggregation (C). Comparisons were made between WT and AC6-KO by two-way ANOVA with Šídák's multiple comparisons test (n=4, ns=not significant, **≤0.01 and ****≤0.0001).

4.6.3. Murine AC6 is not involved PGI_2-mediated inhibition of U44619-stimulated platelet aggregation

Given that AC6-KO platelets display reduced sensitivity to PGI_2 upon PAR-mediated platelet aggregation, we hypothesised whether this defect was G-protein specific. Therefore, we assessed platelet aggregation with and without PGI_2 (100 nM) upon stimulation with U46619 (0.5 µM), the more stable thromboxane (TxA_2) analogue (Figure 57).

We observed no differences in platelet aggregation by U46619 and inhibition by PGI_2 in U46619 stimulated platelets between WT and AC6-KO platelets. WT platelet aggregation was 77.9 ± 5.4 % aggregation (U46619 alone) compared to 4.5 ± 3.7 % aggregation (PGI_2; 100 nM) and aggregation of AC6-KO platelets went from 75.6 ± 3.5 % aggregation (U46619 alone) to 5.6 ± 4.6 % aggregation (PGI_2; 100 nM). These data confirm that the PGI_2 defect observed in AC6-KO platelets in response to thrombin is most likely specific to PAR-mediated signalling pathways rather than overall G-protein signalling.

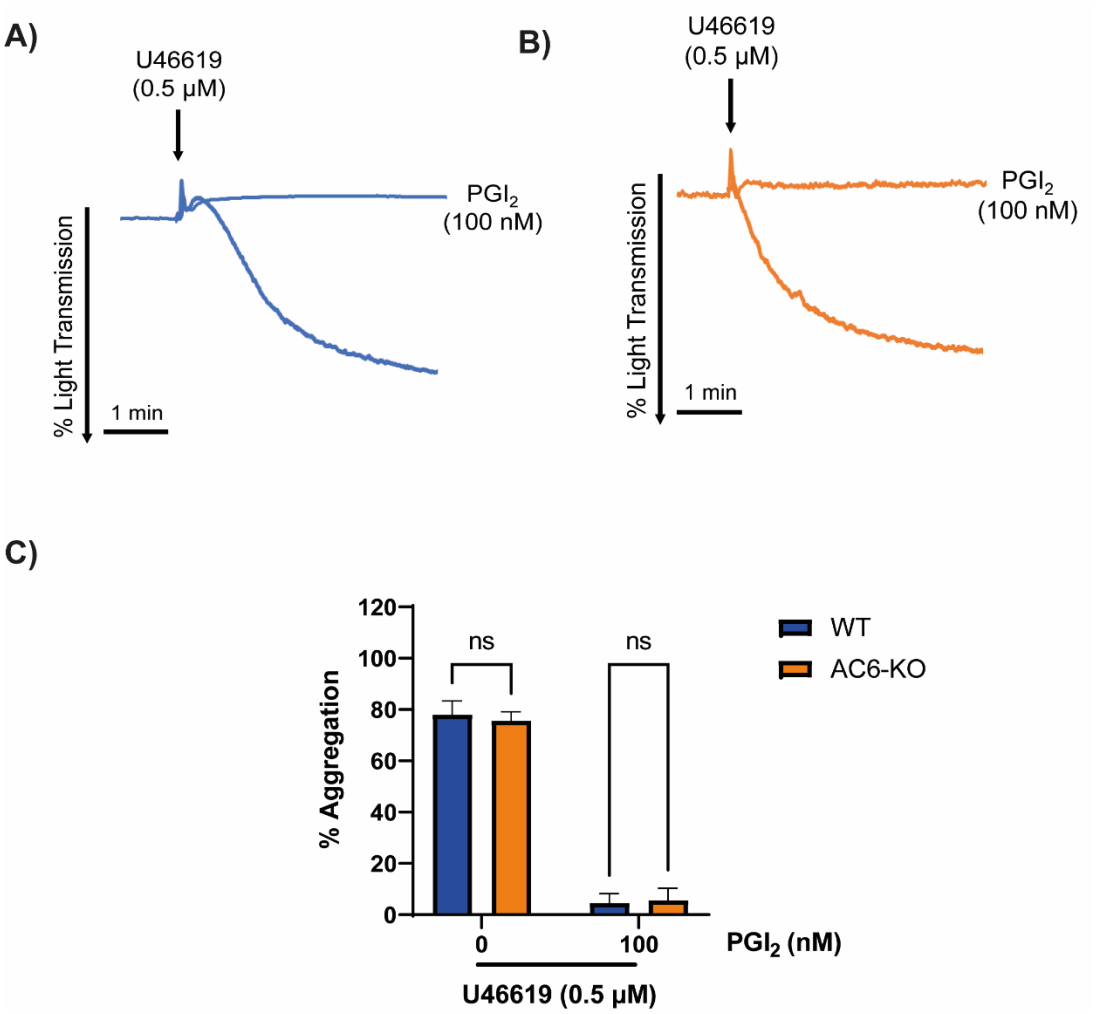

Figure 57. AC6 is not involved in PGI_2 mediated inhibition of TxA_2-stimulated platelet aggregation

Murine washed platelets ($2x10^8$ platelets/ml) were treated with PGI_2 (100 nM) for up to 1 minute prior to the addition of the thromboxane A_2 analogue, U46619 (0.5 µM). Aggregation was observed under constant stirring (800 rpm) at 37°C for up to 10 mins. Representative aggregation traces (A-B) were generated by AggRAM software (Helena Biosciences, UK). Bar graph (C) represents percentage aggregation at 10 mins presented as means ± SD and compared between WT and AC6-KO by two-way ANOVA with Šídák's multiple comparisons test (n=3, ns= not significant).

4.6.4. Murine AC6 is not involved in platelet inhibition by nitric oxide

To ensure that cGMP signalling was not affected by the deletion of AC6, we decided to assess platelet inhibition by GSNO (100 µM) (Archer, 1993), a well-established NO donor, upon stimulation with thrombin (0.035 U/mL) and collagen (2 µg/mL) (Figure 58).

We found no differences in GSNO-mediated inhibition of platelet aggregation between WT and AC6-KO platelets. Aggregation upon thrombin stimulation in WT platelets was 77.3 ± 1.07 % aggregation (thrombin alone) compared to 15.7 ± 4.5 % aggregation (GSNO; 100 µM). AC6-KO thrombin-mediated platelet aggregation went from 76.1 ± 5.29 % aggregation (thrombin alone) to 11.1 ± 5.2 % aggregation (GSNO; 100 µM). Similarly, WT collagen stimulated platelet aggregation went from 71.4 ± 17.1 % aggregation (collagen alone) to 21.5 ± 8.9 % aggregation (GSNO; 100 µM). AC6-KO collagen-mediated platelet aggregation went from 70.7 ± 8.4 % aggregation (collagen alone) to 16.7 ± 2.5 % aggregation (GSNO; 100 µM). Overall, these data demonstrate that AC6 is not implicated in cGMP-mediating signalling.

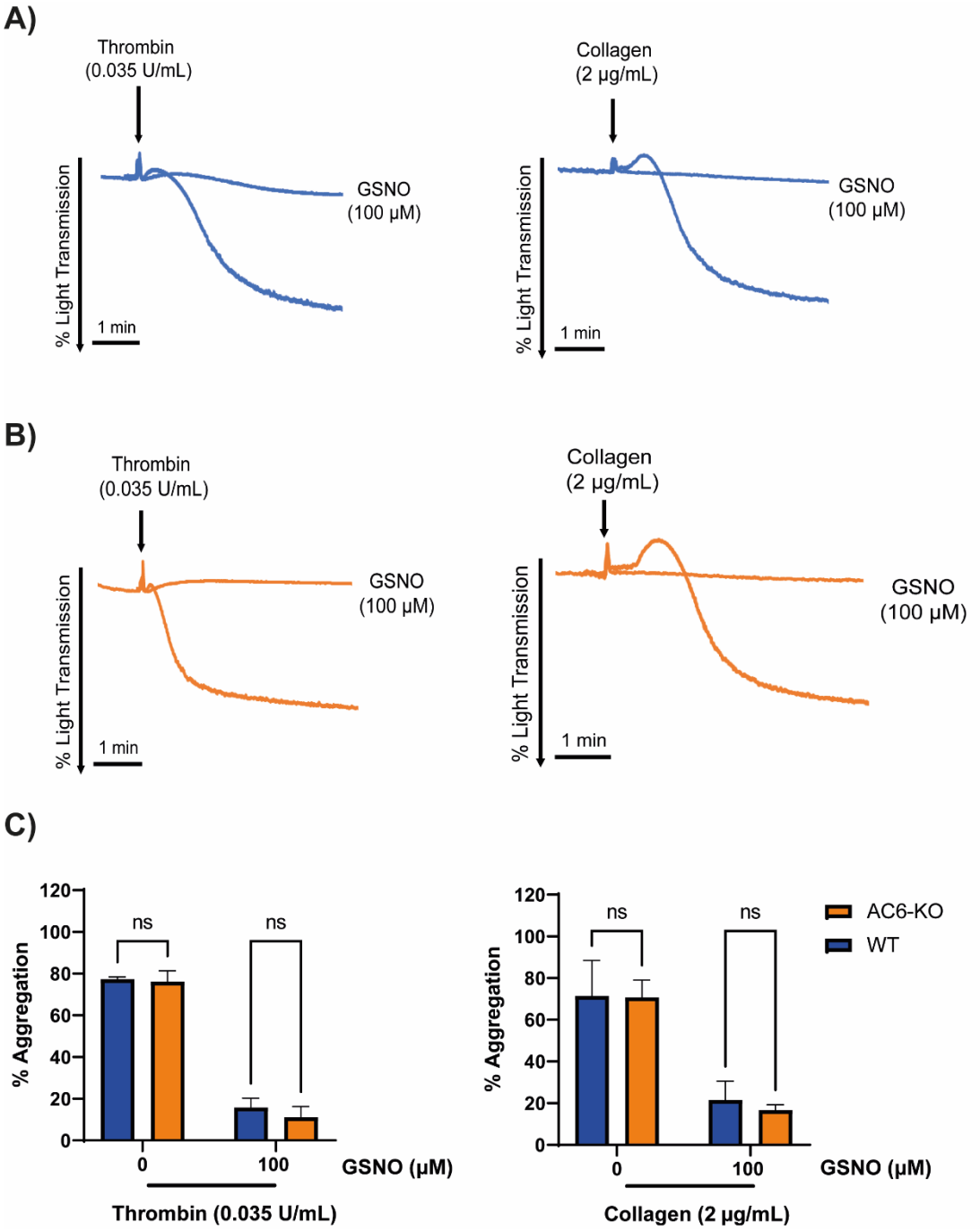

Figure 58. Inhibition of platelet aggregation by GSNO in AC6-KO platelets

Murine washed platelets ($2x10^8$ platelets/ml) were treated with nitric oxide donor, GSNO (100 µM) for up to 1 minute prior to the addition of thrombin (0.035U/mL) (left) or collagen (2 µg/mL) (right). Aggregation was observed under constant stirring (800 rpm) at 37°C for up to 10 mins. Representative aggregation (A – B) traces were generated by AggRAM software (Helena Biosciences, UK). Bar graphs (C) represent percentage aggregation at 10 mins presented as means ± SD and compared between WT and AC6-KO by two-way ANOVA with Šídák's multiple comparisons test (n=3, ns= not significant).

4.7. Expression of platelet surface activation markers

To cross-validate the findings in the platelet aggregation assays, a three-parameter whole blood flow cytometry activation panel was used to assess expression of key platelet activation makers upon stimulation with PAR4 peptide and CRP-XL, with and without PGI_2.

4.7.1. AC6-KO platelets demonstrate impaired PGI_2 sensitivity in response to PAR4 peptide but not CRP-XL

Whole blood was pre-treated with increasing concentrations of PGI_2 (0.1-100 nM) prior to addition of CRP-XL (1 µg/mL) or PAR4 peptide (100 µM) and CD62P (P-selectin) and JON/A (active $\alpha_{IIb}\beta_3$) expression was analysed by flow cytometry (Figure 59).

We found no difference in PGI_2-mediated inhibition of CRP-XL stimulated CD62P expression and JON/A binding between WT and AC6-KO platelets. Inhibition of CRP-XL-mediated CD62P expression and JON/A binding was near maximal inhibition at PGI_2 (20 nM) and did not further increase in both WT and AC6-KO, respectively. The percentage inhibition of CRP-XL mediated CD62P expression in WT platelets was 76.6 ± 14.7 % (PGI_2; 20 nM) and in AC6-KO platelets it was 80.4 ± 8.3 % (PGI_2; 20 nM). This was also observed for the percentage inhibition of CRP-XL mediated JON/A binding. The percentage inhibition of JON/A binding in WT platelets was 76.5 ± 14.7 % (PGI_2; 20 nM), while in AC6-KO platelets it was 80 ± 8.3 % (PGI_2; 20 nM), demonstrating no significant difference in PGI_2-mediated inhibition of CRP-XL driven platelet activity in WT and AC6-KO platelets.

In contrast, upon PAR4 peptide stimulation, AC6-KO platelets displayed markedly impaired PGI_2 sensitivity compared to WT. Inhibition of PAR4-mediated CD62P expression in WT platelets was 80.3 ± 13.6 % inhibition (PGI_2; 20 nM), whereas AC6-KO platelets were inhibited by 30.3 ± 6.7 % inhibition (PGI_2; 20 nM) (PGI_2 20 nM WT vs AC6-KO, $p<0.0001$). This trend was also observed in inhibition of PAR4-mediated JON/A binding, whereby WT platelets showed 85.9 ± 5.9 % inhibition (PGI_2; 20 nM) while AC6-KO platelets demonstrated 65.8 ± 14.9% inhibition (PGI_2; 20 nM) (PGI_2 20 nM, WT vs AC6-KO, $p=0.0003$). Therefore, consistent with platelet aggregation

data, these data demonstrate that AC6 is involved in inhibition of PAR-mediated, but not GPVI-mediated platelet activity by PGI_2.

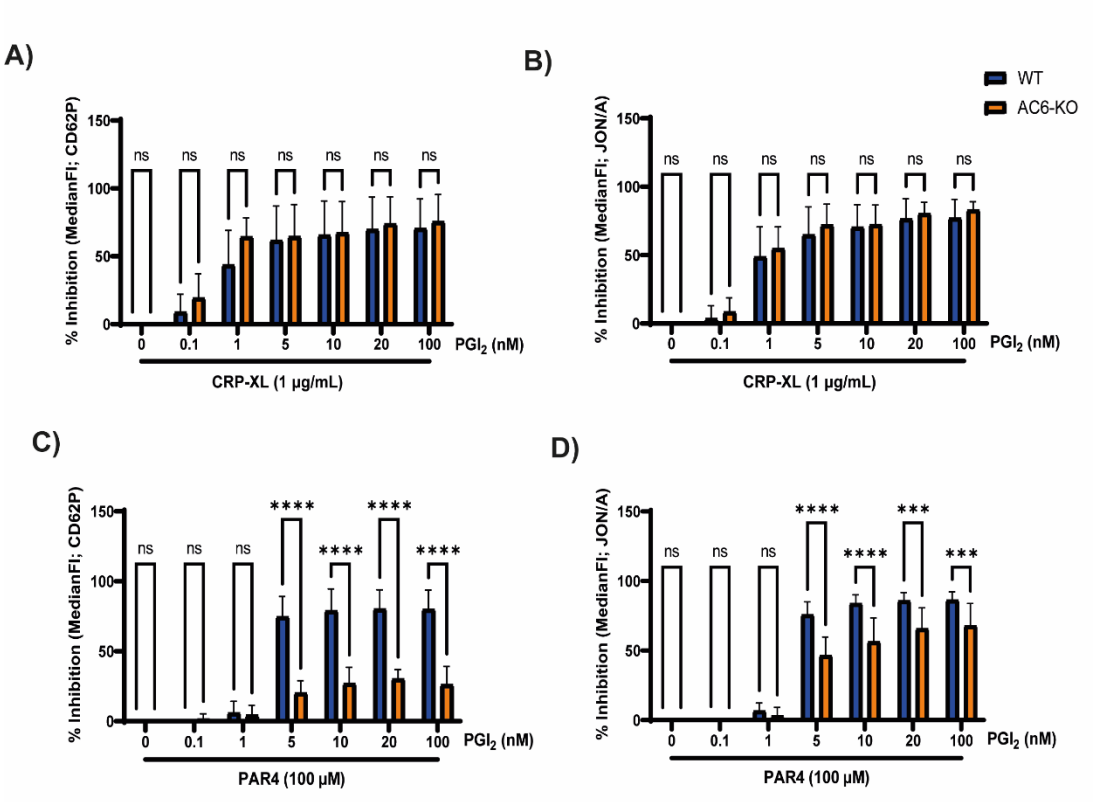

Figure 59. Impaired PGI_2 response upon stimulation with PAR4 peptide by flow cytometry in the AC6-KO mouse

Murine whole blood was stimulated with either PAR4 (100 µM) or CRP-XL (1 µg/mL) and probed CD62P (left) and JON/A (right) for 20 minutes prior to fixation in fix-lyse (BD). CD41-BB700 was used as a platelet marker and samples were analysed for 10,000 platelet positive events. Bar graphs represent percentage inhibition based on median fluorescence intensity. Data presented as means ± SD and compared between WT and AC6-KO by two-way ANOVA with Šídák's multiple comparisons test (n=5, ns = not significant, ***≤0.001, ****≤0.0001).

4.7.2. Effect of PGI_2 on the exposure of phosphatidylserine in AC6-KO platelets

After establishing that inhibition of PAR-mediated platelet activation is impaired in the AC6-KO, we decided to assess whether this defect was present upon inhibition of phosphatidylserine (PS) exposure by PGI_2. Platelet activation by PAR and GPVI receptors leads to the generation of two subpopulations of platelets, pro-aggregatory and pro-coagulant populations (Agbani and Poole, 2017). Pro-aggregatory platelets are defined by activated integrin $\alpha_{IIb}\beta_3$, which acts to support platelet aggregation and clot retraction. While a pro-coagulant platelet population is characterised by mitochondrial membrane depolarisation (Choo et al., 2017), sustained calcium influx (Choo et al., 2012) and exposure of PS on their surface (Podoplelova et al., 2016). Exposure of PS helps to facilitate blood coagulation by binding to coagulation markers to generate thrombin (Monroe et al., 2002) and is, therefore, a key marker for platelet activation. PS exposure is measured by AnnV binding and requires activation of both PAR and GPVI receptors in order to undergo PS translocation to the platelet surface (Tait et al., 1999). Previously we have shown that PS exposure is inhibited by PGI_2 in human platelets (Hindle et al., 2021).

PGI_2 induced a concentration dependent inhibition of both CRP-XL alone and dual agonist stimulation in WT and AC6-KO platelets. However, consistent with data in Figure 59, stimulation with CRP-XL alone presented no difference in percentage inhibition by PGI_2 between WT and AC6-KO (Figure 60 A), therefore we decided to assess whether stimulation of both PAR- and GPVI-mediated signalling pathways would display the defect.

Upon dual agonist stimulation, percentage inhibition by PGI_2 (100 nM) was significantly reduced in AC6-KO platelets compared to WT. The greatest difference observed was at PGI_2 (10 nM) whereby WT platelets displayed 59.7 ± 23.1 % inhibition whereas AC6-KO platelets showed 20.9 ± 20.5 % inhibition of PS exposure ($p=0.003$). The difference was still observed at PGI_2 (100 nM) with WT platelets showing 77.4 ± 11.8 % inhibition while AC6-KO platelets displayed 50.1 ± 17.0 % inhibition of PS exposure ($p=0.03$) (Figure 60 B). In combination with work presented in Figure 59, these data confirm that AC6 is involved in controlling the extent of PAR-mediated platelet activation.

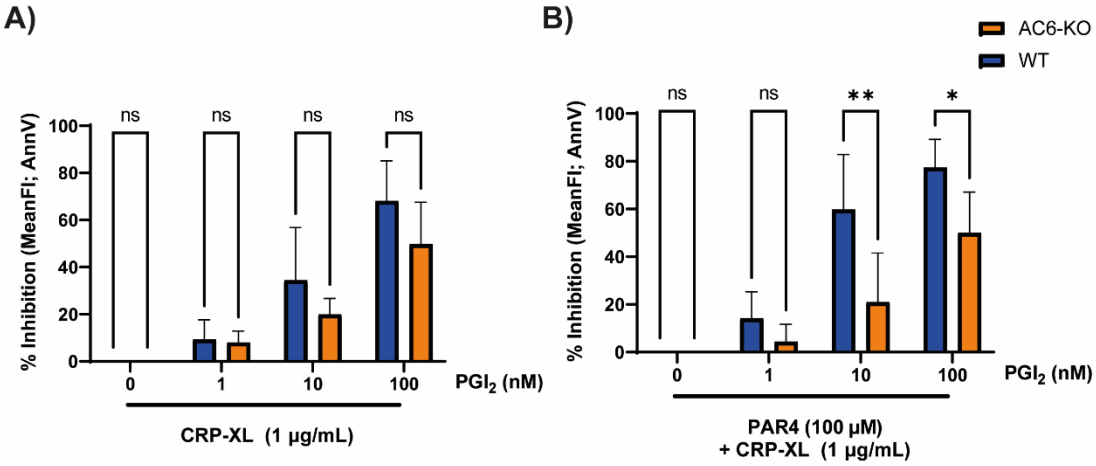

Figure 60. Impaired inhibition of PS exposure by PGI_2 upon stimulation with PAR4 peptide in AC6-KO platelets

Murine whole blood was stimulated with either CRP-XL (1 µg/mL) or in combination with PAR4 peptide (100 µM) and probed with AnnV for 20 minutes prior to fixation in fix-lyse (BD). CD41-BB700 was used as a platelet marker and samples were analysed for 10,000 platelet positive events. Bar graphs represent percentage inhibition based on mean fluorescence intensity (MeanFI). Data presented as means ± SD and compared between WT and AC6-KO by two-way ANOVA with Šídák's multiple comparisons test (n=4, ns = not significant, *≤0.05, and **≤0.01).

4.8. Assessment of thrombosis by $FeCl_3$ injury in the AC6-KO mouse

To apply these findings to a more physiological setting we assessed thrombosis in real-time in response to $FeCl_3$ injury in WT and AC6-KO mice using fluorescent intravital microscopy methods.

4.8.1. Murine platelet AC6 mediates thrombosis

To further assess the physiological role of AC6 in platelet function, we induced thrombosis in mesenteric vessels via $FeCl_3$ injury and measured thrombus formation in real-time. Injury was assessed up to 30 minutes or until vessel occlusion occurred (Figure 61).

We found a striking difference between WT and AC6-KO mice in response to injury. Firstly, AC6-KO mice were observed to have a more rapid vessel occlusion time, 17.7 ± 4.3 min (AC6-KO) compared to 26.3 ± 3.3 min ($p=0.003$) (WT). Furthermore, the percentage size of thrombus over time was markedly increased in AC6-KO mice, for example at 7.5 mins post-injury AC6-KO mice displayed 17.2 ± 10.8 % thrombus size while WT was 1.9 ± 3.5 % thrombus size. These data suggest that platelet AC6 plays a key physiological role in controlling thrombosis.

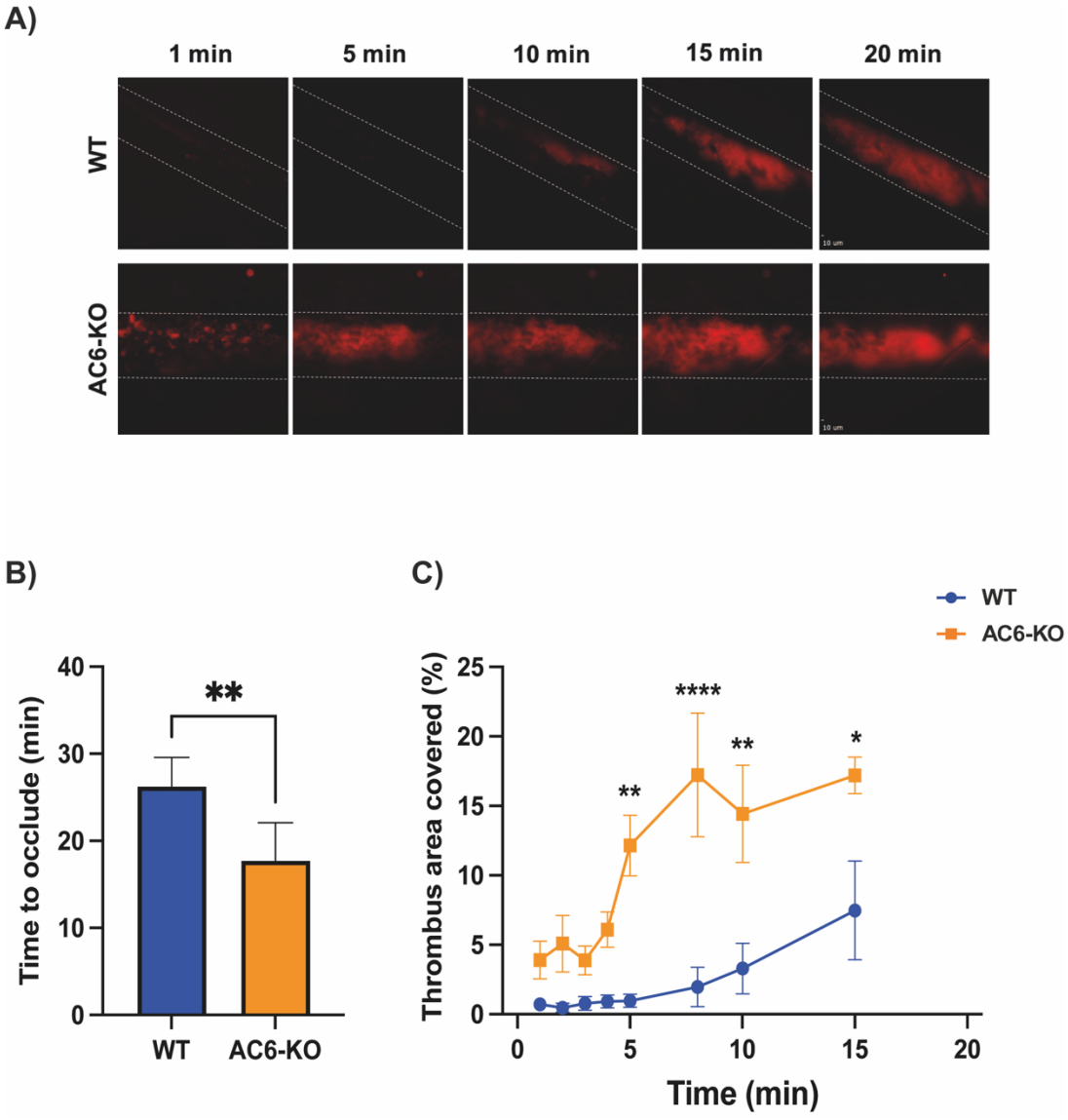

Figure 61. Murine AC6 mediates thrombosis

Filter paper (1mm x 1mm) pre-soaked in $FeCl_3$ (7.5%) was placed on top of exposed mesenteric vessels for 30 seconds of anaesthetized mice. Injury was assessed up to 30 minutes or until vessel occlusion. Images were taken every minute up to 5 minutes, then every 5 minutes up to 30 minutes. Percentage thrombus size over time and occlusion time was taken from an average of two vessels per mouse. Data presented as means ± SD and compared between WT and AC6-KO. Time to occlude analysed by an unpaired students t-test and percentage thrombus size over time was analysed by two-way ANOVA with Šídák's multiple comparisons test (n=6 mice, *≤0.05, **≤0.01, and ****≤0.0001).

4.8.2. AC6-KO mice form clots that are less stable

After establishing that AC6 plays a role in thrombosis we analysed the kinetics of thrombus formation in each individual mouse. This approach examined the levels of fluorescence to determine whether this remains constant over the time course (Figure 63). We used the approach previously described by Duval and colleagues (2021) to determine thrombus stability. A fall in thrombus size (fluorescence) greater than 15% between each time point was considered an embolic event (Figure 62 C). Thrombus size under 5% was considered a background signal and was excluded from analysis.

We observed more falls in thrombus size between subsequent time points in the AC6-KO compared to WT (Figure 62 A-B). AC6-KO mice displayed a 2-fold increase in the number of embolic events compared to WT. Additionally, the percentage decrease in thrombus size per time point in the AC6-KO was 2.7-fold greater compared to WT (Figure 62 D). While the time for the first embolic event to occur was 2.7-fold lower in the AC6-KO compared to WT (Figure 62 E). While not significant, these data represent an emerging phenotype whereby thrombus stability is altered by the loss of AC6.

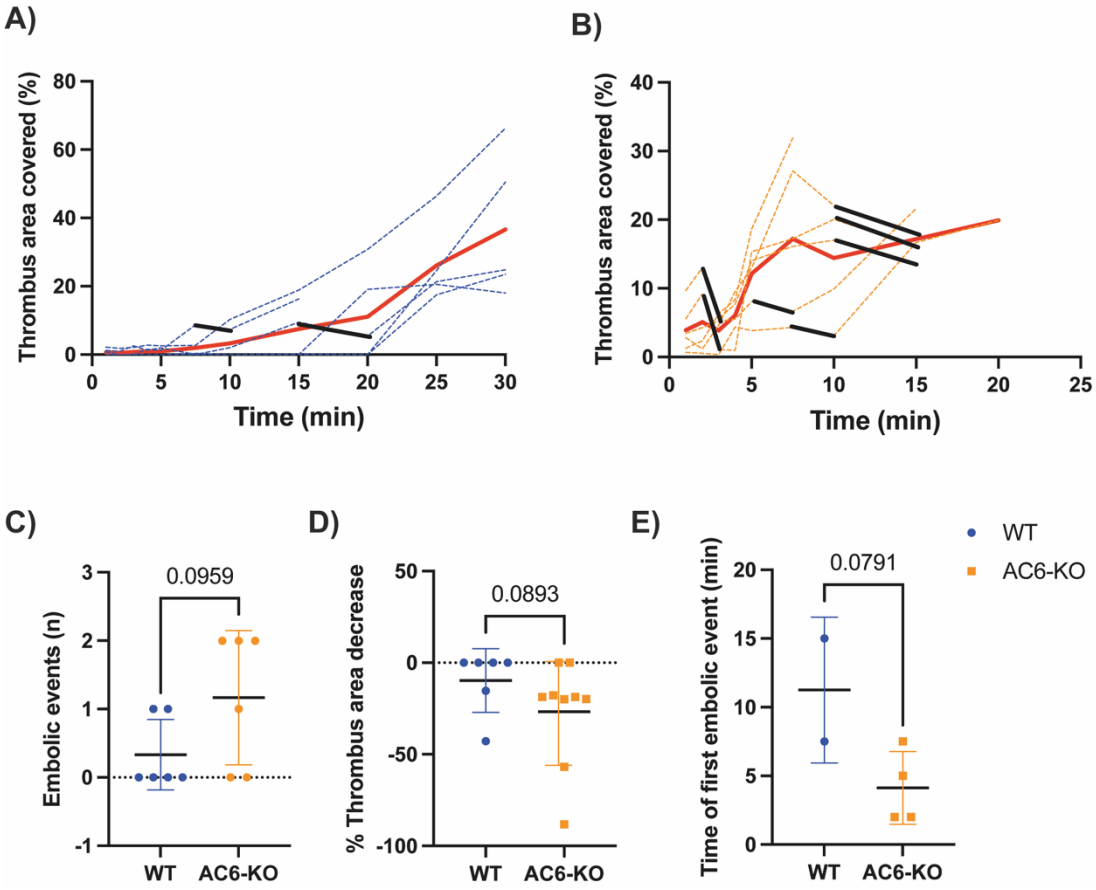

Figure 62. Clot stability is reduced in AC6-KO mice

Following injury to mesenteric vessels with $FeCl_3$ (7.5 %) for 30 secs, clot size was measured over time in WT (A) and AC6-KO (B). Dashed lines represent individual injuries, red line represents average thrombus area and bold lines represent a reduction in thrombus size greater than 15% (embolic event). The number of embolic events (C) was lower in WT mice compared to AC6-KO and the percentage decrease in thrombus area was greater in AC6-KO compared to WT (D). A reduction in time of first embolic event was also observed in AC6-KO compared to WT (E). Data presented as individual values, with horizontal bars indicating means ± SD and analysed by an unpaired students t-test (C and E) and Kolmogorov-Smirnov test (D).

4.9. Discussion

In this part of the study, we have used a conditional genetic approach to investigate the functional role of AC6 in platelet function *in vitro* and *in vivo*. The data suggests that the AC6-KO mouse is specific to platelets and platelet morphology is unchanged between AC6-KO and WT. We have also demonstrated that the AC6-KO mouse displays an impaired response to PGI_2 in PAR but not GPVI mediated platelet activity. In addition, we have found that AC6 mediates thrombosis as well as contributes to thrombus stability.

4.9.1. Confirmation of platelet specific AC6-KO mouse

The development of a platelet specific AC6-KO was vital for this study; therefore, it was important to establish whether our breeding strategy generated an AC6 deletion in platelets alone. In combination with routine genotyping, we used qPCR techniques to assess the absence or presence of the AC6 gene (*ADCY6*) in WT vs AC6-KO platelets. We have shown that *ADCY6* was successfully deleted in platelets and remained intact in other tissues known to express the enzyme (Figure 47). Assessment of expression of AC3 and AC5, showed that AC5 was present in both WT and AC6-KO platelets. While AC3 was not present in either, consistent with other studies (Rowley et al., 2011; Burkhart et al., 2012). This was cross validated by immunoblotting techniques whereby total AC expression was assessed (Figure 48). We found a significant reduction in total AC expression in AC6-KO platelets compared to WT, confirming the presence of another AC, likely AC5 (Rowley et al., 2011; Burkhart et al., 2012). While AC5 is not present in human platelets, the deletion of platelet specific AC6 allows us to identify the role of AC6 on platelet function. These data demonstrate that AC6 is specifically knocked out in platelets and that the other AC, AC5, is intact.

4.9.2. Basic characterisation of the AC6-KO mouse

Examination of the genetically modified mice in terms of body weight, isolated platelet yield, platelet counts in whole blood, reticulated platelets, and surface receptor expression, demonstrated that these parameters were comparable between the two strains.

Critically, we looked at the isolated platelet yields from ~1 mL of whole blood generated by WT and AC6-KO mice as means of estimating platelet count.

We observed no difference in isolated platelet yield in WT and AC6-KO platelets (Figure 49). While not significant, male AC6-KO platelets displayed a higher yield, but this was likely due to the age of the mice.

To cross-validate this, we then measured platelet counts in whole blood using flow cytometry whereby CD41 positive events were recorded for 2.5 minutes and analysed by CD41 positive events per µL of whole blood. Consistent with data in Figure 49 we found no difference in CD41 positive events/µL whole blood between WT and AC6-KO platelets, giving further confirmation that removal of AC6 does not affect platelet counts (Figure 50). Murine platelet counts are variable across different studies (Bull et al., 1965; Levin and Ebbe, 1994; Jirouskova et al., 2007; Fukuda et al., 2017; Aurbach et al., 2019). A study by Aurbach and colleagues (2019) compared blood collection, platelet isolation methods, as well as platelet counting methods via flow cytometry and a bioanalyzer. They found that differences in platelet counts were largely due to mouse strain, genetic modifications, and methodology. We found that our CD41 positive events by cytometry were lower compared to these studies, however, it is important to note that we did not use beads for our platelet count analysis, therefore the data are not directly comparable. Instead, our data demonstrates the number of CD41 positive events, which were first gated by platelet physical characteristics, then by CD41 positive events. Arguably using beads is a more accurate measurement (Nieswandt et al., 2004), as the beads create a comparative standard count, however, counts were consistent between each experiment and we observed no difference between WT and AC6-KO platelets. In addition, to maximise murine blood usage, we collected blood into ACD as described in 2.3.1 to allow for whole blood and washed platelet experiments to be carried out from one mouse, other studies used ETDA or Heparin for whole blood analysis, which could be attributed to the differences we observed (Jin et al., 1997; Banfi et al., 2007; Aurbach et al., 2019). In addition, our yield from washed platelets counts using a coulter particle counter were more consistent with the literature (Figure 49), therefore the low numbers observed in both strains by flow cytometry were no cause for concern.

To establish whether platelet lifespan was affected by deletion of platelet AC6 we measured the presence of reticulated platelets using flow cytometry, as an

indirect method to assess platelet maturity. We observed no difference in the presence of reticulated platelets in AC6-KO compared to WT suggesting that AC6 does not play a key role in platelet lifespan (Figure 51). In hindsight we should have used a platelet marker to establish the percentage of reticulated platelets within the platelet population as described by Hamad et al., (2021). Our data is presented as MedianFI of thiazole orange, on the principle that the more thiazole orange present in a cell, the more genetic material and hence, the younger the platelet is.

We next assessed surface receptor expression in WT and AC6-KO platelets by flow cytometry (Figure 52). We found no difference in surface receptor expression between WT and AC6-KO platelets and were consistent with other studies using genetically modified mice (Pleines et al., 2010; Munzer et al., 2017).

Finally, we assessed platelet morphology via platelet adhesion and spreading upon fibrinogen (Figure 53). We observed no difference in spreading and adhesion between WT and AC6-KO upon fibrinogen (100 µg/mL). Platelet spreading and adhesion was normal in AC6-KO platelets compared to WT, which allowed us to then assess the effect of PGI_2 on platelet spreading and adhesion (Figure 54). While the presence of PGI_2 had no effect on the number of platelets adhered in the AC6-KO compared to WT (Figure 54 B), we did however observe a significant reduction in platelet spreading as displayed by a reduction in percentage area per FoV (Figure 54 C). Though there was a reduction, it was to a much lesser extent than WT platelets, suggesting that AC6 may have a role in PGI_2-mediated inhibition of platelet spreading. Comparison between WT and AC6-KO demonstrated that PGI_2 had a more profound reduction in WT platelets to AC6-KO platelets, however, this was not significant. In theory, a loss of AC6 should reduce the effect of PGI_2, however, we did not observe such a reduction. It's worth noting that platelets were pre-treated with 0.05 U/mL thrombin to initiate spreading and compared to other studies (Mazharian et al., 2007; Pleines et al., 2010) this was a much higher thrombin concentration, which may contribute to a lack of difference upon PGI_2 treatment between WT and AC6-KO platelets. Overall, studies of the basic characterisation of these platelets demonstrates that AC6-KO platelets

are comparable to WT platelets and deletion of AC6 does not affect general platelet morphology.

4.9.3. AC6-KO platelets display impaired response to PGI_2 in PAR but not GPVI-mediated platelet activation

We then set out to establish platelet function in the AC6-KO mouse compared to WT. In the first instance, we assessed platelet aggregation in the presence and absence of PGI_2. Despite the loss of AC6, platelet aggregation upon thrombin or collagen alone remained normal and unchanged between WT and AC6-KO, suggesting that AC6 per se does not influence responsiveness to key agonists. To our surprise we found that sensitivity to PGI_2 was only affected when platelets were stimulated with thrombin but not collagen. This was not linked to all GPCRs since U46619 aggregation was unaffected (Figure 57). Upon activation, platelets release ADP leading to the synthesis of TxA_2 which acts to both promote platelet activation and recruit additional platelets to the site of injury (Offermanns, 2006). To support platelet activation, ADP triggers $G\alpha_i$ leading to the selective inhibition of AC5 and AC6 (Godinho et al., 2015). ADP and TxA_2 work in synergy to enhance platelet activity (Koupenova and Ravid, 2018), while ADP was not tested, the use of U46619 allowed us to assess whether the inhibitory defect observed in response to thrombin-mediated platelet aggregation was PAR-specific or G-protein linked. We observed no such defect in response to PGI_2 upon stimulation with U46619 in AC6-KO platelets compared to WT. Suggesting that the impaired PGI_2 response in AC6-KO platelets (Figure 56) is most likely PAR-mediated.

Previously it was reported that the IP receptor and AC5/6 are co-expressed in microdomains that control the extent of cAMP generation, along with PKA in platelets (Raslan, Z. and Naseem, K.M., 2015; Raslan et al., 2015b). While others document that AC5 and AC6 from rat brains, interact with A-kinase anchoring protein (AKAP) 79/150, directing cAMP signalling via PKA towards a β-adrenergic receptors, G-protein and AC network (Bauman et al., 2006; Dessauer, 2009). Highlighting that ACs could be in close proximity to specific receptors, facilitating the control of cAMP signalling. Therefore, it could be possible that AC6 resides in a complex with PAR receptors, facilitating opposing signals from G_s and G_i.

While cross-talk between cAMP and cGMP signalling does exist this is typically restricted to the action of PDEs (Manns et al., 2002; Moorthy et al., 2011). PDEs act to control the levels of cyclic nucleotides via hydrolysis of cAMP and cGMP. PDE3A regulates cAMP through a cGMP-inhibited mechanism, while PDE2 acts via a cGMP-stimulated process, marrying the two pathways together (Manns et al., 2002; Weber et al., 2017). Previously, a study by Wangorsch et al., (2011), demonstrated stimulation of AC-mediated cAMP production in silico using forskolin and iloprost did not impact cGMP signalling (Wangorsch et al., 2011). Despite this, it was important to examine whether this was the case in murine platelets. Using GSNO as a NO-donor, we found no difference between WT and AC6-KO platelets, with respect to inhibition of aggregation (Figure 58).

Platelet aggregation is the culmination of multiple platelet functions and therefore is important to assess. However, it was also important to ascertain if individual platelet functions were affected. Using flow cytometry to measure integrin activation, α-granule secretion, and PS exposure, we found that the ability of PGI_2 to inhibit each was compromised in AC6-KO but not WT in response to PAR4 peptide. These data highlight a number of important issues. Firstly, the loss of AC6 is linked to PAR activation, secondly, given that multiple functions are affected, compromised cAMP signalling by the absence of AC6 is common to multiple platelet functions and thirdly, the defect is apparent in whole blood (Figure 59 – 60).

Elevation of platelet cAMP levels is regulated by the opposing activity of AC and PDEs (Hunter et al., 2009) with PAR-mediated platelet activity known to increase the hydrolysis of cAMP by PDE3A (Zhang and Colman, 2007). We've demonstrated in both washed platelets and whole blood, that a loss of AC6 is linked PGI_2-mediated inhibition of PAR stimulated platelet activity. Though Hunter and colleagues (2009) demonstrated that PDE3A activity upon platelet activation is PKC mediated, thus linked to both collagen- and thrombin-mediated platelet activation, their work primarily focussed on thrombin-mediated PKC activity. Based on our data, the removal of AC6, therefore, impairs cAMP-mediated inhibition by PGI_2, while the combination of PAR activation increases PDE3A activity, likely resulting in diminished inhibition of PAR-mediated activity.

4.9.4. AC6 plays a key role in mediating thrombosis and thrombus stability in mice

The extent of platelet activity at the site of injury is strictly controlled by cAMP signalling in response to tonic inhibition by PGI_2, as well as NO-stimulated cyclic nucleotide signalling (Beaulieu and Freedman, 2013). In addition, the marginalisation of platelet during blood flow facilitates their exposure to PGI_2. Upon vascular injury, platelets enter the site of injury in a high cAMP/cGMP state, with exposure to high agonist concentrations leading to PDE activity, resulting in reduced inhibitory signalling. Therefore, one could argue that a loss of AC6, and successive impaired cAMP signalling, are likely to present a prothrombotic phenotype.

To establish a physiological function of platelet AC6 we assessed thrombosis in real-time via $FeCl_3$ injury of mesenteric vessels, and we found clear differences between WT and AC6-KO mice (Figure 61). In the absence of platelet AC6, the mice displayed a markedly quicker vessel occlusion time. Furthermore, the size of the thrombus area over time was noticeably increased compared when compared to WT. These data suggest that whilst the reduced sensitivity to the inhibitory effects of PGI_2 *in vitro* relate primarily to PAR-mediated platelet activity, in the complex conditions found *in vivo*, this defect is linked to an abnormal thrombotic response.

Overall, the data suggests that AC5 is still intact in these platelets and that they retain the ability to synthesise some cAMP, though the levels of the cyclic nucleotide produced are not sufficient to maintain a normal response to injury. Further, that AC6 plays a key role in response to injury. Thrombus size can be influenced by its stability and the possibility of embolisation. We examined the potential role of platelet AC6 in mice by assessing “drops or falls” in fluorescence using methods established by Duval and colleagues (2021). Thromboembolic events involve fragments of thrombi leaving the growing thrombus and affecting downstream organs such as the lung or brain. These thromboembolic events include pulmonary embolism and stroke, which affect over 1 million people annually worldwide (Machlus et al., 2011; Huisman et al., 2018; Jame and Barnes, 2020). While we did not track emboli, our analysis observed unstable thrombus formation with an increase in embolic events in the absence of platelet AC6 (Figure 62). The parameters that Duval and

colleagues used, considered anything greater than a 25% loss as an embolic event, whereas we opted for a loss of over 15% as we argued that this is still a substantial loss of the thrombus. Especially as subsequent embolic events occurred at the later stages of thrombus formation, with a loss of over 15% were observed in the AC6-KO compared to WT.

Thrombosis injury models highlight that accelerated thrombosis and unstable thrombi go hand in hand (Duval et al., 2021). Even in studies whereby embolic events have not been analysed, it's clear that data exhibiting an accelerated thrombotic phenotype displays drops in thrombus growth over time (Berger et al., 2020). Instead of relying on anticoagulants for treating thrombotic events, future treatments should account for thrombus quality and stability. We have shown that the loss of AC6 results in unstable thrombus formation, though the mechanisms are unclear, this could be linked to downstream PKA signalling events.

Overall, the data described in this chapter provide an interesting insight to the role of AC6 in platelet function and thrombosis. We've demonstrated that AC6 is linked to inhibition of PAR-mediated signalling but not GPVI, the extent of thrombus formation and stability. Work described in the subsequent chapter will aim to establish the role of AC6 in cAMP signalling.

Chapter 5
Characterisation of AC6-mediated signalling in the AC6-KO mouse

5.1. Introduction

Reduced sensitivity to PGI_2 in cardiovascular disease and diabetes mellitus have been reported several early studies, though the precise mechanisms are yet to be elucidated (Akai et al., 1983; Burghuber et al., 1986). While some studies attribute reduced PGI_2 sensitivity and impaired cAMP signalling to IP receptor expression (Knebel et al., 2015), other factors could be at play. Impaired PGI_2 sensitivity and subsequent cAMP signalling in disease could be attributed to a fault in AC activity. More recently, impaired platelet AC signalling in was identified in ACS and hyperglycaemia (Imam et al., 2019). They also found that post-receptor AC-dependent signalling was a major source of variability in individual patients' responsiveness to $P2Y_{12}$ receptor antagonists, highlighting the importance of understanding AC-mediated cAMP signalling in disease and disease treatment (Imam et al., 2019). Work in this chapter aims to elucidate the relative contribution of AC6 to basal and stimulated cAMP production as well as downstream PKA signalling events.

5.1.1. Aims of chapter

- To assess the relative contribution of AC6 in platelet cAMP production
- To identify PKA substrates linked to AC6 activation
- To identify downstream signalling consequences as a result of AC6 deletion

5.2. Assessment of platelet cAMP production in AC6-KO platelets

After demonstrating a functional defect in response to PAR-mediated inhibition by PGI_2 in AC6-KO platelets as well as accelerated thrombosis (Chapter 4) we decided to assess whether this was linked to altered cAMP signalling as a result of AC6 deletion.

5.2.1. Assessment of cAMP production in response to PGI_2 in AC6-KO platelets

We found no differences in basal cAMP concentrations between AC6-KO and WT, suggesting that AC6 does not contribute significantly to basal cAMP production. In contrast, AC6-KO platelets showed significantly reduced responses to PGI_2-induced cAMP generation (Figure 63). PGI_2 (1 -100 nM) induced a concentration-dependent increase in intracellular cAMP (Figure 63 B) in both strains of mice. However, the concentration of the cyclic nucleotide was significantly lower in AC6-KO platelets (PGI_2 100 nM, $p<0.0001$). Production of cAMP in WT platelets was increased from 237.1 ± 147.4 fmol/10^7 platelets at basal, peaking at 30 secs of PGI_2 (100 nM) to 8167.6 ± 2603.3 fmol/10^7 platelets. While AC6-KO platelets went from 278.6 ± 134.1 fmol/10^7 platelets (basal) to 2359.2 ± 823.6 fmol/10^7 platelets (30 secs; PGI_2 100 nM, $p<0.0001$). (Figure 63 A). Importantly the absence of AC6 did abolish cAMP generation in response to PGI_2.

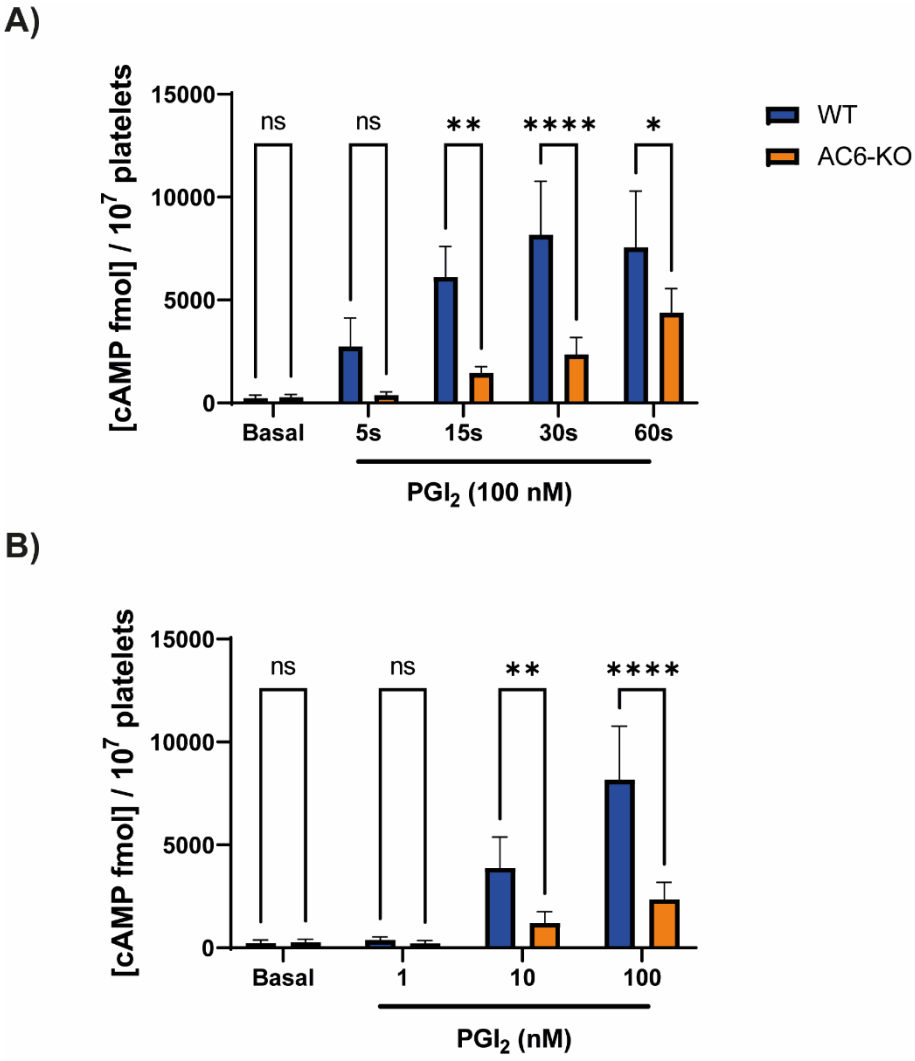

Figure 63. Impaired PGI_2-mediated cAMP production in AC6-KO platelets

Murine washed platelets ($2x10^8$ platelets/mL) were treated with PGI_2 (100 nM) over time (A) or increasing concentrations of PGI_2 (1-100 nM) for 30 secs (B) at RT. Reactions were terminated by the addition of lysis buffer containing 2.5% dodecyltrimethylammonium bromide and cAMP levels were assayed with a commercially available enzyme immunoassay system (Cytiva) and expressed as fmol cAMP/10^7 platelets. All assays were carried out in duplicate, and data presented as means ± SD and compared between WT and AC6-KO by two-way ANOVA with Šídák's multiple comparisons test (n=5, ns=not significant, *≤0.05 **≤0.01, and ****≤0.0001).

5.2.2. Effect of SQ22536 on cAMP production in AC6-KO platelets

In an attempt to understand the source of basal cAMP in the AC6 deficient platelet used the direct AC inhibitor, SQ22536 (Emery et al., 2013). We hypothesised that using SQ22536 would block any remaining AC activity therefore would abolish PGI_2-mediated cAMP production (Figure 64).

Interestingly, we only found a partial reduction in cAMP synthesis in response to SQ22536 in WT, with no effect in AC6-KO platelets. In WT platelets, a significant reduction in cAMP synthesis was only observed at PGI_2 (100 nM), whereby cAMP reduced from 8167.6 ± 2603.4 fmol/10^7 platelets (PGI_2 alone) to 4855.3 ± 1517.7 fmol/10^7 platelets (SQ22536 + PGI_2 100 nM; p=0.02). While AC6-KO platelets displayed no significant difference upon SQ22536 treatment, cAMP production went from 2359.2 ± 823.6 fmol/10^7 platelets (PGI_2 alone) to 3243.3 ± 551.7 fmol/10^7 platelets (SQ22536 + PGI_2 100 nM). These data suggest that SQ22536 may only target AC6 and not AC5 in murine platelets.

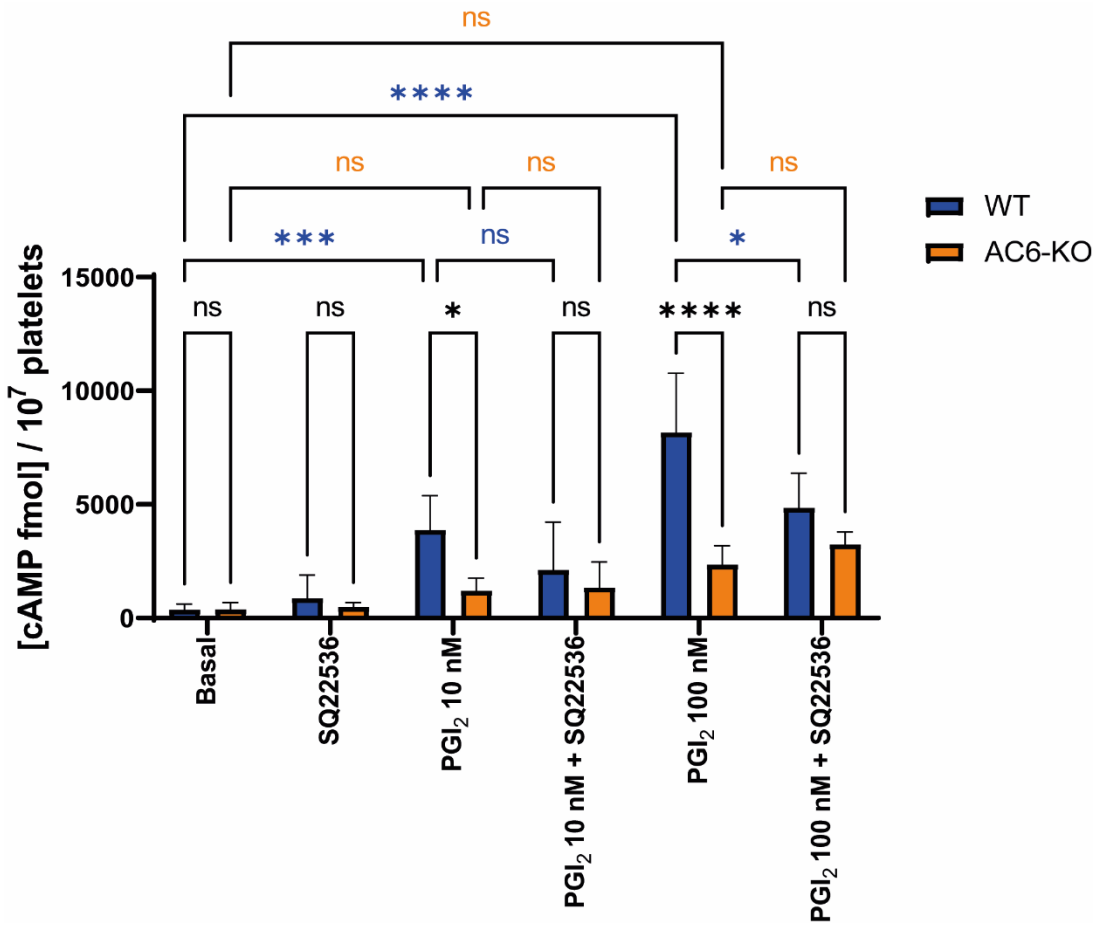

Figure 64. SQ22536 displays no effect on cAMP production in AC6-KO platelets

Murine washed platelets ($2x10^8$ platelets/mL) were pre-treated with and without SQ22536 (100 µM) for 25 minutes at 37°C prior to the addition of PGI_2 (10 – 100 nM) for 30 secs at RT. Reactions were terminated by the addition of lysis buffer containing 2.5% dodecyltrimethylammonium bromide and cAMP levels were assayed with a commercially available enzyme immunoassay system (Cytiva) and expressed as fmol cAMP/10^7 platelets. All assays were carried out in duplicate, and data presented as means ± SD and compared using a two-way ANOVA with Šídák's multiple comparisons. Comparisons were made between WT and AC6-KO (black text), as well as basal versus PGI_2 treatment, and PGI_2 treatment versus PGI_2 with SQ22536 for WT (blue text) and AC6-KO (orange text), (n=3, ns= not significant, *≤0.05, ***≤0.001 and ****≤0.0001).

5.3. Expression of downstream PKA substrates is intact in AC6-KO platelets

The aim of the next series of experiments was to understand the effects of AC6 deletion on cAMP signalling by examining the phosphorylation of known PKA substrates. However, we first examined the expression of two known substrates of PKA to ensure that any changes in phosphorylation were not due to changes in total protein content (Figure 65).

Total VASP expression was 120.3 ± 12.2 % (WT) compared to 135.7 ± 4.4 % (AC6-KO), while total PDE3A expression was 165.4 ± 23.9 % (WT) compared to 138.5 ± 18.1 % (AC6-KO). These data confirm that downstream PKA substrates are intact in the AC6-KO, therefore any potential differences observed in phosphorylation are not attributed to protein expression of VASP and PDE3A.

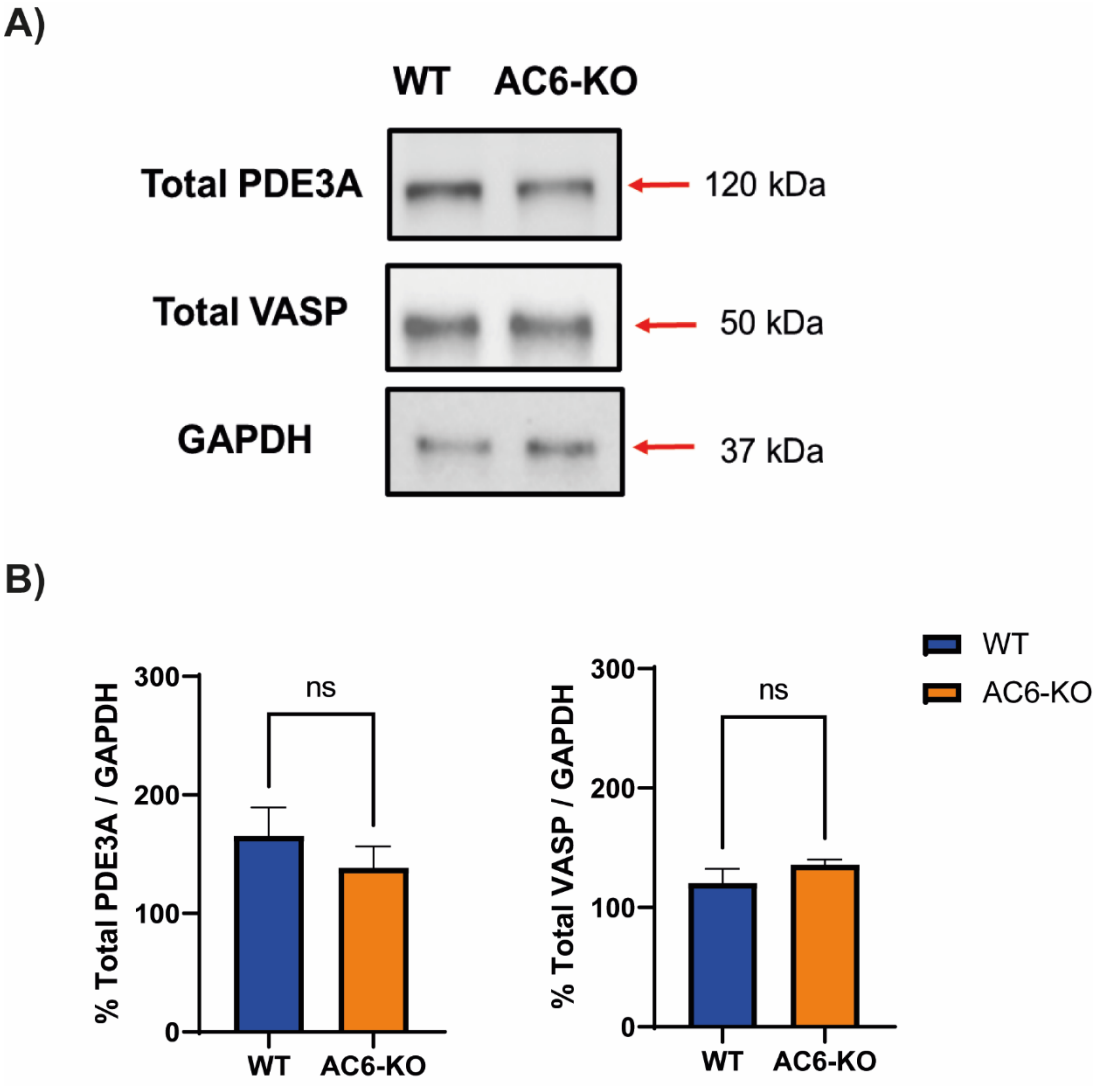

Figure 65. Measurement of downstream PKA substrate expression in AC6-KO platelets

Murine washed platelets ($5x10^8$ platelets/mL) were lysed in 2x Laemmli buffer, separated via SDS-PAGE and immunoblotted for total VASP and total PDE3A with a GAPDH loading control. Representative images (A) and whole lane densitometry bar graphs (B). Data presented as means ± SD and compared between WT and AC6-KO using an unpaired students t-test (n=3, ns = not significant).

5.4. Phosphorylation of PKA substrates in response to cAMP-elevating agents in AC6-KO platelets

After establishing an AC6-specific defect in cAMP production in response to PGI_2 we decided to assess downstream PKA signalling via measurement of phospho-PKA substrates in response to cAMP-elevating agents, including PGI_2, forskolin and 8-CPT-cAMP.

5.4.1. Assessment of phospho-PKA substrates in AC6-KO platelets

Since establishing that protein expression of VASP and PDE3A were intact in the AC6-KO, we first assessed pan phospho-PKA substrates in response to PGI_2 and forskolin (Figure 66).

We observed no difference between WT and AC6-KO in phospho-PKA substrates upon stimulation with PGI_2 or forskolin. Phosphorylation of PKA substrates increased with PGI_2 and forskolin concentration in both WT and AC6-KO platelets. In WT platelets, phosphorylation of PKA substrates went from 23.1 ± 5.5 % (basal) to 157.1 ± 34.1 % (PGI_2; 100 nM) and AC6-KO platelets went from 19.7 ± 11.1 % (basal) to 134.2 ± 27.8 % (PGI_2; 100 nM). Stimulation with forskolin also displayed a similar trend, though to a much lesser extent. In WT platelets, phosphorylation of PKA substrates went from 17.7 ± 2.2 % (basal) to 31.1 ± 8.8 % (forskolin; 10 µM) while AC6-KO platelets went from 11.7 ± 3.0 % (basal) to 37.7 ± 5.8 % (forskolin; 10 µM). Interestingly, representative images do display a subtle reduction in phospho-PKA substrates in AC6-KO compared to WT for both PGI_2 and forskolin treated platelets. Suggesting that there may be some subtle changes to individual PKA substrates that have been lost during whole lane densitometry analysis.

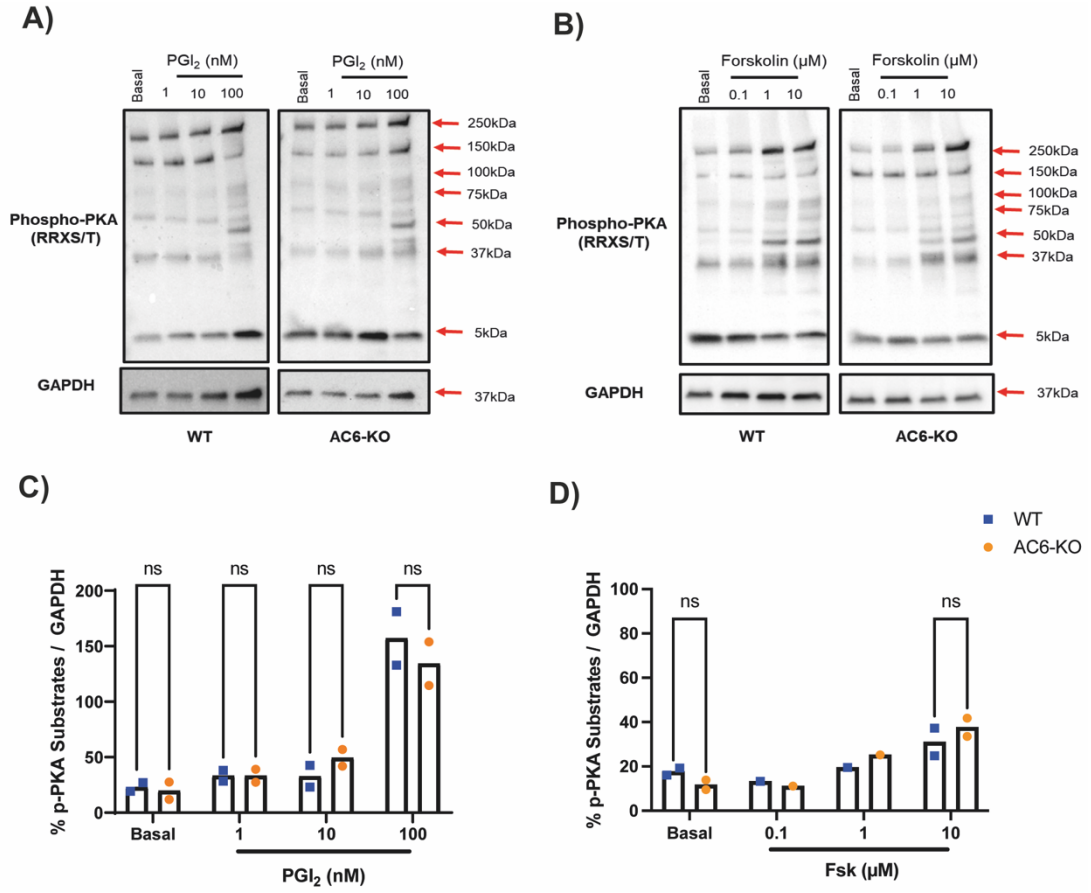

Figure 66. Assessment of phospho-PKA substrates in AC6-KO platelets by immunoblotting

Murine washed platelets ($5x10^8$ platelets/mL) were lysed in 2x Laemmli buffer, separated via SDS-PAGE and immunoblotted for p-PKA substrates (RRXS/T) with a GAPDH loading control. Platelets were stimulated with increasing concentrations of PGI_2 for 2 min (left) or forskolin (right) under constant stirring (800 rpm) at 37˚C. Data presented as images (A-B) and whole lane densitometry bar graphs (C-D) analysed using ImageJ software. Comparisons were made between WT and AC6-KO platelets by two-way ANOVA with Tukey's multiple comparisons test (n=1-2, ns = not significant).

5.4.2. Assessment of individual PKA substrates in AC6-KO platelets in response to PGI_2

Next, we decided to assess phosphorylation of individual PKA substrates upon treatment with PGI_2 to establish whether individual PKA substrates are linked to AC6. Upon treatment with PGI_2 we observed a concentration-dependent increase in both WT and AC6-KO platelets across all the phospho-PKA substrates (Figure 67).

Stimulation with PGI_2, displayed impaired phosphorylation of $VASP^{Ser157}$, $VASP^{Ser239}$ and $GSK3\beta^{Ser9}$ in AC6-KO platelets compared to WT. Differences in $VASP^{Ser157}$ phosphorylation emerged at PGI_2 (10 nM) with WT platelets demonstrating 45.6 ± 29.8 % compared to AC6-KO showing 13.6 ± 2.7 % (p=0.01) (Figure 67 D). The differences were more profound at higher concentrations of PGI_2 (100 nM), whereby $VASP^{Ser157}$ phosphorylation was 136.5 ± 36.8 % in WT platelets whereas AC6-KO platelets displayed 94.7 ± 15.8 % (p=0.003). Differences in $VASP^{Ser239}$ phosphorylation were only present at PGI_2 (100 nM), whereby WT platelets demonstrated 156.2 ± 48.8 % whereas AC6-KO platelets displayed 91.8 ± 24.6 % (p<0.0001) (Figure 67 C). Phosphorylation of $GSK3\beta^{Ser9}$ also displayed a similar level of phosphorylation between WT and AC6-KO at PGI_2 (100 nM). WT platelets were 135.2 ± 24.7 % while, AC6-KO platelets were 91.4 ± 6.6 % (p=0.001) (Figure 67 E). These data demonstrate impaired phosphorylation of certain PKA substrates in AC6-KO platelets compared to WT in response to PGI_2. However, the differences observed are not completely ablated, therefore the other AC must be playing a role here. In contrast we found that the phosphorylation of $PDE3A^{Ser312}$ was unaffected by the absence of AC6 (Figure 67 B).

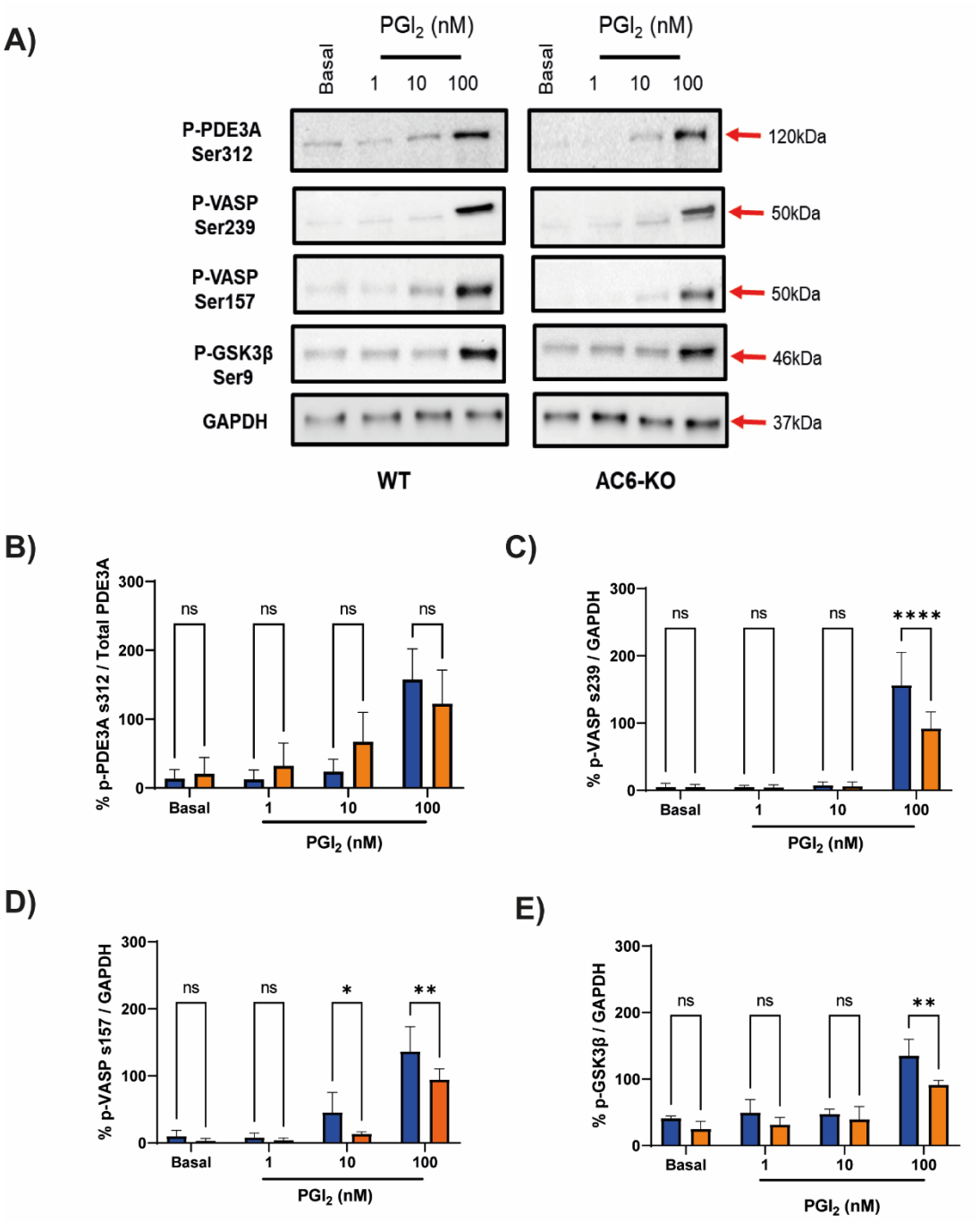

Figure 67. Assessment of individual PKA substrates in AC6-KO platelets upon treatment with PGI_2

Murine washed platelets ($5x10^8$ platelets/mL) were treated with PGI_2 (1 – 100n M) for 2 mins (A). Samples were lysed in 2x Laemmli buffer, separated via SDS-PAGE and immunoblotted for p-PDE3A^{Ser312} (B), p-VASP^{Ser239} (C), p-VASP^{Ser157} (D) and p-GSK3β^{Ser9} (E) with a GAPDH or total PDE3A loading control. Representative images (A) and densitometry bar graphs (B-E) analysed using ImageJ software. Data presented as means ± SD and compared between WT and AC6-KO by two-way ANOVA with Šídák's multiple comparisons test (n=3, ns = not significant, *≤0.05. **≤0.01, and ****≤0.0001).

5.4.3. Assessment of individual PKA substrates in AC6-KO platelets in response to forskolin

Since establishing impaired phosphorylation of certain PKA substrates in AC6-KO platelets in response to PGI_2, we decided to stimulate AC directly using forskolin (Figure 68). The use of forskolin in combination with the AC6-KO allows us to identify contribution of the other AC present (AC5) in PKA substrate phosphorylation.

We observed a defect in PKA substrate phosphorylation in response to forskolin. Phosphorylation of $VASP^{Ser157}$ displayed differences emerging at forskolin (1 µM) with WT platelets at 100.2 ± 31.2 % versus AC6-KO platelets at 66.5 ± 13.6 % (p=0.004). This was also demonstrated at higher concentrations of forskolin (100 µM), whereby WT platelets were 113.2 ± 14.0 % compared to AC6-KO platelets at 81.9 ± 17.0 % (p=0.008) (Figure 68 D). Consistent with this, $VASP^{Ser239}$ phosphorylation followed a similar trend. At forskolin (1 µM), WT platelets were 45.5 ± 9.7 % compared to AC6-KO platelets at 20.9 ± 5.9 % (p=0.04). Differences in $VASP^{Ser239}$ phosphorylation became more significant at higher concentrations of forskolin (10 µM). WT platelets showed $VASP^{Ser239}$ phosphorylation at 135.5 ± 30.3 % whereas AC6-KO platelets displayed 88.8 ± 14.1 % (p<0.0001) (Figure 68 C). $GSK3\beta^{Ser9}$ phosphorylation displayed a clear defect in AC6-KO platelets upon forskolin treatment. Differences emerged at forskolin (1 µM) and remained at higher concentrations of forskolin (10 µM). At forskolin (1 µM), WT platelets were 115.4 ± 4.4 % versus AC6-KO platelets at 47.6 ± 18.7 % (p<0.0001). At a higher concentration of forskolin (10 µM), WT platelets increased to 154.8 ± 34.4 % whereas AC6-KO platelets remained at similar levels of phosphorylation at 48.5 ± 9.0 % (p<0.0001) (Figure 68 E). We observed no difference in $PDE3A^{Ser312}$ phosphorylation between WT and AC6-KO platelets upon treatment with forskolin, this further confirms that AC6 is linked to cAMP production but not breakdown (Figure 68 B). In combination with data presented in Figure 67, we have shown that phosphorylation of VASP and $GSK3\beta^{Ser9}$ are impaired in AC6-KO platelets in response to forskolin, though not completely lost, suggesting that AC5 and AC6 are both linked to these PKA substrates.

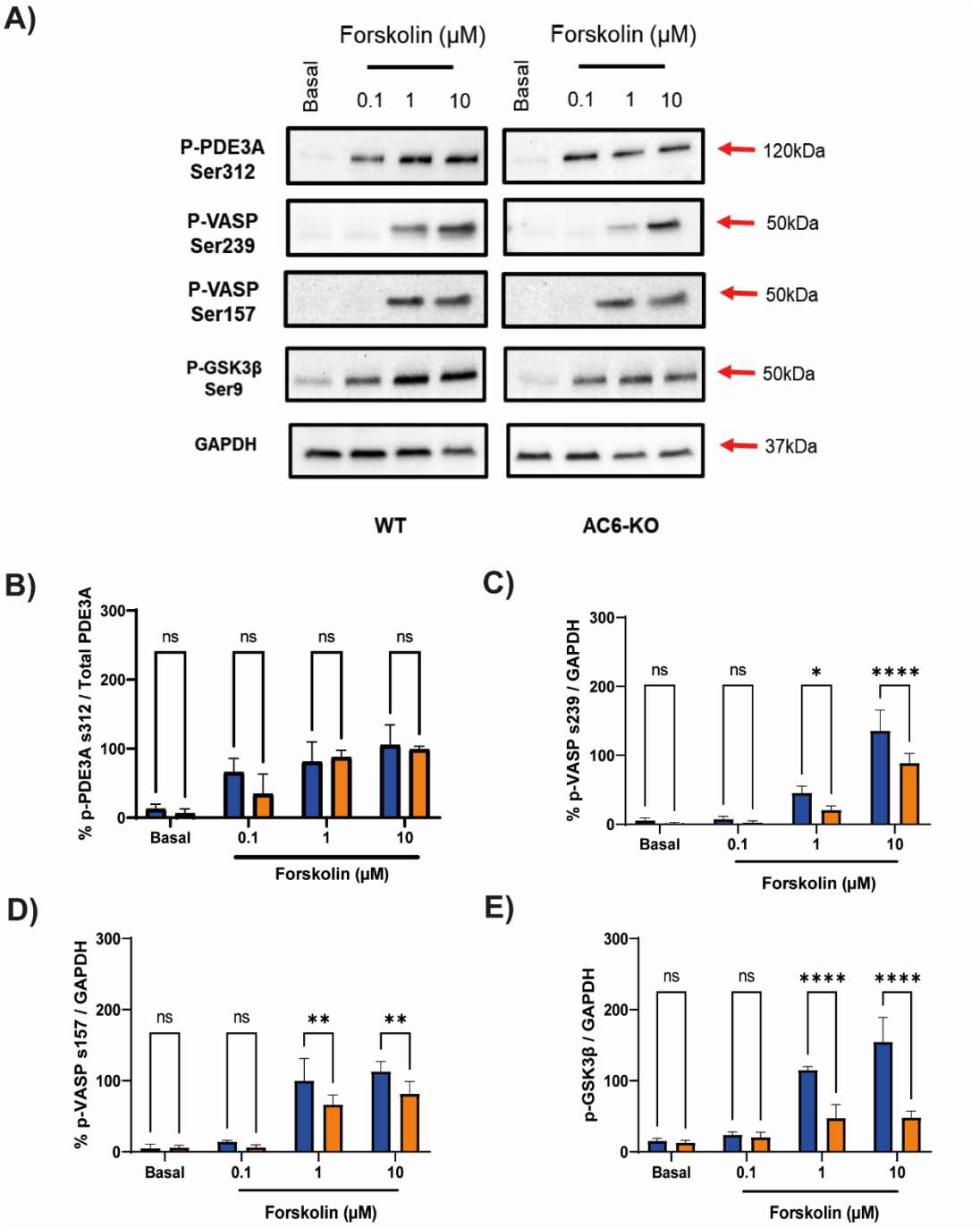

Figure 68. Assessment of individual PKA substrates in AC6-KO platelets upon forskolin treatment

Murine washed platelets (5x10^8 platelets/mL) were treated with forskolin (0.1 – 10 µM) for 5 mins (A). Samples were lysed in 2x Laemmli buffer, separated via SDS-PAGE and immunoblotted for p-PDE3A^{Ser312} (B), p-VASP^{Ser239} (C), p-VASP^{Ser157} (D) and p-GSK3β^{Ser9} (E) with a GAPDH or total PDE3A loading control. Representative images (A) and densitometry bar graphs (B-E) analysed using ImageJ software. Data presented as means ± SD and compared between WT and AC6-KO by two-way ANOVA with Šídák's multiple comparisons test (n=3, ns = not significant, *≤0.05. **≤0.01, and ****≤0.0001).

5.4.4. Assessment of p-VASP in AC6-KO platelets in response to 8-CPT-cAMP

To ensure that downstream PKA phosphorylation events were intact in the AC6-KO, and observed differences are specifically linked to AC6, we employed the use of 8-CPT-cAMP, a direct PKA activator. The use of 8-CPT-cAMP allows us to bypass the IP receptor and ACs to activate PKA directly, therefore allowing us to assess downstream signalling events of PKA (Geiger et al., 1992). We assessed 8-CPT-cAMP mediated phosphorylation of VASP^{Ser157} and found no difference between WT and AC6-KO, suggesting that changes detected are specifically linked to AC6 and not changes to downstream cAMP signalling (Figure 69).

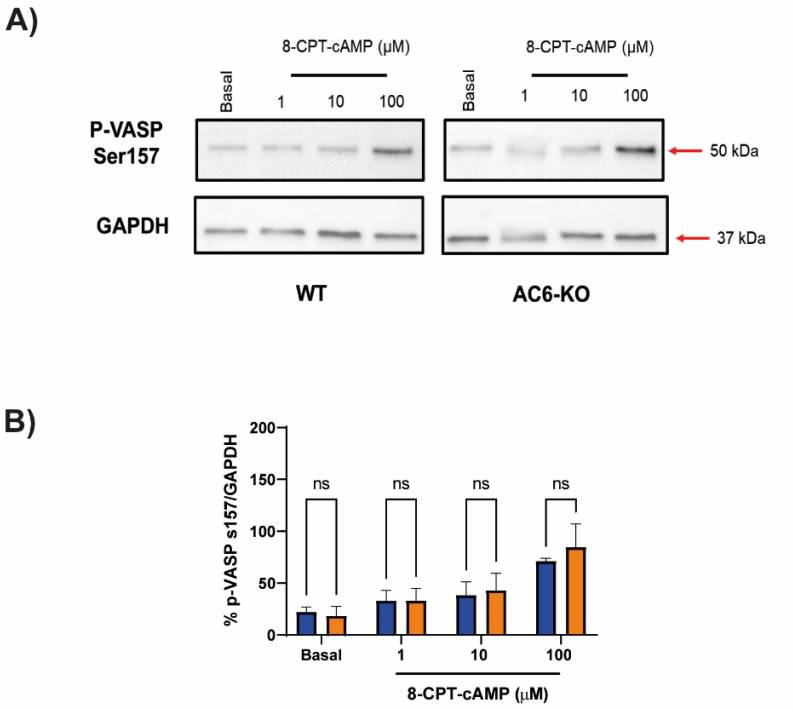

Figure 69. Assessment of p-VASP^{Ser157} in AC6-KO platelets upon 8-CPT-CAMP stimulation

Murine washed platelets (5x10^8 platelets/mL) were treated with 8-CPT-cAMP (1 – 100 μM) for 5 mins (A). Samples were lysed in 2x Laemmli buffer, separated via SDS-PAGE and immunoblotted for p-VASP^{Ser157} with a GAPDH loading control Representative images (A) and densitometry bar graphs (B) analysed using ImageJ software. Data presented as means ± SD and compared between WT and AC6-KO by two-way ANOVA with Šídák's multiple comparisons test (n=3, ns = not significant)

5.4.5. Assessment of p-VASP by phosphoflow in response to PGI_2 in AC6-KO platelets

After establishing a difference in VASP phosphorylation events in the AC6-KO compared to WT in washed platelets. We decided to explore intracellular phosphorylation of VASP in a more physiological setting using whole blood phosphoflow techniques (Hindle et al., 2021; Spurgeon et al., 2014) (Figure 70).

We observed no significant difference in $VASP^{Ser157}$ phosphorylation between WT and AC6-KO platelets upon stimulation with PGI_2 (0.1 – 100 nM). However, heatmaps do indicate a subtle difference in $VASP^{Ser157}$ phosphorylation between WT and AC6-KO at PGI_2 (10 – 100 nM) (Figure 70 A). In contrast, $VASP^{Ser239}$ phosphorylation demonstrated a more profound difference between WT and AC6-KO upon stimulation with PGI_2 (10 - 100nM) (Figure 70 B). At PGI_2 (10 nM), WT platelets displayed 7.6 ± 4.4-fold over basal while AC6-KO showed 2.8 ± 1.3-fold over basal (p=0.03). Phosphorylation of $VASP^{Ser239}$ in WT platelets was 16.9 ± 5.0-fold over basal (PGI_2; 100 nM), whereas AC6-KO platelets displayed 11.9 ± 3.7-fold over basal (PGI_2; 100 nM) (p=0.04).

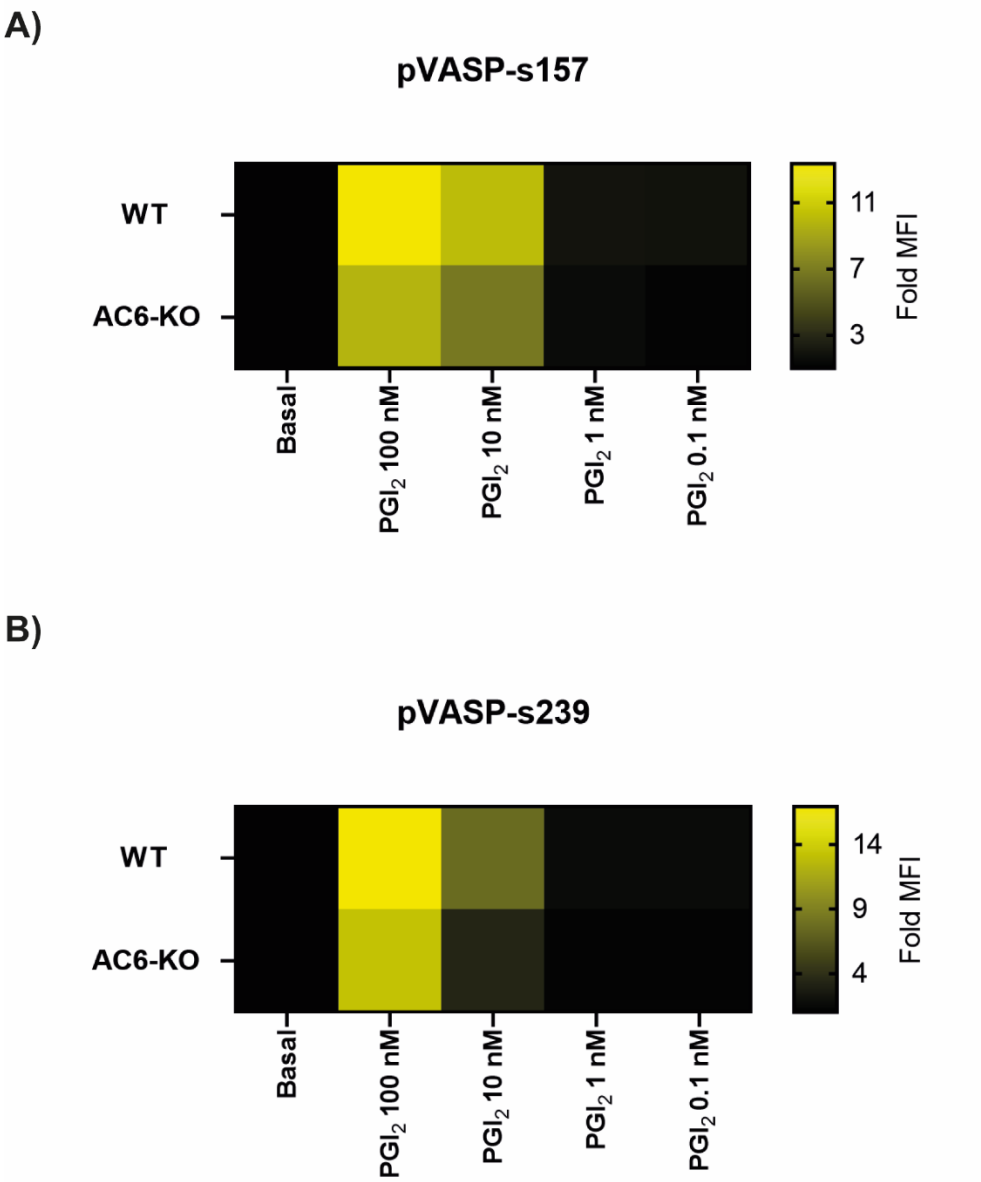

Figure 70. Impaired VASP phosphorylation in response to PGI_2 in AC6-KO platelets

Murine whole blood was treated with increasing concentrations of PGI_2 for 2 min, fixed using PhosFlow Fix/Lyse buffer (BD Biosciences), permeabilised and incubated with phospho-specific antibodies (p-VASP^{ser157}, p-VASP^{ser239} and CD41; 1 µg/mL). Cells were gated on platelet physical properties at 10,000 events and then analysed for p-VASP expression in CD41 positive cells. Data presented as means ± SD fold over basal shown by heatmaps. Data compared between WT and AC6-KO by two-way ANOVA with Šídák's multiple comparisons test (n=5).

5.5. Discussion

The extent of platelet activity is controlled by cyclic nucleotide signalling upon constant exposure to endothelial-derived PGI_2 and NO (Arnold et al., 1977; Moncada, 1982). The cAMP signalling cascade represents a major inhibitory pathway that controls platelet function, haemostasis and thrombosis and our understanding of its specific regulation is limited. Work described in this chapter demonstrates that a loss of AC6 impairs cAMP production and causes subtle changes in downstream PKA substrate phosphorylation in response to cAMP-elevating agents. These signalling defects observed in the AC6-KO are likely to contribute to the functional defects observed in Chapter 4. Here we have used ELISA, immunoblotting and phosphoflow approaches to assess the role of AC6 in platelet cAMP signalling.

5.5.1. Impaired cAMP production upon PGI_2 treatment in AC6-KO

Production of cAMP is a key regulator of platelet function, thus impaired cAMP signalling is linked to reduced sensitivity to PGI_2 in cardiovascular disease (Fisch et al., 1997; Bunting et al., 1983; Berger et al., 2020). We have already demonstrated clear functional defects linked to a loss of AC6, therefore we wanted to assess how the cAMP signalling pathway was impacted by the deletion of AC6. We suspected a loss of AC6 results in diminished cAMP production based on the PAR-mediated functional defect upon treatment with PGI_2 observed in Figure 56 and Figure 59, in addition to accelerated thrombosis as demonstrated in Figure 61. We observed no differences in basal cAMP production between WT and AC6-KO, suggesting that *in vitro,* platelet AC6 does not control 'basal' cAMP production i.e., without exogenous stimulation of AC by PGI_2.

Consistent with this, in the absence of PGI_2-stimulated G_s activity, platelets exhibit ongoing turnover of cAMP to reach an equilibrium sufficient enough to limit spontaneous platelet activation (Feijge et al., 2004). Suggesting that the levels of cAMP at basal are controlled by PDE3A activity, rather than ACs (Feijge et al., 2004). In addition, Noe et al., (2010) attributed basal cAMP generation in platelets to a combination of signalling via G_{i2}, G_z and G_s, though the biochemical role of AC in basal cAMP activity has yet to be explored. Using

FRET analysis Lissandron and colleagues (2005), identified specific pools of cAMP that are localised to distinct PDE isoforms (Stangherlin and Zaccolo, 2012). Remarkably, PKA has been shown to phosphorylate and activate PDE3A in platelets, providing a regulatory feedback mechanism to control platelet cAMP signalling (Macphee et al., 1988; Hunter et al., 2009). Data presented here offers another alternative that basal cAMP synthesis could be attributed to the other AC present, AC5. AC6-KO platelets demonstrated a significantly reduced sensitivity to PGI_2 induced cAMP generation, given that this was not completely ablated, suggests that IP receptors are linked to multiple ACs, which could potentially exist in different locations within a cell.

To further assess the relative contribution of AC6 to cAMP production in response to PGI_2, we used a direct AC inhibitor SQ22536 (Emery et al., 2013). We hypothesised that using SQ22536 would mimic a full-body AC knockout and therefore would prevent PGI_2-mediated cAMP production, allowing us to also assess the contribution of AC5 (Figure 64). Interestingly, only a partial reduction in cAMP generation was observed in the presence of SQ22536 in WT but not AC6-KO platelets. At higher concentrations of PGI_2, WT platelets demonstrated a significant reduction in cAMP generation in response to SQ22536 whereas AC6-KO platelets displayed no such reduction. This could suggest that SQ22536 does not target AC5, however, there have been no reports demonstrating this. Nevertheless, it is possible that the specificity of SQ22536 is questionable. An alternative AC inhibitor does exist, NKY80, though this is said to be less potent than SQ22536 and more selective to AC5 and AC2 (Onda et al., 2001). While this could be useful to inhibit AC5, SQ22536 is more widely used to inhibit ACs. Additionally, the concentrations of SQ22536 used in cell biology studies vary across numerous studies (Haslam, 1973; Kunapuli et al., 1999; Woulfe et al., 2002; Yang et al., 2002; Emery et al., 2013), and further, the use of AC inhibitors typically requires the addition of AC-activators to confirm inhibition, therefore adds complexity to experimental design and output. First reports of SQ22536 on human platelets, identified an IC50 of 13 μM of SQ22536 in the presence of PGE_1 (1 μM) (Haslam, 1973). Interestingly, Yang et al., (2002) demonstrated that the presence of SQ22536, failed to restore a normal response to epinephrine in a $G\alpha_z$ knock-out mouse. They also comment that an SQ22536 concentration of

300 μM is sufficient to inhibit PGI_2-stimulated cAMP formation to the same extent as ADP or epinephrine, although, this data was not shown. Similarly, Woulfe et al., (2002) also report that 300 μM is sufficient to inhibit PGI_2-stimulated cAMP production to levels comparable to AC inhibition by ADP, again this data was not shown and concentrations of PGI_2 were not reported. While Lova et al., (2002) suggests that SQ22536 (300 μM) maximally inhibited forskolin stimulated AC inhibition, again concentrations of forskolin were not reported. Alternatively, in HEK cells an IC50 value of 5 μM (SQ22536) was reported in the presence of forskolin (25 μM), while NS-1 cells demonstrated inhibition of forskolin-stimulated cAMP generation at 1 mM of SQ22536 (Emery et al., 2013). While our data presented in Figure 42, demonstrates, the ability of SQ22536 to reduce PGI_2-mediated VASP phosphorylation in murine platelets at much lower concentrations than reported, we were unable to replicate this in the cAMP ELISA. Either SQ22536 requires further optimisation in experiments assessing cAMP production of murine platelets or it does not target AC5 at the concentrations used in this assay. Arguably, the use of a platelet specific AC-KO mouse negates the need for such inhibitors.

Overall, we have demonstrated that a loss of AC6 contributes to impaired cAMP production in response to PGI_2, though it is not ablated. This could be attributed to AC5 taking on a compensatory role in response to PGI_2, or it's the combination of AC6 and AC5 that control platelet cAMP production. Though this does not compensate for the thrombotic phenotype observed in Figure 61. We have also shown that AC6 is not responsible for basal cAMP production, suggesting that this could be a role for AC5 or PDEs. Lastly, we have found that in the presence of an AC inhibitor (SQ22536), WT platelets displayed a reduction in cAMP generation, while this had no effect on AC6-KO platelets.

5.5.2. The expression of downstream PKA substrates is intact in AC6-KO platelets

Before assessing the impact of impaired cAMP production on downstream PKA substrates, we decided to assess the expression of key PKA substrates via immunoblotting. Our hypothesis was to ensure that the expression of PKA substrates were intact in the AC6-KO before analysing their subsequent phosphorylation events (Figure 65). We found that total VASP and total

PDE3A expression were intact in AC6-KO platelets compared to WT, allowing us to be confident that any changes in phosphorylation were not linked to impaired expression of these proteins.

5.5.3. Impaired PKA substrate phosphorylation in response to PGI_2 and forskolin in AC6-KO platelets

We next set out to establish whether impaired PGI_2-mediated cAMP production, as a result of AC6 deletion, had any downstream PKA signalling implications using a pan phospho-PKA antibody in response to PGI_2 and forskolin (Figure 66). While whole lane densitometry did not demonstrate any significant differences between WT and AC6-KO in response to PGI_2 or forskolin. We did observe a subtle reduction in representative blots at ~50 kDa in AC6-KO platelets. Due to the nature of quantifying pan antibodies via whole-lane densitometry, potential changes may have been lost. It's worth noting that several PKA substrates are ~50 kDa (p-VASP^{Ser157}, p-VASP^{Ser239}, p-GSK3β^{Ser9} and p-GSK3α^{Ser21}) therefore it's likely that these bands may overlap. However, we examined individual PKA substrates in response to cAMP-elevating agents such as PGI_2 (Figure 67), forskolin (Figure 68) and 8-CPT-cAMP (Figure 69) and these data were much clearer. We found that the phosphorylation of VASP was significantly reduced but not completely lost in the AC6-KO, suggesting that AC5 could be playing a role here. Nevertheless, it is important to note that even though the effect on signalling was modest it was significant enough to impair platelet function as demonstrated in Chapter 4. Furthermore, we observed a clear reduction in VASP phosphorylation in response to forskolin, identifying AC6 as a clear mediator of cAMP-mediated PKA activity. The production of cAMP is controlled by the opposing activity of PDE3A and ACs (Raslan et al., 2015a), therefore we wanted to assess whether a loss of AC6 impacted activatory phosphorylation of PDE3A^{Ser312}. In contrast to phosphorylation of VASP, we observed no difference in PDE3A^{Ser312} phosphorylation in AC6-KO platelets upon stimulation with PGI_2 or forskolin, highlighting that AC6 is not involved in the breakdown of cAMP. Notably, this is the first evidence that specific AC isoforms are not linked to all PKA substrates.

Given that PGI_2 stimulation allows us to assess receptor-mediated stimulation of cAMP (including $G\alpha_s$), while forskolin directly activates all ACs (except AC9)

(Seamon and Daly, 1981; Seamon et al., 1981), differences observed in the AC6-KO between PGI_2- and forskolin-mediated PKA phosphorylation events are likely attributed to the IP receptor, G-protein and AC6 signalling relationship. In support, overexpression studies in cardiac fibroblasts show that AC6 selectively enhances β_2-adrenergic receptor signalling, but not other $G\alpha_s$-coupled receptors (Liu et al., 2008) suggesting that distinct AC isoforms are linked to specific $G\alpha_s$-coupled receptors, while direct activation of AC by forskolin does not account for this.

Phosphorylation of VASP is the gold standard for assessment of downstream PKA phosphorylation events, the antibodies are robust and highly reported (Waldmann et al., 1987; Butt et al., 1994; ElDaher et al., 1996). Importantly, phosphorylation of $VASP^{Ser\ 157}$ is proposed to be preferential to PKA, while $VASP^{Ser239}$ is preferential to PKG (Smolenski et al., 1998). Here we show that phosphorylation of VASP at both sites is present in WT platelets treated with PGI_2 or forskolin, demonstrating that cAMP-mediated PKA activation can lead to phosphorylation at both sites. We also measured $VASP^{Ser157}$ phosphorylation in response to the direct PKA activator, 8-CPT-cAMP to assess whether downstream signalling was intact and that the observed differences in Figure 67 and Figure 68 were linked to loss of AC6 (Figure 69). We found no difference between WT and AC6-KO in response to 8-CPT-cAMP, confirming that downstream PKA signalling is preserved in the AC6-KO.

Interestingly, GSK3β has been reported to contribute to thrombus stability (Laurent et al., 2015), based on data described in Chapter 4, we wanted to assess whether a loss of AC6 implicates the phosphorylation of $GSK3\beta^{Ser9}$. It has been documented that GSK3β is active at rest, inhibiting glycogen synthase (GS), which is a key regulator of glycogenesis in platelets and other cell types (Frame and Cohen, 2001; Li et al., 2008). Reports suggest that GSK3β activity at rest primes platelets for aggregation (Laurent et al., 2015), though the exact mechanisms are unclear. However, upon platelet activation, GSK3β becomes phosphorylated by PKB/Akt which in turn, switches off its activity giving rise to glycogen synthase activity, thus glycogenesis. Recent reports have demonstrated that $GSK3\beta^{Ser9}$ is also phosphorylated by PKA, however it is unclear why (Beck et al., 2014). It could be argued that this may

allow resting platelets to metabolise glycogen in a tick over manner. We therefore hypothesised that PKA-mediated phosphorylation of GSK3β^{Ser9} may be impaired upon AC6 loss. Interestingly, we observed reduced PGI_2 and forskolin induced phosphorylation of GSK3β^{Ser9} in AC6-KO platelets (Figure 67 E and Figure 68 E). Notably, the differences were more profound upon forskolin treatment, suggesting that this is primarily AC6 linked, as AC5 has been unable to compensate. Thus, we have found that AC6-KO platelets displayed impaired phosphorylation of VASP^{Ser157}, VASP^{Ser239} and GSK3β^{Ser9} upon stimulation with PGI_2 and forskolin, suggesting that these PKA substrates are linked directly to AC6 activation. While the differences are profound, they are not completely ablated which gives rise to a role for AC5 in the phosphorylation of these PKA substrates.

Overall, the data presented in this chapter demonstrate a clear cAMP/PKA signalling defect in response to PGI_2 and forskolin as a direct result of AC6 loss. These signalling defects are likely to account for the functional differences observed in Chapter 4, especially accelerated thrombosis as described in Figure 61.

Chapter 6
Conclusions and future directions

6.1. Validation of the cAMP signalling pathway in human, murine and patient platelets

Our initial studies validated well-known platelet functional and signalling techniques in human control, human patient, and murine platelets. Strategically it was important to validate known aspects of cAMP signalling to ensure that once the AC6-KO mouse was generated, techniques were optimised, established and translatable to murine platelets. This approach allowed us to have a more streamlined experimental design to ensure maximal output from each mouse, in keeping with the NC3Rs (Burden et al., 2015).

To examine the potential pathophysiological importance of cAMP signalling, we assessed platelet activation and inhibition by PGI_2 in patients with ACS. Consistent with other studies, we found that patients with ACS, exhibit elevated CD62P expression and PS exposure under basal conditions, as well as impaired sensitivity to PGI_2 (Tschoepe et al., 1993; Itoh et al., 1995; Minamino et al., 1998; Bath et al., 1998; Serebruany and Gurbel, 1999; Porreca et al., 2009). Elevated expression of p-selectin (CD62P) has been linked to delayed and unsuccessful thrombolysis is patients post-MI (Gurbel et al., 1998), while elevated PS exposure has been linked to thrombin activation (Hoffman and Monroe, 2001). Increased expression of CD62P and PS exposure at basal could also be linked to impaired sensitivity to endogenous PGI_2 in circulation, thereby shifting platelets to a more activatory and hyperactive state.

Interestingly, we also demonstrate the first evidence of significantly increased sensitivity to PAR1 peptide in platelets from ACS patients. Hyperresponsiveness to PAR1 in combination with elevated PS exposure, and subsequent thrombin activation, can lead to coagulation, therefore perpetuating the cycle of platelet activation and thrombus formation (Hoffman and Monroe, 2001; Monroe et al., 2002). Given that these platelets were pre-

activated and hyperresponsive even after a cardiovascular event suggests that they may be more likely to exhibit recurrent events, despite intervention.

Platelet hyperactivity is a well-known trait of atherothrombosis. While the precise mechanisms are uncertain, some studies suggest this is primarily linked to dyslipidaemia, a known risk factor for MI (Davì et al., 1998; Jackson, 2011; Berger et al., 2018b). Though others suggest this is a result of impaired platelet inhibitory mechanisms (Bunting et al., 1983; Fisch et al., 1997; Van Geet et al., 2009; Berger et al., 2020) or a combination of the two. Impaired platelet sensitivity to PGI_2 in cardiovascular disease has been extensively reported (Bunting et al., 1983; Akai et al., 1983; Burghuber et al., 1986), with our data validating that platelet PGI_2 sensitivity is impaired in patients with ACS, though the distinct mechanisms underpinning this are unclear. Studies have linked impaired cAMP signalling to IP receptor desensitisation, endothelial dysfunction, impaired PGI_2/AC integrity, reduced VASP phosphorylation and accelerated cAMP breakdown by PDEs, (Bunting et al., 1983; Akai et al., 1983; Burghuber et al., 1986; Fisch et al., 1997; Van Geet et al., 2009; Noe et al., 2010; Imam et al., 2019; Berger et al., 2020). Though surprisingly, the distinct role of ACs and their isoforms, had not yet been explored. Further understanding the contribution of AC6, the predominant isoform in human and murine platelets, to cAMP signalling, may give insight into why this protective mechanism fails in cardiovascular disease.

6.1.1. Key findings

- Confirmation of the pH method of platelet isolation to assess platelet function and cAMP signalling in human and murine platelets
- Validation of light transmission aggregometry, static platelet spreading and adhesion, fluorescent flow cytometry, ELISA, immunoblotting and phosphoflow techniques to assess platelet function and cAMP signalling in human and murine platelets to apply to clinical studies and our AC6-KO mouse model
- Elevated platelet activation at basal, impaired PGI_2 sensitivity and elevated PAR1 peptide response in ACS patients

6.2. Characterisation of the platelet specific AC6-KO mouse and the role of AC6 in platelet function

To understand the role of AC6 in platelets, we successfully generated a novel platelet specific AC6-KO mouse. While the other ACs are present, this model still allows us to assess the specific contribution of AC6 to platelet cAMP signalling and function which has not been previously reported. Therefore, this is the first genetic mouse model to assess the cAMP signalling pathway directly.

Numerous mouse models have been used to explore cAMP signalling indirectly within a variety of cell types, for example, IP receptor-null mice display normal platelet aggregation and accelerated thrombosis (Murata et al., 1997), while whole body $G\alpha_{i2}$ knockout mice display impaired AC inhibition by ADP (Jantzen et al., 2001). In skeletal muscle cells, PKA-RIIα knockout mice were found to be normal with no physiological defects and PKA anchoring was not impaired (Burton et al., 1997). In contrast, a microRNA study demonstrated that the absence of the PKA-RII subunit in mouse platelets lead to reduced activation by dual stimulation with adrenalin and PAR4 peptide (Nagalla et al., 2011). In addition mice lacking platelet specific sGC demonstrate accelerated thrombosis in response to injury (Rukoyatkina et al., 2011; Zhang et al., 2011), while patients with mutations that severely reduce sGC expression display impaired NO-mediated cGMP formation and an increased risk of MI (Erdmann et al., 2013). It was not unreasonable to suggest that a loss of AC6 could exhibit a similar phenotype.

Upon assessment of our platelet specific AC6-KO mouse *in vitro,* we found that basal cAMP synthesis was unaffected by the loss of AC6, consistent with earlier studies where basal cAMP was found to be persistently produced regardless of $G\alpha_s$ stimulation in human platelets (Feijge et al., 2004; Noe et al., 2010). Notably, cAMP production was not completely lost, hinting at a potential role in cAMP production for the other AC present, AC5. In contrast to basal cAMP, stimulation with PGI_2 led to diminished production of the cyclic nucleotide in the absence of AC6, demonstrating the IP receptor is linked to AC6-mediated cAMP synthesis. This loss of cAMP was associated diminished p-VASP^{Ser157}, p-VASP^{Ser239} and p-GSK3β^{Ser9}, indicating that PKA

mediated phosphorylation of these substrates were linked, at least in part, to AC6-derived cAMP. Critically, the phosphorylation of PDE3A^{Ser312} in response to PGI_2 or forskolin treatment was unaffected by the absence of AC6 and provides the first crucial evidence that distinct PKA substrates may be linked to specific AC isoforms. Further, the data indicate that loss of PKA substrate phosphorylation observed is linked to cAMP production and not breakdown. Consistent with this, it has been suggested that AC6 is not tightly coupled to cAMP hydrolysis and resides in an area in the cell that is distinct from PDE3A (Gros, R. et al., 2006).

From the perspective of platelets as haemostatic cells we found that platelet counts, adhesion and surface receptor expression were unaffected by the loss of AC6. In addition, functional assessment found that platelet aggregation and activation in response to collagen, CRP-XL, thrombin, PAR4 peptide and TxA_2 were normal in the AC6-KO. Surprisingly, inhibition of PAR- but not GPVI-mediated platelet functions including inhibition of PAR-mediated platelet aggregation, CD62P expression, integrin activation ($\alpha_{IIb}\beta_3$) and PS exposure by PGI_2 were significantly impaired in AC6-KO platelets. Demonstrating that a loss of AC6 does not affect all platelet agonists, whereas PGI_2-mediated inhibition of PAR-stimulated platelet activity is impaired in the absence of AC6.

While our *in vitro* data suggests that AC6 is not linked to basal platelet cAMP activity, it does shed some light on impaired the cAMP signalling which we have shown in ACS patient samples (Figure 29). This is the first evidence of AC6-mediated cAMP signalling, linked to a specific agonist. Given that inhibition of GPVI and TP signalling was unaffected by the loss of AC6, this could suggest that the other AC is reserved for the control of collagen and TxA_2-mediated platelet activity, while AC6 signalling controls PAR-mediated activity. Although our *in vivo* studies demonstrate a clear overall thrombotic phenotype in the absence of AC6, suggesting that AC6 is the main AC isoform responsible for mediating thrombosis.

Our data, and that of others, highlights that ACs in the plasma membrane are likely to exist in complexes to form signalosomes with G-proteins, GPCRs, protein kinases and PDEs (Gros et al., 2006a; Ostrom et al., 2012; Raslan and Naseem, 2015). Compartmentalisation of signalling proteins within

platelets and other cell types often involve lipid rafts, which are specific membrane microdomains that contribute to spatiotemporal organisation. It is thought that lipid rafts provide a specific location for PGI_2-mediated inhibition of platelet activity. It has been demonstrated that the IP receptor and AC5/6 are co-expressed in these types of microdomains and is proposed to control the extent of cAMP production (Raslan et al., 2015b). While many reports suggest that cAMP is constrained to lipid rafts (Liu et al., 2008; Raslan and Naseem, 2015; Raslan et al., 2015a), an alternative hypothesis suggests that cAMP is a diffusible second messenger and therefore has access to large areas of a cell, thus deeming the location of cAMP irrelevant (Johnstone et al., 2018). Consistent with platelet studies, overexpression studies in cardiac fibroblasts show that AC6 selectively enhances β_2-adrenergic receptor signalling, but not other $G\alpha_s$-coupled receptors (Liu et al., 2008) suggesting that AC isoforms could be constrained to lipid rafts along with specific GPCRs. It has also been reported that AC microdomains are consistent among species and stable in their localisation (Ostrom et al., 2002; Cooper and Tabbasum, 2014). While, AC6 is present in both lipid raft and non-raft fractions along with PKA in platelets (Raslan and Naseem, 2015).

In addition to localisation in membrane microdomains, A-anchoring kinase proteins (AKAPs) can tether effector proteins and their downstream targets to facilitate cAMP signalling events (Tasken and Aandahl, 2004). Importantly there is evidence that AKAPs also control upstream signalling events by positioning cAMP effector proteins in close proximity to β-adrenergic receptors and cAMP machinery (Davare et al., 2001; Fraser et al., 2000). In rat brains, AC5 and AC6 interact AKAP79/150, directing cAMP signals via PKA towards a β-adrenergic receptors, G-protein and AC network, though this was shown to facilitate phosphorylation of AC to inhibit cAMP synthesis (Bauman et al., 2006). It could be possible that model is present in platelets to allow control of PAR receptor signalling. While we did not study lipid rafts or AKAPs, the AC6-KO provides insight into its relative contribution to basal and PGI_2-stimulated cAMP production, and its ability to control PAR-mediated activity. Importantly, PAR-mediated platelet activity represents the most potent secondary signalling cascade (Heemskerk et al., 2002). Given that we have demonstrated that a loss of AC6 impairs PGI_2-mediated inhibition of PAR

platelet activation, it begs the question, are PAR receptors and AC6 spatially constrained to microdomains within platelets? A complex containing IP receptors, G_s, AC6, PAR receptors and G_i, along with downstream signalling machinery could pose a mechanism whereby platelet activity is controlled by the opposing action of ACs and PAR receptors.

Tovey and colleagues (2008) defined cAMP signalling in human embryonic kidney cells, as having two nodes of action. Firstly, binary nodes, whereby cAMP passes directly from AC6 to IP3R2, and secondly, analogue nodes, whereby local gradients of cAMP concentration regulate cAMP effectors in a location more remote from AC. They describe binary signalling as a localised delivery of cAMP, while analogue signalling is more dependent on localised cAMP hydrolysis (Tovey et al., 2008). Given that our data demonstrates that AC6 is not linked to PDE3A^{Ser312} phosphorylation, it could suggest that PDE3A activity is dependent on analogue signalling by cGMP and PKA phosphorylation, and could reside elsewhere in the cell, remote from AC6. While control of PAR-mediated activity could be more dependent on binary cAMP signalling. Though we do not yet know specifically which PAR-coupled G-protein is linked to AC6, it could be argued that PARs linked to G_i, which are known to inhibit AC, could reside in microdomains with ACs or specifically AC6.

The current evidence of PAR receptors existing in microdomains, suggests while there is only a weak localisation of PAR1 receptors in cholesterol-rich microdomains, this still contributes to efficient PAR1 signalling in platelets upon PAR1-peptide stimulation (Rabani et al., 2020). While PAR1 is known to be targeted to lipid rafts/caveolae membrane microdomains of endothelial cells (Bae et al., 2007), studies have shown that this membrane targeting regulates PAR1 cleavage specificity by serine proteases in plasma (Bae et al., 2008). Though further work is required to elucidate the location of PAR receptors in relation to AC in platelets.

Taken together we have proposed two updates to the cAMP signalling pathway whereby AC6 and PAR reside in A) lipid rafts or B) close proximity connected by AKAPs as demonstrate in Figure 71.

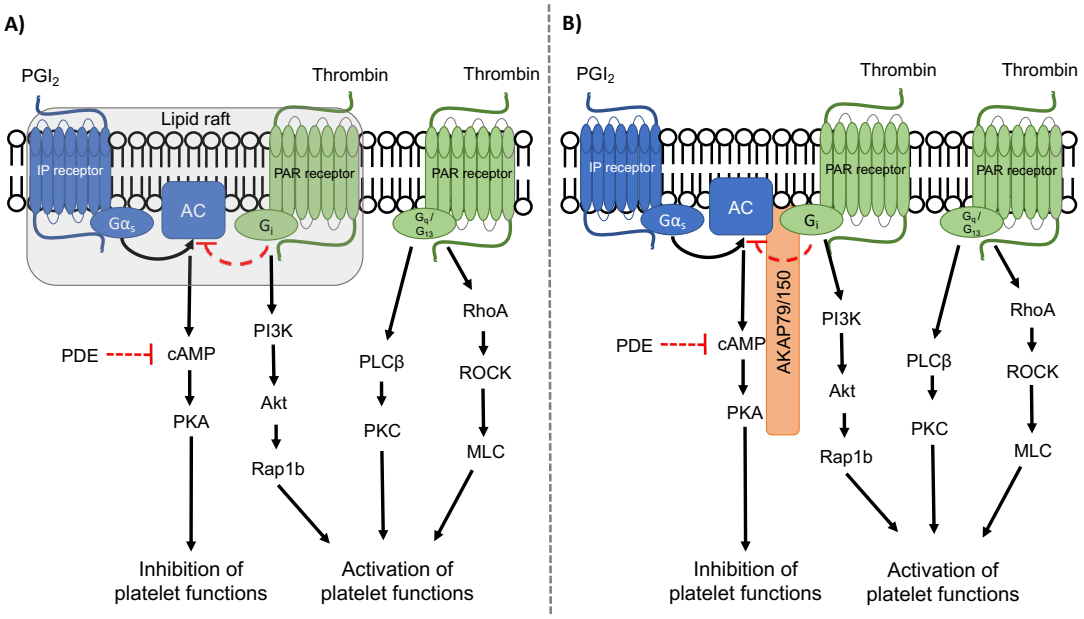

Figure 71. Two proposed cAMP signalling pathways

Proposed cAMP pathways based on data described from this study and adapted from (Dessauer, 2009). A) represents a model of cAMP signalling whereby certain PAR receptors and ACs are connected by lipid raft microdomains, controlling cAMP production and platelet activation. While other PAR receptors remain distinct from AC. B) demonstrates PAR receptors and ACs connected by an AKAP, ensuring close proximity of downstream signalling machinery.

Our physiological data showed that the absence of AC6 in mice results in an accelerated thrombosis phenotype in the context of tonic endothelial inhibition. The assumption is that this is likely attributed to impaired platelet cAMP production and downstream PKA signalling events, due to a loss of AC6. Consistent with our functional data, studies using IP null mice demonstrate normal aggregation, but accelerated thrombosis *in vivo* (Yang et al., 2002). Thus, the loss of different components of the PGI_2-cAMP signalling pathway results in a defective haemostatic response, illustrating the fundamental role of the pathway in normal physiology. Therefore, the targeting of this pathway may have some role in reducing unwanted platelet activation associated with arterial thrombosis. Certain studies by Sim and colleagues (Sim et al., 2004) have shown that inhibition of PDE3A is cardioprotective, whether a strategy of activating specific ACs could also be used remains to be determined.

To our surprise, we also found that the AC6-KO displays impaired thrombus stability, resulting in embolic events. Though the precise mechanisms are unclear and yet to be explored, we suspect this is linked to impaired $GSK3\beta^{Ser9}$ phosphorylation as demonstrated in Figure 67 (Laurent et al., 2015). It has been shown that phosphorylation resistant GSK3β mice, display reduced PAR-mediated platelet activation and impaired *in vitro* thrombus formation (Moore et al., 2021). In contrast, AC6-KO mice demonstrate accelerated thrombosis and impaired PGI_2-mediated inhibition of PAR activity, however thrombi formed were unstable and PGI_2-mediated $GSK3\beta^{Ser9}$ phosphorylation was diminished. Suggesting that, in addition to inhibitory Akt-mediated phosphorylation of $GSK3\beta^{Ser9}$, PKA-mediated $GSK3\beta^{Ser9}$ phosphorylation promotes thrombus stability (Barry et al., 2003). While impaired cAMP signalling leaves $GSK3\beta^{Ser9}$ active, which has been associated with unstable thrombus formation (Zhou et al., 2013; Laurent et al., 2015; Moore et al., 2021). Interestingly, phosphorylation of $GSK3\beta^{Ser9}$ occurs at the same site by PKA and PKB, suggesting it could be possible that PKA- and PKB-mediated phosphorylation of $GSK3\beta^{Ser9}$ control different platelet functions or that $GSK3\beta^{Ser9}$ resides in different locations in close proximity with PKA or PKB (Barry et al., 2003; Beck et al., 2014). In addition, inhibitory phosphorylation of $GSK3\beta^{Ser9}$ was reported to support PAR-

mediated platelet function (Moore et al., 2021). However, in AC6-KO platelets, where phosphorylation of GSK3β^{Ser9} was impaired, PAR-mediated platelet aggregation remained unchanged. Though this defect in GSK3β^{Ser9} phosphorylation is only observed in response to PGI_{2-} and forskolin-stimulated cAMP signalling.

While agonist induced aggregation and activation remain unaffected by the loss of AC6, *in vivo* models represent a more physiological setting whereby we can assess the contribution of AC6 on tonic inhibitory mechanisms in response to injury. Given that basal cAMP synthesis was unaffected by the loss of AC6 in combination with constant exposure to PGI_2 in circulation, suggests that platelets are unlikely to spontaneously activate in the absence of AC6. It's more likely that the extent of platelet activation when challenged in the presence of impaired endogenous inhibitory cAMP signalling, results in this thrombin defect. Differences in function or expression of AC6 in ACS patients, could shed light on the extent of a thrombotic event or risk of subsequent embolic events. It's already been reported that dysfunction of AC activity impacts the efficacy of $P2Y_{12}$ receptor antagonists (Imam et al., 2019), highlighting that this could be an area of interest in terms of whether someone is predisposed to a more profound and/or recurrent thrombotic event (despite intervention).

6.2.1. Key findings

- Successful generation of a novel platelet-specific AC6-KO mouse
- AC6-KO displays impaired cAMP production and specific downstream PKA signalling events
- AC6-KO demonstrates impaired PGI_2 sensitivity in PAR- but not GPVI-mediated platelet activity
- AC6 plays a key physiological role in thrombosis and thrombus stability

6.3. Future directions

6.3.1. Further functional assessment of the AC6-KO mouse

While several approaches were taken to understand the role of AC6 in platelet function and thrombosis, direct analysis of haemostasis was not explored. Given our data demonstrates accelerated thrombosis, we question whether

haemostasis is also affected by the loss of AC6. Further studies using well-established tail bleeding time (TBT) assays could ascertain whether AC6 is involved in haemostasis, or whether it is restricted to mediating thrombosis (Dejana et al., 1979; Dejana et al., 1982; Greene et al., 2010; Liu et al., 2012; Brake et al., 2019; Mohammed et al., 2020).

In addition, while we demonstrated impaired thrombus stability in the AC6-KO mouse, the downstream implications and mechanisms involved are yet to be elucidated. Further *in vivo* thrombosis injury experiments and analysis of embolic events are required to establish whether a loss of AC6 significantly impairs thrombus stability. In addition, using the *in vivo* Xtreme^{TM} (optical and X-ray) imaging system, it would be possible to assess the location of emboli lost from the original injury. This could provide information on whether a loss of AC6 leads to emboli travelling to different locations in the body such as the lung or brain. Using models of inferior vena cava (IVC) thrombosis and pulmonary embolism (PE) in combination with Xtreme^{TM} imaging, would also be advantageous to apply to the AC6-KO mouse (Duval et al., 2021).

We also wonder what impact the loss of AC6 has on other disease models. Murine models of atherosclerosis or diabetes could highlight whether the absence of AC6 is a driver of platelet hyperactivity in these diseases. Platelets from apolipoprotein-E (ApoE) deficient mice, a model used to assess atherosclerosis, demonstrate circulating activated platelets which exacerbate atherosclerosis (Huo et al., 2003). It could be possible that a loss of AC6 and impaired endogenous PGI_2-mediated inhibition of platelets in circulation further elevates platelet hyperactivity and accelerates thrombosis

6.3.2. Further assessment of AC6 signalling

Though we were unable to identify AC6-specific downstream PKA substrates and whether specific G-proteins were implicated by the absence of AC6. Future work involving, phospho- and G-protein arrays would allow us to establish specifically which PKA substrates and G-proteins are affected by the loss of AC6. This would help us to understand the relationship between G-proteins, PAR receptors, ACs and PKA substrates in platelets (Fang et al., 2003; Marcus et al., 2003; Qureshi et al., 2009; Syu et al., 2020). Understanding which phospho-proteins are affected by the loss of AC6

specifically, could also highlight proteins implicated in clot stability, leaning towards a mechanism whereby AC6 controls thrombus stability.

To establish whether AC6 and PAR receptors reside in a complex, along with AC6-specific pools of cAMP and downstream PKA substrates, future work could include subcellular fraction in combination with immunoblotting analysis of G-proteins, AC, PAR receptors and phospho-PKA substrates (Raslan and Naseem, 2015). To establish pools of cAMP as well as PKA activity, ELISAs of subcellular fractions could also be applied. It would be sensible to apply these methods to the AC6-KO though analysis of whether ACs are linked to PAR receptors could also be carried out in human platelets.

Additionally, given that a loss of AC6 results in impaired inhibition of PAR-mediated activity, we postulate that AC6 is linked to PAR receptors either by lipid rafts or AKAPs. Though we did not explore this, future studies could include proximity ligation assays (PLA), dual-colour expansion and confocal microscopy with colocalization analysis to assess whether ACs and PAR receptors are spatially linked in both human and AC6-KO platelets (Jarvius et al., 2007; Hermann et al., 2010; Thulin et al., 2018; Montague et al., 2020; Heil et al., 2022).

6.3.3. Relevance of AC6 in human platelets

As platelets do not contain a nucleus, commonly used *in vitro* genome editing techniques such as siRNA knockdown is not possible. Therefore, understanding the role of genes and subsequent encoded proteins within platelets presents many challenges, largely overcome by the use of mouse models. A clear limitation of this study is the use of mouse models to underpin the role of AC6 in platelets, future work therefore must incorporate translating these findings into man. An alternative to using knockout mouse models are the use of proteolysis-targeting chimeras (PROTACs), whereby a PROTAC molecule with two covalently-linked ligands recruits a target protein and E3 ubiquitin ligase together triggering proteasomal degradation of the target protein (Sakamoto et al., 2001; Schneekloth et al., 2004). Though commonly used to target BCL-XL to alleviate on-target thrombocytopenia associated with BCL-XL inhibition by anti-cancer therapies (Zhang et al., 2020; Li et al., 2022). PROTACs are a new area of platelet biology currently being explored, which

could allow us to assess specific protein function in human platelets. While this has not yet been explored in platelet cAMP signalling, using PROTACs to degrade ACs and their specific isoforms could provide a more relevant model for future studies, reducing the need for knockout mouse models (Burden et al., 2015).

6.3.4. Clinical studies

In contrast to PROTAC studies, patient samples could provide an even more relevant model to explore the role of ACs in disease. To date isoform specific AC antibodies are poor, and isoform specific activators and inhibitors do not yet exist. Therefore, establishing the role of isoform specific ACs in patients does present challenges for future studies. Although given that AC6 is the predominant isoform in human and murine platelets (Rowley et al., 2011; Burkhart et al., 2012; Zeiler et al., 2014), the data presented in this study, hints that AC6 is the main driver of cAMP signalling in platelets. To establish whether AC expression or AC activity is affected in disease, patient samples could be assessed for expression via qPCR and AC activity in response to PGI_2 and forskolin. Analysis of pan-AC expression via immunoblotting in combination with qPCR analysis of specific AC isoforms could allow us to establish whether AC or AC6 expression is impaired in cardiovascular disease. Though this will not reveal functional information, if levels of AC6 expression are lower in disease, it could hint at a potential point of failure and will contribute to our understanding of how platelets become hyperactive in disease. In addition, functional assessment either by platelet aggregation or FFC in the presence of forskolin could tell us whether activation or inhibition is impaired in patients, linked to AC. In combination with the expression analysis this could highlight which AC is potentially implicated in cardiovascular disease. Providing a potential new target for future therapeutics or a diagnostic target to predetermine cardiovascular events.

Bibliography

Abrams, C. and Shattil, S.J. 1991. IMMUNOLOGICAL DETECTION OF ACTIVATED PLATELETS IN CLINICAL DISORDERS. *Thrombosis and Haemostasis.* **65**(5), pp.467-473.

Abramson, S., Korchak, H., Ludewig, R., Edelson, H., Haines, K., Levin, R.I., Herman, R., Rider, L., Kimmel, S. and Weissmann, G. 1985. MODES OF ACTION OF ASPIRIN-LIKE DRUGS. *Proceedings of the National Academy of Sciences of the United States of America.* **82**(21), pp.7227-7231.

Aburima, A., Berger, M., Spurgeon, B.E.J., Webb, B.A., Wraith, K.S., Febbraio, M., Poole, A.W. and Naseem, K.M. 2021. Thrombospondin-1 promotes hemostasis through modulation of cAMP signaling in blood platelets. *Blood.* **137**(5), pp.678-689.

Aburima, A., Wraith, K.S., Raslan, Z., Law, R., Magwenzi, S. and Naseem, K.M. 2013. cAMP signaling regulates platelet myosin light chain (MLC) phosphorylation and shape change through targeting the RhoA-Rho kinase-MLC phosphatase signaling pathway. *Blood.* **122**(20), pp.3533-3545.

Adelman, Michelson, Handin and Ault. 1985. Evaluation of platelet glycoprotein Ib by fluorescence flow cytometry. *Blood.* **66**(2), pp.423-427.

Adelman, B., Gennings, C., Strony, J. and Hanners, E. 1990. SYNERGISTIC INHIBITION OF PLATELET-AGGREGATION BY FIBRINOGEN-RELATED PEPTIDES. *Circulation Research.* **67**(4), pp.941-947.

Adelman, B., Michelson, A., Handin, R. and Ault, K. 1985. Evaluation of platelet glycoprotein Ib by fluorescence flow cytometry. *Blood.* **66**(2), pp.423-427.

Agbani, E.O. and Poole, A.W. 2017. Procoagulant platelets: generation, function, and therapeutic targeting in thrombosis. *Blood.* **130**(20), pp.2171-2179.

Akai, T., Naka, K., Okuda, K., Takemura, T. and Fujii, S. 1983. DECREASED SENSITIVITY OF PLATELETS TO PROSTACYCLIN IN PATIENTS WITH DIABETES-MELLITUS. *Hormone and Metabolic Research.* **15**(11), pp.523-526.

Archer, S. 1993. Measurement of nitric oxide in biological models. *The FASEB Journal.* **7**(2), pp.349-360.

Arikawa, E., Sun, Y., Wang, J., Zhou, Q., Ning, B., Dial, S.L., Guo, L. and Yang, J. 2008. Cross-platform comparison of SYBR® Green real-time PCR with TaqMan PCR, microarrays and other gene expression measurement technologies evaluated in the MicroArray Quality Control (MAQC) study. *BMC Genomics.* **9**(1), p328.

Armstrong, R.A. 1996. Platelet prostanoid receptors. *Pharmacology & Therapeutics.* **72**(3), pp.171-191.

Arnold, W.P., Mittal, C.K., Katsuki, S. and Murad, F. 1977. NITRIC-OXIDE ACTIVATES GUANYLATE CYCLASE AND INCREASES GUANOSINE 3'-5'-CYCLIC MONOPHOSPHATE LEVELS IN VARIOUS TISSUE PREPARATIONS. *Proceedings of the National Academy of Sciences of the United States of America.* **74**(8), pp.3203-3207.

Aslan, J.E. and Mccarty, O.J.T. 2013. Rho GTPases in platelet function. *Journal of Thrombosis and Haemostasis.* **11**(1), pp.35-46.

Atkinson, L., Yusuf, M.Z., Aburima, A., Ahmed, Y., Thomas, S.G., Naseem, K.M. and Calaminus, S.D.J. 2018. Reversal of stress fibre formation by Nitric Oxide mediated RhoA inhibition leads to reduction in the height of preformed thrombi. *Scientific Reports.* **8**(1).

Ault, K.A., Cannon, C.P., Mitchell, J., McCahan, J., Tracy, R.P., Novotny, W.F., Reimann, J.D. and Braunwald, E. 1999. Platelet activation in patients after an acute coronary syndrome: Results from the TIMI-12 trial. *Journal of the American College of Cardiology.* **33**(3), pp.634-639.

Aurbach, K., Spindler, M., Haining, E.J., Bender, M. and Pleines, I. 2019. Blood collection, platelet isolation and measurement of platelet count and size in mice—a practical guide. *Platelets.* **30**(6), pp.698-707.

Azuma, H., Ishikawa, M. and Sekizaki, S. 1986. ENDOTHELIUM-DEPENDENT INHIBITION OF PLATELET-AGGREGATION. *British Journal of Pharmacology.* **88**(2), pp.411-415.

Bae, Yang and Rezaie. 2007. Receptors of the protein C activation and activated protein C signaling pathways are colocalized in lipid rafts of endothelial cells. *Proceedings of the National Academy of Sciences.* **104**(8), pp.2867-2872.

Bae, Yang and Rezaie. 2008. Lipid raft localization regulates the cleavage specificity of protease activated receptor 1 in endothelial cells. *Journal of Thrombosis and Haemostasis.* **6**(6), pp.954-961.

Bain, J., Mclauchlan, H., Elliott, M. and Cohen, P. 2003. The specificities of protein kinase inhibitors: an update. *Biochemical Journal.* **371**(1), pp.199-204.

Banfi, G., Salvagno, G.L. and Lippi, G. 2007. The role of ethylenedimine tetraacetic acid (EDTA) as in vitro anticoagulant for diagnostic purposes. *Clinical Chemistry and Laboratory Medicine.* **45**(5), pp.565-576.

Barry, F.A., Graham, G.J., Fry, M.J. and Gibbins, J.M. 2003. Regulation of glycogen synthase kinase 3 in human platelets: a possible role in platelet function?¹. *FEBS Letters.* **553**(1-2), pp.173-178.

Bath, P.M.W., Blann, A., Smith, N. and Butterworth, R.J. 1998. Von Willebrand factor, P-selectin and fibrinogen levels in patients with acute ischaemic and haemorrhagic stroke, and their relationship with stroke sub-type and functional outcome. *Platelets.* **9**(3-4), pp.155-159.

Bauman, A.L., Soughayer, J., Nguyen, B.T., Willoughby, D., Carnegie, G.K., Wong, W., Hoshi, N., Langeberg, L.K., Cooper, D.M.F., Dessauer, C.W. and Scott, J.D. 2006. Dynamic regulation of cAMP synthesis through anchored PKA-Adenylyl cyclase V/VI complexes. *Molecular Cell.* **23**(6), pp.925-931.

Beaulieu and Freedman. 2013. Inhibition of Platelet Function by the Endothelium. *Platelets.* Third ed. Academic Press, pp.313-342.

Beck, F., Geiger, J., Gambaryan, S., Veit, J., Vaudel, M., Nollau, P., Kohlbacher, O., Martens, L., Walter, U., Sickmann, A. and Zahedi, R.P. 2014. Time-resolved characterization of cAMP/PKA-dependent signaling reveals that platelet inhibition is a concerted process involving multiple signaling pathways. *Blood.* **123**(5), pp.E1-E10.

Becker, R.C., Bassand, J.P., Budaj, A., Wojdyla, D.M., James, S.K., Cornel, J.H., French, J., Held, C., Horrow, J., Husted, S., Lopez-Sendon, J., Lassila, R., Mahaffey, K.W., Storey, R.F., Harrington, R.A. and Wallentin, L. 2011. Bleeding complications with the P2Y12 receptor antagonists clopidogrel and ticagrelor in the PLATelet inhibition and patient Outcomes (PLATO) trial. *European Heart Journal.* **32**(23), pp.2933-2944.

Behnke, O. 1965. FURTHER STUDIES ON MICROTUBULES - A MARGINAL BUNDLE IN HUMAN AND RAT THROMBOCYTES. *Journal of Ultrastructure Research.* **13**(5-6), pp.469-+.

Bennett, H.S. 1963. MORPHOLOGICAL ASPECTS OF EXTRACELLULAR POLYSACCHARIDES. *Journal of Histochemistry & Cytochemistry.* **11**(1), pp.14-&.

Berger, M., Raslan, Z., Aburima, A., Magwenzi, S., Wraith, K.S., Spurgeon, B.E.J., Hindle, M.S., Law, R., Febbraio, M. and Naseem, K.M. 2020. Atherogenic lipid stress induces platelet hyperactivity through CD36-mediated hyposensitivity to prostacyclin: the role of phosphodiesterase 3A. *Haematologica.* **105**(3), pp.808-819.

Berger, M., Wraith, K., Raslan, Z., Magwenzi, S., Aburima, A., Law, R., Rossington, J., Spurgeon, B., Hindle, M., Woodwaard, C., Febbraio, M., Marx, N. and Naseem, K.M. 2018a. Dyslipidemia associated oxidised ldl induces platelet hyperactivity through a cd36-dependent activation of pde3a. *European Heart Journal.* **39**, pp.1047-1048.

Berger, M., Wraith, K., Raslan, Z., Magwenzi, S., Aburima, A., Law, R., Rossington, J., Spurgeon, B., Hindle, M., Woodwaard, C., Febbraio, M., Marx, N. and Naseem, K.M. 2018b. Dyslipidemia-associated atherogenic oxidized lipids induce platelet hyperactivity through phospholipase Cγ2-dependent reactive oxygen species generation. *European Heart Journal.* **39**, pp.1047-1048.

Blair, P. and Flaumenhaft, R. 2009. Platelet α-granules: Basic biology and clinical correlates. *Blood Reviews.* **23**(4), pp.177-189.

Bodnar, R.J., Xi, X.D., Li, Z.Y., Berndt, M.C. and Du, X.P. 2002. Regulation of glycoprotein Ib-IX-von Willebrand factor interaction by cAMP-dependent protein kinase-mediated phosphorylation at Ser(166) of glycoprotein Ib beta. *Journal of Biological Chemistry.* **277**(49), pp.47080-47087.

Bonaccio, M., Di Castelnuovo, A., Costanzo, S., De Curtis, A., Donati, M.B., Cerletti, C., de Gaetano, G., Iacoviello, L. and Investigators, M.-S. 2016. Age-sex-specific ranges of platelet count and all-cause mortality: prospective findings from the MOLI-SANI study. *Blood.* **127**(12), pp.1614-1616.

Bonnard, T. and Hagemeyer, C.E. 2015. Ferric Chloride-induced Thrombosis Mouse Model on Carotid Artery and Mesentery Vessel. *Jove-Journal of Visualized Experiments.* (100).

Born, G.V.R. 1962. AGGREGATION OF BLOOD PLATELETS BY ADENOSINE DIPHOSPHATE AND ITS REVERSAL. *Nature.* **194**(4832), pp.927-&.

Brake, M.A., Ivanciu, L., Maroney, S.A., Martinez, N.D., Mast, A.E. and Westrick, R.J. 2019. Assessing Blood Clotting and Coagulation Factors in Mice. *Current protocols in mouse biology.* **9**(2), pp.e61-e61.

Brass, L.F. 2003. Thrombin and platelet activation. *Chest.* **124**(3), pp.18S-25S.

Brass, L.F., Diamond, S.L. and Stalker, T.J. 2016. Platelets and hemostasis: a new perspective on an old subject. *Blood Advances.* **1**(1), pp.5-9.

Brass, L.F., Wannemacher, K.M., Ma, P. and Stalker, T.J. 2011. Regulating thrombus growth and stability to achieve an optimal response to injury. *Journal of Thrombosis and Haemostasis.* **9**, pp.3-4.

Broos, K., Feys, H.B., De Meyer, S.F., Vanhoorelbeke, K. and Deckmyn, H. 2011. Platelets at work in primary hemostasis. *Blood Reviews.* **25**(4), pp.155-167.

Bull, B.S., Schneiderman, M.A. and Brecher, G. 1965. PLATELET COUNTS WITH COULTER COUNTER. *American Journal of Clinical Pathology.* **44**(6), pp.678-+.

Bunting, S., Moncada, S. and Vane, J.R. 1983. THE PROSTACYCLIN-THROMBOXANE-A2 BALANCE - PATHOPHYSIOLOGICAL AND THERAPEUTIC IMPLICATIONS. *British Medical Bulletin.* **39**(3), pp.271-276.

Burden, N., Chapman, K., Sewell, F. and Robinson, V. 2015. Pioneering Better Science through the 3Rs: An Introduction to the National Centre for the Replacement, Refinement, and Reduction of Animals in Research (NC3Rs).

Journal of the American Association for Laboratory Animal Science. **54**(2), pp.198-208.

Burghuber, O.C., Punzengruber, C., Sinzinger, H., Haber, P. and Silberbauer, K. 1986. PLATELET SENSITIVITY TO PROSTACYCLIN IN SMOKERS AND NONSMOKERS. *Chest.* **90**(1), pp.34-38.

Burkhart, J.M., Vaudel, M., Gambaryan, S., Radau, S., Walter, U., Martens, L., Geiger, J., Sickmann, A. and Zahedi, R.P. 2012. The first comprehensive and quantitative analysis of human platelet protein composition allows the comparative analysis of structural and functional pathways. *Blood.* **120**(15), pp.E73-E82.

Burton, K.A., Johnson, B.D., Hausken, Z.E., Westenbroek, R.E., Idzerda, R.L., Scheuer, T., Scott, J.D., Catterall, W.A. and McKnight, G.S. 1997. Type II regulatory subunits are not required for the anchoring-dependent modulation of Ca2+ channel activity by cAMP-dependent protein kinase. *Proceedings of the National Academy of Sciences of the United States of America.* **94**(20), pp.11067-11072.

Butt, E., Abel, K., Krieger, M., Palm, D., Hoppe, V., Hoppe, J. and Walter, U. 1994. CAMP-DEPENDENT AND CGMP-DEPENDENT PROTEIN-KINASE PHOSPHORYLATION SITES OF THE FOCAL ADHESION VASODILATOR-STIMULATED PHOSPHOPROTEIN (VASP) IN-VITRO AND IN INTACT HUMAN PLATELETS. *Journal of Biological Chemistry.* **269**(20), pp.14509-14517.

Butt, E., Gambaryan, S., Gottfert, N., Galler, A., Marcus, K. and Meyer, H.E. 2003. Actin binding of human LIM and SH3 protein is regulated by cGMP- and cAMP-dependent protein kinase phosphorylation on serine 146. *Journal of Biological Chemistry.* **278**(18), pp.15601-15607.

Cavallini, L., Coassin, M., Borean, A. and Alexandre, A. 1996. Prostacyclin and sodium nitroprusside inhibit the activity of the platelet inositol 1,4,5-trisphosphate receptor and promote its phosphorylation. *Journal of Biological Chemistry.* **271**(10), pp.5545-5551.

Cazenave, J.-P., Ohlmann, P., Cassel, D., Eckly, A., Hechler, B. and Gachet, C. 2004. Preparation of Washed Platelet Suspensions From Human and Rodent Blood. *Platelets and Megakaryocytes.* Humana Press, pp.013-028.

Celi, A., Merrill-Skoloff, G., Gross, P., Falati, S., Sim, D.S., Flaumenhaft, R., Furie, B.C. and Furie, B. 2003. Thrombus formation: direct real-time observation and digital analysis of thrombus assembly in a living mouse by confocal and widefield intravital microscopy. *Journal of Thrombosis and Haemostasis.* **1**(1), pp.60-68.

Chen, Y.B., Harry, A., Li, J.R., Smit, M.J., Bai, X., Magnusson, R., Pieroni, J.P., Weng, G.Z. and Iyengar, R. 1997. Adenylyl cyclase 6 is selectively regulated by protein kinase A phosphorylation in a region involved in G alpha(s), stimulation. *Proceedings of the National Academy of Sciences of the United States of America.* **94**(25), pp.14100-14104.

Cheng, Y., Austin, S.C., Rocca, B., Koller, B.H., Coffman, T.M., Grosser, T., Lawson, J. and FitzGerald, G.A. 2003. Role of prostacyclin in the cardiovascular, response to thromboxane A2. *Faseb Journal.* **17**(5), pp.A1054-A1054.

Chien, A., Edgar, D.B. and Trela, J.M. 1976. Deoxyribonucleic acid polymerase from the extreme thermophile Thermus aquaticus. *Journal of Bacteriology.* **127**(3), pp.1550-1557.

Cho, J., Kim, H., Song, J., Cheong, J.-W., Shin, J.W., Yang, W.I. and Kim, H.O. 2018. Platelet storage induces accelerated desialylation of platelets and increases hepatic thrombopoietin production. *Journal of Translational Medicine.* **16**(1).

Chomczynski, P. and Sacchi, N. 1987. SINGLE-STEP METHOD OF RNA ISOLATION BY ACID GUANIDINIUM THIOCYANATE PHENOL CHLOROFORM EXTRACTION. *Analytical Biochemistry.* **162**(1), pp.156-159.

Choo, H.-J., Kholmukhamedov, A., Zhou, C. and Jobe, S. 2017. Inner Mitochondrial Membrane Disruption Links Apoptotic and Agonist-Initiated Phosphatidylserine Externalization in Platelets. *Arteriosclerosis, Thrombosis, and Vascular Biology.* **37**(8), pp.1503-1512.

Choo, H.-J., Saafir, T.B., Mkumba, L., Wagner, M.B. and Jobe, S.M. 2012. Mitochondrial Calcium and Reactive Oxygen Species Regulate Agonist-Initiated Platelet Phosphatidylserine Exposure. *Arteriosclerosis, Thrombosis, and Vascular Biology.* **32**(12), pp.2946-2955.

Clarke, M.C.H., Savill, J., Jones, D.B., Noble, B.S. and Brown, S.B. 2003. Compartmentalized megakaryocyte death generates functional platelets committed to caspase-independent death. *Journal of Cell Biology.* **160**(4), pp.577-587.

Clemetson, K.J. 2012. Platelets and Primary Haemostasis. *Thrombosis Research.* **129**(3), pp.220-224.

Connolly, T.M., Condra, C., Feng, D.M., Cook, J.J., Stranieri, M.T., Reilly, C.F., Nutt, R.F. and Gould, R.J. 1994. SPECIES VARIABILITY IN PLATELET AND OTHER CELLULAR RESPONSIVENESS TO THROMBIN RECEPTOR-DERIVED PEPTIDES. *Thrombosis and Haemostasis.* **72**(4), pp.627-633.

Conti, M. and Jin, S.L.C. 2000. The molecular biology of cyclic nucleotide phosphodiesterases. *Progress in Nucleic Acid Research and Molecular Biology.* **63**, pp.1-38.

Cooper. 2003. Regulation and organization of adenylyl cyclases and cAMP. *Biochemical Journal.* **375**, pp.517-529.

Cooper and Brooker. 1993. CA-2+-INHIBITED ADENYLYL CYCLASE IN CARDIAC TISSUE. *Trends in Pharmacological Sciences.* **14**(2), pp.34-36.

Cooper and Crossthwaite. 2006. Higher-order organization and regulation of adenylyl cyclases. *Trends in Pharmacological Sciences.* **27**(8), pp.426-431.

Cooper and Tabbasum. 2014. Adenylate cyclase-centred microdomains. *Biochemical Journal.* **462**, pp.199-213.

Corey, E.J., Niwa, H., Falck, J.R., Mioskowski, C., Arai, Y. and Marfat, A. 1980. RECENT STUDIES ON THE CHEMICAL SYNTHESIS OF EICOSANOIDS. *Samuelsson, B., P. W. Ramwell and R. Paoletti (Ed.). Advances in Prostaglandin and Thromboxane Research, Vol. 6. 4th International Prostaglandin Conference, Washington, D.C., USA, May 28-31, 1979. Xlv+600p. Raven Press; New York, N.Y., USA. Illus.* pp.P19-26.

Cossarizza, A., Chang, H.D., Radbruch, A., Akdis, M., Andra, I., Annunziato, F., Bacher, P., Barnaba, V., Battistini, L., Bauer, W.M., Baumgart, S., Becher, B., Beisker, W., Berek, C., Blanco, A., Borsellino, G., Boulais, P.E., Brinkman, R.R., Buscher, M., Busch, D.H., Bushnell, T.P., Cao, X.T., Cavani, A., Chattopadhyay, P.K., Cheng, Q.Y., Chow, S., Clerici, M., Cooke, A., Cosma, A., Cosmi, L., Cumano, A., Dang, V.D., Davies, D., De Biasi, S., Del Zotto, G., Della Bella, S., Dellabona, P., Deniz, G., Dessing, M., Diefenbach, A., Di Santo, J., Dieli, F., Dolf, A., Donnenberg, V.S., Dorner, T., Ehrhardt, G.R.A., Endl, E., Engel, P., Engelhardt, B., Esser, C., Everts, B., Dreher, A., Falk, C.S., Fehniger, T.A., Filby, A., Fillatreau, S., Follo, M., Forster, I., Foster, J.,

Foulds, G.A., Frenette, P.S., Galbraith, D., Garbi, N., Garcia-Godoy, M.D., Geginat, J., Ghoreschi, K., Gibellini, L., Goettlinger, C., Goodyear, C.S., Gori, A., Grogan, J., Gross, M., Grutzkau, A., Grummitt, D., Hahn, J., Hammer, Q., Hauser, A.E., Haviland, D.L., Hedley, D., Herrera, G., Herrmann, M., Hiepe, F., Holland, T., Hombrink, P., Houston, J.P., Hoyer, B.F., Huang, B., Hunter, C.A., Iannone, A., Jack, H.M., Javega, B., Jonjic, S., Juelke, K., Jung, S., Kaiser, T., Kalina, T., Keller, B., Khan, S., Kienhofer, D., Kroneis, T., Kunkel, D., Kurts, C., Kvistborg, P., Lannigan, J., Lantz, O., Larbi, A., LeibundGut-Landmann, S., Leipold, M.D., Levings, M.K., Litwin, V., Liu, Y.L., Lohoff, M., Lombardi, G., Lopez, L., Lovett-Racke, A., Lubberts, E., Ludewig, B., Lugli, E., Maecker, H.T., Martrus, G., Matarese, G., Maueroder, C., McGrath, M., McInnes, I., Mei, H.E., Melchers, F., Melzer, S., Mielenz, D., Mills, K., Mirrer, D., Mjosberg, J., Moore, J., Moran, B., Moretta, A., Moretta, L., Mosmann, T.R., Muller, S., Muller, W., Munz, C., Multhoff, G., Munoz, L.E., Murphy, K.M., Nakayama, T., Nasi, M., Neudorfl, C., Nolan, J., Nourshargh, S., O'Connor, J.E., Ouyang, W.J., Oxenius, A., Palankar, R., Panse, I., Peterson, P., Peth, C., Petriz, J., Philips, D., Pickl, W., Piconese, S., Pinti, M., Pockley, A.G., Podolska, M.J., Pucillo, C., Quataert, S.A., Radstake, T., Rajwa, B., Rebhahn, J.A., Recktenwald, D., Remmerswaal, E.B.M., Rezvani, K., Rico, L.G., Robinson, J.P., Romagnani, C., Rubartelli, A., Ruckert, B., Ruland, J., Sakaguchi, S., Sala-De-Oyanguren, F., Samstag, Y., Sanderson, S., Sawitzki, B., Scheffold, A., Schiemann, M., Schildberg, F., Schimisky, E., Schmid, S.A., Schmitt, S., Schober, K., Schuler, T., Schulz, A.R., Schumacher, T., Scotta, C., Shankey, T.V., Shemer, A., Simon, A.K., Spidlen, J., Stall, A.M., Stark, R., Stehle, C., Stein, M., Steinmetz, T., Stockinger, H., Takahama, Y., Tarnok, A., Tian, Z., Toldi, G., Tornack, J., Traggiai, E., Trotter, J., Ulrich, H., van der Braber, M., van Lier, R.A.W., Veldhoen, M., Vento-Asturias, S., Vieira, P., Voehringer, D., Volk, H.D., von Volkmann, K., Waisman, A., Walker, R., Ward, M.D., Warnatz, K., Warth, S., Watson, J.V., Watzl, C., Wegener, L., Wiedemann, A., Wienands, J., Willimsky, G., Wing, J., Wurst, P., Yu, L.P., Yue, A., Zhang, Q.J., Zhao, Y., Ziegler, S. and Zimmermann, J. 2017. Guidelines for the use of flow cytometry and cell sorting in immunological studies. *European Journal of Immunology.* **47**(10), pp.1584-1797.

Crittenden, J.R., Bergmeier, W., Zhang, Y.Y., Piffath, C.L., Liang, Y.Q., Wagner, D.D., Housman, D.E. and Graybiel, A.M. 2004. CalDAG-GEFI integrates signaling for platelet aggregation and thrombus formation. *Nature Medicine.* **10**(9), pp.982-986.

Crosland-Taylor, P.J. 1953. A Device for Counting Small Particles suspended in a Fluid through a Tube. *Nature.* **171**(4340), pp.37-38.

Darbousset, R., Mezouar, S., Dignat-George, F., Panicot-Dubois, L. and Dubois, C. 2014. Involvement of neutrophils in thrombus formation in living mice. *Pathologie Biologie.* **62**(1), pp.1-9.

Davare, M.A., Avdonin, V., Hall, D.D., Peden, E.M., Burette, A., Weinberg, R.J., Horne, M.C., Hoshi, T. and Hell, J.W. 2001. A beta(2) adrenergic receptor signaling complex assembled with the Ca2+ channel Ca(v)1.2. *Science.* **293**(5527), pp.98-101.

Davies, S.P., Reddy, H., Caivano, M. and Cohen, P. 2000. Specificity and mechanism of action of some commonly used protein kinase inhibitors. *Biochemical Journal.* **351**(1), p95.

Davì, G., Romano, M., Mezzetti, A., Procopio, A., Iacobelli, S., Antidormi, T., Bucciarelli, T., Alessandrini, P., Cuccurullo, F. and Bon, G.B. 1998. Increased

Levels of Soluble P-Selectin in Hypercholesterolemic Patients. *Circulation.* **97**(10), pp.953-957.

De Botton, S. 2002. Platelet formation is the consequence of caspase activation within megakaryocytes. *Blood.* **100**(4), pp.1310-1317.

De Meyer, S.F., Deckmyn, H. and Vanhoorelbeke, K. 2009. von Willebrand factor to the rescue. *Blood.* **113**(21), pp.5049-5057.

Defer, N., Best-Belpomme, M. and Hanoune, J. 2000. Tissue specificity and physiological relevance of various isoforms of adenylyl cyclase. *American Journal of Physiology-Renal Physiology.* **279**(3), pp.F400-F416.

Dejana, E., Callioni, A., Quintana, A. and Degaetano, G. 1979. BLEEDING-TIME IN LABORATORY-ANIMALS .2. COMPARISON OF DIFFERENT ASSAY CONDITIONS IN RATS. *Thrombosis Research.* **15**(1-2), pp.191-197.

Dejana, E., Villa, S. and Degaetano, G. 1982. BLEEDING-TIME IN RATS - A COMPARISON OF DIFFERENT EXPERIMENTAL CONDITIONS. *Thrombosis and Haemostasis.* **48**(1), pp.108-111.

Deng, G., Yu, S., Li, Q., He, Y., Liang, W., Yu, L., Xu, D., Sun, T., Zhang, R. and Li, Q. 2017. Investigation of platelet apoptosis in adult patients with chronic immune thrombocytopenia. *Hematology.* **22**(3), pp.155-161.

Dessauer, C.W. 2009. Adenylyl Cyclase-A-kinase Anchoring Protein Complexes: The Next Dimension in cAMP Signaling. *Molecular Pharmacology.* **76**(5), pp.935-941.

Deutsch, V.R. and Tomer, A. 2006. Megakaryocyte development and platelet production. *British Journal of Haematology.* **134**(5), pp.453-466.

Diamond, S.L. 2016. Systems Analysis of Thrombus Formation. *Circulation Research.* **118**(9), pp.1348-1362.

Dostmann, W.R., Taylor, S.S., Genieser, H.G., Jastorff, B., Døskeland, S.O. and Ogreid, D. 1990. Probing the cyclic nucleotide binding sites of cAMP-dependent protein kinases I and II with analogs of adenosine 3',5'-cyclic phosphorothioates. *Journal of Biological Chemistry.* **265**(18), pp.10484-10491.

Duval, C., Baranauskas, A., Feller, T., Ali, M., Cheah, L.T., Yuldasheva, N.Y., Baker, S.R., McPherson, H.R., Raslan, Z., Bailey, M.A., Cubbon, R.M., Connell, S.D., Ajjan, R.A., Philippou, H., Naseem, K.M., Ridger, V.C. and Ariens, R.A.S. 2021. Elimination of fibrin gamma-chain cross-linking by FXIIIa increases pulmonary embolism arising from murine inferior vena cava thrombi. *Proceedings of the National Academy of Sciences of the United States of America.* **118**(27).

Ebbe, S., Stohlman, F., Donovan, J. and Howard, D. 1965. Megakaryocytopoiesis in the Rat. *Blood.* **26**(1), pp.20-35.

Ebbeling, L., Robertson, C., McNicol, A. and Gerrard, J.M. 1992. RAPID ULTRASTRUCTURAL-CHANGES IN THE DENSE TUBULAR SYSTEM FOLLOWING PLATELET ACTIVATION. *Blood.* **80**(3), pp.718-723.

Eckly, A., Hechler, B., Freund, M., Zerr, M., Cazenave, J.-P., Lanza, F., Mangin, P.H. and Gachet, C. 2011. Mechanisms underlying FeCl3-induced arterial thrombosis. *Journal of Thrombosis and Haemostasis.* **9**(4), pp.779-789.

Edelhoff, S., Villacres, E.C., Storm, D.R. and Disteche, C.M. 1995. Mapping of adenylyl cyclase genes type I, II, III, IV, V, and VI in mouse. *Mammalian Genome.* **6**(2), pp.111-113.

El-Daher, S.S., Patel, Y., Siddiqua, A., Hassock, S., Edmunds, S., Maddison, B., Patel, G., Goulding, D., Lupu, F., Wojcikiewicz, R.J.H. and Authi, K.S. 2000. Distinct localization and function of (IP3)-I-1,4,5 receptor subtypes and the

(IP4)-I-1,3,4,5 receptor GAP1(IP4BP) in highly purified human platelet membranes. *Blood.* **95**(11), pp.3412-3422.

ElDaher, S.S., Eigenthaler, M., Walter, U., Furuichi, T., Miyawaki, A., Mikoshiba, K., Kakkar, V.V. and Authi, K.S. 1996. Distribution and activation of cAMP- and cGMP-dependent protein kinases in highly purified human platelet plasma and intracellular membranes. *Thrombosis and Haemostasis.* **76**(6), pp.1063-1071.

Emery, A.C., Eiden, M.V. and Eiden, L.E. 2013. A New Site and Mechanism of Action for the Widely Used Adenylate Cyclase Inhibitor SQ22,536. *Molecular Pharmacology.* **83**(1), pp.95-105.

Erdmann, J., Stark, K., Esslinger, U.B., Rumpf, P.M., Koesling, D., De Wit, C., Kaiser, F.J., Braunholz, D., Medack, A., Fischer, M., Zimmermann, M.E., Tennstedt, S., Graf, E., Eck, S., Aherrahrou, Z., Nahrstaedt, J., Willenborg, C., Bruse, P., Brænne, I., Nöthen, M.M., Hofmann, P., Braund, P.S., Mergia, E., Reinhard, W., Burgdorf, C., Schreiber, S., Balmforth, A.J., Hall, A.S., Bertram, L., Steinhagen-Thiessen, E., Li, S.-C., März, W., Reilly, M., Kathiresan, S., Mcpherson, R., Walter, U., Ott, J., Samani, N.J., Strom, T.M., Meitinger, T., Hengstenberg, C. and Schunkert, H. 2013. Dysfunctional nitric oxide signalling increases risk of myocardial infarction. *Nature.* **504**(7480), pp.432-436.

Escolar, G. and White, J.G. 1991. THE PLATELET OPEN CANALICULAR SYSTEM - A FINAL COMMON PATHWAY. *Blood Cells.* **17**(3), pp.467-485.

Fadok, V.A., Voelker, D.R., Campbell, P.A., Cohen, J.J., Bratton, D.L. and Henson, P.M. 1992. EXPOSURE OF PHOSPHATIDYLSERINE ON THE SURFACE OF APOPTOTIC LYMPHOCYTES TRIGGERS SPECIFIC RECOGNITION AND REMOVAL BY MACROPHAGES. *Journal of Immunology.* **148**(7), pp.2207-2216.

Falati, S., Gross, P., Merrill-Skoloff, G., Furie, B.C. and Furie, B. 2002. Real-time in vivo imaging of platelets, tissue factor and fibrin during arterial thrombus formation in the mouse. *Nature Medicine.* **8**(10), pp.1175-1180.

Fang, Lahiri and Picard. 2003. G protein-coupled receptor microarrays for drug discovery. *Drug Discovery Today.* **8**(16), pp.755-761.

Fang, Yu, Lu, Bast, Woodgett and Mills. 2000. Phosphorylation and inactivation of glycogen synthase kinase 3 by protein kinase A. *Proceedings of the National Academy of Sciences of the United States of America.* **97**(22), pp.11960-11965.

Feijge, M.A.H., Ansink, K., Vanschoonbeek, K. and Heemskerk, J.W.M. 2004. Control of platelet activation by cyclic AMP turnover and cyclic nucleotide phosphodiesterase type-3. *Biochemical Pharmacology.* **67**(8), pp.1559-1567.

Fisch, A., Tobusch, K., Veit, K., Meyer, J. and Darius, H. 1997. Prostacyclin receptor desensitization is a reversible phenomenon in human platelets. *Circulation.* **96**(3), pp.756-760.

Fontana, P., Zufferey, A., Daali, Y. and Reny, J.-L. 2014. Antiplatelet Therapy: Targeting the TxA2 Pathway. *Journal of Cardiovascular Translational Research.* **7**(1), pp.29-38.

Fox, J.E.B. 1985. LINKAGE OF A MEMBRANE SKELETON TO INTEGRAL MEMBRANE-GLYCOPROTEINS IN HUMAN-PLATELETS - IDENTIFICATION OF ONE OF THE GLYCOPROTEINS AS GLYCOPROTEIN-LB. *Journal of Clinical Investigation.* **76**(4), pp.1673-1683.

Frame, S. and Cohen, P. 2001. GSK3 takes centre stage more than 20 years after its discovery. *Biochemical Journal.* **359**(1), p1.

Fraser, I.D.C., Cong, M., Kim, J., Rollins, E.N., Daaka, Y., Lefkowitz, R.J. and Scott, J.D. 2000. Assembly of an A kinase-anchoring protein-beta(2)-adrenergic receptor complex facilitates receptor phosphorylation and signaling. *Current Biology.* **10**(7), pp.409-412.

Fredholm, B.B., Ijzerman, A.P., Jacobson, K.A., Klotz, K.N. and Linden, J. 2001. International Union of Pharmacology. XXV. Nomenclature and classification of adenosine receptors. *Pharmacological Reviews.* **53**(4), pp.527-552.

Frelinger, A.L., III, Grace, R.F., Gerrits, A.J., Berny-Lang, M.A., Brown, T., Carmichael, S.L., Neufeld, E.J. and Michelson, A.D. 2015. Platelet function tests, independent of platelet count, are associated with bleeding severity in ITP. *Blood.* **126**(7), pp.873-879.

Fukuda, T., Asou, E., Nogi, K. and Goto, K. 2017. Evaluation of mouse red blood cell and platelet counting with an automated hematology analyzer. *Journal of Veterinary Medical Science.* **79**(10), pp.1707-1711.

Fukumoto, S., Koyama, H., Hosoi, M., Yamakawa, K., Tanaka, S., Morii, H. and Nishizawa, Y. 1999. Distinct role of cAMP and cGMP in the cell cycle control of vascular smooth muscle cells - cGMP delays cell cycle transition through suppression of cyclin D1 and cyclin-dependent kinase 4 activation. *Circulation Research.* **85**(11), pp.985-991.

Gachet, C., Leon, C. and Hechler, B. 2006. The platelet P2 receptors in arterial thrombosis. *Blood Cells Molecules and Diseases.* **36**(2), pp.223-227.

Gambaryan, S., Geiger, J.R., Schwarz, U.R., Butt, E., Begonja, A., Obergfell, A. and Walter, U. 2004. Potent inhibition of human platelets by cGMP analogs independent of cGMP-dependent protein kinase. *Blood.* **103**(7), pp.2593-2600.

Garcia Rodriguez, L.A., Martin-Perez, M., Hennekens, C.H., Rothwell, P.M. and Lanas, A. 2016. Bleeding Risk with Long-Term Low-Dose Aspirin: A Systematic Review of Observational Studies. *Plos One.* **11**(8).

Geiger, J., Nolte, C., Butt, E., Sage, S.O. and Walter, U. 1992. ROLE OF CGMP AND CGMP-DEPENDENT PROTEIN-KINASE IN NITROVASODILATOR INHIBITION OF AGONIST-EVOKED CALCIUM ELEVATION IN HUMAN PLATELETS. *Proceedings of the National Academy of Sciences of the United States of America.* **89**(3), pp.1031-1035.

Ghoshal, K. and Bhattacharyya, M. 2014. Overview of Platelet Physiology: Its Hemostatic and Nonhemostatic Role in Disease Pathogenesis. *The Scientific World Journal.* **2014**, pp.1-16.

Gibbins, J.M. 2004. Platelet adhesion signalling and the regulation of thrombus formation. *Journal of Cell Science.* **117**(16), pp.3415-3425.

Gilbert, G.E., Sims, P.J., Wiedmer, T., Furie, B., Furie, B.C. and Shattil, S.J. 1991. PLATELET-DERIVED MICROPARTICLES EXPRESS HIGH-AFFINITY RECEPTORS FOR FACTOR-VIII. *Journal of Biological Chemistry.* **266**(26), pp.17261-17268.

Godinho, R.O., Duarte, T. and Pacini, E.S.A. 2015. New perspectives in signaling mediated by receptors coupled to stimulatory G protein: the emerging significance of cAMP efflux and extracellular cAMP-adenosine pathway. *Frontiers in Pharmacology.* **6**.

Golebiewska, E.M. and Poole, A.W. 2015. Platelet secretion: From haemostasis to wound healing and beyond. *Blood Reviews.* **29**(3), pp.153-162.

Gordge, M.P. 2005. Megakaryocyte apoptosis: sorting out the signals. *British Journal of Pharmacology.* **145**(3), pp.271-273.

Gorman, R.R., Bunting, S. and Miller, O.V. 1977. MODULATION OF HUMAN PLATELET ADENYLATE-CYCLASE BY PROSTACYCLIN (PGX). *Prostaglandins.* **13**(3), pp.377-388.

Graber, S.E. and Hawiger, J. 1982. EVIDENCE THAT CHANGES IN PLATELET CYCLIC-AMP LEVELS REGULATE THE FIBRINOGEN RECEPTOR ON HUMAN-PLATELETS. *Journal of Biological Chemistry.* **257**(24), pp.4606-4609.

Greenberger, L.M. and Ishikawa, Y. 1994. ATP-BINDING CASSETTE PROTEINS - COMMON DENOMINATORS BETWEEN ION CHANNELS, TRANSPORTERS, AND ENZYMES. *Trends in Cardiovascular Medicine.* **4**(4), pp.193-198.

Greene, T.K., Schiviz, A., Hoellriegl, W., Poncz, M. and Muchitsch, E.-M. 2010. Towards a standardization of the murine tail bleeding model. *Journal of Thrombosis and Haemostasis.* **8**(12), pp.2820-2822.

Griesshammer, M., Hornkohl, A., Nichol, J.L., Hecht, T., Raghavachar, A., Heimpel, H. and Schrezenmeier, H. 1998. High levels of thrombopoietin in sera of patients with essential thrombocythemia: Cause or consequence of abnormal platelet production? *Annals of Hematology.* **77**(5), pp.211-215.

Grimsley, G.R. and Pace, C.N. 2003. Spectrophotometric Determination of Protein Concentration. *Current Protocols in Protein Science.* **33**(1).

Gros, Ding, Chorazyczewski, Pickering, Limbird and Feldman. 2006a. Adenylyl cyclase isoform-selective regulation of vascular smooth muscle proliferation and cytoskeletal reorganization. *Circulation Research.* **99**(8), pp.845-852.

Gros, Ding, Pickering and Feldman. 2006b. Regulation of vascular smooth muscle cell function by adenylyl cyclase isoforms. *Faseb Journal.* **20**(5), pp.A1117-A1117.

Gros, R., Ding, Q., Chorazyczewski, J., Pickering, J.G., Limbird, L.E. and Feldman, R.D. 2006. Adenylyl cyclase isoform-selective regulation of vascular smooth muscle proliferation and cytoskeletal reorganization. *Circulation Research.* **99**(8), pp.845-852.

Grozovsky, Begonja, Liu, Visner, Hartwig, Falet and Hoffmeister. 2015a. The Ashwell-Morell receptor regulates hepatic thrombopoietin production via JAK2-STAT3 signaling. *Nature Medicine.* **21**(1), pp.47-54.

Grozovsky, Giannini, Falet and Hoffmeister. 2015b. Regulating billions of blood platelets: glycans and beyond. *Blood.* **126**(16), pp.1877-1884.

Grozovsky, R., Begonja, A.J., Liu, K., Visner, G., Hartwig, J.H., Falet, H. and Hoffmeister, K.M. 2015. The Ashwell-Morell receptor regulates hepatic thrombopoietin production via JAK2-STAT3 signaling. *Nature Medicine.* **21**(1), pp.47-54.

Gryglewski, R.J., Chlopicki, S., Uracz, W. and Marcinkiewicz, E. 2001. Significance of endothelial prostacyclin and nitric oxide in peripheral and pulmonary circulation. *Medical science monitor : international medical journal of experimental and clinical research.* **7**(1), pp.1-16.

Guillou, J.L., Nakata, H. and Cooper, D.M.F. 1999. Inhibition by calcium of mammalian adenylyl cyclases. *Journal of Biological Chemistry.* **274**(50), pp.35539-35545.

Gurbel, P.A., Serebruany, V.L., Shustov, A.R., Dalesandro, M., Gumbs, C.I., Grablutz, L.B., Bahr, R.D., Ohman, E.M. and Topol, E.J. 1998. Increased baseline levels of platelet P-selectin, and platelet-endothelial cell adhesion molecule-1 in patients with acute myocardial infarction as predictors of unsuccessful thrombolysis. *Coronary Artery Disease.* **9**(7), pp.451-456.

Gyulkhandanyan, A.V., Mutlu, A., Freedman, J. and Leytin, V. 2012. Markers of platelet apoptosis: methodology and applications. *Journal of Thrombosis and Thrombolysis.* **33**(4), pp.397-411.

Halbrugge, M. and Walter, U. 1989. PURIFICATION OF A VASODILATOR-REGULATED PHOSPHOPROTEIN FROM HUMAN-PLATELETS. *European Journal of Biochemistry.* **185**(1), pp.41-50.

Halbrügge, M., Friedrich, C., Eigenthaler, M., Schanzenbächer, P. and Walter, U. 1990. Stoichiometric and reversible phosphorylation of a 46-kDa protein in human platelets in response to cGMP- and cAMP-elevating vasodilators. *Journal of Biological Chemistry.* **265**(6), pp.3088-3093.

Hamad, M.A., Schanze, N., Schommer, N., Nührenberg, T. and Duerschmied, D. 2021. Reticulated Platelets—Which Functions Have Been Established by In Vivo and In Vitro Data? *Cells.* **10**(5), p1172.

Hamberg and Samuelss. 1974. PROSTAGLANDIN ENDOPEROXIDES - NOVEL TRANSFORMATIONS OF ARACHIDONIC-ACID IN HUMAN PLATELETS. *Proceedings of the National Academy of Sciences of the United States of America.* **71**(9), pp.3400-3404.

Hammond, H.K., Penny, W.F., Traverse, J.H., Henry, T.D., Watkins, M., Yancy, C., Sweis, R.N., Adler, E.D., Patel, A.N., Murray, D.R., Ross, R.S., Bhargava, V., Maisel, A., Barnard, D.D., Lai, N.C., Dalton, N.D., Lee, M.L., Narayan, S.M., Blanchard, D.G. and Gao, M.H. 2016. Intracoronary Gene Transfer of Adenylyl Cyclase 6 in Patients With Heart Failure A Randomized Clinical Trial. *Jama Cardiology.* **1**(2), pp.163-171.

Hanoune, J. and Defer, N. 2001. Regulation and role of adenylyl cyclase isoforms. *Annual Review of Pharmacology and Toxicology.* **41**, pp.145-174.

Hanoune, J., Pouille, Y., Tzavara, E., Shen, T.S., Lipskaya, L., Miyamoto, N., Suzuki, Y. and Defer, N. 1997. Adenylyl cyclases: Structure, regulation and function in an enzyme superfamily. *Molecular and Cellular Endocrinology.* **128**(1-2), pp.179-194.

Harker, L.A. and Finch, C.A. 1969. Thrombokinetics in man. *Journal of Clinical Investigation.* **48**(6), pp.963-974.

Haslam, R.J. 1973. INTERACTIONS OF PHARMACOLOGICAL RECEPTORS OF BLOOD-PLATELETS WITH ADENYLATE CYCLASE. *Microvascular Research.* **6**(2), pp.255-255.

Haslam, R.J., Dickinson, N.T. and Jang, E.K. 1999. Cyclic nucleotides and phosphodiesterases in platelets. *Thrombosis and Haemostasis.* **82**(2), pp.412-423.

Heemskerk, J.W.M., Bevers, E.M. and Lindhout, T. 2002. Platelet activation and blood coagulation. *Thrombosis and Haemostasis.* **88**(2), pp.186-193.

Heil, H.S., Aigner, M., Maier, S., Gupta, P., Evers, L.M.C., Gob, V., Kusch, C., Meub, M., Nieswandt, B., Stegner, D. and Heinze, K.G. 2022. Mapping densely packed alpha IIb beta 3 receptors in murine blood platelets with expansion microscopy. *Platelets.*

Hermann, M., Nussbaumer, O., Knöfler, R., Hengster, P., Nussbaumer, W. and Streif, W. 2010. Real-Time Live Confocal Fluorescence Microscopy as a New Tool for Assessing Platelet Vitality. *Transfusion Medicine and Hemotherapy.* **37**(5), pp.299-305.

Hettasch, J.M. and Sellers, J.R. 1991. CALDESMON PHOSPHORYLATION IN INTACT HUMAN PLATELETS BY CAMP-DEPENDENT PROTEIN-KINASE AND PROTEIN-KINASE-C. *Journal of Biological Chemistry.* **266**(18), pp.11876-11881.

Higuchi, R., Dollinger, G., Walsh, P.S. and Griffith, R. 1992. SIMULTANEOUS AMPLIFICATION AND DETECTION OF SPECIFIC DNA-SEQUENCES. *Bio-Technology.* **10**(4), pp.413-417.

Hindle, M.S., Spurgeon, B.E.J., Cheah, L.T., Webb, B.A. and Naseem, K.M. 2021. Multidimensional flow cytometry reveals novel platelet subpopulations in response to prostacyclin. *Journal of thrombosis and haemostasis : JTH.*

Hitchcock, I.S. and Kaushansky, K. 2014. Thrombopoietin from beginning to end. *British Journal of Haematology.* **165**(2), pp.259-268.

Hoffman, M. and Monroe, D.M. 2001. A cell-based model of hemostasis. *Thrombosis and Haemostasis.* **85**(6), pp.958-965.

Hoffmeister. 2011. The role of lectins and glycans in platelet clearance. *Journal of Thrombosis and Haemostasis.* **9**, pp.35-43.

Hoffmeister. 2012. Death regulates platelet birth and life. *Blood.* **119**(24), pp.5617-5618.

Hoffmeister and Falet. 2016. Platelet clearance by the hepatic Ashwell-Morrell receptor: mechanisms and biological significance. *Thrombosis Research.* **141**, pp.S68-S72.

Holland, P.M., Abramson, R.D., Watson, R. and Gelfand, D.H. 1991. DETECTION OF SPECIFIC POLYMERASE CHAIN-REACTION PRODUCT BY UTILIZING THE 5'- 3' EXONUCLEASE ACTIVITY OF THERMUS-AQUATICUS DNA-POLYMERASE. *Proceedings of the National Academy of Sciences of the United States of America.* **88**(16), pp.7276-7280.

Holmsen, H. 1989. PHYSIOLOGICAL FUNCTIONS OF PLATELETS. *Annals of Medicine.* **21**(1), pp.23-30.

Horstrup, K., Jablonka, B., Honig-Liedl, P., Just, M., Kochsiek, K. and Walter, U. 1994. Phosphorylation of Focal Adhesion Vasodilator-Stimulated Phosphoprotein at Ser157 in Intact Human Platelets Correlates with Fibrinogen Receptor Inhibition. *European Journal of Biochemistry.* **225**(1), pp.21-27.

Hughan, S.C., Hughes, C.E., Mccarty, O.J.T., Schweighoffer, E., Soultanova, I., Ware, J., Tybulewicz, V.L.J. and Watson, S.P. 2007. GPVI Potentiation of Platelet Activation by Thrombin and Adhesion Molecules Independent of Src Kinases and Syk. *Arteriosclerosis, Thrombosis, and Vascular Biology.* **27**(2), pp.422-429.

Huisman, M.V., Barco, S., Cannegieter, S.C., Le Gal, G., Konstantinides, S.V., Reitsma, P.H., Rodger, M., Noordegraaf, A.V. and Klok, F.A. 2018. Pulmonary embolism. *Nature Reviews Disease Primers.* **4**(1), p18028.

Hunter, R.W., MacKintosh, C. and Hers, I. 2009. Protein Kinase C-mediated Phosphorylation and Activation of PDE3A Regulate cAMP Levels in Human Platelets. *Journal of Biological Chemistry.* **284**(18), pp.12339-12348.

Huo, Y., Schober, A., Forlow, S.B., Smith, D.F., Hyman, M.C., Jung, S., Littman, D.R., Weber, C. and Ley, K. 2003. Circulating activated platelets exacerbate atherosclerosis in mice deficient in apolipoprotein E. *Nature Medicine.* **9**(1), pp.61-67.

Hurley, J.H. 1999. Structure, mechanism, and regulation of mammalian adenylyl cyclase. *Journal of Biological Chemistry.* **274**(12), pp.7599-7602.

Imam, H., Nguyen, T.H., De Caterina, R., Nooney, V.B., Chong, C.R., Horowitz, J.D. and Chirkov, Y.Y. 2019. Impaired adenylate cyclase signaling in acute myocardial ischemia: Impact on effectiveness of P2Y(12) receptor antagonists. *Thrombosis Research.* **181**, pp.92-98.

Ishikawa, Y. and Homcy, C.J. 1997. The adenylyl cyclases as integrators of transmembrane signal transduction. *Circulation Research.* **80**(3), pp.297-304.

Ishikawa, Y. and Homey, C.J. 1997. The adenylyl cyclases as integrators of transmembrane signal transduction. *Circulation Research.* **80**(3), pp.297-304.

Itoh, T., Nakai, K., Ono, M. and Hiramori, K. 1995. CAN THE RISK FOR ACUTE CARDIAC EVENTS IN ACUTE CORONARY SYNDROME BE INDICATED BY PLATELET MEMBRANE ACTIVATION MARKER P-SELECTIN. *Coronary Artery Disease.* **6**(8), pp.645-650.

Iwami, G., Kawabe, J., Ebina, T., Cannon, P.J., Homcy, C.J. and Ishikawa, Y. 1995. REGULATION OF ADENYLYL-CYCLASE BY PROTEIN-KINASE-A. *Journal of Biological Chemistry.* **270**(21), pp.12481-12484.

Iyengar, R. 1993. MOLECULAR AND FUNCTIONAL DIVERSITY OF MAMMALIAN G(S)-STIMULATED ADENYLYL CYCLASES. *Faseb Journal.* **7**(9), pp.768-775.

Jackson. 2007. The growing complexity of platelet aggregation. *Blood.* **109**(12), pp.5087-5095.

Jackson. 2011. Arterial thrombosis—insidious, unpredictable and deadly. *Nature Medicine.* **17**(11), pp.1423-1436.

Jackson, Nesbitt and Kulkarni. 2003. Signaling events underlying thrombus formation. *Journal of Thrombosis and Haemostasis.* **1**(7), pp.1602-1612.

Jame, S. and Barnes, G. 2020. Stroke and thromboembolism prevention in atrial fibrillation. *Heart.* **106**(1), pp.10-17.

Jandrot-Perrus, M., Lagrue, A.-H., Okuma, M. and Bon, C. 1997. Adhesion and Activation of Human Platelets Induced by Convulxin Involve Glycoprotein VI and Integrin α2β1. *Journal of Biological Chemistry.* **272**(43), pp.27035-27041.

Jantzen, H.-M., Milstone, D.S., Gousset, L., Conley, P.B. and Mortensen, R.M. 2001. Impaired activation of murine platelets lacking Gαi2. *Journal of Clinical Investigation.* **108**(3), pp.477-483.

Jarvius, M., Paulsson, J., Weibrecht, I., Leuchowius, K.-J., Andersson, A.-C., Wahlby, C., Gullberg, M., Botling, J., Sjoblom, T., Markova, B., Ostman, A., Landegren, U. and Soderberg, O. 2007. In situ detection of phosphorylated platelet-derived growth factor receptor beta using a generalized proximity ligation method. *Molecular & Cellular Proteomics.* **6**(9), pp.1500-1509.

Jennings, L.K. 2009. Mechanisms of platelet activation: Need for new strategies to protect against platelet-mediated atherothrombosis. *Thrombosis and Haemostasis.* **102**(2), pp.248-257.

Jin, Abrahams, Skinner, Petitou, Pike and Carrell. 1997. The anticoagulant activation of antithrombin by heparin. *Proceedings of the National Academy of Sciences.* **94**(26), pp.14683-14688.

Jin, Inoue, Tamura, Suzuki-Inoue, Satoh, Berndt, Handa, Goto and Ozaki. 2007. A role for glycosphingolipid-enriched microdomains in platelet glycoprotein Ib-mediated platelet activation. *Journal of Thrombosis and Haemostasis.* **5**(5), pp.1034-1040.

Jirouskova, M., Shet, A.S. and Johnson, G.J. 2007. A guide to murine platelet structure, function, assays, and genetic alterations. *Journal of Thrombosis and Haemostasis.* **5**(4), pp.661-669.

Johnston-Cox, H.A. and Ravid, K. 2011. Adenosine and blood platelets. *Purinergic Signalling.* **7**(3), pp.357-365.

Johnstone, T.B., Agarwal, S.R., Harvey, R.D. and Ostrom, R.S. 2018. cAMP Signaling Compartmentation: Adenylyl Cyclases as Anchors of Dynamic Signaling Complexes. *Molecular Pharmacology.* **93**(4), pp.270-276.

Josefsson, E.C., Burnett, D.L., Lebois, M., Debrincat, M.A., White, M.J., Henley, K.J., Lane, R.M., Moujalled, D., Preston, S.P., O'Reilly, L.A., Pellegrini, M., Metcalf, D., Strasser, A. and Kile, B.T. 2014. Platelet production proceeds independently of the intrinsic and extrinsic apoptosis pathways. *Nature Communications.* **5**(1).

Josefsson, E.C., James, C., Henley, K.J., Debrincat, M.A., Rogers, K.L., Dowling, M.R., White, M.J., Kruse, E.A., Lane, R.M., Ellis, S., Nurden, P., Mason, K.D., O'Reilly, L.A., Roberts, A.W., Metcalf, D., Huang, D.C.S. and Kile, B.T. 2011. Megakaryocytes possess a functional intrinsic apoptosis pathway that must be restrained to survive and produce platelets. *Journal of Experimental Medicine.* **208**(10), pp.2017-2031.

Kacian, D.L. and Myers, J.C. 1976. Synthesis of extensive, possibly complete, DNA copies of poliovirus RNA in high yields and at high specific activities. *Proceedings of the National Academy of Sciences.* **73**(7), pp.2191-2195.

Kahn, M.L., Zheng, Y.-W., Huang, W., Bigornia, V., Zeng, D., Moff, S., Farese, R.V., Tam, C. and Coughlin, S.R. 1998. A dual thrombin receptor system for platelet activation. *Nature.* **394**(6694), pp.690-694.

Kaluzhny, Y. and Ravid, K. 2004. Role of Apoptotic Processes in Platelet Biogenesis. *Acta haematologica.* **111**(1-2), pp.67-77.

Kaluzhny, Y., Yu, G., Sun, S., Toselli, P.A., Nieswandt, B., Jackson, C.W. and Ravid, K. 2002. BclxL overexpression in megakaryocytes leads to impaired platelet fragmentation. *Blood.* **100**(5), pp.1670-1678.

Kappelmayer, J., Nagy, B., Miszti-Blasius, K., Hevessy, Z. and Setiadi, H. 2004. The emerging value of P-selectin as a disease marker. *Clinical Chemistry and Laboratory Medicine.* **42**(5), pp.475-486.

Kasahara, K., Takagi, J., Sekiya, F., Inada, Y. and Saito, Y. 1987. ANALYSIS OF DISTRIBUTION OF RECEPTORS AMONG PLATELETS BY FLOW-CYTOMETRY. *Thrombosis Research.* **45**(6), pp.763-770.

Kawabe, J., Iwami, G., Ebina, T., Ohno, S., Katada, T., Ueda, Y., Homcy, C.J. and Ishikawa, Y. 1994. DIFFERENTIAL ACTIVATION OF ADENYLYL-CYCLASE BY PROTEIN-KINASE-C ISOENZYMES. *Journal of Biological Chemistry.* **269**(24), pp.16554-16558.

Kelemen, E., Cserhati, I. and Tanos, B. 1958. Demonstration and some properties of human thrombopoietin in thrombocythaemic sera. *Acta haematologica.* **20**(6), pp.350-355.

Kennedy, S.D., Igarashi, Y. and Kickler, T.S. 1997. Measurement of in vitro P-selectin expression by flow cytometry. *American Journal of Clinical Pathology.* **107**(1), pp.99-104.

Khan, A.O., Maclachlan, A., Lowe, G.C., Nicolson, P.L.R., Ghaithi, R.A., Thomas, S.G., Watson, S.P., Pike, J.A. and Morgan, N.V. 2020. High-throughput platelet spreading analysis: a tool for the diagnosis of platelet-based bleeding disorders. *Haematologica.* **105**(3), pp.e124-e128.

Knebel, S.M., Sprague, R.S. and Stephenson, A.H. 2015. Prostacyclin receptor expression on platelets of humans with type 2 diabetes is inversely correlated with hemoglobin A1c levels. *Prostaglandins & Other Lipid Mediators.* **116**, pp.131-135.

Kosaki, G. 2005. In Vivo Platelet Production from Mature Megakaryocytes: Does Platelet Release Occur via Proplatelets? *International Journal of Hematology.* **81**(3), pp.208-219.

Koupenova and Ravid. 2018. Biology of Platelet Purinergic Receptors and Implications for Platelet Heterogeneity. *Frontiers in Pharmacology.* **9**.

Koupenova, M., Clancy, L., Corkrey, H.A. and Freedman, J.E. 2018. Circulating Platelets as Mediators of Immunity, Inflammation, and Thrombosis. *Circulation Research.* **122**(2), pp.337-351.

Krupinski, J., Coussen, F., Bakalyar, H.A., Tang, W.J., Feinstein, P.G., Orth, K., Slaughter, C., Reed, R.R. and Gilman, A.G. 1989. ADENYLYL CYCLASE AMINO-ACID SEQUENCE - POSSIBLE CHANNEL-LIKE OR TRANSPORTER-LIKE STRUCTURE. *Science.* **244**(4912), pp.1558-1564.

Kulkarni, S., Dopheide, S.M., Yap, C.L., Ravanat, C., Freund, M., Mangin, P., Heel, K.A., Street, A., Harper, I.S., Lanza, F. and Jackson, S.P. 2000. A revised model of platelet aggregation. *Journal of Clinical Investigation.* **105**(6), pp.783-791.

Kunapuli, S.P., Dangelmaier, C., Jin, J.G., Kim, Y.B. and Daniel, J.L. 1999. Role of intracellular signaling events in ADP-induced platelet aggregation. *Thrombosis and Haemostasis.* pp.714-714.

Kurz, K.D., Main, B.W. and Sandusky, G.E. 1990. RAT MODEL OF ARTERIAL THROMBOSIS INDUCED BY FERRIC-CHLORIDE. *Thrombosis Research.* **60**(4), pp.269-280.

Kuter, D.J. and Gernsheimer, T.B. 2009. Thrombopoietin and Platelet Production in Chronic Immune Thrombocytopenia. *Hematology-Oncology Clinics of North America.* **23**(6), pp.1193-+.

Laemmli, U.K. 1970. CLEAVAGE OF STRUCTURAL PROTEINS DURING ASSEMBLY OF HEAD OF BACTERIOPHAGE-T4. *Nature.* **227**(5259), pp.680-+.

Laurent, P.-A., Séverin, S., Hechler, B., Vanhaesebroeck, B., Payrastre, B. and Gratacap, M.-P. 2015. Platelet PI3Kβ and GSK3 regulate thrombus stability at a high shear rate. *Blood.* **125**(5), pp.881-888.

Lefkimmiatis, K. and Zaccolo, M. 2014. cAMP signaling in subcellular compartments. *Pharmacology & Therapeutics.* **143**(3), pp.295-304.

Lefrançais, E., Ortiz-Muñoz, G., Caudrillier, A., Mallavia, B., Liu, F., Sayah, D.M., Thornton, E.E., Headley, M.B., David, T., Coughlin, S.R., Krummel, M.F., Leavitt, A.D., Passegué, E. and Looney, M.R. 2017. The lung is a site of platelet biogenesis and a reservoir for haematopoietic progenitors. *Nature.* **544**(7648), pp.105-109.

Leng, X.-H., Hong, S.Y., Larrucea, S., Zhang, W., Li, T.-T., LóPez, J.A. and Bray, P.F. 2004. Platelets of Female Mice Are Intrinsically More Sensitive to Agonists Than Are Platelets of Males. *Arteriosclerosis, Thrombosis, and Vascular Biology.* **24**(2), pp.376-381.

Levin, J. and Ebbe, S. 1994. WHY ARE RECENTLY PUBLISHED PLATELET COUNTS IN NORMAL MICE SO LOW. *Blood.* **83**(12), pp.3829-3830.

Leytin, V. 2012. Apoptosis in the anucleate platelet. *Blood Reviews.* **26**(2), pp.51-63.

Lhermusier, T., Chap, H. and Payrastre, B. 2011. Platelet membrane phospholipid asymmetry: from the characterization of a scramblase activity to the identification of an essential protein mutated in Scott syndrome. *Journal of Thrombosis and Haemostasis.* **9**(10), pp.1883-1891.

Li, August and Woulfe. 2008. GSK3β is a negative regulator of platelet function and thrombosis. *Blood.* **111**(7), pp.3522-3530.

Li, McIntyre and Silverstein. 2013. Ferric chloride-induced murine carotid arterial injury: A model of redox pathology. *Redox Biology.* **1**(1), pp.50-55.

Li, Pu, Zheng, Ai, Chen and Peng. 2022. Proteolysis-targeting chimeras (PROTACs) in cancer therapy. *Molecular Cancer.* **21**(1).

Libby, P. 2001. Current Concepts of the Pathogenesis of the Acute Coronary Syndromes. *Circulation.* **104**(3), pp.365-372.

Lindemann, S., Krämer, B., Seizer, P. and Gawaz, M. 2007. Platelets, inflammation and atherosclerosis. *Journal of Thrombosis and Haemostasis.* **5**, pp.203-211.

Lissandron, V., Terrin, A., Collini, M., D'Alfonso, L., Chirico, G., Pantano, S. and Zaccolo, M. 2005. Improvement of a FRET-based indicator for cAMP by linker design and stabilization of donor-acceptor interaction. *Journal of Molecular Biology.* **354**(3), pp.546-555.

Liu, Jennings, Dart and Du. 2012. Standardizing a simpler, more sensitive and accurate tail bleeding assay in mice. *World journal of experimental medicine.* **2**(2), pp.30-36.

Liu, Ruoho, Rao and Hurley. 1997. Catalytic mechanism of the adenylyl and guanylyl cyclases: Modeling and mutational analysis. *Proceedings of the National Academy of Sciences of the United States of America.* **94**(25), pp.13414-13419.

Liu, Thangavel, Sun, Kaminsky, Mahautmr, Stitham, Hwa and Ostrom. 2008. Adenylyl cyclase type 6 overexpression selectively enhances beta-adrenergic and prostacyclin receptor-mediated inhibition of cardiac fibroblast function because of colocalization in lipid rafts. *Naunyn-Schmiedebergs Archives of Pharmacology.* **377**(4-6), pp.359-369.

Livak, K.J. and Schmittgen, T.D. 2001. Analysis of relative gene expression data using real-time quantitative PCR and the 2(T)(-Delta Delta C) method. *Methods.* **25**(4), pp.402-408.

Lochner, A. and Moolman, J.A. 2006. The many faces of H89: A review. *Cardiovascular Drug Reviews.* **24**(3-4), pp.261-274.

Locke, D., Chen, H., Liu, Y., Liu, C. and Kahn, M.L. 2002. Lipid Rafts Orchestrate Signaling by the Platelet Receptor Glycoprotein VI. *Journal of Biological Chemistry.* **277**(21), pp.18801-18809.

Lohse, M.J., Hein, P., Hoffmann, C., Nikolaev, V.O., Vilardaga, J.P. and Buenemann, M. 2008. Kinetics of G-protein-coupled receptor signals in intact cells. *British Journal of Pharmacology.* **153**, pp.S125-S132.

Lopez, J.A., Del Conde, I. and Shrimpton, C.N. 2005. Receptors, rafts, and microvesicles in thrombosis and inflammation. *Journal of Thrombosis and Haemostasis.* **3**(8), pp.1737-1744.

Lova, P., Paganini, S., Sinigaglia, F., Balduini, C. and Torti, M. 2002. A G(i)-dependent pathway is required for activation of the small GTPase Rap1B in human platelets. *Journal of Biological Chemistry.* **277**(14), pp.12009-12015.

Lowry, O.H., Rosebrough, N.J., Farr, A.L. and Randall, R.J. 1951. PROTEIN MEASUREMENT WITH THE FOLIN PHENOL REAGENT. *Journal of Biological Chemistry.* **193**(1), pp.265-275.

Ludwig, M.G. and Seuwen, K. 2002. Characterization of the human adenylyl cyclase gene family: cDNA, gene structure, and tissue distribution of the nine isoforms. *Journal of Receptor and Signal Transduction Research.* **22**(1-4), pp.79-110.

Machlus, K.R., Aleman, M.M. and Wolberg, A.S. 2011. Update on Venous Thromboembolism. *Arteriosclerosis, Thrombosis, and Vascular Biology.* **31**(3), pp.476-478.

Macphee, C.H., Reifsnyder, D.H., Moore, T.A., Lerea, K.M. and Beavo, J.A. 1988. PHOSPHORYLATION RESULTS IN ACTIVATION OF A CAMP PHOSPHODIESTERASE IN HUMAN-PLATELETS. *Journal of Biological Chemistry.* **263**(21), pp.10353-10358.

Majed, B.H. and Khalil, R.A. 2012. Molecular Mechanisms Regulating the Vascular Prostacyclin Pathways and Their Adaptation during Pregnancy and in the Newborn. *Pharmacological Reviews.* **64**(3), pp.540-582.

Manganello, J.M., Djellas, Y., Borg, C., Antonakis, K. and Le Breton, G.C. 1999. Cyclic AMP-dependent phosphorylation of thromboxane A(2) receptor-associated G alpha(13). *Journal of Biological Chemistry.* **274**(39), pp.28003-28010.

Mangin, P.H., Onselaer, M.-B., Receveur, N., Le Lay, N., Hardy, A.T., Wilson, C., Sanchez, X., Loyau, S., Dupuis, A., Babar, A.K., Miller, J.L., Philippou, H., Hughes, C.E., Herr, A.B., Ariëns, R.A., Mezzano, D., Jandrot-Perrus, M., Gachet, C. and Watson, S.P. 2018. Immobilized fibrinogen activates human platelets through glycoprotein VI. *Haematologica.* **103**(5), pp.898-907.

Manns, Brennan, Colman and Sheth. 2002. Differential Regulation of Human Platelet Responses by cGMP Inhibited and Stimulated cAMP Phosphodiesterases. *Thromb Haemost.* **87**, pp.873-879.

Manrique, R.V. and Manrique, V. 1987. PLATELET RESISTANCE TO PROSTACYCLIN - ENHANCEMENT OF THE ANTIAGGREGATORY EFFECT OF PROSTACYCLIN BY PENTOXIFYLLINE. *Angiology.* **38**(2), pp.101-108.

Marcus, K., Moebius, J. and Meyer, H.E. 2003. Differential analysis of phosphorylated proteins in resting and thrombin-stimulated human platelets. *Analytical and Bioanalytical Chemistry.* **376**(7), pp.973-993.

Martin, J.F., Kristensen, S.D., Mathur, A., Grove, E.L. and Choudry, F.A. 2012. The causal role of megakaryocyte–platelet hyperactivity in acute coronary syndromes. *Nature Reviews Cardiology.* **9**(11), pp.658-670.

Mason, K.D., Carpinelli, M.R., Fletcher, J.I., Collinge, J.E., Hilton, A.A., Ellis, S., Kelly, P.N., Ekert, P.G., Metcalf, D., Roberts, A.W., Huang, D.C.S. and Kile, B.T. 2007. Programmed Anuclear Cell Death Delimits Platelet Life Span. *Cell.* **128**(6), pp.1173-1186.

Mazharian, A., Roger, S., Berrou, E., Adam, F., Kauskot, A., Nurden, P., Jandrot-Perrus, M. and Bryckaert, M. 2007. Protease-activating receptor-4 induces full platelet spreading on a fibrinogen - Involvement of Erk2 and p38 and Ca2+ matrix mobilization. *Journal of Biological Chemistry.* **282**(8), pp.5478-5487.

Mcarthur, K., Chappaz, S. and Kile, B.T. 2018. Apoptosis in megakaryocytes and platelets: the life and death of a lineage. *Blood.* **131**(6), pp.605-610.

Mellion, B.T., Ignarro, L.J., Ohlstein, E.H., Pontecorvo, E.G., Hyman, A.L. and Kadowitz, P.J. 1981. EVIDENCE FOR THE INHIBITORY ROLE OF GUANOSINE 3',5'-MONOPHOSPHATE IN ADP-INDUCED HUMAN-PLATELET AGGREGATION IN THE PRESENCE OF NITRIC-OXIDE AND RELATED VASODILATORS. *Blood.* **57**(5), pp.946-955.

Metcalfe, P., Williamson, L.M., Reutelingsperger, C.P.M., Swann, I., Ouwehand, W.H. and Goodall, A.H. 1997. Activation during preparation of therapeutic platelets affects deterioration during storage: a comparative flow cytometric study of different production methods. *British Journal of Haematology.* **98**(1), pp.86-95.

Metharom, P., Berndt, M.C., Baker, R.I. and Andrews, R.K. 2015. Current State and Novel Approaches of Antiplatelet Therapy. *Arteriosclerosis, Thrombosis, and Vascular Biology.* **35**(6), pp.1327-1338.

Michelson, A.D. 1994. PLATELET ACTIVATION BY THROMBIN CAN BE DIRECTLY MEASURED IN WHOLE-BLOOD THROUGH THE USE OF THE

PEPTIDE GPRP AND FLOW-CYTOMETRY - METHODS AND CLINICAL-APPLICATIONS. *Blood Coagulation & Fibrinolysis.* **5**(1), pp.121-131.

Michelson, A.D., Koganov, E.S., Forde, E.E., Carmichael, S.L. and Frelinger, A.L., III. 2018. Avatrombopag increases platelet count but not platelet activation in patients with thrombocytopenia resulting from liver disease. *Journal of Thrombosis and Haemostasis.* **16**(12), pp.2515-2519.

Minamino, T., Kitakaze, M., Sanada, S., Asanuama, H., Kurotobi, T., Koretsune, Y., Fukunami, M., Kuzuya, T., Hoki, N. and Hori, M. 1998. Increased Expression of P-Selectin on Platelets Is a Risk Factor for Silent Cerebral Infarction in Patients With Atrial Fibrillation. *Circulation.* **98**(17), pp.1721-1727.

Mitchell, J.A., Ali, F., Bailey, L., Moreno, L. and Harrington, L.S. 2008. Role of nitric oxide and prostacyclin as vasoactive hormones released by the endothelium. *Experimental Physiology.* **93**(1), pp.141-147.

Mohammed, B.M., Monroe, D.M. and Gailani, D. 2020. Mouse models of hemostasis. *Platelets.* **31**(4), pp.417-422.

Moncada, S. 1982. PROSTACYCLIN AND ARTERIAL-WALL BIOLOGY. *Arteriosclerosis.* **2**(3), pp.193-207.

Moncada, S., Gryglewski, R., Bunting, S. and Vane, J.R. 1976. ENZYME ISOLATED FROM ARTERIES TRANSFORMS PROSTAGLANDIN ENDOPEROXIDES TO AN UNSTABLE SUBSTANCE THAT INHIBITS PLATELET-AGGREGATION. *Nature.* **263**(5579), pp.663-665.

Monroe, D.M., Hoffman, M. and Roberts, H.R. 2002. Platelets and Thrombin Generation. *Arteriosclerosis, Thrombosis, and Vascular Biology.* **22**(9), pp.1381-1389.

Montague, S.J., Lim, Y.J., Lee, W.M. and Gardiner, E.E. 2020. Imaging Platelet Processes and Function-Current and Emerging Approaches for Imaging in vitro and in vivo. *Frontiers in Immunology.* **11**.

Moore, S.F., Agbani, E.O., Wersäll, A., Poole, A.W., Williams, C.M., Zhao, X., Li, Y., Hutchinson, J.L., Hunter, R.W. and Hers, I. 2021. Opposing Roles of GSK3α and GSK3β Phosphorylation in Platelet Function and Thrombosis. *International Journal of Molecular Sciences.* **22**(19), p10656.

Moorthy, B.S., Gao, Y.F. and Anand, G.S. 2011. Phosphodiesterases Catalyze Hydrolysis of cAMP-bound to Regulatory Subunit of Protein Kinase A and Mediate Signal Termination. *Molecular & Cellular Proteomics.* **10**(2).

Morgenstern, E. 1997. *Human Platelet Morphology/Ultrastructure. In: von Bruchhausen, F., Walter, U. (eds) Platelets and Their Factors. Handbook of Experimental Pharmacology,.* Berlin, Heidelberg: Springer Berlin Heidelberg.

Munnix, I.C.A., Harmsma, M., Giddings, J.C., Collins, P.W., Feijge, M.A.H., Comfurius, P., Heemskerk, J.W.M. and Bevers, E.M. 2003. Store-mediated calcium entry in the regulation of phosphatidylserine exposure in blood cells from Scott patients. *Thrombosis and Haemostasis.* **89**(4), pp.687-695.

Munzer, P., Walker-Allgaier, B., Geue, S., Langhauser, F., Geuss, E., Stegner, D., Aurbach, K., Semeniak, D., Chatterjee, M., Menendez, I.G., Marklin, M., Quintanilla-Martinez, L., Salih, H.R., Litchfield, D.W., Buchou, T., Kleinschnitz, C., Lang, F., Nieswandt, B., Pleines, I., Schulze, H., Gawaz, M. and Borst, O. 2017. CK2 beta regulates thrombopoiesis and Ca2+-triggered platelet activation in arterial thrombosis. *Blood.* **130**(25), pp.2774-2785.

Murata, T., Ushikubi, F., Matsuoka, T., Hirata, M., Yamasaki, A., Sugimoto, Y., Ichikawa, A., Aze, Y., Tanaka, T., Yoshida, N., Ueno, A., Oh-Ishi, S. and Narumiya, S. 1997. Altered pain perception and inflammatory response in mice lacking prostacyclin receptor. *Nature.* **388**(6643), pp.678-682.

Murthy, K.S., Zhou, H.P. and Makhlouf, G.M. 2002. PKA-dependent activation of PDE3A and PDE4 and inhibition of adenylyl cyclase V/VI in smooth muscle. *American Journal of Physiology-Cell Physiology.* **282**(3), pp.C508-C517.

Mustard, J.F., Kinlough-Rathbone, R.L. and Packham, M.A. 1989. ISOLATION OF HUMAN PLATELETS FROM PLASMA BY CENTRIFUGATION AND WASHING. *Hawiger, J. (Ed.). Methods in Enzymology, Vol. 169. Platelets: Receptors, Adhesion, Secretion, Part a. Xxviii+512p. Academic Press, Inc.: San Diego, California, USA; London, England, Uk. Illus.* pp.3-11.

Nagalla, S., Shaw, C., Kong, X., Kondkar, A.A., Edelstein, L.C., Ma, L., Chen, J., Mcknight, G.S., López, J.A., Yang, L., Jin, Y., Bray, M.S., Leal, S.M., Dong, J.-F. and Bray, P.F. 2011. Platelet microRNA-mRNA coexpression profiles correlate with platelet reactivity. *Blood.* **117**(19), pp.5189-5197.

Nagy, Z. and Smolenski, A. 2018. Cyclic nucleotide-dependent inhibitory signaling interweaves with activating pathways to determine platelet responses. *Research and Practice in Thrombosis and Haemostasis.* **2**(3), pp.558-571.

Neer, E.J. 1975. THE SIZE OF ADENYLATE CYCLASE. *J Supramol Struct.* pp.810-810.

Nelson, C.P., Rainbow, R.D., Brignell, J.L., Perry, M.D., Willets, J.M., Davies, N.W., Standen, N.B. and Challiss, R.A.J. 2011. Principal role of adenylyl cyclase 6 in K+ channel regulation and vasodilator signalling in vascular smooth muscle cells. *Cardiovascular Research.* **91**(4), pp.694-702.

Nieswandt, Pleines and Bender. 2011. Platelet adhesion and activation mechanisms in arterial thrombosis and ischaemic stroke. *Journal of Thrombosis and Haemostasis.* **9**, pp.92-104.

Nieswandt, Schulte and Bergmeier. 2004. Flow-Cytometric Analysis of Mouse Platelet Function. *Platelets and Megakaryocytes.* Humana Press, pp.255-268.

Nieswandt, B., Schulte, V. and Bergmeier, W. 2004. Flow-Cytometric Analysis of Mouse Platelet Function. *Platelets and Megakaryocytes.* Humana Press, pp.255-268.

Noe, L., Peeters, K., Izzi, B., Van Geet, C. and Freson, K. 2010. Regulators of Platelet cAMP Levels: Clinical and Therapeutic Implications. *Current Medicinal Chemistry.* **17**(26), pp.2897-2905.

Oberprieler, N.G. and Tasken, K. 2011. Analysing phosphorylation-based signalling networks by phospho flow cytometry. *Cellular Signalling.* **23**(1), pp.14-18.

Odell, T.T., Jackson, C.W. and Reiter, R.S. 1968. Generation cycle of rat megakaryocytes. *Experimental Cell Research.* **53**(2-3), pp.321-328.

Offermanns, S. 2006. Activation of platelet function through G protein-coupled receptors. *Circulation Research.* **99**(12), pp.1293-1304.

Ogilvy, S., Metcalf, D., Print, C.G., Bath, M.L., Harris, A.W. and Adams, J.M. 1999. Constitutive Bcl-2 expression throughout the hematopoietic compartment affects multiple lineages and enhances progenitor cell survival. *Proceedings of the National Academy of Sciences.* **96**(26), pp.14943-14948.

Onda, T., Hashimoto, Y., Nagai, M., Kuramochi, H., Saito, S., Yamazaki, H., Toya, Y., Sakai, I., Homcy, C.J., Nishikawa, K. and Ishikawa, Y. 2001. Type-specific Regulation of Adenylyl Cyclase. *Journal of Biological Chemistry.* **276**(51), pp.47785-47793.

Orth, M.F., Cazes, A., Butt, E. and Grunewald, T.G.P. 2015. An update on the LIM and SH3 domain protein 1 (LASP1): a versatile structural, signaling, and biomarker protein. *Oncotarget.* **6**(1), pp.26-42.

Ostrom, Bogard, Gros and Feldman. 2012. Choreographing the adenylyl cyclase signalosome: sorting out the partners and the steps. *Naunyn-Schmiedeberg's Archives of Pharmacology.* **385**(1), pp.5-12.

Ostrom, Liu, Head, Gregorian, Seasholtz and Insel. 2002. Localization of adenylyl cyclase Isoforms and G protein-coupled receptors in vascular smooth muscle cells: Expression in caveolin-rich and noncaveolin domains. *Molecular Pharmacology.* **62**(5), pp.983-992.

Patel, S.R. 2005. The biogenesis of platelets from megakaryocyte proplatelets. *Journal of Clinical Investigation.* **115**(12), pp.3348-3354.

Pidoux, G. and Tasken, K. 2010. Specificity and spatial dynamics of protein kinase A signaling organized by A-kinase-anchoring proteins. *Journal of Molecular Endocrinology.* **44**(5), pp.271-284.

Pierce, K.L., Premont, R.T. and Lefkowitz, R.J. 2002. Seven-transmembrane receptors. *Nature Reviews Molecular Cell Biology.* **3**(9), pp.639-650.

Pleines, I., Eckly, A., Elvers, M., Hagedorn, I., Eliautou, S., Bender, M., Wu, X., Lanza, F., Gachet, C., Brakebusch, C. and Nieswandt, B. 2010. Multiple alterations of platelet functions dominated by increased secretion in mice lacking Cdc42 in platelets. *Blood.* **115**(16), pp.3364-3373.

Pluthero, F.G. and Kahr, W.H.A. 2018. The Birth and Death of Platelets in Health and Disease. *Physiology.* **33**(3), pp.225-234.

Podoplelova, N.A., Sveshnikova, A.N., Kotova, Y.N., Eckly, A., Receveur, N., Nechipurenko, D.Y., Obydennyi, S.I., Kireev, I.I., Gachet, C., Ataullakhanov, F.I., Mangin, P.H. and Panteleev, M.A. 2016. Coagulation factors bound to procoagulant platelets concentrate in cap structures to promote clotting. *Blood.* **128**(13), pp.1745-1755.

Polgár, J., Clemetson, J.M., Kehrel, B.E., Wiedemann, M., Magnenat, E.M., Wells, T.N.C. and Clemetson, K.J. 1997. Platelet Activation and Signal Transduction by Convulxin, a C-type Lectin from Crotalus durissus terrificus (Tropical Rattlesnake) Venom via the p62/GPVI Collagen Receptor. *Journal of Biological Chemistry.* **272**(21), pp.13576-13583.

Porreca, E., Di Nisio, M., Moretta, V., Cuccurullo, F., Marchisio, M., Lanuti, P., Pierdomenico, L. and Miscia, S. 2009. Increased phosphatidylserine exposure on platelets from hospitalized patients with acute medical illnesses. *Thrombosis Research.* **124**(4), pp.502-504.

Qureshi, A.H., Chaoji, V., Maiguel, D., Faridi, M.H., Barth, C.J., Salem, S.M., Singhal, M., Stoub, D., Krastins, B., Ogihara, M., Zaki, M.J. and Gupta, V. 2009. Proteomic and Phospho-Proteomic Profile of Human Platelets in Basal, Resting State: Insights into Integrin Signaling. *PLoS ONE.* **4**(10), pe7627.

Rabani, V., Lagoutte-Renosi, J., Series, J., Valot, B., Xuereb, J.-M. and Davani, S. 2020. Cholesterol-Rich Microdomains Contribute to PAR1 Signaling in Platelets Despite a Weak Localization of the Receptor in These Microdomains. *International Journal of Molecular Sciences.* **21**(21), p8065.

Radomski, Palmer and Moncada. 1987a. ENDOGENOUS NITRIC-OXIDE INHIBITS HUMAN-PLATELET ADHESION TO VASCULAR ENDOTHELIUM. *Lancet.* **2**(8567), pp.1057-1058.

Radomski, Palmer and Moncada. 1987b. THE ANTI-AGGREGATING PROPERTIES OF VASCULAR ENDOTHELIUM - INTERACTIONS BETWEEN PROSTACYCLIN AND NITRIC-OXIDE. *British Journal of Pharmacology.* **92**(3), pp.639-646.

Radomski, M.W., Palmer, R.M.J. and Moncada, S. 1987. Comparative pharmacology of endothelium-derived relaxing factor, nitric oxide and prostacyclin in platelets. *British Journal of Pharmacology.* **92**(1), pp.181-187.

Radomski, M.W., Palmer, R.M.J. and Moncada, S. 1987. THE ANTI-AGGREGATING PROPERTIES OF VASCULAR ENDOTHELIUM - INTERACTIONS BETWEEN PROSTACYCLIN AND NITRIC-OXIDE. *British Journal of Pharmacology.* **92**(3), pp.639-646.

Raslan, Aburima and Naseem. 2015a. The Spatiotemporal Regulation of cAMP Signaling in Blood Platelets-Old Friends and New Players. *Frontiers in Pharmacology.* **6**.

Raslan, Magwenzi, Aburima, Taskén and Naseem. 2015b. Targeting of type I protein kinase A to lipid rafts is required for platelet inhibition by the 3′,5′-cyclic adenosine monophosphate-signaling pathway. *Journal of Thrombosis and Haemostasis.* **13**(9), pp.1721-1734.

Raslan and Naseem. 2014. The control of blood platelets by cAMP signalling. *Biochemical Society Transactions.* **42**, pp.289-294.

Raslan and Naseem. 2015. Compartmentalisation of cAMP-dependent signalling in blood platelets: The role of lipid rafts and actin polymerisation. *Platelets.* **26**(4), pp.349-357.

Raslan, Z. and Naseem, K.M. 2015. Compartmentalisation of cAMP-dependent signalling in blood platelets: The role of lipid rafts and actin polymerisation. *Platelets.* **26**(4), pp.349-357.

Ravid, K., Lu, J., Zimmet, J.M. and Jones, M.R. 2002. Roads to polyploidy: The megakaryocyte example. *Journal of Cellular Physiology.* **190**(1), pp.7-20.

Ribatti, D. and Crivellato, E. 2007. Giulio Bizzozero and the discovery of platelets. *Leukemia Research.* **31**(10), pp.1339-1341.

Rivera, J., Luisa Lozano, M., Navarro-Nunez, L. and Vicente, V. 2009. Platelet receptors and signaling in the dynamics of thrombus formation. *Haematologica-the Hematology Journal.* **94**(5), pp.700-711.

Roberts, W., Magwenzi, S., Aburima, A. and Naseem, K.M. 2010. Thrombospondin-1 induces platelet activation through CD36-dependent inhibition of the cAMP/protein kinase A signaling cascade. *Blood.* **116**(20), pp.4297-4306.

Rosen, E.D., Raymond, S., Zollman, A., Noria, F., Sandoval-Cooper, M., Shulman, A., Merz, J.L. and Castellino, F.J. 2001. Laser-Induced Noninvasive Vascular Injury Models in Mice Generate Platelet- and Coagulation-Dependent Thrombi. *The American Journal of Pathology.* **158**(5), pp.1613-1622.

Rowley, J.W., Oler, A.J., Tolley, N.D., Hunter, B.N., Low, E.N., Nix, D.A., Yost, C.C., Zimmerman, G.A. and Weyrich, A.S. 2011. Genome-wide RNA-seq analysis of human and mouse platelet transcriptomes. *Blood.* **118**(14), pp.E101-E111.

Ruggeri, Z.M. 2002. Platelets in atherothrombosis. *Nature Medicine.* **8**(11), pp.1227-1234.

Ruggeri, Z.M. and Mendolicchio, G.L. 2007. Adhesion Mechanisms in Platelet Function. *Circulation Research.* **100**(12), pp.1673-1685.

Rukoyatkina, N., Walter, U., Friebe, A. and Gambaryan, S. 2011. Differentiation of cGMP-dependent and -independent nitric oxide effects on platelet apoptosis and reactive oxygen species production using platelets lacking soluble guanylyl cyclase. *Thrombosis and Haemostasis.* **106**(5), pp.922-933.

Rumjantseva and Hoffmeister. 2010. Novel and unexpected clearance mechanisms for cold platelets. *Transfusion and Apheresis Science.* **42**(1), pp.63-70.

Sadana, R. and Dessauer, C.W. 2009. Physiological Roles for G Protein-Regulated Adenylyl Cyclase Isoforms: Insights from Knockout and Overexpression Studies. *Neurosignals.* **17**(1), pp.5-22.

Saiki, R.K., Gelfand, D.H., Stoffel, S., Scharf, S.J., Higuchi, R., Horn, G.T., Mullis, K.B. and Erlich, H.A. 1988. PRIMER-DIRECTED ENZYMATIC AMPLIFICATION OF DNA WITH A THERMOSTABLE DNA-POLYMERASE. *Science.* **239**(4839), pp.487-491.

Saiki, R.K., Scharf, S., Faloona, F., Mullis, K.B., Horn, G.T., Erlich, H.A. and Arnheim, N. 1985. ENZYMATIC AMPLIFICATION OF BETA-GLOBIN GENOMIC SEQUENCES AND RESTRICTION SITE ANALYSIS FOR DIAGNOSIS OF SICKLE-CELL ANEMIA. *Science.* **230**(4732), pp.1350-1354.

Sakamoto, K.M., Kim, K.B., Kumagai, A., Mercurio, F., Crews, C.M. and Deshaies, R.J. 2001. Protacs: Chimeric molecules that target proteins to the Skp1-Cullin-F box complex for ubiquitination and degradation. *Proceedings of the National Academy of Sciences of the United States of America.* **98**(15), pp.8554-8559.

Salles, I.I., Feys, H.B., Iserbyt, B.F., De Meyer, S.F., Vanhoorelbeke, K. and Deckmyn, H. 2008. Inherited traits affecting platelet function. *Blood Reviews.* **22**(3), pp.155-172.

Samuelss. 1965. ON INCORPORATION OF OXYGEN IN CONVERSION OF 8,11,14-EICOSATRIENOIC ACID TO PROSTAGLANDIN E1. *Journal of the American Chemical Society.* **87**(13), pp.3011-&.

Sandoo, A., van Zanten, J.J.C.S.V., Metsios, G.S., Carroll, D. and Kitas, G.D. 2010. The endothelium and its role in regulating vascular tone. *The open cardiovascular medicine journal.* **4**, pp.302-312.

Sassone-Corsi, P. 2012. The Cyclic AMP Pathway. *Cold Spring Harbor Perspectives in Biology.* **4**(12).

Schneekloth, J.S., Fonseca, F.N., Koldobskiy, M., Mandal, A., Deshaies, R., Sakamoto, K. and Crews, C.M. 2004. Chemical genetic control of protein levels: Selective in vivo targeted degradation. *Journal of the American Chemical Society.* **126**(12), pp.3748-3754.

Schror, K. 1997. Aspirin and platelets: The antiplatelet action of aspirin and its role in thrombosis treatment and prophylaxis. *Seminars in Thrombosis and Hemostasis.* **23**(4), pp.349-356.

Scott, J.D. and Pawson, T. 2009. Cell Signaling in Space and Time: Where Proteins Come Together and When They're Apart. *Science.* **326**(5957), pp.1220-1224.

Seamon, K.B. and Daly, J.W. 1981. FORSKOLIN - A UNIQUE DITERPENE ACTIVATOR OF CYCLIC AMP-GENERATING SYSTEMS. *Journal of Cyclic Nucleotide Research.* **7**(4), pp.201-224.

Seamon, K.B., Padgett, W. and Daly, J.W. 1981. FORSKOLIN - UNIQUE DITERPENE ACTIVATOR OF ADENYLATE-CYCLASE IN MEMBRANES AND IN INTACT-CELLS. *Proceedings of the National Academy of Sciences of the United States of America-Biological Sciences.* **78**(6), pp.3363-3367.

Selvadurai, M.V. and Hamilton, J.R. 2018. Structure and function of the open canalicular system – the platelet's specialized internal membrane network. *Platelets.* **29**(4), pp.319-325.

Serebruany, V.L. and Gurbel, P.A. 1999. Assessment of platelet activity by measuring platelet-derived substances in plasma from patients with acute myocardial infarction: Surprising lessons from the GUSTO-III platelet study. *Thrombosis Research.* **93**(3), pp.149-150.

Shakur, Y., Holst, L.S., Landstrom, T.R., Movsesian, M., Degerman, E. and Manganiello, V. 2001. Regulation and function of the cyclic nucleotide

phosphodiesterase (PDE3) gene family. *Progress in Nucleic Acid Research and Molecular Biology, Vol 66.* **66**, pp.241-277.

Shattil, Hoxie, Cunningham and Brass. 1985. Changes in the platelet membrane glycoprotein IIb.IIIa complex during platelet activation. *Journal of Biological Chemistry.* **260**(20), pp.11107-11114.

Shattil, Kim and Ginsberg. 2010. The final steps of integrin activation: the end game. *Nature Reviews Molecular Cell Biology.* **11**(4), pp.288-300.

Shattil, S.J., Hoxie, J.A., Cunningham, M. and Brass, L.F. 1985. Changes in the platelet membrane glycoprotein IIb.IIIa complex during platelet activation. *Journal of Biological Chemistry.* **260**(20), pp.11107-11114.

Siess, W. 1989. MOLECULAR MECHANISMS OF PLATELET ACTIVATION. *Physiological Reviews.* **69**(1), pp.58-178.

Sim, D.S., Merrill-Skoloff, G., Furie, B.C., Furie, B. and Flaumenhaft, R. 2004. Initial accumulation of platelets during arterial thrombus formation in vivo is inhibited by elevation of basal cAMP levels. *Blood.* **103**(6), pp.2127-2134.

Simonds, W.F. 1999. G protein regulation of adenylate cyclase. *Trends in Pharmacological Sciences.* **20**(2), pp.66-73.

Simons, K. and Gerl, M.J. 2010. Revitalizing membrane rafts: new tools and insights. *Nature Reviews Molecular Cell Biology.* **11**(10), pp.688-699.

Smolenski, A., Bachmann, C., Reinhard, K., Hönig-Liedl, P., Jarchau, T., Hoschuetzky, H. and Walter, U. 1998. Analysis and Regulation of Vasodilator-stimulated Phosphoprotein Serine 239 Phosphorylation in Vitro and in Intact Cells Using a Phosphospecific Monoclonal Antibody. *Journal of Biological Chemistry.* **273**(32), pp.20029-20035.

Smrcka, A.V. 2008. G protein beta gamma subunits: Central mediators of G protein-coupled receptor signaling. *Cellular and Molecular Life Sciences.* **65**(14), pp.2191-2214.

Spurgeon, Aburima, Oberprieler, Tasken and Naseem. 2014. Multiplexed phosphospecific flow cytometry enables large-scale signaling profiling and drug screening in blood platelets. *Journal of Thrombosis and Haemostasis.* **12**(10), pp.1733-1743.

Spurgeon, B.E.J. and Naseem, K.M. 2018. High-Throughput Signaling Profiling in Blood Platelets by Multiplexed Phosphoflow Cytometry. *Methods in molecular biology (Clifton, N.J.).* **1812**, pp.95-111.

Stalker, T.J., Newman, D.K., Ma, P., Wannemacher, K.M. and Brass, L.F. 2012. Platelet signaling. *Handbook of experimental pharmacology.* (210), pp.59-85.

Stalker, T.J., Traxler, E.A., Wu, J., Wannemacher, K.M., Cermignano, S.L., Voronov, R., Diamond, S.L. and Brass, L.F. 2013. Hierarchical organization in the hemostatic response and its relationship to the platelet-signaling network. *Blood.* **121**(10), pp.1875-1885.

Stangherlin, A. and Zaccolo, M. 2012. Phosphodiesterases and subcellular compartmentalized cAMP signaling in the cardiovascular system. *American Journal of Physiology-Heart and Circulatory Physiology.* **302**(2), pp.H379-H390.

Stepanyan, M.G., Filkova, A.A., Garzon Dasgupta, A.K., Martyanov, A.A. and Sveshnikova, A.N. 2021. Platelet Activation through GPVI Receptor: Variability of the Response. *Biochemistry (Moscow), Supplement Series A: Membrane and Cell Biology.* **15**(1), pp.73-81.

Subramanian, H., Zahedi, R.P., Sickmann, A., Walter, U. and Gambaryan, S. 2013. Phosphorylation of CalDAG-GEFI by protein kinase A prevents Rap1b activation. *Journal of Thrombosis and Haemostasis.* **11**(8), pp.1574-1582.

Sun, B., Li, H., Shakur, Y., Hensley, J., Hockman, S., Kambayashi, J., Mangamello, V.C. and Liu, Y. 2007. Role of phosphodiesterase type 3A and 3B in regulating platelet and cardiac function using subtype-selective knockout mice. *Cellular Signalling.* **19**(8), pp.1765-1771.

Sunahara, R.K., Dessauer, C.W. and Gilman, A.G. 1996. Complexity and diversity of mammalian adenylyl cyclases. *Annual Review of Pharmacology and Toxicology.* **36**, pp.461-480.

Syu, G.-D., Dunn, J. and Zhu, H. 2020. Developments and Applications of Functional Protein Microarrays. *Molecular & Cellular Proteomics.* **19**(6), pp.916-927.

Tait, J.F., Smith, C. and Wood, B.L. 1999. Measurement of Phosphatidylserine Exposure in Leukocytes and Platelets by Whole-Blood Flow Cytometry with Annexin V. *Blood Cells, Molecules, and Diseases.* **25**(5), pp.271-278.

Tasken, K. and Aandahl, E.M. 2004. Localized effects of cAMP mediated by distinct routes of protein kinase A. *Physiological Reviews.* **84**(1), pp.137-167.

Tello-Montoliu, A., Tomasello, S.D., Ueno, M. and Angiolillo, D.J. 2011. Antiplatelet therapy: thrombin receptor antagonists. *British Journal of Clinical Pharmacology.* **72**(4), pp.658-671.

Tesmer, J.J.G., Sunahara, R.K., Gilman, A.G. and Sprang, S.R. 1997. Crystal structure of the catalytic domains of adenylyl cyclase in a complex with G(s alpha).GTP gamma S. *Science.* **278**(5345), pp.1907-1916.

Thomas, M.R. and Storey, R.F. 2015. The role of platelets in inflammation. *Thrombosis and Haemostasis.* **114**(3), pp.449-458.

Thulin, Å., Yan, J., Åberg, M., Christersson, C., Kamali-Moghaddam, M. and Siegbahn, A. 2018. Sensitive and Specific Detection of Platelet-Derived and Tissue Factor–Positive Extracellular Vesicles in Plasma Using Solid-Phase Proximity Ligation Assay. *TH Open.* **02**(03), pp.e250-e260.

Tiedt, R., Schomber, T., Hui, H.S. and Skoda, R.C. 2007. Pf4-Cre transgenic mice allow the generation of lineage-restricted gene knockouts for studying megakaryocyte and platelet function in vivo. *Blood.* **109**(4), pp.1503-1506.

Tomaiuolo, M., Brass, L.F. and Stalker, T.J. 2017. Regulation of Platelet Activation and Coagulation and Its Role in Vascular Injury and Arterial Thrombosis. *Interventional cardiology clinics.* **6**(1), pp.1-12.

Tovey, S.C., Dedos, S.G., Taylor, E.J.A., Church, J.E. and Taylor, C.W. 2008. Selective coupling of type 6 adenylyl cyclase with type 2 IP3 receptors mediates direct sensitization of IP3 receptors by cAMP. *Journal of Cell Biology.* **183**(2), pp.297-311.

Tschoepe, D., Schultheiss, H.P., Kolarov, P., Schwippert, B., Dannehl, K., Nieuwenhuis, H.K., Kehrel, B., Strauer, B. and Gries, F.A. 1993. PLATELET MEMBRANE ACTIVATION MARKERS ARE PREDICTIVE FOR INCREASED RISK OF ACUTE ISCHEMIC EVENTS AFTER PTCA. *Circulation.* **88**(1), pp.37-42.

Van Geet, C., Izzi, B., Labarque, V. and Freson, K. 2009. Human platelet pathology related to defects in the G-protein signaling cascade. *Journal of Thrombosis and Haemostasis.* **7**, pp.282-286.

Varga-Szabo, D., Pleines, I. and Nieswandt, B. 2008. Cell adhesion mechanisms in platelets. *Arteriosclerosis Thrombosis and Vascular Biology.* **28**(3), pp.403-412.

Vargas, J.R., Radomski, M. and Moncada, S. 1982. THE USE OF PROSTACYCLIN IN THE SEPARATION FROM PLASMA AND WASHING OF HUMAN-PLATELETS. *Prostaglandins.* **23**(6), pp.929-945.

Versteeg, H.H., Heemskerk, J.W.M., Levi, M. and Reitsma, P.H. 2013. NEW FUNDAMENTALS IN HEMOSTASIS. *Physiological Reviews.* **93**(1), pp.327-358.

Vogler, M., Hamali, H.A., Sun, X.-M., Bampton, E.T.W., Dinsdale, D., Snowden, R.T., Dyer, M.J.S., Goodall, A.H. and Cohen, G.M. 2011. BCL2/BCL-XL inhibition induces apoptosis, disrupts cellular calcium homeostasis, and prevents platelet activation. *Blood.* **117**(26), pp.7145-7154.

Waldmann, Nieberding and Walter. 1987. VASODILATOR-STIMULATED PROTEIN-PHOSPHORYLATION IN PLATELETS IS MEDIATED BY CAMP-DEPENDENT AND CGMP-DEPENDENT PROTEIN-KINASES. *European Journal of Biochemistry.* **167**(3), pp.441-448.

Wangorsch, G., Butt, E., Mark, R., Hubertus, K., Geiger, J., Dandekar, T. and Dittrich, M. 2011. Time-resolved in silico modeling of fine-tuned cAMP signaling in platelets: feedback loops, titrated phosphorylations and pharmacological modulation. *BMC Systems Biology.* **5**(1), p178.

Wardell, M.R., Reynolds, C.C., Berndt, M.C., Wallace, R.W. and Fox, J.E.B. 1989. PLATELET GLYCOPROTEIN IB-BETA IS PHOSPHORYLATED ON SERINE 166 BY CYCLIC AMP-DEPENDENT PROTEIN-KINASE. *Journal of Biological Chemistry.* **264**(26), pp.15656-15661.

Warlo, E.M.K., Arnesen, H. and Seljeflot, I. 2019. A brief review on resistance to P2Y(12) receptor antagonism in coronary artery disease. *Thrombosis Journal.* **17**.

Warner, T.D., Nylander, S. and Whatling, C. 2011. Anti-platelet therapy: cyclo-oxygenase inhibition and the use of aspirin with particular regard to dual anti-platelet therapy. *British Journal of Clinical Pharmacology.* **72**(4), pp.619-633.

Watson, S.P., Auger, J.M., McCarty, O.J.T. and Pearce, A.C. 2005. GPVI and integrin alpha II beta 3 signaling in platelets. *Journal of Thrombosis and Haemostasis.* **3**(8), pp.1752-1762.

Weber, S., Zeller, M., Guan, K., Wunder, F., Wagner, M. and El-Armouche, A. 2017. PDE2 at the crossway between cAMP and cGMP signalling in the heart. *Cellular Signalling.* **38**, pp.76-84.

White, J.G. 2004. Electron microscopy methods for studying platelet structure and function. *Methods in molecular biology (Clifton, N.J.).* **272**, pp.47-63.

Wijeyeratne, Y.D. and Heptinstall, S. 2011. Anti-platelet therapy: ADP receptor antagonists. *British Journal of Clinical Pharmacology.* **72**(4), pp.647-657.

Willoughby, D. and Cooper, D.M.F. 2007. Organization and Ca2+ regulation of adenylyl cyclases in cAMP microdomains. *Physiological Reviews.* **87**(3), pp.965-1010.

Wong, S.T., Baker, L.P., Trinh, K., Hetman, M., Suzuki, L.A., Storm, D.R. and Bornfeldt, K.E. 2001. Adenylyl cyclase 3 mediates prostaglandin E-2-induced growth inhibition in arterial smooth muscle cells. *Journal of Biological Chemistry.* **276**(36), pp.34206-34212.

Woulfe, D., Jiang, H., Mortensen, R., Yang, J. and Brass, L.F. 2002. Activation of Rap1B by Gi Family Members in Platelets. *Journal of Biological Chemistry.* **277**(26), pp.23382-23390.

Wurzinger, L.J. 1990. HISTOPHYSIOLOGY OF THE CIRCULATING PLATELET. *Advances in Anatomy Embryology and Cell Biology.* **120**, pp.1-92.

Yang, J., Wu, J., Jiang, H., Mortensen, R., Austin, S., Manning, D.R., Woulfe, D. and Brass, L.F. 2002. Signaling through G(i) family members in platelets - Redundancy and specificity in the regulation of adenylyl cyclase and other effectors. *Journal of Biological Chemistry.* **277**(48), pp.46035-46042.

Yusuf, M.Z., Raslan, Z., Atkinson, L., Aburima, A., Thomas, S.G., Naseem, K.M. and Calaminus, S.D.J. 2017. Prostacyclin reverses platelet stress fibre formation causing platelet aggregate instability. *Scientific Reports.* **7**.

Zaccolo, M. 2009. cAMP signal transduction in the heart: understanding spatial control for the development of novel therapeutic strategies. *British Journal of Pharmacology.* **158**(1), pp.50-60.

Zaccolo, M. 2011. Spatial control of cAMP signalling in health and disease. *Current Opinion in Pharmacology.* **11**(6), pp.649-655.

Zaccolo, M., Zerio, A. and Lobo, M.J. 2021. Subcellular Organization of the cAMP Signaling Pathway. *Pharmacological Reviews.* **73**(1), pp.278-309.

Zeiler, M., Moser, M. and Mann, M. 2014. Copy Number Analysis of the Murine Platelet Proteome Spanning the Complete Abundance Range. *Molecular & Cellular Proteomics.* **13**(12), pp.3435-3445.

Zhang and Colman. 2007. Thrombin regulates intracellular cyclic AMP concentration in human platelets through phosphorylation/activation of phosphodiesterase 3A. *Blood.* **110**(5), pp.1475-1482.

Zhang, Liu, Ruoho and Hurley. 1997. Structure of the adenylyl cyclase catalytic core. *Nature.* **386**(6622), pp.247-253.

Zhang, Xiang, Dong, Skoda, Daugherty, Smyth, Du and Li. 2011. Biphasic roles for soluble guanylyl cyclase (sGC) in platelet activation. *Blood.* **118**(13), pp.3670-3679.

Zhang, Zhang and Ding. 2017. Role of P2Y(12) Receptor in Thrombosis. *Thrombosis and Embolism: from Research to Clinical Practice, Vol 1.* **906**, pp.307-324.

Zhang, Zhang, Liu, Khan, Zhou and Zheng. 2020. PROTACs are effective in addressing the platelet toxicity associated with BCL-XL inhibitors. *Exploration of Targeted Anti-tumor Therapy.* **1**(4), pp.259-272.

Zhao, L., Liu, J., He, C., Yan, R., Zhou, K., Cui, Q., Meng, X., Li, X., Zhang, Y., Nie, Y., Zhang, Y., Hu, R., Liu, Y., Zhao, L., Chen, M., Xiao, W., Tian, J., Zhao, Y., Cao, L., Zhou, L., Lin, A., Ruan, C. and Dai, K. 2017. Protein kinase A determines platelet life span and survival by regulating apoptosis. *Journal of Clinical Investigation.* **127**(12), pp.4338-4351.

Zhou, X., Wang, H., Burg, M.B. and Ferraris, J.D. 2013. Inhibitory phosphorylation of GSK-3 beta by AKT, PKA, and PI3K contributes to high NaCl-induced activation of the transcription factor NFAT5 (TonEBP/OREBP). *American Journal of Physiology-Renal Physiology.* **304**(7), pp.F908-F917.

Zimmermann, G., Zhou, D.M. and Taussig, R. 1998. Genetic selection of mammalian adenylyl cyclases insensitive to stimulation by G(s alpha). *Journal of Biological Chemistry.* **273**(12), pp.6968-6975.